Sustainable catalytic process for the one-pot formation of cyclic carbonates through oxidation of alkenes and CO2 cycloaddition

Matthieu Balas

Sorbonne Université

ED 397

Institut des matériaux de Paris Centre IMPC / Laboratoire de Réactivité de Surface LRS in collaboration with Institut Parisien de Chimie Moléculaire IPCM

Sustainable catalytic process for the *one-pot* formation of cyclic carbonates through oxidation of alkenes and CO_2 cycloaddition

Par Matthieu Balas

Thèse de doctorat de Physique et Chimie des Matériaux

Dirigée par Franck Launay et Richard Villanneau

Présentée et soutenue publiquement le 15/04/2021

Devant un jury composé de :

Mr Hesemann Peter	Directeur de recherche, Université de Montpellier	Rapporteur
Mme Dufaud-Nicolai Veronique	Directrice de recherche, Université Lyon 1	Rapporteur
Mr Tassaing Thierry	Directeur de recherche, Université de Bordeaux	Examinateur
Mr Nicolas Emmanuel	Chercheur, CEA Saclay (Gif sur Yvette)	Examinateur
Mme Christ Lorraine	Maître de conférences, Université Lyon 1	Examinatrice
Mme Cassaignon Sophie	Professeur, Sorbonne Université Paris	Examinatrice
Mr Launay Franck	Professeur, Sorbonne Université Paris	Directeur de thèse
Mr Villanneau Richard	Maître de conférences, Sorbonne Université Paris	Co-directeur de thèse

Table of contents

GLOSSARY

ACN	Acetonitrile
BET	Brunauer–Emmett–Teller
BPTMS	Bromopropyltrimethoxysilane
CCS	Carbon Capture and Storage
CCU	Carbon Capture and Utilization
CHP	Cumene Hydroperoxide
CPTMS	Chloropropyltrimethoxysilane
DBU	1,8-Diazabicyclo[5.4.0]undéc-7-ène
DCM	Dichloromethane
GC-FID	Gas Chromatography - Flame Ionization Detector
Im	Imidazolium
MOF	Metal-Organic Framework
MTO	Methyltrioxorhenium
QAS	Quaternary Ammonium Salt
r.t.	Room temperature
SBA	Santa Barbara Amorphous
SC	Styrene Carbonate
SO	Styrene Oxide
TACN	1,4,7-Triazacyclononane
TBABr	Tetrabutylammonium bromide
TBHP	*Tert*-butyl Hydroperoxide
TGA	Thermogravimetric Analysis
THF	Tetrahydrofuran

GENERAL INTRODUCTION

It is now widely accepted within the scientific community that "Human activities are estimated to have caused approximately 1.0°C of global warming above pre-industrial levels, […] and that warming due to anthropogenic emissions from the pre-industrial period to the present will persist for centuries to millennia and will continue to cause further long-term changes in the climate system". [1] It is therefore becoming urgent to reduce our CO_2 emissions in order to curb the global temperature increase (**Figure 1**).

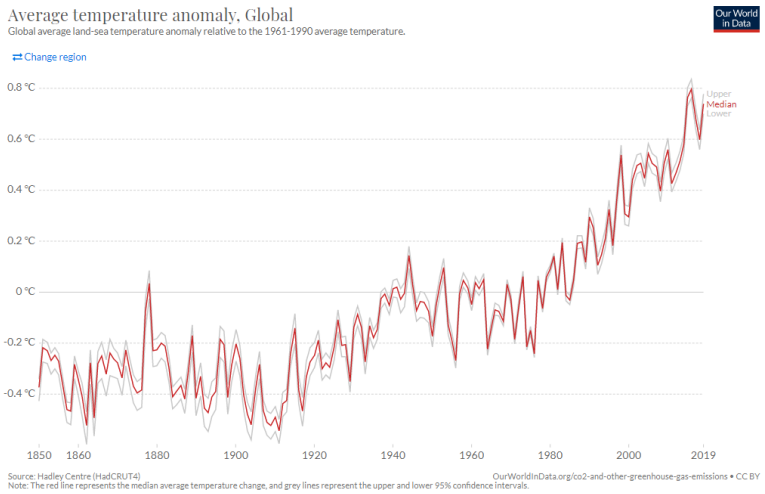

Figure 1: *Global average land-sea temperature anomaly relative to the 1961-1990 average temperature[2]*

The main source of CO_2 comes from the consumption of energy of fossil origin. Indeed, the use of machines makes our daily lives easier, but also releases a large amount of CO_2 into the atmosphere. Many solutions exist to limit our CO_2 emissions:

- the decarbonation of our way of life implying a decrease in the use of fossil fuels
- the capture and sequestration of CO_2 in geological faults
- the use of CO_2 in chemical or technological application.

This last option not only allows us to reduce our CO_2 emissions by reusing it afterwards, but also offers the potential to replace fossil fuel sources, which are now in the majority in our energy production. Nowadays, the utilization of CO_2 for the global production of chemicals ranges only 170 Mt/y worldwide and is dominated by the synthesis of urea (140 Mt/y).[3] Among these chemicals, cyclic carbonates offer many advantages as they are widely used in the manufacture of industrial products such as solvents, paint-strippers, lithium batteries, and biodegradable packaging.[4] Their typical industrial synthesis involves the reaction of glycols

with phosgene, leading to the generation of environmentally harmful chlorinated wastes. However, a greener pathway involving the use of CO_2 as C1 building blocks still exists, requiring cycloaddition reaction of CO_2 onto epoxides.[5] CO_2 being a very stable molecule, drastic reaction conditions alongside with a catalyst are required to obtain high yields of carbonate products. Nowadays, BASF and Chimei-Asahi are currently synthesising ethylene cyclic carbonate using CO_2 with the presence of quaternary ammonium salts (such as Et_4NBr).[6] The process is carried out at high temperature (120-160°C) and CO_2 pressure (30-80 bar) and the development of new processes to lower these reaction conditions is currently an important area of research.[7–9]

Furthermore, epoxides used as starting materials for the cycloaddition reaction can be obtained at laboratory or industrial scale either from chlorohydrin process (nearly 50% of the industrial production of propylene oxide) or by the transfer of an oxygen atom from an oxidant to the corresponding alkene. The most common oxidants are peracids, but catalytic systems involving NaOCl[10], iodobenzene PhIO[11] or organic hydroperoxide such as *tert*-butyl-hydroperoxide (TBHP) are also used.[12] The common drawback of all of these oxidants is that they afford stoichiometric amounts of non-valuable by-products. In this context, there is a constant search for catalytic processes using dioxygen or hydrogen peroxide, i.e. “green” reagents that could substitute technologies based on conventional oxidants. They offer the advantages of having a high atomic efficiency (50% for O_2 and 47% for H_2O_2) and releasing water as only side-product.[13] Industrial production of epoxide using O_2 actually exist only in the case of propylene oxide in the presence of a silver-based catalyst.[14] In the case of longer alkyl chains, the activation of the kinetically stable O_2 molecule implies the use of electron donors. One example of such approach is the so-called Mukaiyama epoxidation reaction that can be considered as a promising way of utilising O_2 in mild conditions.[15]

As a logical development, it would then be possible to synthesize styrene carbonate from styrene in mild conditions by coupling two steps in only one vessel: a first step leading to the epoxide synthesis in the presence of a green oxidant, followed by a cycloaddition reaction in the presence of CO_2 (see **Figure 2**). However, setting up a two-step global reaction is not simple and raises many challenges:

- the implementation of reactions operating under similar solvent, temperature, and pressure conditions,

- the presence of one or more catalysts that can work for one or both reaction steps,
- simultaneous or delayed addition of compounds can also greatly influence the overall catalytic activity.

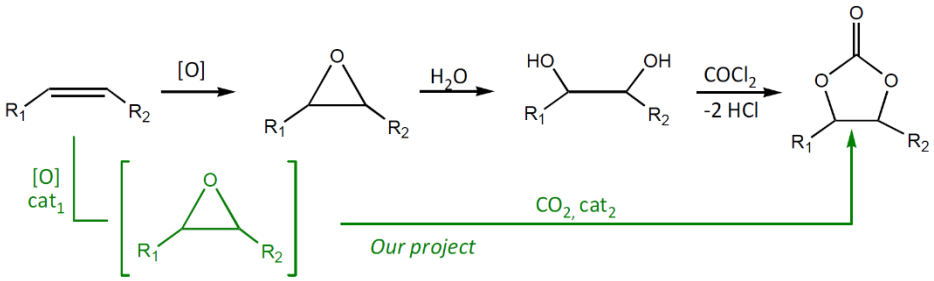

Figure 2: *One pot green process for the synthesis of cyclic carbonates from olefins*

In summary, the objective of this thesis (OxCyCat_CO_2, ANR-17-CE06-0009) is to develop an efficient catalytic system, allowing the synthesis of cyclic carbonates from alkenes under operating conditions common to both reactions. A second equally important objective will also consist in proposing the immobilisation through covalent grafting of these catalysts on a mesoporous silica support, in order to improve their recyclability.

Consequently, the strategy adopted in this manuscript is based on the synthesis of a material bearing several active catalytic phases, at least one for epoxidation and one for cycloaddition. The present manuscript is thus divided as follows:

First, a bibliography section develops a state of the art of oxidation reactions performed in the presence of O_2 and H_2O_2 (**Chapter I**), as well as of the cycloaddition of CO_2 onto epoxides (**Chapter II**). Finally, an updated review of the existing catalytic systems proposed for the transformation of styrene into styrene carbonate in the presence of CO_2 will be proposed in **Chapter III**. The aim of the latter is to identify the advantages and drawbacks of the common reaction conditions and catalysts that have already been used for the whole transformation.

Secondly, our experimental results will be presented in the following **Chapter IV to Chapter VIII** as follows :

- Optimisation of the cycloaddition reaction alone will be studied in **Chapter IV**, including the synthesis of the co-catalysts and their grafting on silica.

- Grafting of quaternary ammonium salts onto silica will be presented in **Chapter V** and the catalytic activity of the resulting materials reported for the cycloaddition of CO_2 onto styrene oxide in the absence of any co-catalyst.
- Oxidation step to convert styrene into styrene oxide using either O_2 in the Mukaiyama reaction or H_2O_2 will be investigated in homogeneous conditions in **Chapter VI.**

Finally, the global reaction running either with O_2/CO_2 or H_2O_2/CO_2 and the adequate catalysts in homogeneous conditions will be presented in **Chapter VII**. At the end, an exploratory study dealing with silica supports bearing active catalytic functions with potentialities for the epoxidation and cycloaddition reactions will be carried out in **Chapter VIII**.

After the general conclusion, the manuscript ends with an appendix section where the description of the equipment and conditions is provided.

References:

[1] D. Roberts, R. Pidcock, Y. Chen, S. Connors, M. Tignor, IPCC Report 2019: Global warming of 1.5°C, *IPCC.*, (**2019**)

[2] C.P. Morice, J.J. Kennedy, N. A. Rayner, P.D. Jones, Our world in data, temperature anomaly : https://ourworldindata.org/grapher/temperature-anomaly, (**2019**)

[3] A. Rafiee, K. Rajab Khalilpour, D. Milani, M. Panahi, Trends in CO_2 conversion and utilization: A review from process systems perspective, *J. Environ. Chem. Eng.*, (**2018**), 6, 5771–5794.

[4] M. Cokoja, M.E. Wilhelm, M.H. Anthofer, W.A. Herrmann, F.E. Kühn, Synthesis of Cyclic Carbonates from Epoxides and Carbon Dioxide by Using Organocatalysts, *ChemSusChem*., (**2015**), 8, 2436–2454.

[5] M. Aresta, A. Dibenedetto, A. Angelini, The changing paradigm in CO_2 utilization, *J. CO_2 Util.*, (**2013**), 3–4, 65–73.

[6] E.A. Quadrelli, G. Centi, J.L. Duplan, S. Perathoner, Carbon dioxide recycling: Emerging large-scale technologies with industrial potential, *ChemSusChem*., (**2011**), 4, 1194–1215.

[7] F. Lagarde, H. Srour, N. Berthet, N. Oueslati, B. Bousquet, A. Nunes, A. Martinez, V. Dufaud, Investigating the role of SBA-15 silica on the activity of quaternary ammonium halides in the coupling of epoxides and CO_2, *J. CO_2 Util.*, (**2019**), 34, 34–39.

[8] C. Kohrt, T. Werner, Recyclable Bifunctional Polystyrene and Silica Gel-Supported Organocatalyst for the Coupling of CO_2 with Epoxides, *ChemSusChem*., (**2015**), 8, 2031–2034.

[9] B. Motos-Pérez, J. Roeser, A. Thomas, P. Hesemann, Imidazolium-functionalized SBA-15 type silica: Efficient organocatalysts for Henry and cycloaddition reactions, *Appl. Organomet. Chem.*, (**2013**), 27, 290–299.

[10] B. Meunier, E. Guilmet, M.E. De Carvalho, R. Poilblanc, Sodium hypochlorite: a convenient oxygen source for olefin epoxidation catalyzed by (porphyrinato)manganese complexes, *J. Am. Chem. Soc.*, (**1984**), 106, 6668–6676.

[11] Y. Yang, F. Diederich, J.S. Valentine, Lewis acidic catalysts for olefin epoxidation by iodosylbenzene, *J. Am. Chem. Soc.*, (**1991**), 113, 7195–7205.

[12] M. Moghadam, V. Mirkhani, S. Tangestaninejad, I. Mohammadpoor-Baltork, M.M. Javadi, Molybdenum Schiff base-polyoxometalate hybrid compound: A heterogeneous catalyst for alkene epoxidation with tert-BuOOH, *Polyhedron*., (**2010**), 29, 648–654.

[13] R.A. Sheldon, E factors, green chemistry and catalysis: An odyssey, *Chem. Commun.*, (**2008**), 3352–3365.

[14] J. Tsuji, J. Yamamoth, M. Ishino, N. Oku, Development of New Propylene Oxide Process, (**2006**), 1–8. http://www.sumitomo-chem.co.jp/english/rd/report/theses/docs/20060100_ely.pdf.

[15] T. Yamada, T. Takai, O. Rhode, T. Mukaiyama, Direct Epoxidation of Olefins Catalyzed by Nickel(II) Complexes with Molecular Oxygen and Aldehydes, *Bull. Chem. Soc. Jpn.*, (**1991**), 64, 2109–2117.

PART I : BIBLIOGRAPHY SECTION

CHAPTER I

TOWARDS THE SYNTHESIS OF EPOXIDES USING GREEN OXIDANTS

I.1 Introduction

High attention in organic synthesis has been paid to epoxides, as they exhibit a versatile reactivity (see **Figure 3**). These strained three-membered heterocycles can be opened by a number of different nucleophilic species with high control over stereo- and regioselectivity.[1], thus leading to the formation of multiple 1,2-difunctionalized products.

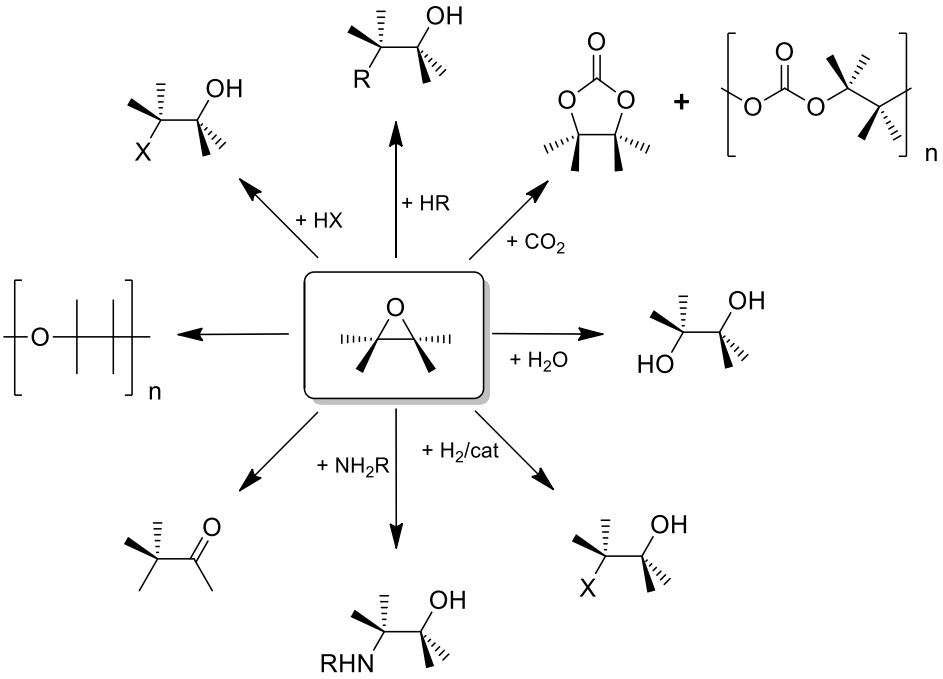

Figure 3: *Representative overview of epoxides reactions*

The most used method to prepare epoxides is the direct oxidation of olefins, by reaction with a peracid (Prilezhaev epoxidation reaction (see **Figure 4.c**)). Various other oxidants, such as alkyl hydroperoxides or hydrogen peroxide (see **Figure 4.a)**) are also used but via a metal catalysed reaction.[2,3] Otherwise, epoxides, especially propene oxide (30 million tons in 2016[4]) and epichlorohydrin[5–7], are also prepared in two steps by ring closing of halohydrins induced by a base, halohydrin being initially produced by reaction of hypochlorous acid with an olefin (**Figure 4.b**). However, sodium chloride waste is formed in molar equivalent quantities with a potential impact on the environment.[8]

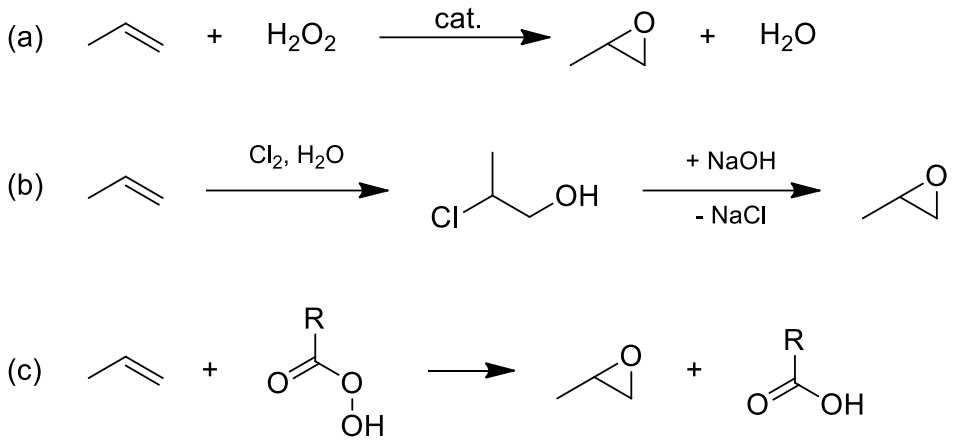

Figure 4: *General methods of preparation of epoxides*

Regarding other pathways, other parameters can be considered. Epoxidation reactions with peracids (*e.g. m*-chloro perbenzoic acid (*m*-CPBA) and peracetic acid) and hydroperoxides (*e.g. tert*-butyl hydroperoxide) show a poor atom economy since the delivery of the oxygen atom occurs at the expense of the production of by-products with relatively high molecular weight (*e.g. m*-chloro benzoic acid, acetic acid, *tert*-butanol). Oxygen atom availabilities in various oxidants used in the laboratory or at industrial scale for different kind of reactions are presented in **Table** 1. The more economic, the higher the % active oxygen will be. In addition, epoxide selectivity remains a critical aspect due to the rich reactivity of these molecules with strong oxidants and acidic conditions. Despite all these limiting aspects, Prilezhaev epoxidation reaction is still widely used in organic synthesis (**Figure 4**.**c**).[9]

Table 1: *Common oxidants ordered by active oxygen content*

Oxidant	**Active oxygen content (wt.%)**	**Waste product**
O_2	100.0	Nothing or H_2O
O_2/sacrificial reductant	50.0	Oxidized form of the sacrificial reductant
H_2O_2	47.0	H_2O
HNO_3	25.0	NO_x
NaOCl	21.6	NaCl
t-BuOOH	21.1	CH_3COOH
m-CPBA	9.3	$mClC_6H_4COOH$
$NaIO_4$	7.5	$NaIO_3$
PhIO	7.3	PhI

Only one epoxide, ethylene oxide, which is actually economically the most important epoxide due to its applications as fumigant, to make antifreeze, ethylene glycol and other

useful compounds.[10], is made by reaction of O_2 with the corresponding alkene, *i.e.* ethylene over a silver catalyst.[11] Other industrially important epoxides are :

- epichlorohydrin, made by a high-temperature chlorination of propylene and which is mainly used for the production of glycerol, unmodified epoxy resin and elastomers [12],
- styrene oxide[13], prepared either via the chlorohydrin route or catalytically with hydrogen peroxide and which is used industrially as reactive diluent for epoxy resins [9],
- α-pinene oxide, synthesized industrially from α-pinene oxidation by a percarboxylic acid [14]and which is a key intermediate in the synthesis of flavours, fragrances and therapeutics agents[15].

O_2 or H_2O_2 are particularly attractive for their high atom economy, lack of toxicity and low cost.[16–19] It should also be noted that water is the only by-product generated from these reagents. Thus, O_2 or H_2O_2, provided that catalysts are used, have the potential to be developed into large-scale green processes. Earth abundant metal-based catalysts such as those involving Co, Mn, Fe, Cu and Ni seem to be the most promising and interesting because of availability and toxicity consideration. Hydrogen peroxide is one of the best terminal oxidants in terms of environmental and economic considerations, but H_2O_2 must be produced from O_2 and H_2 by the anthraquinone route. However, such a process, which is at the origin of about 95% of the world's H_2O_2 production, is handicapped by its economy, which depends heavily on effective recycling of extraction solvents, hydrogenation catalyst and expensive quinone.[20] The tars produced by the *in-situ* oxidation of quinone during H_2O_2 production render the epoxidation process by H_2O_2 less environmentally friendly as expected in the end.[21] This explains why a lot of research is being carried out on an alternative way of producing H_2O_2.[22]

In mild oxidation processes such as epoxidation, only one oxygen atom of molecular oxygen is used (50% atom efficiency, [23]) which is a little bit more than with H_2O_2. However, most of the oxidation strategy for selective oxidation with O_2 often require reducing agents to capture the extra oxygen atom during the reaction. Moreover, aerobic oxidation is often difficult to control and a commonly used scheme is to work at low conversion in order to avoid

over-oxidation. Furthermore, in certain circumstances, O_2 /organic mixtures have to be handled with caution due to some spontaneously ignition risks.

According to these statements the following chapter focuses on epoxidation methods which uses H_2O_2 and O_2 as oxidants and their respective catalysts. A first part will focus on the H_2O_2 oxidation process, developing the different catalysts and processes used and the most recent works developed in the last 4 years in the epoxidation of styrene and limonene. A second part will be directed toward the aerobic epoxidation of styrene. Distinction will be made between systems operating in the presence or absence of a co-substrate.

Different alkenes will be considered in this review since the performances of a catalyst may vary from one substrate to another one. Indeed, terminal aliphatic alkenes (*e.g*. 1-octene) are notoriously more challenging than alkenes conjugated with aromatics (*e.g.* styrene) or endocyclic olefins (*e.g*. cyclooctene or cyclohexene). It has also to be noted that some epoxides such as aromatic epoxides (e.g. styrene oxide) are highly sensitive to acidic conditions, as they tend to isomerize to carbonyl compound by the Meinwald rearrangement.[24]

I.2 Epoxidation with H_2O_2

The literature in the field of epoxidation with H_2O_2 is extensive.[16,25–27] In this section, we will look at catalytic reactions involving metal complexes. We will not discuss reactions carried out in basic medium on functionalized olefins ("hydroperoxide anion mechanism", **Table 2**), nor organocatalyzed reactions. **Table 2** specifies the main mechanisms encountered. In those involving hydroperoxo complexes with metals (M-OOH) at their highest oxidation state, the O-O bond is weakened by the metal which facilitates the transfer either of the oxygen atom directly connected to the metal ("Lewis acid mechanism" which also works with hydroperoxides), or of the most distant one ("hydroperoxy mechanism"). Peroxo complexes are also able to transfer one of the two oxygen atoms. Note that with incompletely oxidized metals, such as Fe(III) or Mn(III), the hydroperoxo complex initially formed by interaction with H_2O_2 can also transfer one of the two oxygen atoms, but this evolution is rather rare. It is the result of a very specific choice of ligands. More often, these hydroperoxo

complexes are only intermediates. They can lead to i) either to hydroxyl radicals ("Homolytic breakdown mechanism") not very susceptible to give epoxidation reactions but rather access to allylic oxidation products, or ii) to biomimetic metaloxo species ("Metal-oxo mechanism") capable of transferring the oxygen atom in oxidation state -II to the alkene. The purpose of this part is first to review the main catalysts used over the years making a distinction between three kinds of catalysts precursors, i.e. “heterogeneous catalysts”, “soluble metal oxides”, and “soluble coordination complexes”. Then, we propose to have a closer look at papers published since 2018.

I.2.1 Heterogeneous systems

Epoxidation of olefins with hydrogen peroxide can be performed with the assistance of various heterogeneous catalysts that mainly include Ti or Al that will be discussed in a first part. [28] These catalysts are able to perform oxidation reaction through the hydroperoxy mechanism (see **Table 2**). In the case of Ti, most of them are crystalline microporous zeolites (especially, TS-1), ordered mesoporous Ti-Si mixed oxides, or supported Ti-on-silica species. In the case of Al, most common solid catalysts consist on hydrotalcite components. species are the most common catalysts. Other strategy to obtain heterogeneous processes consist on grafting homogeneous catalysts onto the surface of solid support. A short presentation of soluble catalysts covalently bonded onto inorganic supports will be presented in a second part.

Table 2: *Classification of the mechanisms encountered for H_2O_2 epoxidation*

Name	Mechanism	Metal centers	Comments
Lewis acid mechanism	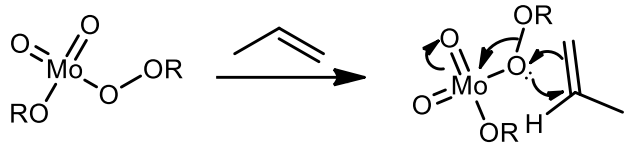	Mostly early transition metals (e.g., Mo, V, Re)	Concerted step leaving the oxidation state of the metal unchanged
Hydroperoxy mechanism	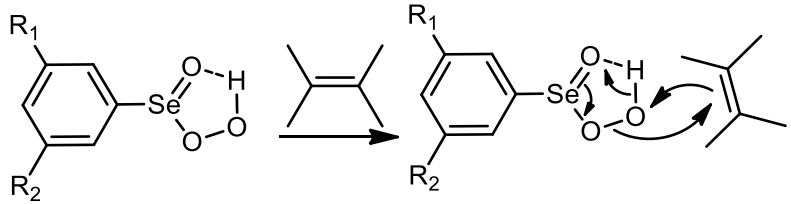	Main group Se, B, As, Al and C	Oxygen atom transferred is the distal one
Peroxy mechanism	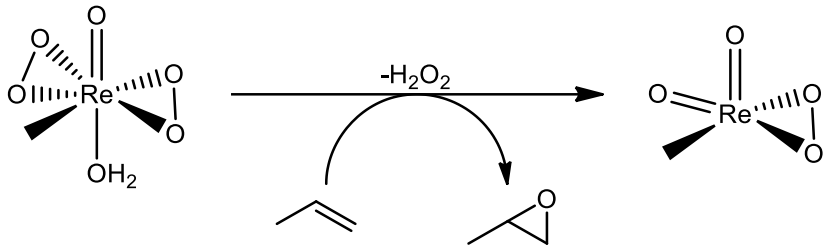	Early transition Ti, V, Nb, Ta, Cr, Mo, W and Re	Oxygen atom transferred is the proximal one (directly link to the metal)
Hydroperoxide anion mechanism	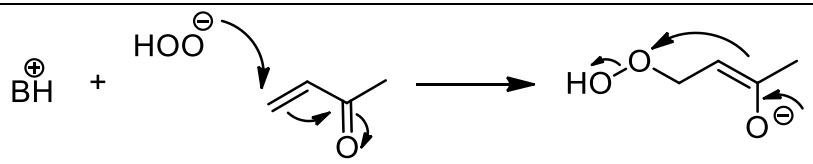	Cu, Mg-Al mixed oxides	Nucleophilic anion able to epoxidize electron-poor alkenes.
Metal-oxo mechanism	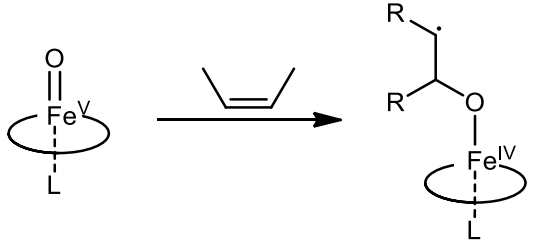	Late transition metal such as Mn, Fe and Ru	Mechanism involves the formation of a radical intermediate with salens and porphyrins

I.2.1.1 Catalysis by silica-based materials or alumina itself

Otherwise "truly" heterogeneous catalysts for epoxidation of olefins with H_2O_2 are typically mineral-type catalysts based on solids such as zeolites[29–31], boehmite[32–34] or hydrotalcite[35–37]. Titanium is probably the most used metal[27] since the discovery of titanium-silicalite-1 (TS-1).[38]. This zeolite, containing four-coordinated Ti centers in a microporous siliceous framework, catalyses the epoxidation of linear small-sized alkenes, such as propene or allyl chloride in methanol under mild condition, affording good turnovers with more than 90% epoxide selectivity. Some of the key for its success are probably (1) its hydrophobic pores that prevent the massive presence of water and favours the olefins adsorption, and (2) the good dispersion of Ti in tetrahedral coordination. As a consequence, TS-1 is the only catalyst successfully applied in the industry to produce propylene oxide with aqueous H_2O_2.[27] However, due to its small-sized circular pores, with dimension of 5.3x5.6 Å, access to its active sites is only restricted to linear alkenes. Other zeolites with larger pores have been since developed to address this selectivity issue. For instance, Ti-MWW, a zeolite with large 10-membered rings, allows formation of cyclo C_6-C_8 epoxides in 80-85% yield.[39,40] However, such system tend to operate at slightly higher temperature (e.g., 60-70°C), which may lead to decomposition of sensitive products. As seen in **Table 2**, Ti(IV) based materials always involve a peroxy mechanism based on an oxidation catalysis carried out with Lewis acid materials such as Al(III) or W(VI). In the case of Ti, interaction between Ti(IV) and H_2O_2 is the key to allow the epoxidation reaction. Coordination between electronic deficient Ti(IV) and HOO^- is able to promotes the necessary breaking of the O-O bond.

More recently, aluminium oxyhydroxide, also known as boehmite [γ-AlO(OH)], has also been reported to behave as an active heterogeneous catalyst in the epoxidation of alkenes with H_2O_2.[34,41] Hence, Al_2O_3 was successfully utilised by Schul'pin and co-workers for the epoxidation of limonene into high-value products at moderate temperature. With a particular set of parameters (molar H_2O_2/limonene = 2.4 and 0.08 g of Al_2O_3 for 2,5 mmol of limonene) 1,2-epoxylimonene was obtained with 63% yield and 90% selectivity after 10h reaction. By increasing the amount of catalyst and oxidant per limonene equivalent, a remarkable 99% yield of diepoxy limonene was obtained. X-ray diffraction analysis confirmed the presence of boehmite containing Al-OOH fragments which play the role of active species. At least 5 runs

were conducted with no noticeable loss of conversion. Earlier, Rebek and McCready also proposed that Al-OOH species [42] can be formed by the interaction of H_2O_2 with basic alumina affording the epoxidation of different unfunctionalized olefins but with moderate yields.

It is also noteworthy that hydrotalcites are able to promote the epoxidation of a large scope of substrates by H_2O_2 but nitriles[36] or amides[37] have to be introduced in stoichiometric amount (or more) with the oxidant. Indeed, such basic solids, allow the *in-situ* formation of peroxycarboxylic acids[43]. Hydrotalcites, hence, behave as substitutes to bicarbonate in excess in Payne epoxidation[44] but with the advantage of being recycled.

I.2.1.2 "Homogeneous catalysts" attached to solid supports

A convenient general approach to get efficient heterogeneous catalysts may be to anchor performant homogeneous catalysts onto solid supports. Different strategies regarding epoxidation catalysts were detailed by K. Burgess and co-workers [19,25,26,45]. Main strategies for immobilization of metallic homogeneous catalysts are 1) their covalent binding/coordination onto modified inorganic mesoporous materials such as silica[25], zeolite or other metal oxides[46], 2) the encapsulation of inorganic complexes within cavities in modified silica or zeolites[47] or 3) the ion-exchange to bind ionic catalysts[48]. Supports with three-dimensional open pore network structures, porosity and high surface area are privileged for an optimized diffusion.[49]

However, as a general trend, supported homogeneous catalysts tend to have reduced catalytic activity compared to their homogeneous analogues[50]. Such drawback often compensates with the easily recovery of the catalyst and reduction of the contamination of the products by traces of metal provided that leaching is avoided.

I.2.2 Catalysis with soluble metal oxides

Alkylhydroperoxo complexes issued from the interaction of transition metals with alkylhydroperoxides (such as *tert*-butyl hydroperoxide) have been widely described and their activity in olefin epoxidation tested. On the contrary, equivalent complexes obtained with hydrogen peroxide were less successful due to their instability towards H_2O_2 and/or H_2O.[51] An exception is that of soluble metal oxides, [18,25,26,51] such as polyoxometalates (POM)

and methyltrioxorhenium (MTO), since these complexes, without organic ligands, are expected to be much more resistant to self-oxidation than conventional complexes.

I.2.2.1 Polyoxometalates

Polyoxometalates (POM) are anionic clusters composed by early transition metals in their highest oxidation state (W (VI), Mo(V), Mo(VI), V(IV) and V(V), *etc*) and connected by oxo ligands.[52] They were first reported in 1826 by Berzelius who described the behaviour of transition metal in aqueous solution and the formation of polyanions, as exemplified in **Equation 1** and **Equation 2**.[53]

$$8H^+ + 7[WO_4]^{2-} \longrightarrow [W_7O_{24}]^{6-} + 4H_2O \qquad \textit{Equation 1}$$

$$23H^+ + [HPO_4]^{2-} + 12[MoO_4]^{2-} \rightarrow [PMo_{12}O_{40}]^{3-} + 12H_2O \qquad \textit{Equation 2}$$

POMs can be prepared starting from d^0 metal oxides such as WO_3, MoO_3 and V_2O_5. The latter "dissolve" at high pH value affording the corresponding orthometalates (WO_4^{2-}, MoO_4^{2-}, VO_4^{3-}, respectively). As the pH is lowered, these orthometalates protonate to give oxide-hydroxide compounds such as $W(OH)O_3^-$ and $Mo(OH)O_3^{2-}$ that are able to condensate via olation and oxolation processes, leading to the formation of M-O-M or M-(OH)M linkages with H_2O release.[54],[55] Metal-oxo and metal-hydroxo polymers are then generated in solution until the electrostatic repulsion developed in edge-sharing polyhedral is too strong.

Isopolyanions are one of the two main types of POMs and are represented by the formula $[M_mO_y]^{n-}$, where M is the addendum (usually molybdenum or tungsten, less frequently niobium, vanadium or tantalum).[56]. On the other hand, heteropolyanions are formed by the incorporation of other anions (referred to the heteroatoms, hence the terminology) and are represented by the general formula $[X_xM_mO_y]^{n-}$ ($x \leq m$). A large variety of elements from the periodic table can be classified as heteroatom, most commons are As^{5+}, P^{5+}, Ge^{4+}, Si^{4+} and B^{3+}.[57]

The most well-known and studied structure is the so-called Keggin structure with the general formula $[X^{n+}M_{12}O_{40}]^{(8-n)-}$. These highly stable and easily synthesized compounds are generally formed with P^{5+} or Si^{4+} heteroatom X and Mo^{6+} and W^{6+} as addenda M atoms. In 1933, Keggin solved the structure of $H_3[PW_{12}O_{40}]$ by powder X-ray diffraction from the

association of 12 edge and corner-sharing MO_6 octahedra surrounding the central XO_4 tetrahedron.[58]

Applications of POMs to catalysis is stimulated by their properties, such as high thermal stability, tuneable redox and acidity properties, sensitivity to light and inherent resistance to oxidative decomposition allowing them to be involved in a large scope of oxidation reactions [59],[60–62].

In 1983, Venturello and co-workers reported that a Keggin type phosphotungstate was able to catalyse the epoxidation of a series of diversified olefins by H_2O_2 with selectivity of ca. 95% and products yields in the range of 85-95% at 70°C.[63] However, it was later demonstrated by several groups, that the true catalytically active species is the peroxo complex reported in **Figure 5**.[64]

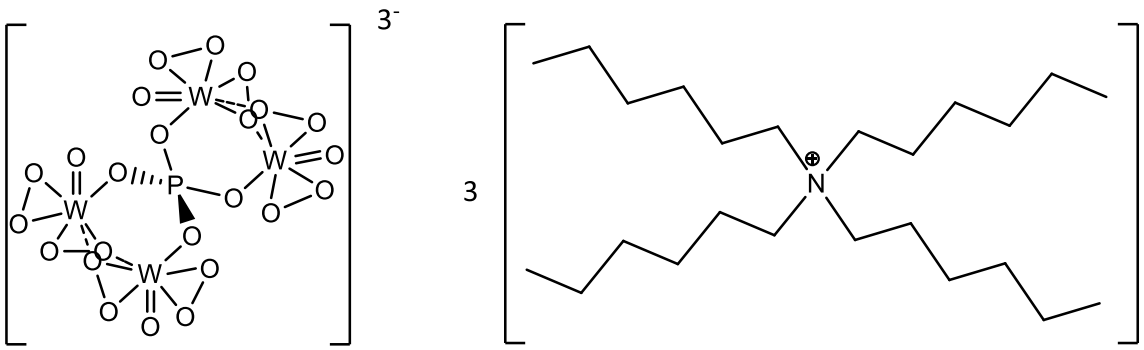

Figure 5: *Ishii-Venturello catalyst derived from the Keggin type phosphotungstate*

This salt showed favourable characteristics such as stability to oxidation, solubility in both water and organic solvent, effectiveness as phase transfer catalyst (due to the counter-cation), ease of synthesis and good thermal stability. Since, this catalyst has found industrial application in the epoxidation of olefins and in their oxidative cleavage to carboxylic acids.

Recently, Villanneau *et al* obtained an almost complete conversion of cyclooctene into cyclooctene oxide by H_2O_2 in acetonitrile after 6h at room temperature using as catalyst, B,α-$[AsW_9O_{33}\{P(O)CH_2CH_2CO_2H\}_2]^{5-}$, an hybrid trivacant-type Keggin bearing two phosphonopropionic groups (see **Figure 6**).[65] B,α-$[AsW_9O_{33}\{P(O)CH_2CH_2CO_2H\}_2]^{5-}$ could be also immobilized, through an amide linkage, onto mesoporous silica functionalized by aminopropyl groups without losing any catalytic activity.[66–68]

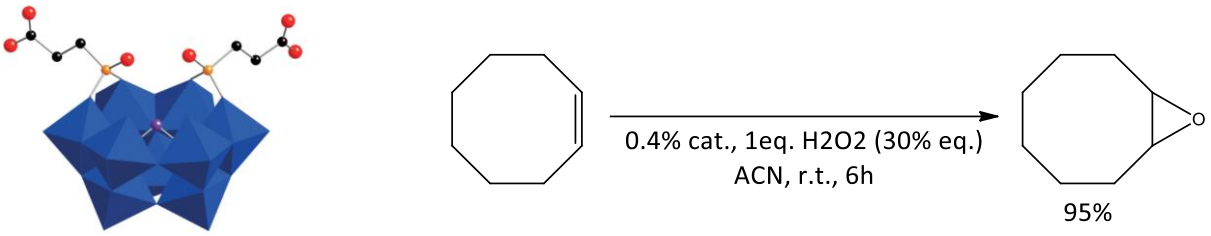

Figure 6: Structural representation of B,α-[$AsW_9O_{33}\{P(O)CH_2CH_2CO_2H\}_2]^{5-}$ (counter-cations are omitted for sake of clarity) and catalysis results obtained with cyclooctene

Catalytic oxidation of bio-sourced molecules contained in essential oils of citrus has also been investigated. Indeed, unsaturated terpenic hydrocarbons such as limonene are a starting point for various oxygenated compounds used in fine chemistry industry and whose sustainable production is of major concern. However, limonene oxidation is a particularly versatile reaction, as various products can be obtained (see **Figure 7**).

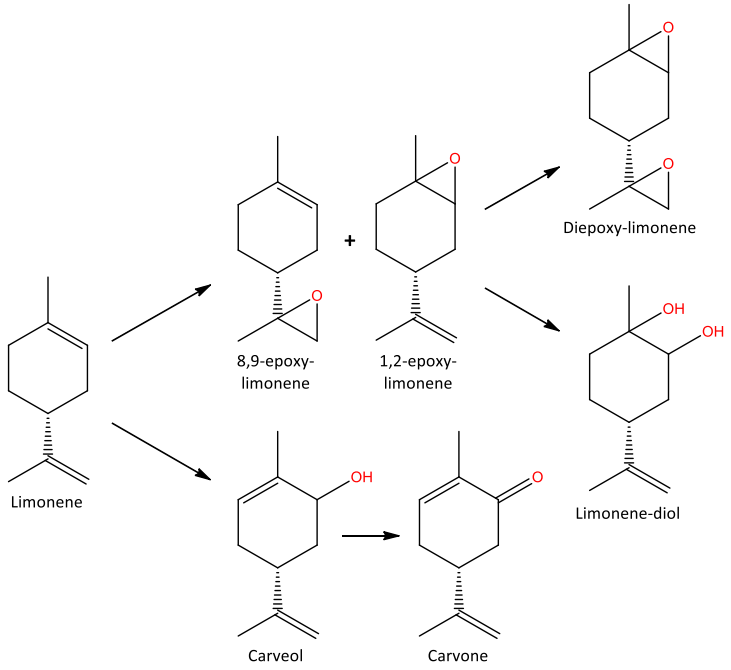

Figure 7: *Typical reaction scheme for the epoxidation of limonene and its most frequent oxidized forms with hydrogen peroxide (H_2O_2)*

In this regard, W-based POMs seem to be in the front line.[69,70] Hence, Villanneau and co-worker were able to get significant amounts of 1,2-limonene oxide with a total yield of 84% of both diastereomers after 24h reaction at room temperature with 100% conversion of limonene.

I.2.2.2 Methyltrioxorhenium

Since the discovery of methyltrioxorhenium ($MeReO_3$ or MTO) by Hermann and co-workers, epoxidation of a variety of olefins was conducted at room temperature or below using 0.1-1 mol% of this catalyst in THF or *tert*-butyl alcohol with anhydrous H_2O_2.[71] As seen in

Figure 8, Re oxidation state in MTO remains at +VII throughout the whole reaction. Like Ti(IV), W(VI) before, Re(VII) does not undergo redox chemistry but it activates H_2O_2 through the equilibrium formation of two η^2-peroxo species **1** and **2**.[72]

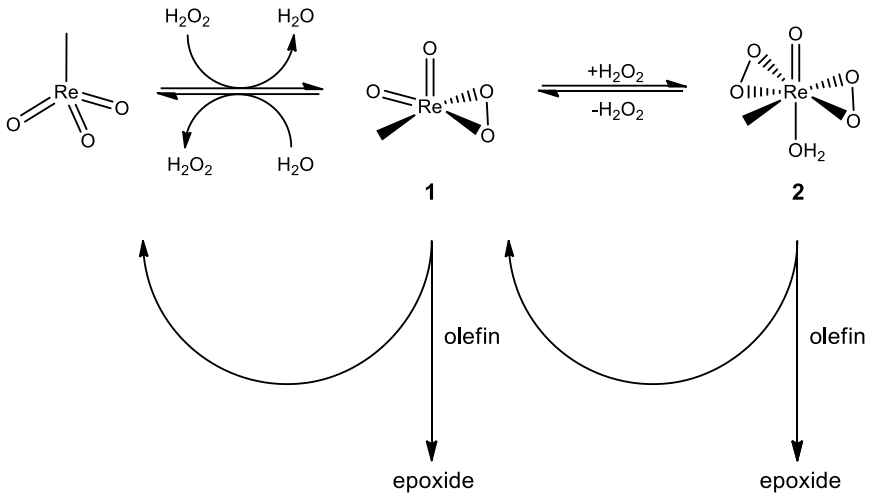

Figure 8: *Catalytic cycles for MTO assisted-epoxidation by H_2O_2*

The main drawback in MTO assisted epoxidations by H_2O_2 is related to the inherent acidity of the reaction medium that causes the ring opening of sensitive epoxides to diols. None of the modifications and optimisations added to the MTO epoxidation system were able to avoid such drawback until Sharpless and co-workers tested the use of pyridine.[73] Pyridine has two important effects. First, it makes the environment slightly basic avoiding unwanted ring opening event and, second, it accelerates the rate of the reaction. Following the same strategy, use of aprotic media like nitromethane or CH_2Cl_2 allows a biphasic system, allowing a better separation of water from the organic phase where the epoxidation takes place. Opening of the epoxide formed can then be avoided, which improves the overall selectivity of the desired product. However, it seems that the pK_a of the amine is determining since the more basic ones are able to deactivate MTO. Best nitrogen donors are resistant to oxidation themselves, and not too basic to avoid MTO decomposition into inert perrhenic acid and methanol.[74]-[75] However this complex suffers from its cost and the use of aprotic media

like nitromethane or chlorinated solvent, which makes it incompatible for large-scale reaction due to toxicity issues and risk of explosion. Nevertheless, MTO remains an attractive option for small-scale epoxidation of different alkenes with aliphatic and aromatic substituents.[19]

I.2.3 Coordination complexes

Coordination complexes play a major role in the green epoxidation catalysis. Major metal centres found in most recent literature are Iron(III) and Manganese(III) and will be especially emphasizes in the following parts. A particular attention will be paid to their organic ligand, including porphyrins, Schiff-base ligands salen, TACN (Triazacyclononane) and amine pyridyls complexes. Historical state-of-art will be presented as well as a few examples of the most recent processes found in literature.

I.2.3.1 Iron and Manganese porphyrins complexes

Porphyrins are naturally occurring macrocyclic ligands playing a key role in some life processes like oxidation with molecular dioxygen via Cytochrome P450 enzymes.[76] With the progress done in synthetic chemistry and the known ability of porphyrins to tune the metal reactivity and afford very stable complexes, metalloporphyrins have naturally emerged as an important class of biomimetic or bioinspired catalysts for controlled oxidation with different oxygen donors (see **Figure 9).** Iron and Manganese porphyrins are the most efficient for epoxidation reactions. Other metalloporphyrins such as those containing molybdenum give lower conversions and selectivity.[77]

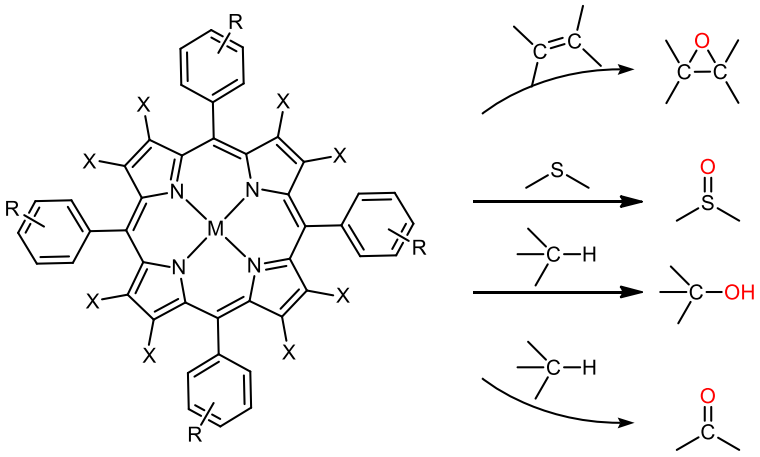

Figure 9: *Some important transformations catalysed by porphyrins*

Iron porphyrins are able to catalyse both the epoxidation of olefins and the hydroxylation of hydrocarbons by various oxidants among which H_2O_2.[78] In the proposed mechanisms, hydrogen peroxide is first activated through its coordination with iron. This coordination allows the transfer of an oxygen atom to the olefin (monooxygenase activity) but iron porphyrins may also cause the decomposition of hydrogen peroxide to water and oxygen (catalase activity).[79] That is the reason why reports on efficient epoxidation with H_2O_2 are rather limited. The activity and selectivity of such iron-based-catalysts is strongly affected by the nature of the porphyrin ligand, the substrate concentration and the solvent composition.[80,81] Other oxidants such as iodosylbenzene are preferred.[82].

Manganese porphyrins tend to be more active regarding the conversions and selectivities obtained. Mn-porphyrin complexes and their effectiveness for olefin epoxidation with H_2O_2 were first discovered by Mansuy and co-workers.[83] Chlorinated porphyrin ligands were proposed to resist side-oxidation of the catalyst. However, addition of imidazole or a combination of imidazole and carboxylic acids was required to improve the reactivity, with a 91% yield of cyclooctene in only 15 min in the presence of carboxylic acid. Experiment was conducted with a cyclooctene : H_2O_2 : Mn(TDCPP)CI : cocatalyst molar ratio = 700 : 20 : 1 : 10, at room temperature during 2h.

I.2.3.2 Manganese Salen/Salophen complexes

Salen and salophen are two classes of ligands that are Schiff bases prepared via the condensation of two salicylaldehyde molecules or their substituted derivatives with aliphatic and aromatic diamines, respectively.[84]. Salen ligands are easily synthesized and are able to form stable complexes with a wide variety of metal ions.[85] Most popular salen is the one obtained from 3,5-*di*-*tert*-butyl-salicylaldehyde and chiral cyclohexane-1,2-diamine (**Figure 10).** Manganese complexe of this ligand was first reported as asymmetric epoxidation catalyst (Jacobsen's catalyst) by Jacobsen and Katsuki in 1990. It has since been recognized as one of the most efficient and practical catalyst for the asymmetric epoxidation of non-functionalized olefins.[86]

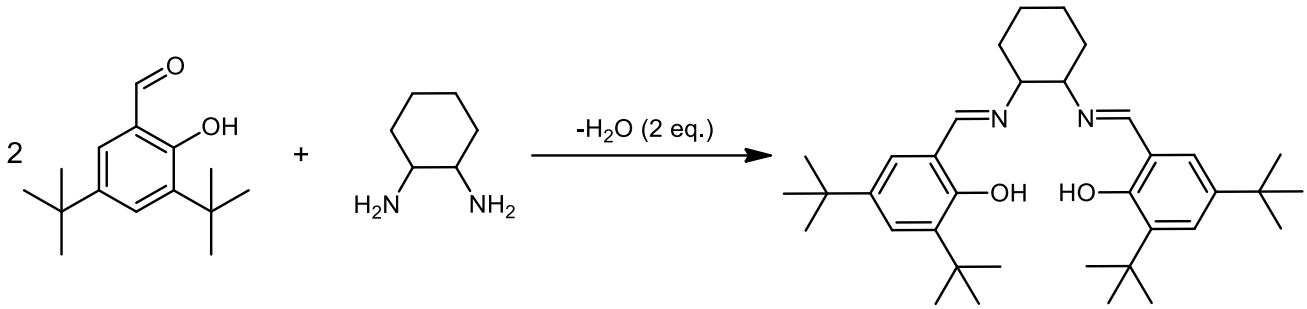

***Figure 10**: Synthesis of N,N'-bis(3,5-di-tert-butylsalicylidene)-1,2-cyclohexanediamine salen ligand*

Primary oxidants used for the epoxidation of various olefins were iodosylbenzene, sodium hypochlorite and *m*-CPBA. Surprisingly, there has been little consideration on the use of H_2O_2 as oxidant with manganese salen complexes since its first utilization by Berkessel.[87] As mentioned in **Table 2**, the mechanistic scheme commonly proposed consists of a two-step catalytic cycle. In a first step, an intermediate Mn^{V}-oxo complex is generated, which in a second step carries the activated oxygen to the olefinic double bond.[88] Actually, most Mn coordination complexes require additives such as imidazole, pyridines or tertiary amine N-oxides to generate the requisite Mn-oxo intermediates via heterolytic cleavage of H_2O_2.[89]

Recently, Toscano and co-workers carried out enantioselective epoxidation of various alkenes using H_2O_2, chiral Mn^{III} salen catalyst in water and diethyltetradecylamine to get corresponding epoxide with enantiomeric excess values up to 95%.[90]

I.2.3.3 Iron and Manganese TACN complexes

Manganese complexes which ligands are derived from facially coordinating 1,4,7-triaza-cyclononane (TACN) system were first published in the 1990s.[91] Metal based TACN catalysts have been found to efficiently epoxidize olefins in the presence of acid additives (typically oxalic, but also ascorbic and squaric acid) and H_2O_2. Efficiency was also improved by using oxalate buffer.[92] However, reactions performing without additive usually require huge excess of hydrogen peroxide for efficient epoxidation.[19] Depending on the additive used, reactivities and selectivities change in unpredictable ways.

In recent years, both Watkinson[93] and Yin and co-workers[93] developed a catalytic system combining trimethyl Mn-TACN as main catalyst with $Sc(OTf)_3$ as a co-catalyst. Indeed, Fukuzumi, Nam and co-workers showed earlier that the addition of Lewis acids (LA) would increase the oxygen atom transfer effectiveness in mechanisms involving high valent metal-oxo species.[94] Hence, Yin and co-workers obtained excellent conversion of epoxides starting

from various olefins (e.g., from 93 to 100%, **Figure 11**) at 0°C after 2h reaction.[95] An optimal Mn_2^{IV}: Sc^{3+} molar ratio of 1 : 2 was required to obtain high yields of epoxides. As explained by the authors, higher molar ratio of 1 : 4 would lead to a decrease in conversion of olefin. In the case of Watkinson and co-workers, a molar ratio of 1 : 0.5 was enough to obtain 91% yield of styrene oxide at room temperature after 3 minutes.[96]

To conclude, TACN are ligands that afford very reactive complexes, but they are more difficult to functionalize than salen. Alternative ligands easier to synthesize that provide a similar coordination environment (e.g., polyamine coordination groups) are therefore promising and will be discussed in the next part.

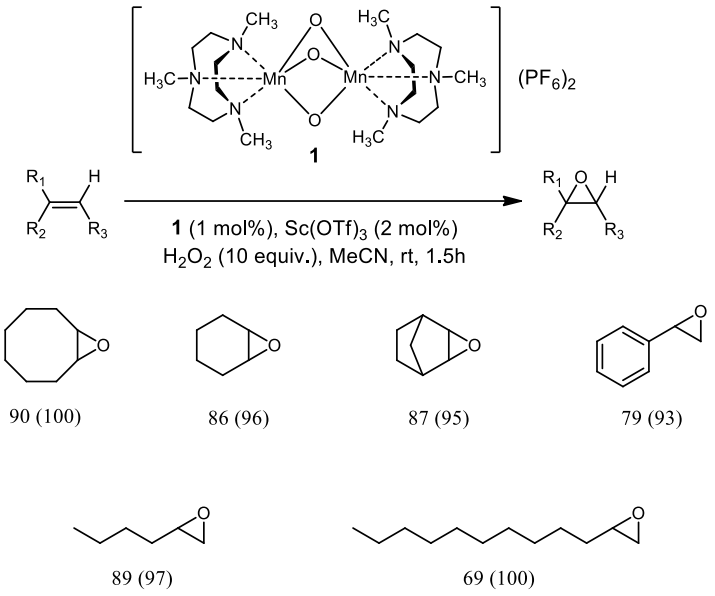

Figure 11: *Epoxidation results based on a Mn-TMTACN : $Sc(OTf)_3$ catalytic system and respective yields (conversion %) obtained from various epoxides*

I.2.3.4 Iron and Manganese pyridyl-amine complexes

Ligands containing pyridine and amine coordinating groups have been investigated by Que and co-workers in their search for oxidation catalysts used as biomimetic models of non-heme monooxygenases enzymes.[97] Most of these catalytically active models are octahedral iron(II) complexes with tetradentate N-donor ligands (primarily consisting of amines, pyridines and pyrrolidines) and two labile triflate or acetonitrile ligands.[98] Que and co-workers suggested that Fe^{III}-OOH hydroperoxo intermediates are produced upon reaction. Through either homolytic or heterolytic O-O cleavage, Fe^{III}-OOH would afford iron(IV) or iron(V) oxo

species that are potential catalytically active species in olefins epoxidation. It is also noteworthy that $HO^{\cdot}$ radicals, which are not synonymous of selective processes, are co-produced in the case of homolytic cleavage. The formation of diols that are usually considered as epoxide co-products issued from the subsequent hydrolysis processes could also be explained by the direct interaction of alkenes with *cis*-$HOFe^{V}$=O oxo species.[99] In different studies, the activity of these model catalysts was improved significantly by using additives such as Lewis acids (e.g., $Sc(OTf)_3$ as mentioned previously) or non-coordinating (e.g. perchloric acid)[100] and coordinating (e.g., acetic acid)[101] Brønsted acids. Acetic acid considerably increases the selectivity towards epoxides as the result of the suppression of the competing coordination of water, that affords diol through the participation of *cis*-$HOFe^{V}$=O species.[101]

Another limitation observed is the catalyst deactivation upon the oxidative degradation of the organic ligands.[102] Various pathways have been described such as the oxidation of alkyl and aryl C-H bonds [103] and/or the oxidative N-dealkylation of amine-based ligands.[104] Different strategies have been applied in order to reduce the catalyst decomposition, such as the slow addition of H_2O_2, the addition of acetic acid, or the modifications of the ligands by increasing the bulkiness of the pyridine fragments.[105]

In a rather recent work, from Gebbink *et al* reported the development of an iron-N_2Py_2 (bis-alkylamine-bis-pyridine ligand) able to successfully achieve epoxidation of various olefins such as cyclooctene with 80% yield of corresponding oxide.[106] The reaction occurs in short amount of time (30 min) at 0°C in the presence of non-aqueous H_2O_2 and acetic acid. Authors showed also that the lifetime of their catalyst could be increased by adding deuterated sites on the N_2Py_2 ligand.

Examples of efficient Manganese epoxidation catalysts with pyridyl-amine ligands have also been reported. Hence, Sun and co-workers obtained pretty high yields of various epoxides (up to 95%) in the presence of aminopyridine complexes derived from L-proline with H_2O_2.[107] The reaction occurred under 30 min at -30°C in the presence of 2,2-dimethylbutanoic acid, used as an additive.

I.2.4 Most recent works published since 2018

The literature in this area is extensive and difficult to segregate into categories. As an attempt to classify the latest results regarding this field, recent results shall be presented according to the catalysts precursors: “Heterogeneous complexes”, “soluble metal oxides”, and “homogeneous coordination complexes”. The most recent studies involving H_2O_2 have been gathered in **Table 4** for styrene oxide product, showing the catalyst category, the solvent used, the reaction conditions (temperature and reaction time), the catalyst loading and the resulting yield of styrene oxide. A colour classification has been proposed in *Table 3* in order to expose the best parameters and yields obtained: the greener the best. Therefore, a system allowing 95% yield of styrene oxide at room temperature with a catalyst loading of 0.1% will be part of the top tier catalytic systems

Table 3: *Colour classification proposed to classify the catalytic systems*

Parameters	++++	+++	++	+	-
Yield (%)	90-100	80-90	70-80	60-70	<60
Molar cat. loading (%)	<0.2%	0.2-0.25%	0.25-0.4%	0.4-1%	>1%
Temperature	<30 °C	30-50 °C	50-60 °C	60-80 °C	> 80 °C

First catalytic processes displayed are part of the heterogeneous class, including supported homogeneous catalysts (**Table 4 entries 1-8**), nanoparticles (**Table 4 entries 9-10**) , and other functionalized inorganic materials (**Table 4 entries 11-15**). Most recent works report Schiff base complexes supported on inorganic supports such as silica SiO_2, Graphene Oxide or polymer resin. Experiments were conducted in ACN solvent in most cases (**Table 4 entries 4-8**) with metal concentration as low as 50 ppm (**entry 2**), able to obtain styrene oxide with high yield of 90% minimum. It is noteworthy that some processes are efficient at room temperature (**entries 3, 5-6**) with low reaction time (minimum 3h). Best systems reported with heterogeneous catalyst were developed by Dasgupta and co-workers involving a copper(II) Schiff base supported on magnetic nanoparticle Fe_3O_4.[108] High yield of styrene oxide of 96% was obtained after 3h reaction at room temperature. Catalyst was used in very low molar ratio of only 50 ppm. It is remarkable that the reaction was conducted in H_2O medium with equivalent molar ratio of H_2O_2 and styrene. Catalyst was reused up to 6 times without loss of reactivity or leaching phenomenon.

The next catalytic systems belong to the metal oxides class (**Table 4 entries 16-25**), including peroxomolybdates (**entries 16-19**) or polyoxometalates species (**entries 20-21**). As

seen in previous processes, most of the system evolve in ACN solvent, at mild temperature of 60°C with molar H_2O_2:styrene ratio of 2 to 5. Remarkable yields of styrene oxide were generally obtained in a lesser time compared to supported homogeneous catalyst (time reaction from 0.75 to 6h.) Best system so far was developed by Kurup and co-workers, involving a dioxidomolybdenum(VI) complex chelated with N^4-(3-methoxyphenyl) thiosemicarbazone.[109] High yield of styrene oxide of 97% was obtained in 4h at 60°C with very low concentration of catalyst (200 ppm). Styrene oxide was obtained via a peroxy mechanism (**Table 2**) as detailed by the authors. As a down-side, utilization of co-catalyst $NaHCO_3$ leading to the active specie $[Mo(VI)O(O_2)]^{2+}$ was needed to obtain high yield of corresponding product.

Homogeneous complexes catalysts are then presented in the last part of **Table 2 entries 24-31**. Recent processes involve the use of manganese centre inside either TACN ligands (**entries 24-25**) or Schiff base (**entries 26**). Like the previous heterogeneous and metal oxides catalysts described, they are able to perform well in ACN in most cases with high yields of styrene oxide from 60 to 93%, at temperature close to 0°C or below. However, a large scale of these systems tends to have higher concentration of catalyst : styrene molar ratio (close to 1%). Best catalyst so far was developed by Watkinson *et al.* with the utilization of Mn-TACN associated to $Sc(OTf)_3$ as a co-catalyst.[96] Such system was already presented in previous TACN part and is closely related to the one presented in **Figure 11**. High yields (92-99%) were obtained for substituted styrene oxides after only 3 min at room temperature in ACN.

I.2.5 Conclusion

Catalytic processes involved in the green epoxidation reaction of alkenes using H_2O_2 have been displayed in this part. Most general group of catalysts have been classified and a non-extensive review of systems developed in recent years has been presented. Improvements have been made over the years to afford high yield of corresponding epoxide with low temperature and reaction time conditions. Systems requiring low molar ratio and no additive needed are preferable, but it is noteworthy that the best methods always depend on the desired substrate and the reaction scale. To our sight, it is clear that the best systems shall display good catalytic activity, low metal toxicity and the ability of the catalyst to be supported on solid support.

Table 4: Most recent studies involving the catalytic epoxidation of styrene in the presence of green oxidant hydrogen peroxide H_2O_2.

Entry	Catalyst category	Catalyst subcategory	Catalyst	Solvent	Condition[a]	cat : alkene : H_2O_2[b]	Yld [c] (%)	Ref.
1	Heterogeneous	SHC[d]	[V] Schiff base@GO	$Et_2(OH)_2$	90°C / 3h	- : 1 : 1	99	[110]
2	Heterogeneous	SHC	[Ta] complex@resin	-	80°C / 6h	1 : 2 000 : 4 000	99	[111]
3	Heterogeneous	SHC	[Co] Schiff base@Fe_3O_4	H_2O	r.t. / 3h	1 : 1 700 : 1 700	96	[108]
4	Heterogeneous	SHC	[Co] Schiff base@Al_2O_3	ACN[e]	50°C / 5h	- : 1 : 1,4	93	[112]
5	Heterogeneous	SHC	MIL-101-guanidine-Fe	ACN	r.t. / 8h	- : 1 : 2	81	[113]
6	Heterogeneous	SHC	Mn Salen-DIC@MCM-41	ACN	r.t. / 8h	1 : 30 : 100	45	[114]
7	Heterogeneous	SHC	[Cu] Schiff base@GO	ACN	75°C / 5h	-	44	[115]
8	Heterogeneous	SHC	$[Te_2W_{20}O_{70}\{Re(CO)_3\}_2]^{12-}$	ACN	75°C / 3h	1 : 200 : 600	20	[116]
9	Heterogeneous	CNP[f]	5%Au/CeO_2-nancubes	-	80°C / 18h	-	86	[117]
10	Heterogeneous	CNP	$NiCo_2O_4$	ACN	70°C / 10h	- : 1 : 3	52	[118]
11	Heterogeneous	Boehmite and silica	Mn-Silicalite-1	DMF	r.t. / 4h	-	92	[119]
12	Heterogeneous	Boehmite and silica	V-Silicalite-1	ACN	85°C / 4h	-	17	[120]
13	Heterogeneous	Other supports	Pyr-Mn_2	t-BuOH/Me_2CO	30°C / 2h	1 : 17 000 : 160 000	91	[121]
14	Heterogeneous	Other supports	AuNPs@GO	ACN	60°C / 5h	- : 1 : 3	90	[122]
15	Heterogeneous	Other supports	$\{2(Him).[Cu(pdc)2]\}_n$	EtOH	60°C / 8h	- : 1 : 1,5	78	[123]
16	Metal Oxides	Peroxomolybdates	$[\{MoO_2(H_2O)\}_3ptk(bhz)_3]$	ACN	60°C / 2h	- : 1 : 2	98	[124]
17	Metal Oxides	Peroxomolybdates	MoO_2LD	ACN	60°C / 4h	1 : 5 000 : 20 000	97	[109]
18	Metal Oxides	Peroxomolybdates	$[Mo(VI)O_2L_6(DMSO)]$	ACN	60°C / 4h	1 : 280 000 : -	96	[125]
19	Metal Oxides	Peroxomolybdates	[Mo] Schiff base	DCEt[g]	r.t. / 45 min	- : 1 : 3	22	[126]
20	Metal Oxides	Polyoxometalates	$\{Mo_{72}Fe_{30}\}$-type Keplerate	EtOH	78°C / 3,5h	1 : 500 : 1500	76	[127]
21	Metal Oxides	Polyoxometalates	$[As_6W_{58}O_{206}]^{38-}$	BuOH	65°C / 4h	1 : 2 000 : 6 000	46	[128]
22	Metal Oxides	Other	$(NH_4)_3[FeMo_6O_{18}(OH)_6]$	ACN	50°C / 6h	1 : 1 000 : 1 500	85	[129]
23	Metal Oxides	Other	[TBA][$NbO(OH)_2$(LA)]	ACN	30°C / 4h	1 : 60 : 60	68	[130]

24	Complexes	TACN[(h)]	[Mn]TMTACN	ACN	r.t. / 3 min	1 : 100 : 300	92	[96]
25	Complexes	TACN	Mn-Me_3tacn	ACN	0°C / 2h	1 : 100 : 300	74	[95]
26	Complexes	Pyridyl-Amine	[Mn] Schiff base	ACN	-30°C / 30 min	1 : 500 : 2 000	41	[107]
27	Complexes	Other	[VO_2(dar-inh)]	ACN	80°C / 6h	- : 1 : 3	93	[131]
28	Complexes	Other	enzyme [Fe]	ACN	r.t. / 30 min	1 : 20 : 40	88	[132]
29	Complexes	Other	[VO_2L]	ACN	70°C / 5h	1 : 75 : 150	78	[133]
30	Complexes	Other	[Ru(pydic)(hcptpyDP)]	DCM/MeOH	r.t. / 2,5h	1 : 200 : 400 (UHP)	60	[134]
31	Complexes	Other	[Cu_2(oxalate)]	ACN	50°C / 3h	- : 1 : 2	60	[135]

(a) r.t. stands for room temperature, (b) molar ratios, (c) Yield of styrene oxide, (d) SHC: Supported Homogeneous Catalyst, (e) ACN: Acetonitrile, (f) CNP: Crystalized Nanoparticles, (g) DCEt : dichloroethane, (h) TACN: 1,4,7-triazacyclononane

I.3 Epoxidation reaction using green oxidant O_2

The use of O_2 in synthetic epoxidation reactions is an important challenge since only one epoxide, ethylene oxide, is produced at industrial scale with this oxidant. Indeed, for kinetic reasons, molecular oxygen is insufficiently reactive under relatively mild conditions.[37] This is explained by the triplet ground state of molecular oxygen (presence of 2 unpaired electrons) since, according to Wigner rule[136], reactions occurring between triplet molecules and singlet molecules such as alkenes (with paired electrons) are kinetically unfavourable. Therefore, one should use an appropriate activation mechanism, compatible with the reactants. Different approaches can be implemented for the activation of O_2 and alkenes such as the use of heat, catalysis, electrocatalysis or photocatalysis. Only then the high-energy spin forbidden pathways can be bypassed, for example, by a more efficient free radical mechanism in which *in-situ* formed peroxyl radicals act as the active oxidant instead of O_2. This poses serious difficulties as unwanted oxidation side-reaction are more likely to happen, leading to the formation of mixtures of by-products that lower the yield of epoxide yield. Other strategies rely on the use of co-substrate able to give away 2 electrons to the system. The following part will be organized according to systems able to perform with or without these co-substrates.

I.3.1 O_2 with sacrificial reagent

Use of co-substrates that act as $2e^-$ reducing agents in mild conditions can be a good strategy for synthetic organic chemistry. Indeed, Nature provides many examples of enzyme assisted oxidation reactions using O_2 that are of great inspiration for chemists. In monooxygenases, the cleavage of the O=O bond and the transfer of one of the two oxygen atoms of O_2 to the substrate systematically goes through a reduction of the two oxygen atoms to their -I oxidation state with the assistance of catalysts and external electron sources such as NADH, or NADPH. By analogy, chemists have used numerous sacrificial reagents such as inorganic compounds (Zn, BH_4^-, H_2…)[137–139] or organic molecules (alcohol, aldehydes…)[140,141] or the assistance of electrodes. Several metal complexes catalyse the aerobic epoxidation of olefins in the presence of aldehydes (as seen in **Figure 12**). This process in known as the Mukaiyama epoxidation reaction.[142] Original Mukaiyama-type catalytic systems based on the use of O_2 and an aldehyde offered interesting applications, for example,

in the regioselective epoxidation of steroids.[143] First studies reported involved nickel-β-diketonate metal complexes, showing efficient alkene conversion and selectivity toward the epoxide.[144] It was shown that catalytic activity is strongly sensitive to the nature of the aldehyde, which is converted to the corresponding carboxylic acid (best known were isobutyraldehyde IBA and pivalaldehyde PA). Indeed, aldehydes containing a secondary or tertiary carbon next to the carbonyl moiety provide the best results.

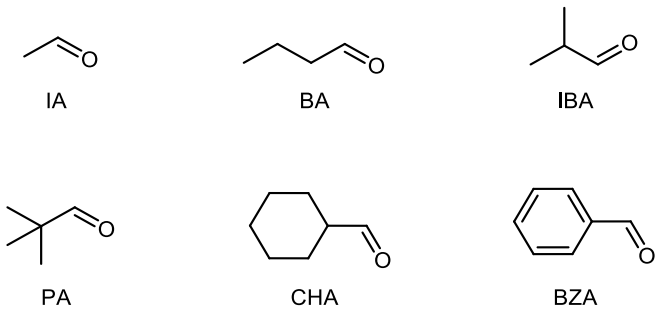

Figure 12: *Structures of some aldehydes used as additives in epoxidations with O_2*

The mechanism of Mukaiyama reaction has long been investigated. It is nowadays agreed that it remains dependent on specific reaction conditions and catalysts. As seen in Figure 13**,** an acylperoxy radical **(a)** is most likely formed by the autoxidation of the aldehyde.

- In one pathway (I, in **red**), **(a)** would be later involved in a radical chain, where the metal's role appears first to be the initiator, affording the corresponding percarboxylic acid **(b)** that needs further activation through its coordination to M^{n+} **(c)**. Subsequent heterolytic cleavage of the O-O bond in the resulting acylperoxy complexe **(c)** would afford a metaloxo species ($M^{(n+2)+}$=O), that would be the real reagent for oxygen transfer onto the alkene substrate ("metal-oxo mechanism" in **Table 2**).
- In the second pathway (II, in **blue**), **(a)** would directly interact with M^{n+} affording another acylperoxy complexe **(d)** with a higher metal oxidation state than **(c)** that would be able to transfer an oxygen atom to the alkene substrate ("Lewis acid mechanism" in **Table 2**) but a non-metal assisted epoxidation by **(a)** cannot be totally excluded in some cases.

Mukaiyama reactions are operationally simple, and work with several metal catalysts. As concerns metals, manganese(III), cobalt(II), iron(III) or iron(II), and copper(II) complexes have been widely used (see recent developments based on Fe-porphyrins [146] and Co-Schiff base

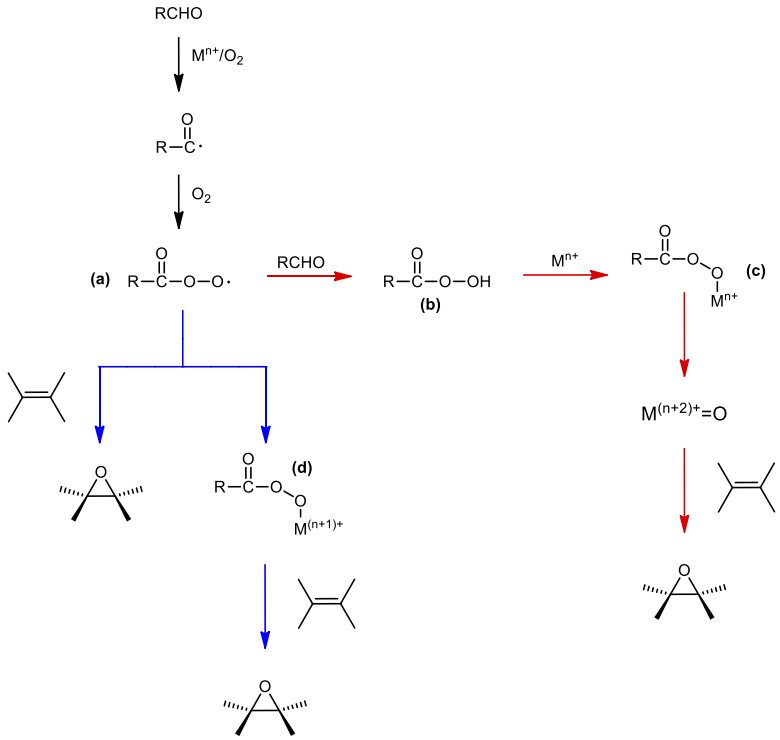

Figure 13: *Proposed mechanisms for the "acylperoxy and peroxy carboxylic" metal-assisted epoxidation of olefins with O_2* [145]

based catalysts.[51]) However, these reactions have the drawback that the corresponding oxidized co-substrate (carboxylic acid here) is produced in stoichiometric amounts. In this mater, a promising Mukaiyama reaction would be one catalytic system generating high-value carboxylic acids with the expected epoxide product.

Manganese turns out to be the metal of choice for the development of aerobic epoxidation of olefins with Mukaiyama type systems. As early as in 1991, chiral manganese(III) salen complexes have been proposed by Mukaiyama and co-workers as catalysts for the epoxidation of conjugated olefins using molecular dioxygen.[147] The system involved catalyst **1a (Figure 14)** as main catalyst working with O_2 and pivalaldehyde. According to the authors, the chiral manganese(III) salen complexes coupled with O_2 and an aldehyde[143] (typically pivalaldehyde in 3-fold excess) work like monooxygenase enzymes, following pathway **b (Figure 13)** [148].

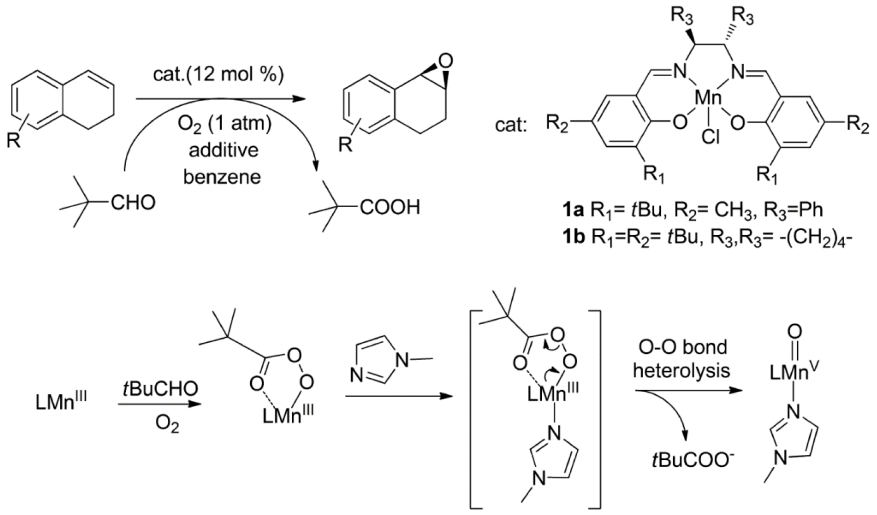

Figure 14: *Mukaiyama catalyst system for the green epoxidation of olefin using O_2 as oxidant and proposed mechanism*

The impact of nitrogen bases such as imidazole was also investigated with O_2. Moderately high yields (from 40 to 60%) were obtained, with the best results in the presence of alkyl imidazole additives. Actually, results were related to the length of the alkyl chains in the following order: CH_3 < *n*-C_2H_5 < *n*-C_8H_{17}.

Other reductants were used instead aldehydes avoiding the formation of carboxylic acids in the reaction mixture. Hence, in 1996, Nolte and Gosling reported a dual catalytic system for olefin epoxidation involving both Mn(III)TPPCl and [Rh(III)bipyCp*]Cl complexes as well as sodium formate[149]. Making the hypothesis that Mn(III) needs to be reduced to Mn(II) in order to interact with O_2 like Fe(III) in Cytochrome P450 enzymes, the authors introduced the Rh(I) form of [Rh(III)bipyCp*]Cl, also in catalytic amount, that can be made in-situ using formate as reductant (see **Figure 15**). Such reaction has the disadvantage of producing CO_2 in stoichiometric quantity but in the frame of the carboxylation of alkenes with O_2 and CO_2 (present experimental study), such approach for the aerobic oxidation of olefins could be suitable.

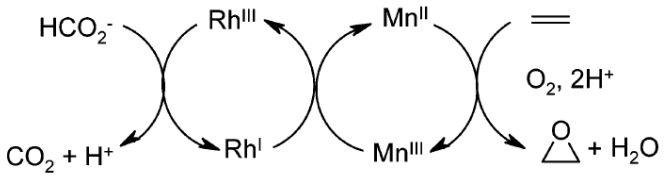

Figure 15: *Proposed mechanism of the dual catalytic epoxidation system involving Mn and Rh in the presence of formiate.*

Lots of manganese salen complexes, including chiral ones, have been tested for the aerobic epoxidation in the presence of sacrificial reductants. Several alkenes were investigated, including styrene, a compound well known for its difficulty of epoxidation.

- Moderate to good yields were obtained for example with manganese salen complexes **I** and **II** (see **Table 5 entries 1-3, 6 and 7**) using PA (Pivalaldehyde) as co-reductant. The reaction was conducted in fluorobenzene (fluorous solvents have a high affinity with O_2) in the presence of N-methylimidazole (NMI) acting as an axial ligand.

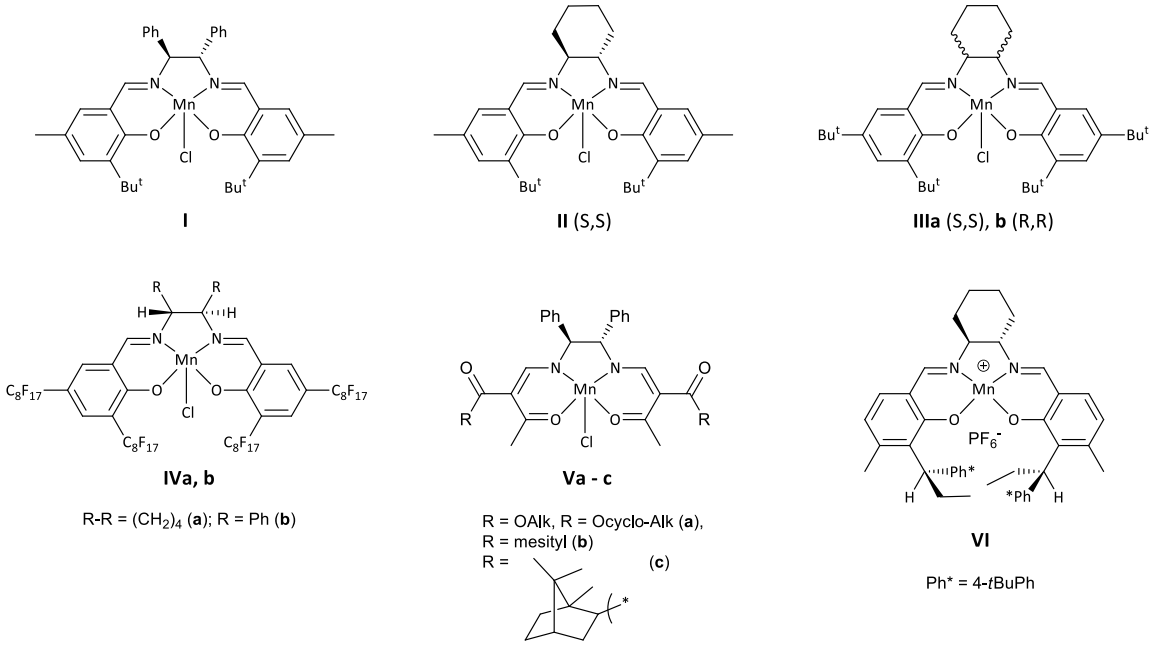

Figure 16: *Manganese complexes used in aerobic epoxidation ion Mukaiyama reactions*

- Lee *et al.* [150] described a co-reductant free system based on complex **III** (also known as Jacobsen catalyst), $CHCl_3$, NaOH and TBABr for the asymmetric epoxidation of alkenes (see **Table 5 entries 4,15-17**). According to the authors, the oxygen capture, in that case, would be related to the *in-situ* generation of $:CCl_2$ carbene species responsible for the production of dichlorocarbonyl peroxide, the actual terminal oxidant. However, low yields of epoxides were obtained and the addition of NMI was necessary, otherwise only dichlorocyclopropanes were found among the reaction products. Other authors such as Woodward *et al.*[151] were able to test a large scope of alkenes such as styrene and chromene using complex **III** in the presence of 2-oxocyclopentanecarboxylates as co-reductants instead of aldehydes. Poor yields of epoxides were obtained with 38% of styrene oxide with moderate selectivity of 47%.

- Variations of the solvents were also reported in some studies. Pozzi and co-workers suggested fluorous biphasic conditions (perfluorohydrocarbons : CH_2Cl_2 = 1:1) for aerobic epoxidations in the presence of manganese complexes **IV** (see **Table 5 entries 10-11**). Such conditions allowed utilization of the catalyst with quantities as low as 1.5 mol%. Authors were able to obtain good yields of epoxides from corresponding alkenes after 5h at 20°C under atmospheric O_2 pressure.

- Mukaiyama *et al.* published a series of papers introducing β-ketoiminato manganese optically active complexes (see **Table 5,** complexes **V** and **VI**) that were tested in reaction conditions analogous to those used in Mukaiyama Mn-salen epoxidation system described here (12% cat. loading, PA, room temperature, 4 h and 1 atm O_2).[152] Catalysts **V** present moderate to good yields of epoxides (from 52 to 70%).

The above survey of the literature shows that manganese salen complexes are interesting epoxidation catalysts that can be used with a large scope of alkenes. They are easy to synthesize, and their substituents can be tuned to optimize their catalytic performances. The reaction not only requires a co-reductant (aldehydes, or the solvent itself in the case of $CHCl_3$) but also an imidazole ligand. Even though the reaction occurs in the absence of aldehydes in some case, the resulting conversion remains pretty low (see **Table 5 entries 4, 15-17**).

Table 5: *Epoxidation reactions of conjugated olefins with O_2 in the presence of manganese salen complexes[17,153]*

Entry	Substrate	Catalyst	Sacrificial reductant	Additive	Yield (%)	t (h)	T (°C)	ref.
1	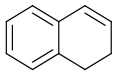	**I**	PA	-	42	12	r.t.	[143]
2		**I**	PA	N-Me-Imd	62	12	r.t.	[143]
3		**II**	PA	N-Me-Imd	62	12	r.t.	[143]
4		**III**	$CHCl_3$	Imd	12	12	r.t.	[154]
5		**Vc**	$CHCl_3$	Imd	70	12	r.t.	[154]
6	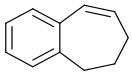	**I**	PA	N-Me-Imd	52	12	r.t.	[143]
7		**II**	PA	N-Me-Imd	52	12	r.t.	[143]
8		**Vb**	PA	-	79	1	r.t.	[152]
9		**Vc**	PA	-	52	1	r.t.	[155]
10	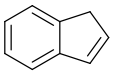	**IVa**	PA	N-Hex-Imd	83	2	20	[156]
11		**IVb**	PA	N-Hex-Imd	77	2	20	[156]
12	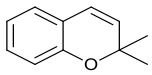	**III**	PA	N-Me-Imd	12	12	r.t.	[143]
13		**III**	PA	N-Bu-Imd	26	12	r.t.	[143]
14		**III**	PA	N-Oct-Imd	37	12	r.t.	[143]
15	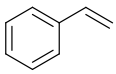	**III**	$CHCl_3$	Imd	19	12	r.t.	[154]
16		**III**	$CHCl_3$	N-Me-Imd	17	12	r.t.	[154]
17		**III**	$CHCl_3$	N-Oct-Imd	10	12	r.t.	[154]
18		**IVa**	PA	N-Hex-Imd	86	5	20	[156]
19		**IVb**	PA	N-Hex-Imd	81	5	20	[156]
20	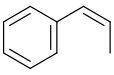	**Vb**	PA	-	28	1	r.t.	[152]
21		**VI**	PA	N-Me-Imd	14	12	r.t.	[154]
22	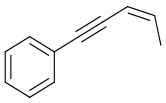	**Va**	PA	-	53	1	r.t.	[157]

PA = pivalaldehyde, N-Me-Imd = N-methylimidazole, N-Bu-Imd = N-n-butylimidazole, N-Hex-Imd = N-n-hexylimidazole, and N-Oct-Imd = N-n-octylimidazole

More recently, Hemmat and co-worker [158] showed that a Salen-Mn complex anchored onto the surface of a magnetic silica nanocomposite (1 : 45 molar eq.) could be efficient at room temperature within 90 min. Numerous epoxides could be prepared, such as styrene oxide obtained with a yield of 100%. Oxygen in the presence of IBA was found to be the most effective compared to other oxidants such as *m*-CPBA, $NaIO_4$ or even H_2O_2. The radical character of the reaction could be emphasized by radical scavenger, i.e. BHT (2,6-*tert*-butyl-4-methylphenol).

However, most of the recent research works seem to focus on porphyrin complexes, as presented in Table 8. Recently, epoxidation of multiple unfunctionalized alkenes has been investigated using manganese porphyrin Mn(TPP) (5,10,15,20-tetraphenylporphyrinato

complex), in the presence of molecular dioxygen and isobutyraldehyde[145]. In that case, the metal complex would be involved in the initiation step allowing the free radical autoxidation of the aldehyde, leading to the active epoxidizing agent.

Last three years, several supported MnTPP complexes were used successfully in the aerobic epoxidation of styrene in the presence of IBA under mild conditions (O_2 atmosphere, balloon or bubbling, and temperature always below 60°C). Catalysts were used in a wide scope of styrene/metal concentration, from 11% in the worst case (**Table 6 entries 13**) to 7 ppm in the last case (**Table 6 entries 12**). Silica, graphene oxide (GO), carbon nanotubes (CNTs) or magnetite (Fe_3O_4) nanoparticles were used as shown in Table 8. In some cases, reactions perform very well at room temperature providing styrene oxide with high yields from 60 to 100% (see **Table 6 entries 1,3,6-8, 12 and 13**). Sacrificial reductor IBA is always added in 3 to 5 molar equivalent vs. the alkene.

Table 6: Most recent studies involving the epoxidation of styrene by O_2 in the presence of Manganese based catalysts

Entry	Catalyst	Aldehyde	Solvent	Conditions[a]	cat : alkene : Ald[b]	Conv. (%)	Yield (%)[c]	Ref
1	Mn-salen@SiO_2	IBA[d]	ACN[e]	25°C / 1,5h	1:45:225	100	100	[158]
2	MnTPP@SiO_2[f]	IBA	ACN	52°C / 6h	? : 1 : 3[j]	100	100	[159]
3	MnTPP@SiO_2	IBA	butyronitrile	25°C / 2h	1 : 10000 : 50000	99	95	[160]
4	MnTPP@GO	IBA	ACN	60°C / 2h	1 :10000 : 25000	100	89	[161]
5	MnTPP@SiO_2	IBA	ACN	45°C / 4h	1 : 9 500 : 24 000	100	86	[162]
6	MnTPP@GO[g]	IBA	Me_2CO	r.t. / 2h	1 : 90 : 450	100	85	[163]
7	MOF-525-Mn	IBA	DCM	r.t. / 2,5h	? : 1 : 5	99	83	[164]
8	MnTPP@SiO_2	IBA	Me_2CO	r.t. / 30 min	1 : 180 : 900	85	82	[165]
9	MnTPP@p(APTMACl) [h]	IBA	ACN	60°C / 7h	1 : 31 200 : 78 000	83	79	[166]
10	Mn(L)(OH)@Fe_3O_4	IBA	ACN	40°C / 8h	1 : 3000 : 7500	100	78	[167]
11	MnTPP@Fe_3O_4	IBA	ACN	r.t. / 8h	1 : 12 000 : 30 000	100	67	[168]
12	MnTPP@Fe_3O_4	IBA	iPrCHO/ACN	25°C / 8h	1 : 142 000 : 350 000	100	63	[169]
13	MnTPP@SiO_2	IBA	ACN	50°C / 1h	1 : 9 : 27	90	62	[170]
14	MnTPP@MWCNTs[i]	IBA	ACN	40°C / 4h	1 : 45 : 135	87	56	[171]

(a) r.t. stands for room temperature, (b) molar ratios, (c) yields are for styrene oxide, (d) IBA: Isobutyraldehyde, (e) ACN: Acetonitrile, (f) TPP: Tetraphenylporphyrine (see Figure 9), (g) GO: Graphene Oxide, (h) APTMA: (3-acrylamidopropyl)trimethylammonium, (i) MWCNTs: multi-walled carbon nanotubes, (j) no information found regarding the catalyst concentration

I.3.2 O_2 without sacrificial reagent

As already stated in the Introduction, the use of a heterogeneous silver catalyst for the synthesis of ethylene oxide from ethylene and O_2 remains the most notable example of aerobic oxidation performed in the absence of a sacrificial reductant. Selective monooxygenation is very difficult to achieve with other heterogeneous metal catalysts, which tend to fully oxidize the organic compound to form water and CO_2 in the temperature conditions used for ethylene in the presence of Ag. However, the extension toward of O_2/Ag to substituted alkenes remains a challenge because alkyl substituents are more prone to oxidation and even combustion. Most of the catalytic systems developed recently involve the use of Co and Au (also known as coinage metals). Cobalt is especially preferred with systems involving the use of DMF solvent and will be developed in a first part. Gold surfaces for more active and selective catalysts are investigated in a second part.

I.3.2.1 Cases without announced sacrificial reductants

Several papers have reported the successful aerobic epoxidation of olefins with cobalt nanocatalysts in DMF without adding any sacrificial reductants (see **Table 7, entries 1-7**). Actually, the use of the amide solvent (DMF, here) is required for catalytic activity. DMF would behave as a ligand for Co atoms at the surface of the nanoparticles. This gives rise to a Co-DMF complex that reacts with dioxygen affording a Co superoxo species able to transfer an oxygen atom to the olefin. Such solvent effect has already been noted on several oxidation reactions. Tang and co-workers suggested that the tetrahedrally coordinated Co^{2+} sites, including DMF as a ligand, play an important role in the activation of dioxygen.

Another explanation would be the role of solvent as a co-reductant. Indeed, a closer look of the product distribution made by Baiker *et al.* revealed an oxidation product of DMF: *N*-formyl-*N*-methyl formamide (FMF).[172] The authors suggested that DMF may be an active component in the oxidative transformation of styrene, with the parallel formation of FMF with the conversion of styrene. As seen in **Figure 17**, the autoxidation of *N,N*- dialkyl-amide resulted in the formation of hydroperoxide, later decomposed into *N*-formyl-amide. Addition of hydroquinone proved a free-radical mechanism. Peroxy-radical may propagate a chain reaction by abstracting hydrogen from a further molecule.[173]

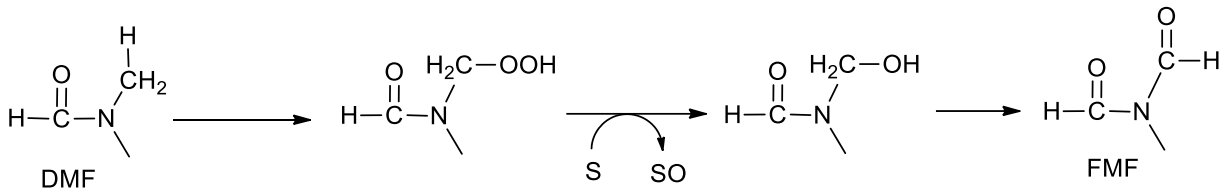

Figure 17: *Autoxidation of DMF via the thermal oxidation of DMF and epoxidation of styrene (S) into styrene oxide (SO)*

Many examples in **Table 7 (entries 1-6)** are involving heterogeneous catalysts made by Co doping of oxides or carbons. A general conclusion of these papers was that isolated Co species are more active than aggregates which means that low Co loadings can be used.[174]

I.3.2.2 Au nanoparticles

Nanocrystalline gold catalysts allow the epoxidation of styrene under relatively mild conditions (80°C) providing the epoxide as the major product, with low to good (40-90%) selectivities as seen in **Table 7 (entries 8 and 15-17)**. Due to poor lack of reactivity, a peroxide initiator (TBHP) is often required in these reactions as radical initiators (**Table 7 entries 15 and 16**). Lambert et al have reported that the use of very small gold entities (~1.4 nm) derived from 55-atom gold clusters and supported on inorganic support are efficient and robust catalysts for the selective oxidation of styrene by dioxygen.[175] In these reactions, even though the processes are remarkable because no initiator was used (see **Table 7 entry 17**), epoxide was obtained with a low selectivity (up to 18%) with much more drastic temperature conditions (100°C). It is proposed that O_2 activation at the gold clusters takes place by splitting the O–O bond.[175,176]

Table 7: Most recent studies involving the epoxidation of styrene in the presence of O_2 without adding any sacrificial reagent and with (top) or without (down) DMF.

Entry	Catalyst subcategory	Catalyst	Aldehyde	Solvent	Condition	cat : alkene : Ald[a]	Conv. (%)	Yld (%)[b]	Ref
1	Co NP[c]	**Co**-CeO_2	-	DMF[d]	140°C / 4h	-	100	90	[177]
2	Co NP	**Co**$_3O_4$	-	DMF	130°C / 5h	-	99	89	[178]
3	Co NP	**Co**/SiO_2	-	DMF	100°C / 3h	-	98	92	[179]
4	Co NP	**Co**-CeO_2	TBHP 15%	DMF	140°C / 4h	1 : 420 : 2 000	99	89	[177]
5	Co NP	**Co**/CNTs(in)[e]	-	DMF	100°C / 1h	-	93	86	[180]
6	Co NP	**Co**–SiO_2	-	DMF	80°C / 24h	-	50	45	[181]
7	Co complex	**Co**$(acac)_2$@SiO_2[f]	-	DMF	100°C / 12h	-	74	44	[182]
8	Au NP	**Au**@Pd	LED[g]	DMF	80°C / 10h	1 : 1 400	65	37	[183]
9	Co complex	**Co**-PAA@GO[h]	-	ACN	60°C / 3h	1 : 500 : -	93	90	[184]
10	Co complex	**Co**-schiff base	-	ACN	60°C / 5.5h	-	84	67	[185]
11	Co complex	**Co**Ox/MOR[i]	CHP 10% [j]	-	60°C / 7h	1 : 200 : 2 000	70	64	[186]
12	Co complex	[**Co**$(HL)_2$]NO_3	-	ACN	60°C / 3.5h	1 : 1000 : -	100	46	[187]
13	Co NP	**Co**PMA@UIO-67[k]	t-BuOOH	-	80°C / 6h	- : 1 : 50	80	47	[188]
14	Co NP	**Co**-Al_2O_3	-	dioxane	90°C / 5h	-	76	43	[189]
15	Au NP	**Au**@HTCo/Al[l]	TBHP	-	80°C / 80h	1 : 100 : -	87	38	[190]
16	Au NP	**Au**-HT	TBHP 5%	Toluene	80°C / 24h	1 : 100 : -	42	33	[191]
17	Au NP	**Au**/TiO_2	-	Toluene	100°C / 15h	-	56	10	[176]

(a) molar ratios, (b) yields are for styrene oxide, (c) NP: nanoparticles, (d) DMF: Dimethylformamide, (e) CNTs: Carbon nanotubes, (f) acac: acetylacetonate, (g) LED: Light emitting diode, (h) PAA: polyacrylic acid; GO: Graphene oxide, (i) MOR: mordenite ($Al_2Si_{10}O_{24}{\cdot}7H_2O$), (j) CHP: Cumene hydroperoxide, (k) PMA: Phosphomolybdic acid, (l) HT: Hydrotalcite, (m) BTAM: benzyl trimethylammonium, (n) TPP: Tetraphenylporphyrin.

I.4 Conclusion

Epoxidation methodologies that can be considered satisfactory from a sustainable perspective are currently available for most classes of olefins. H_2O_2 (even if synthesized from H_2 and O_2 by a not so green industrial process) and molecular dioxygen can be reliably and efficiently used as green oxidants with the presence of proper metal-based catalysts. However, important problems remain. First of all, catalytic epoxidations with O_2 usually require the introduction of a cosubstrate. Methods that could use dioxygen alone will represent an extraordinary advance, but major breakthroughs in the discovery of O_2 activation and of the catalysts that engage in these processes are needed. There are now catalysts, like polyoxometalates, that allow their use in an extraordinarily efficient manner, limiting or avoiding disproportionation reactions.

This review highlights main catalysts for the epoxidation reaction in the presence of green oxidants H_2O_2/O_2 such as polyoxometalates, TACN, porphyrins, and Salen ligands. Among these complexes, salen are represented in systems requiring either H_2O_2 or O_2 oxidant. They are simple to synthesize, easily tuneable and presents interesting catalytic properties: high epoxide yields with only little molar ratio below 1%. One of the most well-known salen is the Jacobsen catalyst (Salen-Mn(III)Cl), tested both in homogeneous and heterogeneous conditions. Complexes salen have been grafted at the surface of numerous inorganic materials such as alumina, magnetite, graphene oxide, silica, or polymer resin. Salen-Mn(III)Cl complex have been bonded to silica support SiO_2, which present good thermal resistance and interesting tuneable properties. As seen before, one of the best catalytic system consists on a supported Mn-Salen grafted on SiO_2 silica support, affording 100% yield of styrene oxide after 1.5h at 25°C.

The review encouraged the use of homogeneous and supported Salen-Mn(III)Cl to study the epoxidation of styrene with the aerobic Mukaiyama system oxidant system. In the case of H_2O_2 oxidant, a system involving a Polyoxometalate catalyst either in solution or grafted in silica support will be preferred.

References

[1] U. Sundermeier, C. Doebler, M. Beller, Recent Developments in the Osmium-Catalyzed Dihydroxylation of Olefins, *ChemInform*., (**2005**), 36, 1–20.

[2] S.A. Hauser, M. Cokoja, F.E. Kühn, Epoxidation of olefins with homogeneous catalysts-quo vadis?, *Catal. Sci. Technol.*, (**2013**), 3, 552–561.

[3] K.A. Jørgensen, Transition-Metal-Catalyzed Epoxidations, *Chem. Rev.*, (**1989**), 89, 431–458.

[4] M.& P. Nexant, Market Analytics : Propylene Oxide, **2018**.

[5] T.A. Nijhuis, M. Makkee, J.A. Moulijn, B.M. Weckhuysen, The production of propene oxide: Catalytic processes and recent developments, *Ind. Eng. Chem. Res.*, (**2006**), 45, 3447–3459.

[6] F. Cavani, J.H. Teles, Sustainability in catalytic oxidation: An alternative approach or a structural evolution?, *ChemSusChem*., (**2009**), 2, 508–534.

[7] R.R. and K.T.R. G. Sienel, Ullmann's Encyclopedia of Organic Chemicals, *Wiley-VCH*., (**1999**),.

[8] F. Asinger, the Chlorination of the Olefins, *Mono-Olefins*., (**1968**), 506–627.

[9] G. Sienel, Epoxides, *Ullmann's Encycl. Ind. Chem.*, (**2000**), 13, 139–154.

[10] Wikipedia, Ethylene oxide, (n.d.),. https://en.wikipedia.org/wiki/Ethylene_oxide.

[11] P.A. Kilty, W.M.H. Sachtler, The mecanism of the selective oxidation of ethylene to ethylene oxide, *Catal. Rev. Sci. Eng.*, (**1974**), 10, 37–41.

[12] Jean-marc Brignon, Epichlorhydrine, in: INERIS, Données Tech. Sur Les Subst. Chim. En Fr., **2017**: pp. 1–45.

[13] Dow Chemical, Styrene Oxide, in: Tech. Serv. Dev., Midland Michigan, **1958**.

[14] F.S. H. H¨aberlein, Hoechst, DE-OS 2 835 940, **1978**.

[15] M. Golets, S. Ajaikumar, J.P. Mikkola, Catalytic Upgrading of Extractives to Chemicals: Monoterpenes to "eXICALS," *Chem. Rev.*, (**2015**), 115, 3141–3169.

[16] C. Wang, H. Yamamoto, Asymmetric Epoxidation Using Hydrogen Peroxide as Oxidant, *Chem. - An Asian J.*, (**2015**), 10, 2056–2068.

[17] K.P. Bryliakov, Catalytic Asymmetric Oxygenations with the Environmentally Benign Oxidants H_2O_2 and O_2, *Chem. Rev.*, (**2017**), 117, 11406–11459.

[18] K. Sato, Green oxidation with aqueous hydrogen peroxide, *AIST Today (International Ed.*, (**2004**), 32.

[19] B.S. Lane, K. Burgess, Metal-catalyzed epoxidations of alkenes with hydrogen peroxide, *Chem. Rev.*, (**2003**), 103, 2457–2473.

[20] R. Lewis, G.J. Hutchings, A review of recent advances in the direct synthesis of H2O2, *ChemCatChem*., (**2019**), 11, 298–308.

[21] H. J. Rledl, G. Pfleiderer, US2158525A, **1939**.

[22] J.M. Campos-Martin, G. Blanco-Brieva, J.L.G. Fierro, Hydrogen Peroxide Synthesis: An Outlook beyond the Anthraquinone Process, *Angew. Chemie Int. Ed.*, (**2006**), 45, 6962–6984.

[23] I.E. Markó, P.R. Giles, M. Tsukazaki, S.M. Brown, C.J. Urch, Copper-catalyzed oxidation of alcohols to aldehydes and ketones: An efficient, aerobic alternative, *Science (80-.).*, (**1996**), 274, 2044–2046.

[24] J.L. Jat, G. Kumar, Isomerization of Epoxides, *Adv. Synth. Catal.*, (**2019**), 361, 4426–4441.

[25] M.J.F. Calvete, M. Piñeiro, L.D. Dias, M.M. Pereira, Hydrogen Peroxide and Metalloporphyrins in Oxidation Catalysis: Old Dogs with Some New Tricks, *ChemCatChem*., (**2018**), 10, 3615–3635.

[26] M.S. Batra, R. Dwivedi, R. Prasad, Recent Developments in Heterogeneous Catalyzed Epoxidation of Styrene to Styrene Oxide, *ChemistrySelect*., (**2019**), 4, 11636–11673.

[27] J.M. Fraile, Solid Catalysts for Epoxidation with Dilute Hydrogen Peroxide, *Encycl. Inorg. Bioinorg. Chem.*, (**2016**), 1–9.

[28] I. Kirm, F. Medina, X. Rodríguez, Y. Cesteros, P. Salagre, J. Sueiras, Epoxidation of styrene with hydrogen peroxide using hydrotalcites as heterogeneous catalysts, *Appl. Catal. A Gen.*, (**2004**), 272, 175–185.

[29] U. Clerici, M. G.; Bellussi, G.; Romano, Synthesis of propylene oxide from propylene and hydrogen peroxide catalyzed by titanium silicalite, *J. Catal.*, (**1991**), 129, 159.

[30] Y. Wang, Q. Zhang, T. Shishido, K. Takehira, Characterizations of iron-containing MCM-41 and its catalytic properties in epoxidation of styrene with hydrogen peroxide, *J. Catal.*, (**2002**), 209, 186–196.

[31] P. Wu, T. Tatsumi, Extremely high trans selectivity of Ti-MWW in epoxidation of alkenes with hydrogen peroxide, *Chem. Commun.*, (**2001**), 897–898.

[32] R. Rinaldi, U. Schuchardt, Factors responsible for the activity of alumina surfaces in the catalytic epoxidation of cis-cyclooctene with aqueous H_2O_2, *J. Catal.*, (**2004**), 227, 109–116.

[33] R. Rinaldi, U. Schuchardt, On the paradox of transition metal-free alumina-catalyzed epoxidation with aqueous hydrogen peroxide, *J. Catal.*, (**2005**), 236, 335–345.

[34] V.R. Choudhary, N.S. Patil, N.K. Chaudhari, S.K. Bhargava, Epoxidation of styrene by anhydrous hydrogen peroxide over boehmite and alumina catalysts with continuous removal of the reaction water, *J. Mol. Catal. A Chem.*, (**2005**), 227, 217–222.
[35] O.D. Pavel, B. Cojocaru, E. Angelescu, V.I. Pârvulescu, The activity of yttrium-modified Mg,Al hydrotalcites in the epoxidation of styrene with hydrogen peroxide, *Appl. Catal. A Gen.*, (**2011**), 403, 83–90.
[36] S. Ueno, K. Yamaguchi, K. Yoshida, K. Ebitani, K. Kaneda, Hydrotalcite catalysis: Heterogeneous epoxidation of olefins using hydrogen peroxide in the presence of nitriles, *Chem. Commun.*, (**1998**), 295–296.
[37] K. Yamaguchi, K. Ebitani, K. Kaneda, Hydrotalcite-catalyzed epoxidation of olefins using hydrogen peroxide and amide compounds, *J. Org. Chem.*, (**1999**), 64, 2966–2968.
[38] M.G. Clerici, P. Ingallina, Epoxidation of lower olefins with hydrogen peroxide and titanium silicalite, *J. Catal.*, (**1993**), 140, 71–83.
[39] O.A. Kholdeeva, A.Y. Derevyankin, A.N. Shmakov, N.N. Trukhan, E.A. Paukshtis, A. Tuel, V.N. Romannikov, Alkene and thioether oxidations with H_2O_2 over Ti-containing mesoporous mesophase catalysts, *J. Mol. Catal. A Chem.*, (**2000**), 158, 417–421.
[40] P. Wu, T. Tatsumi, T. Komatsu, T. Yashimay, A novel titanosilicate with MWW structure: II. Catalytic properties in the selective oxidation of alkenes, *J. Catal.*, (**2001**), 202, 245–255.
[41] A.J. Bonon, Y.N. Kozlov, J.O. Bahú, R.M. Filho, D. Mandelli, G.B. Shul'pin, Limonene epoxidation with H_2O_2 promoted by Al_2O_2: Kinetic study, experimental design, *J. Catal.*, (**2014**), 319, 71–86.
[42] R.M. J.Rebek, New epoxidation reagents derived from alumina and silicon, *Tetrahedron Lett.*, (**1979**), 45, 4337–4338.
[43] W.T. Reichle, S.Y. Kang, D.S. Everhardt, The nature of the thermal decomposition of a catalytically active anionic clay mineral, *J. Catal.*, (**1986**), 101, 352–359.
[44] G.B. Payne, A simplified procedure for epoxidation by benzonitrile-hydrogen peroxide. Selective oxidation of 2-allylcyclohexanone, *Tetrahedron*., (**1962**), 18, 763–765.
[45] H.L. Xie, Y.X. Fan, C.H. Zhou, Z.X. Du, E.Z. Min, Z.H. Ge, X.N. Li, A review on heterogeneous solid catalysts and related catalytic mechanisms for epoxidation of olefins with H_2O_2, *Chem. Biochem. Eng. Q.*, (**2008**), 22, 25–39.
[46] N. Pal, A. Bhaumik, Mesoporous materials: Versatile supports in heterogeneous catalysis for liquid phase catalytic transformations, *RSC Adv.*, (**2015**), 5, 24363–24391.
[47] P.P. Knops-Gerrits, M. L'abbé, P.A. Jacobs, Epoxidation with manganese N,N'-bis(2-Pyridinecarboxamide) complexes encapsulated in zeolite y, *Stud. Surf. Sci. Catal.*, (**1997**), 108, 445–452.
[48] C. Peng, X.H. Lu, X.T. Ma, Y. Shen, C.C. Wei, J. He, D. Zhou, Q.H. Xia, Highly efficient epoxidation of cyclohexene with aqueous H_2O_2 over powdered anion-resin supported solid catalysts, *J. Mol. Catal. A Chem.*, (**2016**), 423, 393–399.
[49] A. Kumar, V.P. Kumar, B.P. Kumar, V. Vishwanathan, K.V.R. Chary, Vapor phase oxidation of benzyl alcohol over gold nanoparticles supported on mesoporous TiO_2, *Catal. Letters*., (**2014**), 144, 1450–1459.
[50] S.T. Oyama, Mechanisms in Homogeneous and Heterogeneous Epoxidation Catalysis, **2008**.
[51] G. Grigoropoulou, J.H. Clark, J.A. Elings, Recent developments on the epoxidation of alkenes using hydrogen peroxide as an oxidant, *Green Chem.*, (**2003**), 5, 1–7.
[52] V.I. Isaeva, O.M. Nefedov, L.M. Kustov, Metal–organic frameworks-based catalysts for biomass processing, *Catalysts*., (**2018**), 8,.
[53] J. Berzelius, The preparation of the phosphomolybdate ion [PMo12O40]2-, *Pogg. Ann. Phys*., (**1826**), 6, 369--371.
[54] A. Greenwood, N. N.; Earnshaw, Chemistry of the Elements (2nd ed.), **1997**.
[55] D. Tytko, Karl-Heinz, Gras, Mo Oxomolybdenum Species in Aqueous Solutions, **2013**.
[56] D.L. Kepert, Structures of polyanions, *Inorg. Chem.*, (**1969**), 8, 1556–1558.
[57] C. Albert, S.W. Geoffrey, Advanced Inorganic Chemistry: A comprehensive text. Third Edition, (**1972**), 1145.
[58] J.F. Keggin, Structure of the Molecule of 12-Phosphotungstic Acid., *Nature*., (**1933**), 131, 908–909.
[59] C.L. Hill, Introduction: PolyoxometalatesMulticomponent Molecular Vehicles To Probe Fundamental Issues and Practical Problems, *Chem. Rev.*, (**1998**), 98, 1–2.
[60] A. Proust, B. Matt, R. Villanneau, G. Guillemot, P. Gouzerh, G. Izzet, Functionalization and post-functionalization: A step towards polyoxometalate-based materials, *Chem. Soc. Rev.*, (**2012**), 41, 7605–7622.
[61] S.S. Wang, G.Y. Yang, Recent Advances in Polyoxometalate-Catalyzed Reactions, *Chem. Rev.*, (**2015**), 115, 4893–4962.

[62] Y. Ren, M. Wang, X. Chen, B. Yue, H. He, Heterogeneous catalysis of polyoxometalate based organic-inorganic hybrids, *Materials (Basel).*, (**2015**), 8, 1545–1567.
[63] C. Venturello, E. Alneri, M. Ricci, A New, Effective Catalytic System for Epoxidation of Olefins by Hydrogen Peroxide under Phase-Transfer Conditions, *J. Org. Chem.*, (**1983**), 48, 3831–3833.
[64] I. V. Kozhevnikov, Catalysis by heteropoly acids and multicomponent polyoxometalates in liquid-phase reactions, *Chem. Rev.*, (**1998**), 98, 171–198.
[65] O. Makrygenni, L. Vanmairis, S. Taourit, F. Launay, A. Shum Cheong Sing, A. Proust, H. Gérard, R. Villanneau, Selective Formation of Epoxylimonene Catalyzed by Phosphonyl/Arsonyl Derivatives of Trivacant Polyoxotungstates at Low Temperature, *Eur. J. Inorg. Chem.*, (**2020**), 2020, 605–612.
[66] O. Makrygenni, D. Brouri, A. Proust, F. Launay, R. Villanneau, Immobilization of polyoxometalate hybrid catalysts onto mesoporous silica supports using phenylene diisothiocyanate as a cross-linking agent, *Microporous Mesoporous Mater.*, (**2019**), 278, 314–321.
[67] R. Villanneau, A. Marzouk, Y. Wang, A. Ben Djamaa, G. Laugel, A. Proust, F. Launay, Covalent grafting of organic-inorganic polyoxometalates hybrids onto mesoporous SBA-15: A key step for new anchored homogeneous catalysts, *Inorg. Chem.*, (**2013**), 52, 2958–2965.
[68] F. Bentaleb, O. Makrygenni, D. Brouri, C. Coelho Diogo, A. Mehdi, A. Proust, F. Launay, R. Villanneau, Efficiency of Polyoxometalate-Based Mesoporous Hybrids as Covalently Anchored Catalysts, *Inorg. Chem.*, (**2015**), 54, 7607–7616.
[69] J.L. Bicas, A.P. Dionísio, G.M. Pastore, Bio-oxidation of terpenes: An approach for the flavor Industry, *Chem. Rev.*, (**2009**), 109, 4518–4531.
[70] E. V. Gusevskaya, Reactions of terpenes catalyzed by heteropoly compounds: Valorization of biorenewables, *ChemCatChem*., (**2014**), 6, 1506–1515.
[71] W.A. Herrmann, R.W. Fischer, D.W. Marz, metals, molybdenum and tungsten, could also be optimized in this way. Moreover, catalytic properties are expected for the organic oxides of the neighboring element, osmium. Simple compounds such as O=Os(CH,), are known.[’31, *Angew. Chem. Int Ed. Engl.*, (**1991**), 30, 1638–1641.
[72] Y.D. Wu, J. Sun, Transition Structures of Epoxidation by $CH_3Re(O)_2(O_2)$ and $CH_3Re(O)(O_2)_2$ and Their Water Adducts, *J. Org. Chem.*, (**1998**), 63, 1752–1753.
[73] J. Rudolph, K.L. Reddy, J.P. Chiang, B.K. Sharpless, Highly efficient epoxidation of olefins using aqueous H_2O_2 and catalytic methyltrioxorhenium/pyridine: Pyridine-mediated ligand acceleration, *J. Am. Chem. Soc.*, (**1997**), 119, 6189–6190.
[74] S. Yamazaki, An improved methyltrioxorhenium-catalyzed epoxidation of alkenes with hydrogen peroxide, *Org. Biomol. Chem.*, (**2007**), 5, 2109–2113.
[75] H. Adolfsson, C. Copéret, J.P. Chiang, A.K. Yudin, Efficient epoxidation of alkenes with aqueous hydrogen peroxide catalyzed by methyltrioxorhenium and 3-cyanopyridine, *J. Org. Chem.*, (**2000**), 65, 8651–8658.
[76] J.C. Barona-Castaño, C.C. Carmona-Vargas, T.J. Brocksom, K.T. De Oliveira, M. Graça, P.M.S. Neves, M. Amparo, F. Faustino, Porphyrins as catalysts in scalable organic reactions, *Molecules*., (**2016**), 21, 1–27.
[77] G. Legemaat, W. Drenth, M. Schmidt, G. Prescher, G. Goor, Epoxidation of alkenes by hydrogen peroxide catalysed by oxo(5,10,15,20-tetraphenylporphyiiinato)-molybdenum(V) complexes, *J. Mol. Catal.*, (**1990**), 62, 119–133.
[78] R.A. Sheldon, Oxidations catalysis by metalloporphyrins, Dekker: New York, **1994**.
[79] P. Jones, D. Mantle, I. Wilson, Influence of ligand modification on the kinetics of the reactions of iron(III) porphyrins with hydrogen peroxide in aqueous solutions, *J. Chem. Soc.{,} Dalt. Trans.*, (**1983**), 161–164.
[80] W. Nam, S.Y. Oh, Y.J. Sun, J. Kim, W.K. Kim, S.K. Woo, W. Shin, Factors affecting the catalytic epoxidation of olefins by iron porphyrin complexes and H_2O_2 in protic solvents, *J. Org. Chem.*, (**2003**), 68, 7903–7906.
[81] N.A. Stephenson, A.T. Bell, Influence of solvent composition on the kinetics of cyclooctene epoxidation by hydrogen peroxide catalyzed by iron(III) [tetrakis(pentafluorophenyl)] porphyrin chloride [(F_{20}TPP)FeCl], *Inorg. Chem.*, (**2006**), 45, 2758–2766.
[82] T.G. Traylor, F. Xu, A Biomimetic Model for Catalase: The Mechanisms of Reaction of Hydrogen Peroxide and Hydroperoxides with Iron(III) Porphyrins, *J. Am. Chem. Soc.*, (**1987**), 109, 6201–6202.
[83] A. Thellend, P. Battioni, D. Mansuy, Ammonium acetate as a very simple and efficient cocatalyst for manganese porphyrin-catalysed oxygenation of hydrocarbons by hydrogen peroxide, *J. Chem. Soc. Chem. Commun.*, (**1994**), 202, 1035–1036.
[84] P.G. Cozzi, Metal-Salen Schiff base complexes in catalysis: Practical aspects, *Chem. Soc. Rev.*, (**2004**), 33, 410–421.
[85] D.A. Atwood, M.J. Harvey, Group 13 compounds incorporating Salen ligands, *Chem. Rev.*, (**2001**), 101, 37–52.

[86] W. Zhang, J.L. Loebach, S.R. Wilson, E.N. Jacobsen, Enantioselective Epoxidation of Unfunctionalized Olefins Catalyzed by (Saien)manganese Complexes, *J. Am. Chem. Soc.*, (**1990**), 112, 2801–2803.

[87] T. Schwenkreis, A. Berkessel, A biomimetic catalyst for the asymmetric epoxidation of unfunctionalized olefins with hydrogen peroxide, *Tetrahedron Lett.*, (**1993**), 34, 4785–4788.

[88] L. Cavallo, H. Jacobsen, Electronic effects in (salen)Mn-based epoxidation catalysts, *J. Org. Chem.*, (**2003**), 68, 6202–6207.

[89] V. La Paglia Fragola, F. Lupo, A. Pappalardo, G. Trusso Sfrazzetto, R.M. Toscano, F.P. Ballistreri, G.A. Tomaselli, A. Gulino, A surface-confined O=MnV(salen) oxene catalyst and high turnover values in asymmetric epoxidation of unfunctionalized olefins, *J. Mater. Chem.*, (**2012**), 22, 20561–20565.

[90] F.P. Ballistreri, C.M.A. Gangemi, A. Pappalardo, G.A. Tomaselli, R.M. Toscano, G. Trusso Sfrazzetto, (Salen)Mn(III) Catalyzed Asymmetric Epoxidation Reactions by Hydrogen Peroxide in Water: A Green Protocol, *Int. J. Mol. Sci.*, (**2016**), 17, 1112–1121.

[91] S. Shylesh, M. Jia, W.R. Thiel, Recent progress in the heterogenization of complexes for single-site epoxidation catalysis, *Eur. J. Inorg. Chem.*, (**2010**), 369, 4395–4410.

[92] D.E. De Vos, B.F. Sels, M. Reynaers, Y. V. Subba Rao, P.A. Jacobs, Epoxidation of terminal or electron-deficient olefins with H_2O_2, catalysed by Mn-trimethyltriazacyclonane complexes in the presence of an oxalate buffer, *Tetrahedron Lett.*, (**1998**), 39, 3221–3224.

[93] G. De Faveri, G. Ilyashenko, M. Watkinson, Recent advances in catalytic asymmetric epoxidation using the environmentally benign oxidant hydrogen peroxide and its derivatives, *Chem. Soc. Rev.*, (**2011**), 40, 1722–1760.

[94] S. Fukuzumi, K. Ohkubo, Y.M. Lee, W. Nam, Lewis Acid Coupled Electron Transfer of Metal-Oxygen Intermediates, *Chem. - A Eur. J.*, (**2015**), 21, 17548–17559.

[95] Z. Lv, C. Choe, Y. Wu, H. Wang, Z. Chen, G. Li, G. Yin, Non-redox metal ions accelerated oxygen atom transfer by Mn-Me_3tacn complex with H_2O_2 as oxygen resource, *Mol. Catal.*, (**2018**), 448, 46–52.

[96] A. Nodzewska, M. Watkinson, Remarkable increase in the rate of the catalytic epoxidation of electron deficient styrenes through the addition of $Sc(OTf)_3$ to the MnTMTACN catalyst, *Chem. Commun.*, (**2018**), 54, 1461–1464.

[97] L. Que, Jr., W.B. Tolman, Bis(μ-oxo)dimetal "Diamond" Cores in Copper and Iron Complexes Relevant to Biocatalysis, *Angew. Chemie Int. Ed.*, (**2002**), 41, 1821.

[98] P.C.A. Bruijnincx, I.L.C. Buurmans, S. Gosiewska, M.A.H. Moelands, M. Lutz, A.L. Spek, G. Van Koten, R.J.M.K. Gebbink, Iron(II) complexes with bio-inspired N,N,O ligands as oxidation catalysts: Olefin epoxidation and cis-dihydroxylation, *Chem. - A Eur. J.*, (**2008**), 14, 1228–1237.

[99] K. Chen, Q. Lawrence, cis-Dihydroxylation of olefins by a non-heme iron catalyst: A functional model for Rieske dioxygenases, *Angew. Chemie - Int. Ed.*, (**1999**), 38, 2227–2229.

[100] and L.Q.J. Subhasree Kal, Apparao Draksharapu, Sc^{3+} (or $HClO_4$) Activation of a Nonheme FeIII–OOH Intermediate for the Rapid Hydroxylation of Cyclohexane and Benzene, *J Am Chem Soc*., (**2018**), 140, 5798–5804.

[101] R. Mas-Ballesté, L. Que, Iron-catalyzed olefin epoxidation in the presence of acetic acid: Insights into the nature of the metal-based oxidant, *J. Am. Chem. Soc.*, (**2007**), 129, 15964–15972.

[102] M. Grau, A. Kyriacou, F. Cabedo Martinez, I.M. De Wispelaere, A.J.P. White, G.J.P. Britovsek, Unraveling the origins of catalyst degradation in non-heme iron-based alkane oxidation, *Dalt. Trans.*, (**2014**), 43, 17108–17119.

[103] A. Nielsen, F.B. Larsen, A.D. Bond, C.J. McKenzie, Regiospecific ligand oxygenation in iron complexes of a carboxylate-containing ligand mediated by a proposed FeV-oxo species, *Angew. Chemie - Int. Ed.*, (**2006**), 45, 1602–1606.

[104] B. Sonnberger, P. Hühn, A. Waßerburger, F. Wasgestian, Base promoted decomposition of bis(1,4,7-triazacyclononane)nickel(III) in aqueous solution, *Inorganica Chim. Acta*., (**1992**), 196, 65–71.

[105] A. Thibon, J.F. Bartoli, S. Bourcier, F. Banse, Mononuclear iron complexes relevant to nonheme iron oxygenases. Synthesis, characterizations and reactivity of Fe-Oxo and Fe-Peroxo intermediates, *Dalt. Trans.*, (**2009**), 9587–9594.

[106] J. Chen, R.J.M. Klein Gebbink, Deuterated N_2Py_2 Ligands: Building More Robust Non-Heme Iron Oxidation Catalysts, *ACS Catal.*, (**2019**), 9, 3564–3575.

[107] W. Wang, Q. Sun, C. Xia, W. Sun, Enantioselective epoxidation of olefins with hydrogen peroxide catalyzed by bioinspired aminopyridine manganese complexes derived from L-proline, *Cuihua Xuebao/Chinese J. Catal.*, (**2018**), 39, 1463–1469.

[108] S. Dasgupta, S. Chatterjee, T. Chattopadhyay, Designing of a magnetically separable Fe_3O_4@dopa@ML nano-catalyst for multiple organic transformations (epoxidation, reduction, and coupling) in aqueous

medium, *J. Coord. Chem.*, (**2019**), 72, 550–568.
[109] T.M. Asha, M. Sithambaresan, M.R. Prathapachandra Kurup, Dioxidomolybdenum(VI) complexes chelated with N4-(3-methoxyphenyl)thiosemicarbazone as molybdenum(IV) precursors in oxygen atom transfer process and oxidation of styrene, *Polyhedron*., (**2019**), 171, 530–541.
[110] R. Vithalani, D.S. Patel, C.K. Modi, V. Sharma, P.K. Jha, Graphene Oxide Supported Oxovanadium (IV) Complex for Catalytic Peroxidative Epoxidation of Styrene: An Eye-Catching Impact of Solvent, *Appl. Organomet. Chem.*, (**2020**), 34, 1–17.
[111] G. Saikia, K. Ahmed, C. Rajkhowa, M. Sharma, H. Talukdar, N.S. Islam, Polymer immobilized tantalum(v)-amino acid complexes as selective and recyclable heterogeneous catalysts for oxidation of olefins and sulfides with aqueous H_2O_2, *New J. Chem.*, (**2019**), 43, 17251–17266.
[112] T. Chakraborty, A. Chakraborty, S. Maity, D. Das, T. Chattopadhyay, Conglomerated system of Ag nanoparticles decorated Al_2O_3 supported cobalt and copper complexes with enhanced catalytic activity for oxidation reactions, *Mol. Catal.*, (**2019**), 462, 104–113.
[113] A. Shaabani, R. Mohammadian, H. Farhid, M. Karimi Alavijeh, M.M. Amini, Iron-Decorated, Guanidine Functionalized Metal-Organic Framework as a Non-heme Iron-Based Enzyme Mimic System for Catalytic Oxidation of Organic Substrates, *Catal. Letters*., (**2019**), 149, 1237–1249.
[114] H. Zakeri, S. Rayati, G. Zarei, Synthesis and characterization of a Mn-Schiff base complex anchored on modified MCM-41 as a novel and recyclable catalyst for oxidation of olefins, *Appl. Organomet. Chem.*, (**2018**), 32, 1–9.
[115] S.R. Pour, A. Abdolmaleki, M. Dinari, Immobilization of new macrocyclic Schiff base copper complex on graphene oxide nanosheets and its catalytic activity for olefins epoxidation, *J. Mater. Sci.*, (**2019**), 54, 2885–2896.
[116] J. Lu, X. Ma, P. Wang, J. Feng, P. Ma, J. Niu, J. Wang, Synthesis, characterization and catalytic epoxidation properties of a new tellurotungstate(iv)-supported rhenium carbonyl derivative, *Dalt. Trans.*, (**2019**), 48, 628–634.
[117] M. Alhumaimess, O. Aldosari, H. Alshammari, M.M. Kamel, M.A. Betiha, H.M.A. Hassan, Ionic liquid green synthesis of CeO_2 nanorods and nano-cubes: Investigation of the shape dependent on catalytic performance, *J. Mol. Liq.*, (**2019**), 279, 649–656.
[118] B. Paul, S.K. Sharma, R. Khatun, S. Adak, G. Singh, V. Joshi, M.K. Poddar, A. Bordoloi, T. Sasaki, R. Bal, Development of Highly Efficient and Durable Three-Dimensional Octahedron $NiCo_2O_4$ Spinel Nanoparticles toward the Selective Oxidation of Styrene, *Ind. Eng. Chem. Res.*, (**2019**), 58, 18168–18177.
[119] J. Zhao, Y. Zhang, S. Zhang, Q. Wang, M. Chen, T. Hu, C. Meng, Synthesis and characterization of Mn-Silicalite-1 by the hydrothermal conversion of Mn-magadiite under the neutral condition and its catalytic performance on selective oxidation of styrene, *Microporous Mesoporous Mater.*, (**2018**), 268, 16–24.
[120] J. Zhao, Y. Zhang, F. Tian, Y. Zuo, Y. Mu, C. Meng, High pH promoting the synthesis of V-Silicalite-1 with high vanadium content in the framework and its catalytic performance in selective oxidation of styrene, *Dalt. Trans.*, (**2018**), 47, 11375–11385.
[121] C. Bihanic, A. Stanovych, F. Pelissier, C. Grison, Putting Waste to Work: The Demonstrative Example of Pyrite Quarry Effluents Turned into Green Oxidative Catalysts, *ACS Sustain. Chem. Eng.*, (**2019**), 7, 6223–6233.
[122] W. Zheng, H. Hu, Y. Chen, R. Tan, D. Yin, Diamine-Decorated Graphene Oxide with Immobilized Gold Nanoparticles of Small Size for Alkenes Epoxidation with H_2O_2, *Catal. Letters*., (**2019**), 149, 3328–3337.
[123] D. Saha, S. Gayen, S. Koner, Cu(II)/Cu(II)-Mg(II) containing pyridine-2,5-dicarboxylate frameworks: Synthesis, structural diversity, inter-conversion and heterogeneous catalytic epoxidation, *Polyhedron*., (**2018**), 146, 93–98.
[124] M.R. Maurya, R. Tomar, L. Rana, F. Avecilla, Trinuclear Dioxidomolybdenum(VI) Complexes of Tritopic Phloroglucinol-Based Ligands and Their Catalytic Applications for the Selective Epoxidation of Olefins, *Eur. J. Inorg. Chem.*, (**2018**), 2018, 2952–2964.
[125] S. Roy, Saswati, S. Lima, S. Dhaka, M.R. Maurya, R. Acharyya, C. Eagle, R. Dinda, Synthesis, structural studies and catalytic activity of a series of dioxidomolybdenum(VI)-thiosemicarbazone complexes, *Inorganica Chim. Acta*., (**2018**), 474, 134–143.
[126] G. Romanowski, J. Kira, M. Wera, Synthesis, structure, spectroscopic characterization and catalytic activity of chiral dioxidomolybdenum(VI) Schiff base complexes derived from R(−)-2-amino-1-propanol, *Inorganica Chim. Acta*., (**2018**), 483, 156–164.
[127] H. Taghiyar, B. Yadollahi, New perspective to catalytic epoxidation of olefins by Keplerate containing Keggin polyoxometalates, *Polyhedron*., (**2018**), 156, 98–104.
[128] X. Ma, P. He, B. Xu, J. Lu, R. Wan, H. Wu, Y. Wang, P. Ma, J. Niu, J. Wang, Pyrazine dicarboxylate-bridged

arsenotungstate: Synthesis, characterization, and catalytic activities in epoxidation of olefins and oxidation of alcohols, *Dalt. Trans.*, (**2019**), 48, 12956–12963.
[129] Z. Zhou, G. Dai, S. Ru, H. Yu, Y. Wei, Highly selective and efficient olefin epoxidation with pure inorganic-ligand supported iron catalysts, *Dalt. Trans.*, (**2019**), 48, 14201–14205.
[130] W. Ma, H. Yuan, H. Wang, Q. Zhou, K. Kong, D. Li, Y. Yao, Z. Hou, Identifying catalytically active mononuclear peroxoniobate anion of ionic liquids in the epoxidation of olefins, *ACS Catal.*, (**2018**), 8, 4645–4659.
[131] M.R. Maurya, N. Jangra, F. Avecilla, I. Correia, 4,6-Diacetyl Resorcinol Based Vanadium(V) Complexes: Reactivity and Catalytic Applications, *Eur. J. Inorg. Chem.*, (**2019**), 2019, 314–329.
[132] L. Li, H.J. Song, X.G. Meng, R.Q. Yang, N. Zhang, Efficient epoxidation reaction of terminal olefins with hydrogen peroxide catalyzed by an iron (II) complex, *Tetrahedron Lett.*, (**2018**), 59, 2436–2439.
[133] L. Hao, A.M. Lebuis, J.F. Harrod, Synthesis and structural characterization of $Cp_2Ti(SiH_3)(PMe_3)$, *Chem. Commun.*, (**1998**), 1089–1090.
[134] O. Porcar-Tost, B. Pi-Boleda, J. García-Anton, O. Illa, R.M. Ortuño, Cyclobutane-based peptides/terpyridine conjugates: Their use in metal catalysis and as functional organogelators, *Tetrahedron*., (**2018**), 74, 7252–7260.
[135] S. Goswami, S. Singha, R. Saha, A. Singha Roy, M. Islam, S. Kumar, A bi-nuclear Cu(II)-complex for selective epoxidation of alkenes: Crystal structure, thermal, photoluminescence and cyclic voltammetry, *Inorganica Chim. Acta*., (**2019**), 486, 352–360.
[136] R. A. Sheldon, Metal Catalyzed Epoxidation of Olefins with Hydroperoxides, in: Asp. Homog. Catal., **1981**: pp. 3–70.
[137] R. Meiers, U. Dingerdissen, W.F. Hölderich, Synthesis of propylene oxide from propylene, oxygen, and hydrogen catalyzed by palladium-platinum-containing titanium silicalite, *J. Catal.*, (**1998**), 176, 376–386.
[138] M.P. Kapoor, A.K. Sinha, S. Seelan, S. Inagaki, S. Tsubota, H. Yoshida, M. Haruta, Hydrophobicity induced vapor-phase oxidation of propene over gold supported on titanium incorporated hybrid mesoporous silsesquioxane, *Chem. Commun.*, (**2002**), 23, 2902–2903.
[139] A.K. Sinha, S. Seelan, S. Tsubota, M. Haruta, A three-dimemional mesoporous titanosilicate support for gold nanoparticles: Vapor-phase epoxidation of propene with high conversion, *Angew. Chemie - Int. Ed.*, (**2004**), 43, 1546–1548.
[140] B. Meunier, Metalloporphyrins as Versatile Catalysts for Oxidation Reactions and Oxidative DNA Cleavage, *Chem. Rev.*, (**1992**), 92, 1411–1456.
[141] J.R. Monnier, The direct epoxidation of higher olefins using molecular oxygen, *Appl. Catal. A Gen.*, (**2001**), 221, 73–91.
[142] T. Punniyamurthy, S. Velusamy, J. Iqbal, Recent Advances in Transition Metal Catalyzed Oxidation of Organic Substrates with Molecular Oxygen, *Chem. Rev.*, (**2005**), 105, 2329–2364.
[143] T. Yamada, K. Imagawa, T. Nagata, T. Mukaiyama, Enantioselective Epoxidation of Unfunctionalized Olefins with Molecular Oxygen and Aldehyde Catalyzed by Optically Active Manganese(III) Complexes, *Chem. Lett.*, (**1992**), 21, 2231–2234.
[144] B. B. Wentzel, P. A. Gosling, M. C. Feiters, R. J. M. Nolte, Mechanistic studies on the epoxidation of alkenes with molecular oxygen and aldehydes catalysed by transition metal–β-diketonate complexes, *J. Chem. Soc.{,} Dalt. Trans.*, (**1998**), 2241–2246.
[145] W. Nam, H.J. Kim, S.H. Kim, R.Y.N. Ho, J.S. Valentine, Metal Complex-Catalyzed Epoxidation of Olefins by Dioxygen with Co-Oxidation of Aldehydes. A Mechanistic Study, *Inorg. Chem.*, (**1996**), 35, 1045–1049.
[146] S. Rayati, F. Nejabat, The catalytic efficiency of Fe-porphyrins supported on multi-walled carbon nanotubes in the oxidation of olefins and sulfides with molecular oxygen, *New J. Chem.*, (**2017**), 41, 7987–7991.
[147] T. Yamada, T. Takai, O. Rhode, T. Mukaiyama, Direct Epoxidation of Olefins Catalyzed by Nickel(II) Complexes with Molecular Oxygen and Aldehydes, *Bull. Chem. Soc. Jpn.*, (**1991**), 64, 2109–2117.
[148] L. Que, W.B. Tolman, Biologically inspired oxidation catalysis, *Nature*., (**2008**), 455, 333–340.
[149] P.A. Gosling, R.J.M. Nolte, A manganese(III) porphyrin/rhodium(III) bipyridine/formate catalyst system for the reductive activation of molecular oxygen, *J. Mol. Catal. A Chem.*, (**1996**), 113, 257–267.
[150] J. Byun, C. Han, Y. Park, N. Lee, J. Baik, Synthesis and Characterization of Mn(Ⅲ) Chloro Complexes with Salen-Type Ligands, *J. Korean Chem. Soc.*, (**2002**), 46, 194–204.
[151] B. Rhodes, S. Rowling, P. Tidswell, S. Woodward, S.M. Brown, Aerobic epoxidation via alkyl-2-oxocyclopentanecarboxylate co-oxidation with cobalt or manganese Jacobsen-type catalysts, *J. Mol. Catal. A Chem.*, (**1997**), 116, 375–384.
[152] T. Nagata, K. Imagawa, T. Yamada, T. Mukaiyama, Enantioselective Aerobic Epoxidation of Acyclic Simple

Olefins Catalyzed by the Optically Active β-Ketoiminato Manganese(III) Complex, *Chem. Lett.*, (**1994**), 23, 1259–1262.
[153] R. V Ottenbacher, E.P. Talsi, K.P. Bryliakov, Catalytic asymmetric oxidations using molecular oxygen, *Russ. Chem. Rev.*, (**2018**), 87, 821–830.
[154] N.H. Lee, J.S. Balk, S. Bin Han, Trapping of the Dichlorocarbonyl Oxide Using a Chiral (Salen)Mn(III) Complex, *Bull. Korean Chem. Soc.*, (**1997**), 18, 796–798.
[155] T. Mukaiyama, T. Yamada, T. Nagata, K. Imagawa, Asymmetric Aerobic Epoxidation of Unfunctionalized Olefins Catalyzed by Optically Active α-Alkoxycarbonyl-β-ketoiminato Manganese(III) Complexes, *Chem. Lett.*, (**1993**), 22, 327–330.
[156] G. Pozzi, F. Cinato, F. Montanari, S. Quici, C. Cnr, C. Organica, Efficient aerobic epoxidation of alkenes in perfluorinated solvents catalysed by chiral (salen) Mn complexes Chiral complexes selectively soluble in perfluorocarbons have been synthesized for the first time and tested as catalysts for the epoxidation of, *Chem. Commun.*, (**1998**), 877–878.
[157] T. Nagata, K. Imagawa, T. Yamada, T. Mukaiyama, Optically Active N , N ′-Bis(3-oxobutylidene)diaminatomanganese(III) Complexes as Novel and Efficient Catalysts for Aerobic Enantioselective Epoxidation of Simple Olefins , *Bull. Chem. Soc. Jpn.*, (**1995**), 68, 1455–1465.
[158] K. Hemmat, M.A. Nasseri, A. Allahresani, Olefins oxidation with molecular O2 in the presence of chiral Mn(III) salen complex supported on magnetic CoFe2O4@SiO2@CPTMS, *Appl. Organomet. Chem.*, (**2019**), 33, 4937–4949.
[159] E. Ahadi, H. Hosseini-Monfared, C. Schlüsener, C. Janiak, A. Farokhi, Chirally-Modified Graphite Oxide as Chirality Inducing Support for Asymmetric Epoxidation of Olefins with Grafted Manganese Porphyrin, *Catal. Letters*., (**2020**), 150, 861–873.
[160] L.D. Dias, R.M.B. Carrilho, C.A. Henriques, G. Piccirillo, A. Fernandes, L.M. Rossi, M. Filipa Ribeiro, M.J.F. Calvete, M.M. Pereira, A recyclable hybrid manganese(III) porphyrin magnetic catalyst for selective olefin epoxidation using molecular oxygen, *J. Porphyr. Phthalocyanines*., (**2018**), 22, 331–341.
[161] K. Berijani, A. Farokhi, H. Hosseini-Monfared, C. Janiak, Enhanced enantioselective oxidation of olefins catalyzed by Mn-porphyrin immobilized on graphene oxide, *Tetrahedron*., (**2018**), 74, 2202–2210.
[162] K. Berijani, H. Hosseini-Monfared, Collaborative effect of Mn-porphyrin and mesoporous SBA-15 in the enantioselective epoxidation of olefins with oxygen, *Inorganica Chim. Acta*., (**2018**), 471, 113–120.
[163] S. Rayati, S. Rezaie, F. Nejabat, Mn(III)-porphyrin/graphene oxide nanocomposite as an efficient catalyst for the aerobic oxidation of hydrocarbons, *Comptes Rendus Chim.*, (**2018**), 21, 696–703.
[164] J.W. Brown, Q.T. Nguyen, T. Otto, N.N. Jarenwattananon, S. Glöggler, L.S. Bouchard, Epoxidation of alkenes with molecular oxygen catalyzed by a manganese porphyrin-based metal-organic framework, *Catal. Commun.*, (**2015**), 59, 50–54.
[165] S. Rayati, F. Nejabat, F. Panjiali, Aerobic oxidation of olefins in the presence of a new amine functionalized core–shell magnetic nanocatalyst, *Catal. Commun.*, (**2019**), 122, 52–57.
[166] T.M. Yazdely, M. Ghorbanloo, H. Hosseini-Monfared, Polymeric ionic liquid material-anchored Mn–porphyrin anion: Heterogeneous catalyst for aerobic oxidation of olefins, *Appl. Organomet. Chem.*, (**2018**), 32, 4388–4400.
[167] V. Abbasi, H. Hosseini-Monfared, S.M. Hosseini, A heterogenized chiral imino indanol complex of manganese as an efficient catalyst for aerobic epoxidation of olefins, *New J. Chem.*, (**2017**), 41, 9866–9874.
[168] A. Farokhi, H. Hosseini-Monfared, A recyclable Mn-porphyrin catalyst for enantioselective epoxidation of unfunctionalized olefins using molecular dioxygen, *New J. Chem.*, (**2016**), 40, 5032–5043.
[169] A. Farokhi, K. Berijani, H. Hosseini-Monfared, Manganes-Porphyrin as Efficient Enantioselective Catalyst for Aerobic Epoxidation of Olefins, *Catal. Letters*., (**2018**), 148, 2608–2618.
[170] S. Rayati, P. Nafarieh, M.M. Amini, The synthesis, characterization and catalytic application of manganese porphyrins bonded to novel modified SBA-15, *New J. Chem.*, (**2018**), 42, 6464–6471.
[171] A. Rezaeifard, M. Jafarpour, A. Naeimi, A practical innovative method for highly selective oxidation of alcohols in neat water using water-insoluble iron and manganese porphyrins as reusable heterogeneous catalysts, *Catal. Commun.*, (**2011**), 16, 240–244.
[172] Z. Opre, T. Mallat, A. Baiker, Epoxidation of styrene with cobalt-hydroxyapatite and oxygen in dimethylformamide: A green technology?, *J. Catal.*, (**2007**), 245, 482–486.
[173] Q. Tang, Q. Zhang, H. Wu, Y. Wang, Epoxidation of styrene with molecular oxygen catalyzed by cobalt(II)-containing molecular sieves, *J. Catal.*, (**2005**), 230, 384–397.
[174] M.J. Beier, W. Kleist, M.T. Wharmby, R. Kissner, B. Kimmerle, P.A. Wright, J.D. Grunwaldt, A. Baiker, Aerobic epoxidation of olefins catalyzed by the cobalt-based metal-organic framework STA-12(Co),

Chem. - A Eur. J., (**2012**), 18, 887–898.
[175] M. Turner, V.B. Golovko, O.P.H. Vaughan, P. Abdulkin, A. Berenguer-Murcia, M.S. Tikhov, B.F.G. Johnson, R.M. Lambert, Selective oxidation with dioxygen by gold nanoparticle catalysts derived from 55-atom clusters, *Nature*., (**2008**), 454, 981–983.
[176] L. Wang, H. Wang, A.E. Rice, W. Zhang, X. Li, M. Chen, X. Meng, J.P. Lewis, F.-S.S. Xiao, Design and Preparation of Supported Au Catalyst with Enhanced Catalytic Activities by Rationally Positioning Au Nanoparticles on Anatase, *J. Phys. Chem. Lett.*, (**2015**), 6, 2345–2349.
[177] S. Hassan, R. Kumar, A. Tiwari, W. Song, L. van Haandel, J.K. Pandey, E. Hensen, B. Chowdhury, Role of oxygen vacancy in cobalt doped ceria catalyst for styrene epoxidation using molecular oxygen, *Mol. Catal.*, (**2018**), 451, 238–246.
[178] R. Jain, C.S. Gopinath, Morphology-dependent, green, and selective catalytic styrene oxidation on Co_3O_4, *Dalt. Trans.*, (**2019**), 48, 4574–4581.
[179] Z.Q. Shi, L.X. Jiao, J. Sun, Z.B. Chen, Y.Z. Chen, X.H. Zhu, J.H. Zhou, X.C. Zhou, X.Z. Li, R. Li, Cobalt nanoparticles in hollow mesoporous spheres as a highly efficient and rapid magnetically separable catalyst for selective epoxidation of styrene with molecular oxygen, *RSC Adv.*, (**2014**), 4, 47–53.
[180] Z.Q. Shi, Z.P. Dong, J. Sun, F.W. Zhang, H.L. Yang, J.H. Zhou, X.H. Zhu, R. Li, Filled cobalt nanoparticles into carbon nanotubes as a rapid and high-efficiency catalyst for selective epoxidation of styrene with molecular oxygen, *Chem. Eng. J.*, (**2014**), 237, 81–87.
[181] S. Bhunia, S. Jana, D. Saha, B. Dutta, S. Koner, Catalytic olefin epoxidation over cobalt(II)-containing mesoporous silica by molecular oxygen in dimethylformamide medium, *Catal. Sci. Technol.*, (**2014**), 4, 1820–1828.
[182] Q. Tang, Y. Wang, J. Zhang, R. Qiao, X. Xie, Y. Wang, Y. Yang, Cobalt(II) acetylacetonate complex immobilized on aminosilane-modified SBA-15 as an efficient catalyst for epoxidation of trans-stilbene with molecular oxygen, *Appl. Organomet. Chem.*, (**2016**), 30, 435–440.
[183] C. Hu, X. Xia, J. Jin, H. Ju, D. Wu, Z. Qi, S. Hu, R. Long, J. Zhu, L. Song, Y. Xiong, Surface Modification on Pd Nanostructures for Selective Styrene Oxidation with Molecular Oxygen, *ChemNanoMat*., (**2018**), 4, 467–471.
[184] M. Kazemnejadi, B. Mahmoudi, Z. Sharafi, M.A. Nasseri, A. Allahresani, M. Esmaeilpour, Synthesis and characterization of a new poly α-amino acid Co(II)-complex supported on magnetite graphene oxide as an efficient heterogeneous magnetically recyclable catalyst for efficient free-coreductant gram-scale epoxidation of olefins with molecular o, *J. Organomet. Chem.*, (**2019**), 896, 59–69.
[185] M. Kazemnejadi, A. Shakeri, M. Nikookar, M. Mohammadi, M. Esmaeilpour, Co(II) Schiff base complex decorated on polysalicylaldehyde as an efficient, selective, heterogeneous and reusable catalyst for epoxidation of olefins in mild and self-coreductant conditions, *Res. Chem. Intermed.*, (**2017**), 43, 6889–6910.
[186] P. Tao, X. Lu, H. Zhang, R. Jing, F. Huang, S. Wu, D. Zhou, Q. Xia, Enhanced activity of microwave-activated CoO_x/MOR catalyst for the epoxidation of α-pinene with air, *Mol. Catal.*, (**2019**), 463, 8–15.
[187] D. Saha, T. Maity, R. Bera, S. Koner, Cobalt(III) Schiff base complex: Synthesis, X-ray structure and aerobic epoxidation of olefins, *Polyhedron*., (**2013**), 56, 230–236.
[188] X. Song, D. Hu, X. Yang, H. Zhang, W. Zhang, J. Li, M. Jia, J. Yu, Polyoxomolybdic Cobalt Encapsulated within Zr-Based Metal–Organic Frameworks as Efficient Heterogeneous Catalysts for Olefins Epoxidation, *ACS Sustain. Chem. Eng.*, (**2019**), 7, 3624–3631.
[189] D. Pan, Q. Xu, Z. Dong, S. Chen, F. Yu, X. Yan, B. Fan, R. Li, Facile synthesis of highly ordered mesoporous cobalt-alumina catalysts and their application in liquid phase selective oxidation of styrene, *RSC Adv.*, (**2015**), 5, 98377–98390.
[190] S.R. Leandro, C.I. Fernandes, A.S. Viana, A.C. Mourato, P.D. Vaz, C.D. Nunes, Catalytic performance of bulk and colloidal Co/Al layered double hydroxide with Au nanoparticles in aerobic olefin oxidation, *Appl. Catal. A Gen.*, (**2019**), 584, 117155.
[191] S.R. Leandro, A.C. Mourato, U. Łapińska, O.C. Monteiro, C.I. Fernandes, P.D. Vaz, C.D. Nunes, Exploring bulk and colloidal Mg/Al hydrotalcite–Au nanoparticles hybrid materials in aerobic olefin epoxidation, *J. Catal.*, (**2018**), 358, 187–198.

CHAPTER II

GREEN STRSTEGY IN SYNTHESIS OF CYCLIC CARBONATES VIA CO_2 CYCLOADDITION TO EPOXIDES

II.1 State of the climatic urgency

Since the industrial revolution and the invention of the steam engine, mankind has been constantly meeting a growing need for energy. This growing energy consumption is reflected in the many machines that now populate our daily lives, from the car to the clothes we wear, from the heating for our homes to the millions of connected computers around the world. This energy requires the combustion of fossil fuels, which are free and abundant on Earth and are considered to be the main source of CO_2 emissions into the atmosphere.[1] This greenhouse gas (GHG) has always been present and is at the centre of many exchanges between the earth's surface, the ocean and the atmosphere via its carbon cycle. However, this balance has been broken, and a surplus of CO_2 equivalent to 1400 billion tons has since been emitted into the atmosphere between 1850 and 2014.[2] The concentration of CO_2 in the atmosphere has thus reached an all-time high of 416 ppm in 2020, compared to 280 ppm before the industrial revolution (which already represented a high concentration on the geological time scale of the last 800,000 years).[3]

CO_2 emissions have been increasing steadily since the industrial revolution of 1850. In spite of the awareness of nations and the holding of numerous international agreements aimed at reducing greenhouse gas emissions (creation IPCC 1988, Rio Summit 1992, Kyoto Protocol 1993, Copenhagen Agreement 2009 and Paris Agreement COP21 in 2015 to name but a few), the only reductions in CO_2 emissions have only been observed in the wake of sudden economic crises (see **Figure 18**). In summary, no policy has so far led to an effective reduction of CO_2 emissions.

An increase of 25 to 90% (compared to the year 2000) in global GHG emissions is estimated in 2030 at an increase in CO_2 concentration of between 600 and 1550 ppm. Such an increase would, in the worst-case scenario, result in a global temperature increase of 4.8°C. [4] As a reference, the global temperature difference between the pre-industrial area and the last ice age was only -5°C. This temperature rising up to our time occurred in a very long geological time of 0.1 °C per century, whereas today it is 2 °C per century and is therefore not to be taken lightly.[4] At 2°C, food insecurity is expected to occur in several areas of the globe, probably leading to political instability (see **Figure 19**).

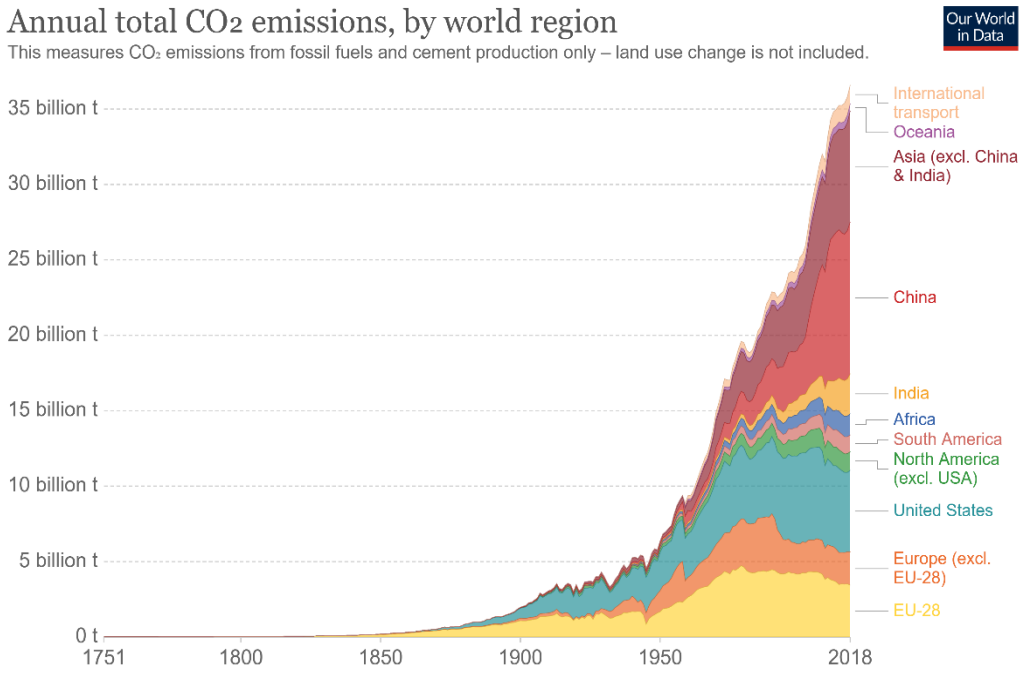

Figure 18: *Annual total CO_2 emission (source: OurWorldInData)*

At 4°C, living conditions in equatorial zones become fatally unliveable for more than 100 days a year for more than 3 billion human beings.[5] As a result, a target of 2°C above pre-industrial levels was confirmed in the Paris agreements in 2015 by a large majority of countries (main CO_2 emitters such as China or India are out of it).

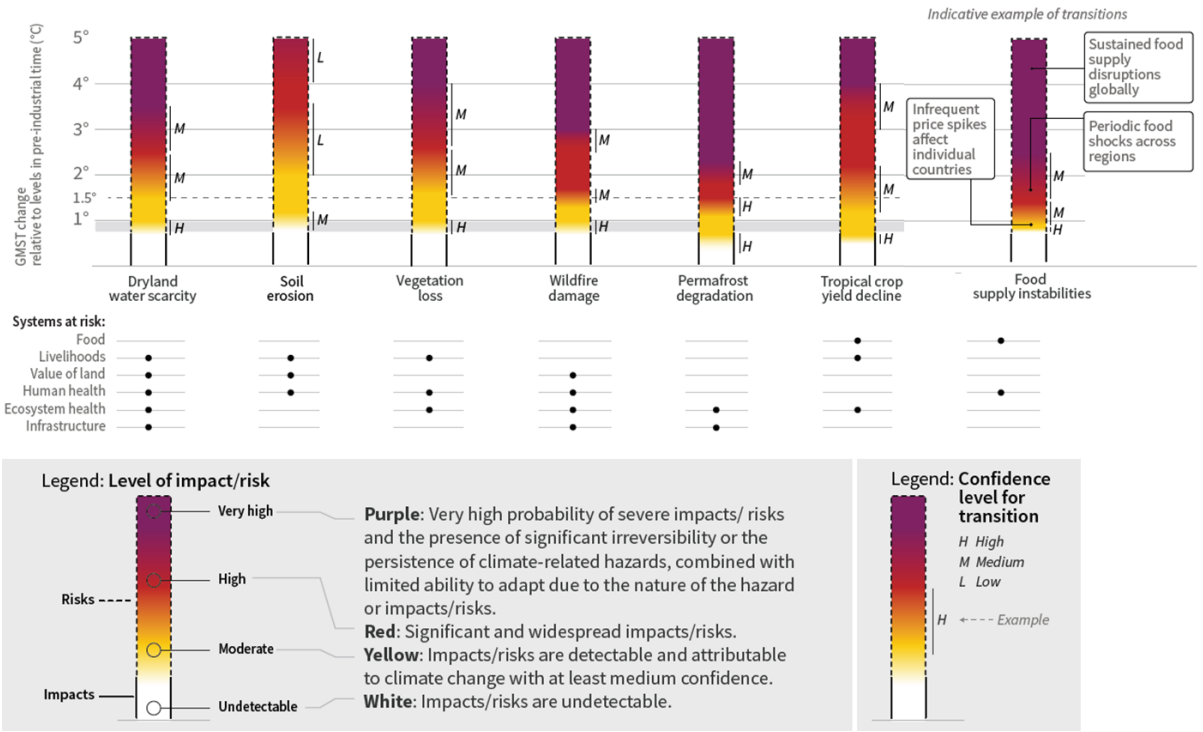

Figure 19: *Evaluation of main risks of global warming depending on the increase of temperature*[6]

CO_2 emissions need to be regulated and reduced worldwide by 78-118% by 2100 compared to the 2010 level. Since fossil fuel are the main source of energy, these emissions are closely related to our economic activity. Which means that a drop in CO_2 emissions, and therefore in energy consumption, will probably lead the world into an economic recession.[7] In France, this would amount to a 5% decline in growth per year, which would correspond to the effects of a COVID health crisis every year.

II.2 Main strategies to reduce CO_2 emissions

The reduction of anthropogenic CO_2 emissions is an urgent matter and three main strategies are now at work to stem its increasing concentration. The first, outlined above, would be to significantly reduce our energy needs, thus lowering the quantity of CO_2 emitted. This method would have to be implemented sufficiently in advance to avoid a transition that would be too abrupt for governments. A resilient economy study may be considered in order to face not only a decreasing energy demand, but also a depletion of available raw materials (peak oil for Europe in 2008).[8] A second strategy consisting on the Carbon Capture and Sequestration (CCS) is attracting growing interest. The capture and concentration of CO_2 by chemical absorption with amines represents the most mature capture solution to date (estimated cost between 40 and 60 €/tCO_2 captured).[9] Monoethanolamine (MEA) remains the most currently studied compound for CO_2 adsorption. They can be grafted on Polyethylene glycol (PEG) as solid support. A CO_2 purity higher than 99% can thus be achieved. However, a compromise must be found between the purity targeted and the operating costs of the capture process. Depending on the final concentration obtained, the CO_2 can either be buried in geological faults if its purity remains below 95%: this strategy is called Carbon Capture and Sequestration (CCS).[10] For example, Total plans to store 40 million metric tons of CO_2 over 25 years. However, this capture strategy is not optimized for every type of industry. It is therefore preferable to the steel or cement industries that produce fumes with a higher concentration of CO_2.

These strategies increase the amount of highly concentrated CO_2 available as a raw material. Consequently, the use of CO_2 as an abundant renewable and non-toxic C1 carbon resource allows the synthesis of high value-added products.[11] This is referred to as Carbon Capture and Utilization (CCU). This strategy would allow to mitigate CO_2 emissions, but also

to slow down the depletion of fossil resources by offering an alternative by synthesis to products that were previously in limited quantities. However, such a strategy remains difficult and time-consuming to implement compared to CCS strategy. Furthermore, in order to confirm if the process is able to prevent more CO_2 release, rigorous study of the life cycle of the product formed will allow us to conclude on the effectiveness of this technology.[12] Other feasibility, time and cost parameters come into play and will not be discussed in this section.

II.2.1 Mains reactions for CO_2 utilization

CO_2 is a very stable molecule ($\Delta_r G^\circ$ = -396 kJ/mol):[12] which is found as waste in any combustion process. For a long time, CO_2 has been considered as a "spent" form of carbon. Such a molecule is nevertheless utilised in nature, the most well-known reaction being photosynthesis, which converts carbon dioxide into carbohydrates and dioxygen using energy from sunlight.

Nowadays, the utilization of CO_2 for the global production of chemicals ranges (see **Figure 20**) around 170 Mt/y **worldwide** and is dominated by the synthesis of urea, then inorganic carbonates. Carbonate production shows the greatest growth, with a **5 000**% evolution from 2014 to 2020, confirming the growing interest and technological development for this process.[13] Non-chemical and technological employments of CO_2 range around 30 Mt/y worldwide and present a number of applications where CO_2 acts essentially as a fluid. Such utilizations refer to the substitution of CO_2 to chlorofluorocarbons (CFC) in air conditioners[14], to perchloroethene in dry washing[15], to complex chemicals in food conservation[16], and so on. The dual use of supercritical CO_2 (sc-CO_2) as reagent or solvent, in chemical process, like the caffeine extraction from coffee beans[17], is another innovative application.

Conversion of CO_2, as well as attempts to produce $H(C^{+II})OOH$, $(C^{+II})O$, $H_2(C^0)O$, $H_3(C^{-II})OH$, or $(C^{-IV})H_4$ hydrocarbons, are based on the reduction of carbon from its oxidation state +IV in CO_2 [18] and require quite a lot of energy.[19–24] These will not be discussed in this part therefore. On the other hand, reactions where carbon dioxide is incorporated into target chemicals without any change of its carbon oxidation state are more favourable. It includes

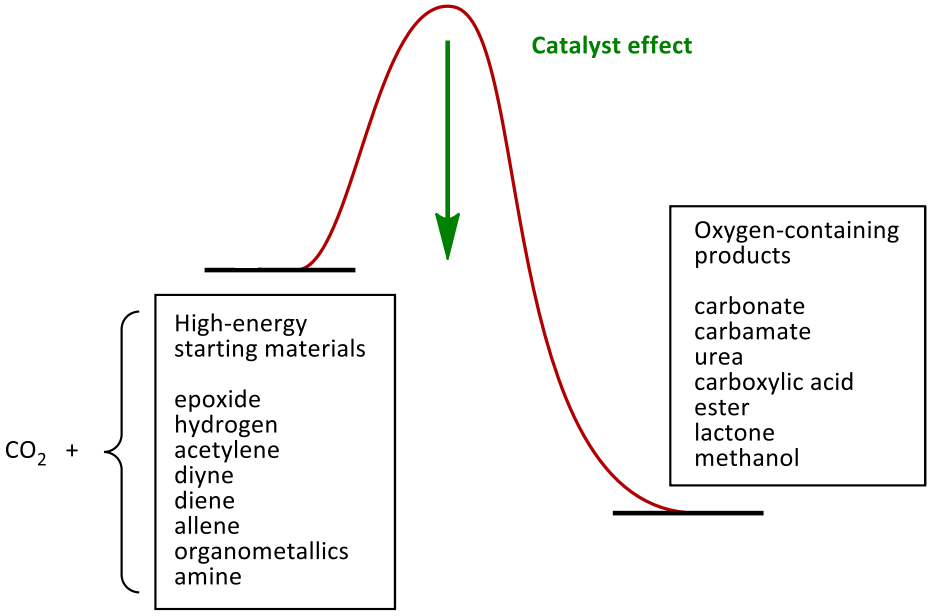

Figure 20: *Main substrates and products obtained from catalytic reaction using CO_2 as C1 material*

carboxylation reactions, such as the formation of carbamates (RR'N(C^{+IV})(O)OR"), carbonates ($(RO)_2(C^{+IV})O$), ureas ($(RNH)_2(C^{+IV})(O)$) and polymeric materials. Previous processes for the industrial synthesis of these different classes of chemicals utilising toxic intensive species[25] such as $COCl_2$ are increasingly reconsidered with the progresses of an inherently safer green chemistry.[26] Consequently, there is now a crucial need for applications showing that CO_2 is a good starting material or building block for the synthesis of bulk or fine chemical. As one example, recovery and utilization of carbon dioxide to produce carbonates is a well-known technology since the 70s where the carboxylation of epoxides into cyclic carbonates catalysed by quaternary ammonium salts was discovered[27]. Nowadays, new catalysts have been developed for this application.

II.3 About cyclic carbonates and epoxides

Cyclic carbonates are widely used in the manufacture of industrial products such as solvents, paint-strippers, epoxy glue, lithium batteries, and biodegradable packaging[28–30]. They also have application in the medicinal chemistry, such as controlled drug release[31], surgical implant substances[32], or even as anti-depressant.[33] Cyclic, acyclic and poly-carbonates are all commercialized,[34,35] and industrially important organic carbonates include dimethyl carbonate, diphenyl carbonate, ethylene carbonate and propylene carbonate (see **Figure 21**).[36]

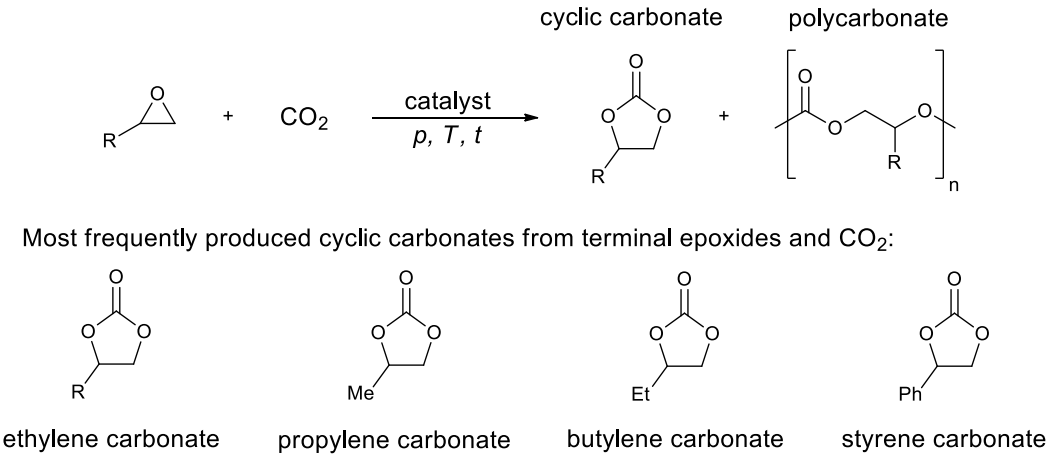

Figure 21: *Most frequently obtained products of cycloaddition reaction as well as their corresponding epoxides*

Various sources of C1 carbon can react with diols such as dimethyl carbonate, urea or CO to produce cyclic carbonates (see **Figure 22**), but the most seducing route in green and sustainable chemistry remains the cycloaddition of CO_2 to epoxides. Furthermore, the latter pathways to synthesize cyclic carbonates is one of the few methods that allows a 100% atom-economical efficient assimilation and has been industrialized for more than 40 years[37].

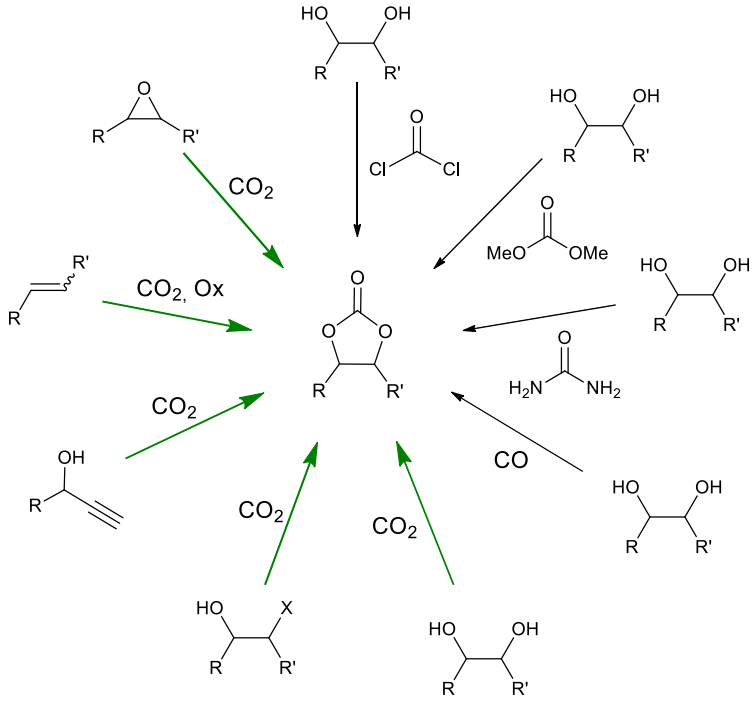

Figure 22: *Cyclic carbonate synthesis pathways*

Coupling CO_2 with epoxide is a chemical reaction known since 1969 when Inoue *et al.* combined $ZnEt_2$, water, CO_2 and propylene oxide to yield a small quantity of polymeric material[38,39]. Such a reaction path is much more environmentally respectful than the multi-step phosgenation reaction pathway.[37] The latter thus involves the formation of an intermediate diol by hydrolysis of the epoxide and its reaction with phosgene. This last step is particularly troublesome due to the use of a toxic reagent, *i.e.* phosgene, and to the production of hydrochloric acid (see **Figure 23**). However, the subsequent studies in this area frequently faced low catalytic activities and competitive formation of polycarbonates and/or undesired by-products, such as higher degrees of ether linkages in the polymer chains.

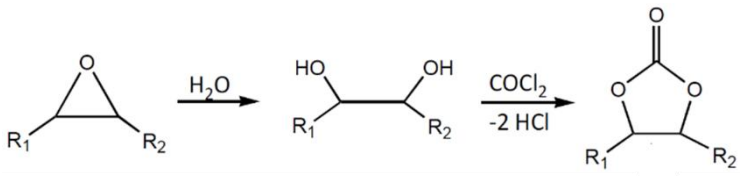

Figure 23: *Synthesis route of cyclic carbonate from epoxide with phosgene as C1 source*

The fundamental transformations of CO_2 require the C=O polarization, with a partial negative charge (-0.296) on the O atoms and a positive partial charge (+0.592) on the center C. This polarization allows nucleophilic attack of amines, halides or phenolates at the central atom C. The concomitant use of a catalyst can induce significant changes in chemical reactivity by modifying both its molecular geometry (from linear geometry to bent) and its electronic distribution (less electron-deficient carbon during coordination).

In the context of the CO_2 activation, many different catalysts that can efficiently convert CO_2 into high-value molecules were studied until now, but the quest for new catalysts able to significantly reduce drastic reaction conditions remains an intensified research area.

The efficiency of ammonium salts as catalysts in this CO_2/epoxide coupling reaction was first developed by Steinbauer *et al.* who studied the kinetics of the butylene oxide conversion without solvent in the presence of ammonium salts (2 mol%) for 6 hours at 90°C under 10 bar of CO_2.[40] The activity of different ammonium salts was found strongly depending on the nature of the anion according to the order $Cl^- > Br^- > I^-$ (see **Table 8**) in this work**.** In particular *n*-Bu_4NCl (TBACl) **(a)** has proven to be the most active monofunctional ammonium salt. First-order kinetics were found for the conversion of 1,2-epoxybutane with CO_2 at constant pressure. The rate constants k_{obs} were determined for the reaction in the

presence of ammonium salts decreasing in the order of 0.178 h^{-1} **(a)** > 0.051 h^{-1} **(b)** > 0.028 h^{-1} **(c)**.

Table 8: *Kinetic constants of cycloaddition reaction of butylene oxide using ammonium salts*

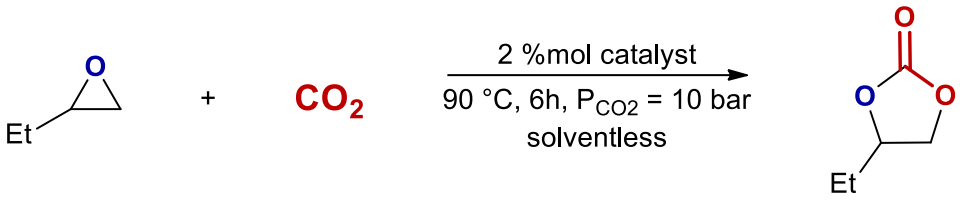

Entry	catalyst	K_{obs} (h^{-1})
1	*n*-Bu_4NCl **(a)**	0.178
2	*n*-Bu_4NBr **(b)**	0.051
3	*n*-Bu_4NI **(c)**	0.028

Lots of examples of catalysts developed for the cycloaddition of CO_2 onto epoxides were based on the use of easily accessible and commercially available quaternary ammonium or onium salts. This made them the most used catalysts for laboratory research and industrial production,[41] alone or combined with co-catalysts such as metal complexes [42,43] or hydrogen bond donors[12,41,44],[45] in order to enhance the catalytic activity and improve epoxide conversion. Zhang and co-workers compared the catalytic performances of several onium salts in the conversion of propene oxide (used as a model epoxide) into propylene carbonate. The catalytic activity of the salts decreased following the order: PPh_3Bu^+ > Bu_4N^+ >> K^+ > Na^+.[41],[46] Thus, in the case of onium salts it was shown that longer alkyl chains led to higher activity and selectivity. More generally the larger the steric hindrance, the greater the anion lability, due to reduced electrostatic interactions.[47] In parallel, it was shown that the activity of the anions varies in the order I^- > Br^- > Cl^- > PF_6^-, BF_4^- in the presence of water. However, the activity of I^- is very sensitive to water since the following order Br^- > Cl^- > I^- > PF_6^-, BF_4^- was observed in the absence of water Thus, tetrabutylammonium bromide (*n*-Bu_4NBr) is generally considered as a good compromise and is still the most used catalyst for the addition of CO_2 to epoxide.[50,51] In a general way, tetraalkylammonium or imidazolium-based ionic liquids are widely used as both solvents and catalysts[52–55] due to their extremely low vapour pressure and high boiling point, their thermal stability and their tremendous variety (various libraries of cations and anions are available to tune their properties[56,57]).

As stated above, metal complexes or salts as well as hydrogen bond donors thus act as Lewis acids.[58–61] In some cases, CO_2 is adsorbed on a Lewis base site (Nu), thus forming a Nu^+-COO^- carbonate-type species, whereas the epoxide is coordinated on the Lewis acid site. In a second step, the ring-opening of the coordinated epoxide occurred through the nucleophile attack of the pre-formed carbonate. This led to an oxy-anion of which evolution afforded the expected cyclic carbonate as a product. Arai *et al.* studied the catalytic activity of various metal salts in the presence of 1-butyl-3-methylimidazolium chloride for the conversion of styrene oxide[47], hence showing that the nature of the metal cation had a significant impact. The catalytic activity decreased in the order $Zn^{2+} > Fe^{3+} > Fe^{2+} > Mg^{2+} > Li^+ > Na^+$, which is in accordance with the order of Lewis acidity strength of the metal cations.[47] Compared to Fe^{3+}, Zn^{2+} has indeed a weaker ionization potential but a stronger ionic radius. According to the literature, other metals such as Mn, Cr, Co, Ni and Al that can also act as effective catalysts for CO_2/epoxide coupling. This included complexes with various ligands such as porphyrins N4, Schiff bases N4, Schiff bases Salophen and Salen 2N2O, macrocyclic ligands 4N2O, and phenolic derivatives (see **Figure 24**).

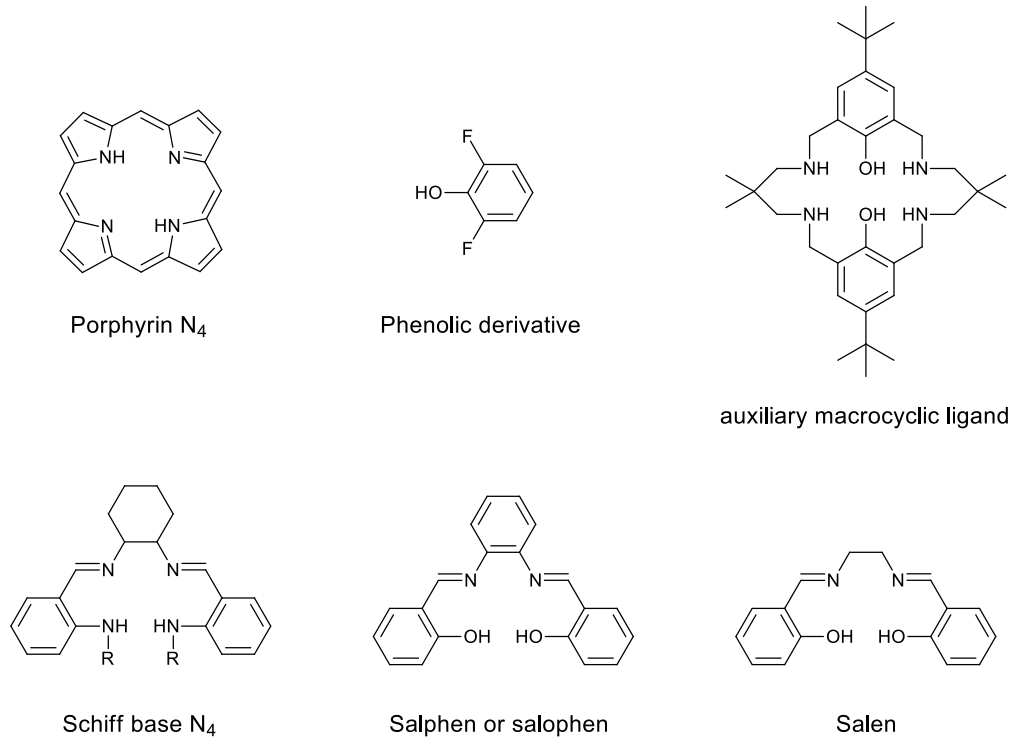

Figure 24: *Efficient ligands for CO_2/epoxide coupling after metal complexing*

Cycloaddition of CO_2 to epoxides can be carried out using nucleophilic catalysts, binary systems composed by Lewis acid/base dual components, or a single-component catalyst displaying both functions. As seen in **Figure 25**, nucleophilic compounds such as guanidine base TBD (1,5,7-triazabicyclo[4.4.0]dec-5-ene),[62] amidine base DBU (1,8-diazabicyclo[5.4.0]undec-7-ene),[63,64] or N-heterocyclic carbenes (NHCs)[65] are known to perform nucleophilic attack onto the electrophilic C-atom of CO_2, leading to the corresponding CO_2-adducts. Such adducts (**A-1**, **Figure 25**, Cycle 1 left ; nucleophiles in this class are referred to Nu^1) can then attack an epoxide (or a Lewis-acid (LA) activated epoxide **A-2**) leading to the alkoxy-ester **I-1**. Target carbonate product was then obtained after intramolecular cyclization of the latter and restored the nucleophile for a new catalytic cycle.

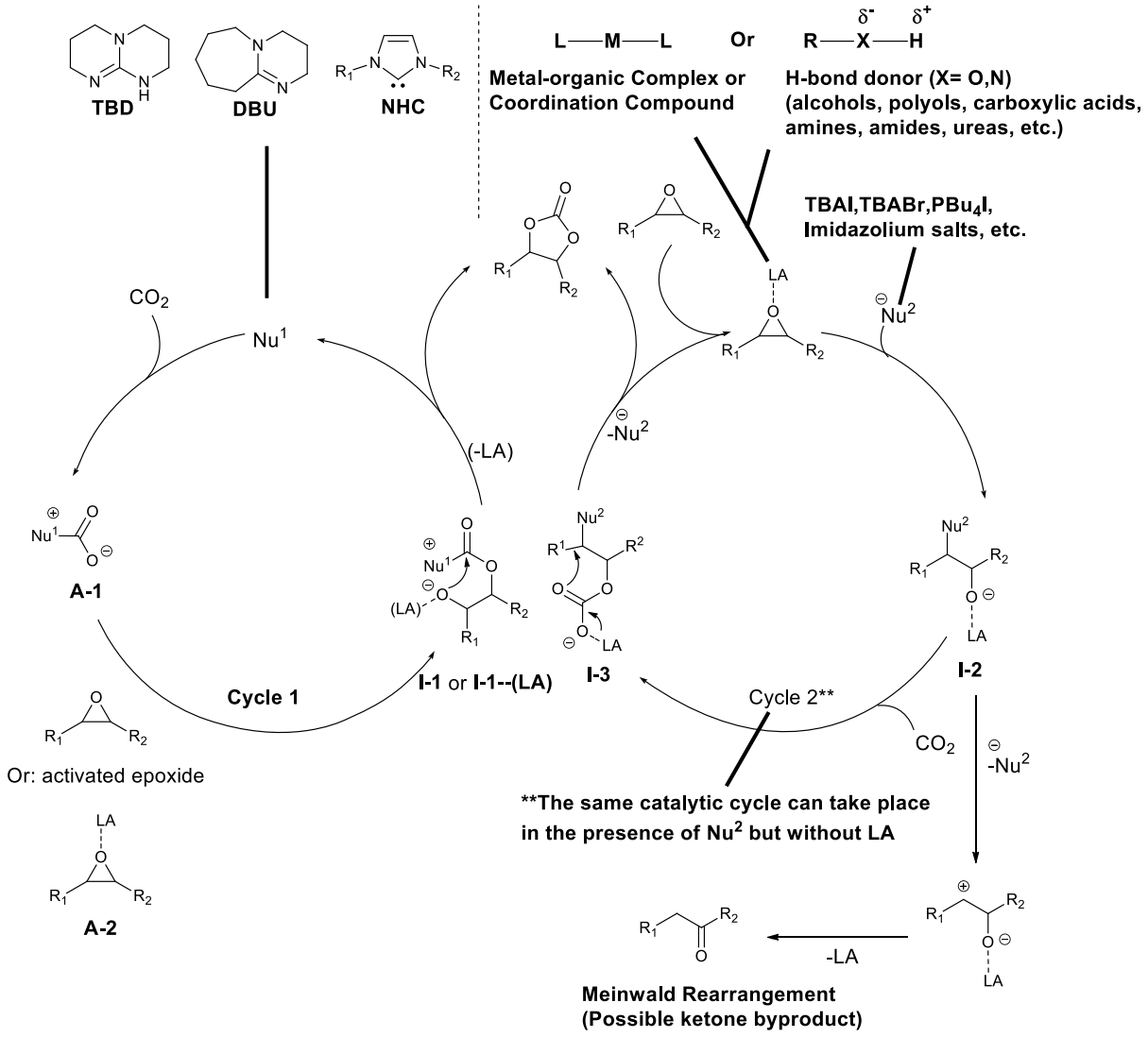

Figure 25: *General mechanistic pathways for the cycloaddition of CO_2 to epoxides[62]*

Alternative mechanistic routes (**Figure 25**, Cycle 2 right, the nucleophilic species in this cycle are referred to Nu^2), were also described. Ammonium and phosphonium salts and ionic liquids (ILs) bearing nucleophilic counter-anions (see **Figure 26**) were thus able to perform the ring-opening of the epoxide after the nucleophilic attack of the anion, leading to the formation of the targeted cyclic carbonate. Such organic catalysts were most of the time not efficient enough to afford efficient cycloaddition reaction on their own. Consequently, the presence of hydrogen bond donors or of a Lewis acidic compound (such as metal-organic complexes and coordination compounds) were able to act as a Lewis acid and to activate the epoxide. This facilitated its opening and often led to a remarkable acceleration of the reaction rate. From a mechanistical standpoint, CO_2 inserted into the metal-alkoxide bond of **I-2** leading to the intermediate **I-3** whose cyclization yielded the cyclic carbonate product (**Figure 25**, Cycle 2).

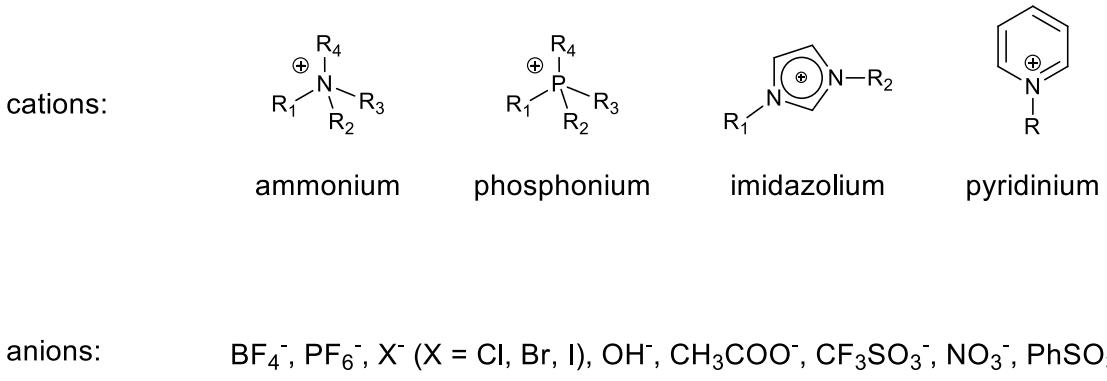

Figure 26: *Representative anions and cations of ammonium salts and ionic liquids (ILs)*

This binary system is a representative of many cycloaddition reactions of CO_2 to epoxides. In this context, the Lewis acidic component is referred as the “catalyst” and the Lewis basic component as the “co-catalyst” in a majority of works. However, this convention is misleading, as the Lewis acidic “catalyst” may generally be not active in the absence of a nucleophilic “co-catalyst”, the latter sufficient on its own to promote the catalytic reaction. Therefore, it is not used in this manuscript and the main “catalyst” should always refer to the nucleophilic specie and the “co-catalyst” term referring to the Lewis acid catalyst.

At the same time, the quest for more gentle conditions for this type of reaction allows now temperatures set under ambient condition. Such performances were obtained in recent works *via* catalytic systems involving the binary use of LA-BA catalysts and following the mechanism shown in cycle 2 of **Figure 25.** In this context, most of the recent literature reports described the application of Lewis acidic complexes and compounds acting as co-catalyst in

the presence of well-established source of nucleophilic anions such as quaternary onium salts or ionic liquids. Therefore, some recent reviews focused on the cycloaddition of CO_2 and epoxides. These reviews were generally organized according to the class of Lewis-acid employed and categorized these Lewis acids according to their chemical structure.

Finally, it is noteworthy that organocatalysis, working thus without metal centre, recently drew attention these last years, the processes being inexpensive (absence of noble metals), and the compounds used generally stable and in particular not sensitive to air.

II.3.1 Recent homogeneous catalytic systems developed

As seen in previous part, a large variety of catalytic systems were developed in the past few decades in the context of the cycloaddition reaction of CO_2 onto epoxides. The majority of these systems involved the use of *n*-Bu_4NBr as the main catalyst. Furthermore, the use of Schiff base (Salen type) catalysts regularly appeared in the literature, being mono-, bi- or trimetallic. In parallel, a few number of epoxides were studied over the years. A non-exhaustive list of these is presented in and a selection of representative recent works is reported in **Table 9**, that will be commented in the next paragraph. The same classification of co-catalysts was used as seen in **Figure 27.**

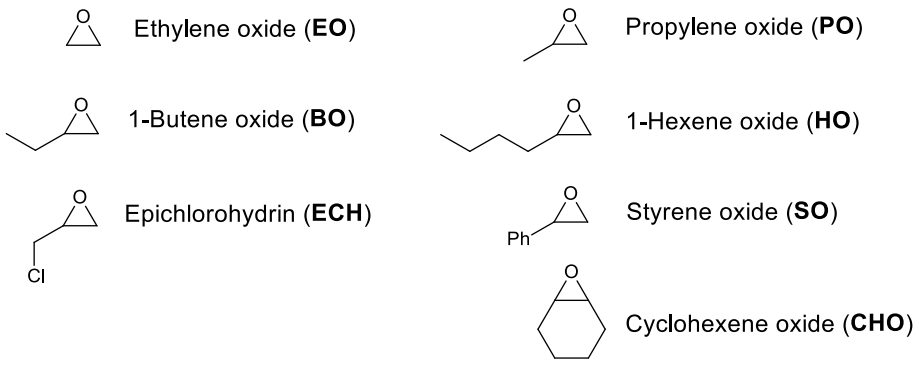

Figure 27: *Commonly used terminal epoxides and their relative's abbreviations*

Table 9: *Experimental conditions and the corresponding outputs from the CO_2 cycloaddition reactions*

Entry	oxide	Cat	Co-cat (molar%)	T (°C)	P (bar)	t (h)	Yield (%)	Ref.
Organocatalysts								
1	PO	-	$[BMIm]BF_4$ IL (5%)	110	25	6	91	[66]
2	SO	TBACl (2%)	-	90	10	6	20	[40]
3		TBABr (2%)	-	90	10	6	23	
4		TBAI (2%)	-	90	10	6	16	
Monometallic salen complexes								
5	SO	TBABr (2.5%)	Salophen-Cr (2.5%)	25	1	3	37	[67]
6				25	1	6	60	
7				25	1	24	100	
8		TBABr (2.5%)	Salophen-Al (2.5%)	25	1	3	44	
9				25	1	6	71	
10				25	1	24	100	
Bimetallic salen complexes								
11	PO	TBABr (7%)	Bimetallic Salen-Co (0.5%)	25	10	48	76	[68]
12		TBABr (7%)	Bimetallic Salen-Al (0.5%)	25	10	48	73	
13		TBABr (7%)	Bimetallic Salen-Zn (0.5%)	25	10	48	72	
Monometallic non-salen complexes								
14	SO	-	Zn(II) TPP (0.01%)	120	17	9	94	[69]
15	PO	TBABr (5%)	Co-cryptand (0.05%)	0	1	8	43	[70]
16	SO	TBABr (5%)		20	1	12	32	
17	ECH	TBABr (5%)		20	1	24	48	
18		-		20	1	48	6	
19		TBABr (5%)	-	20	1	48	11	
Bimetallic non-salen complexes								
20	SO	TBABr (5%)	Bi-aluminium scorpionate (5%)	r.t.	1	24	75	[71]
21		TBABr (5%)		r.t.	10	24	97	
22		TBABr (5%)		r.t.	10	24	59	
Trimetallic non-salen complexes								
23	CHO	TBABr (1%)	Trimetallic-Co (0.1%)	80	21	24	66	[72]
24		TBAI (1%)		80	21	24	39	
25		TBABr (1%)	Trimetallic-Zn (0.1%)	80	21	24	90	
26		TBAI (1%)		80	21	24	87	
27		TBABr (1%)	Trimetallic-Ni (0.1%)	80	21	24	43	

II.3.2 Impact of the temperature

The catalytic activity of the processes implemented for the cycloaddition reaction is very sensitive to the temperature. Indeed, an increase of the yield in carbonate product was generally observed in most cases when the temperature increased. However, it has been reported by Sun *et al* that in the case of the global formation of styrene carbonate from styrene, an increase of the temperature from 80 to 90°C led to a decrease in styrene carbonate yield.[73] According to the authors, this decrease was actually linked to an increase in the formation of benzaldehyde, a side-product caused by the oxidative cleavage of styrene, as the temperature rises. In this particular case, the cycloaddition reaction that led to the formation of styrene carbonate being faster than the epoxidation step, the formation of benzaldehyde and styrene carbonate ultimately occurred together over time.

II.3.3 Impact of CO_2 pressure

Typical conditions observed for the synthesis of cyclic carbonate in the literature required 15 to 30 bar of CO_2 to reach a significant catalytic activity. However, several recent works reported reactions operating at pressures close to 1 bar (see **Table 9 entries 5-10** and **15-20**). It was demonstrated that a decrease as well as an increase from the optimal value of CO_2 pressure led to a dramatic decrease of the catalytic activity. In the latter case, it was found that the presence of an excess of CO_2 led to slow down the epoxides interaction with the catalyst.[74] Indeed, this resulted in a lower substrate concentration and consequently a reduction in the substrate conversion.

II.4 Heterogenization of cycloaddition catalysts

Various heterogeneous catalytic systems were developed in the past decades. Simple separation process and possibly to work in gas flow are the main reasons for the high demand for heterogeneous catalysts.[75]

II.4.1 Strategies for supporting homogeneous catalysts over silica support

Many studies in the literature dealt with the immobilization of homogeneous catalysts for the cycloaddition reaction, varying at once the nature of the catalysts and the supports. Representative examples in recent literature were based on the grafting of ionic liquid onto polymer matrix,[76,77] on the functionalization of MCM-41 silica with imidazolium,[78] or on SBA-15 with triazolium-based ionic liquids.[79] The nature of the support was important and must meet pertinent criteria since it had 1) to be chemically compatible with the active phase, 2) to show high stability within the drastic conditions used during the reaction, and 3) to prevent negative interaction, and if possible, to enhance the catalytic activity. Interestingly, with regard to this last point, it is now admitted that supports bearing H-donor groups such as -OH could greatly improve the conversion of the epoxide (see **Figure 25**). Thus, SBA-15 silica supports that bear -OH groups was considered as a good candidate for the immobilization of either homogeneous ammonium salts catalysts or Salophen co-catalysts. Valuable examples of co-catalysts Salophen grafted on silica will be further developed in the following part. On the other hand, grafting of main catalyst quaternary ammonium salts will be further developed in the **Chapter V** and related to the covalent grafted of ammonium salt on silica support.

II.4.2 Grafting salen over silica support

Covalent immobilization is a key to obtain robust bond and can efficiently prevent from the leaching of active sites from the support. Chromium salen complexes were anchored successfully by Baleizâo *et al.* on aminopropyl-functionalized SiO_2 silica.[80] Two strategies of anchoring were developed by the authors: the grafting was made either by coordination with Cr (see **Figure 28** (**a**)), or by covalent linkage to the ligand (see **Figure 28** (**b**)). In the case of a grafting through the metal coordination, a severe leaching of the complex into solution was observed. It has to be noted that non-covalent immobilization strategies led to materials much more sensitive to the experimental conditions, especially the polarity of the solvent. However, non-covalent anchoring led to more difficulties to control the immobilized amount. In the case of a covalent linkage (see **Figure 28.b**), leaching of the ligand was not observed, while the styrene oxide conversion remained low, with 59% yield obtained compared to 74% in the case

of coordinated catalyst (**a**) (see **Table 10 entries 1-2**). Experiments were conducted at 80°C during 6h under a high CO_2 pressure of 100 bar.

However, this contrast between grafting by coordination or covalent linkage was not systematically observed. It was thus shown by *Alvaro* et al,[82] *Ramin* et al,[81] and Jutz *et al*.[83] that better yield of carbonate was obtained in the case of covalently grafted catalyst at the surface of silica support. In the case of Chromium(III) supported catalyst, 30% yield of propylene carbonate was obtained with coordinated bonded catalyst while 41% was obtained in the case of covalent bond anchoring (see **Table 10 entries 3-4**). Cycloaddition was occurring at 140°C under 35 bar during 3h in the absence of homogeneous quaternary ammonium salt. In the case of silylated Salen-Mn(III) [83], covalent grafting (see **Figure 28** (**f**)) allowed better catalytic performances. Indeed, 95% yield of styrene carbonate was obtained after 3h reaction at 140°C under 35 bar of CO_2 (**Table 10 entry 6**) with catalyst (**f**) while 6% was obtained with coordinated compound (**e**) (**Table 10 entry 5**). However, in these works, significant loss of the catalytic activity was observed after the first cycle despite the immobilization of the metal co-catalyst. 95% yield of styrene carbonate was obtained after 3h reaction at 140°C under 35 bar of CO_2 (**Table 10 entry 6**) while 0.6% was obtained after a second run. The authors thus attributed this decrease in reactivity to the formation of inactive species on the surface of the silica due to the loss of Br halide. Therefore, addition of homogeneous Et_4NBr catalysts was necessary to increase the catalytic activity (85% and 78% yields obtained after 2nd and 3rd runs). In another case, Lu *et al.* demonstrated the ability for immobilized metal complex (Co-Salen) to be effectively used in a flow rector for continuous cycloaddition reaction.[84]

Table 10: *Experimental parameters of cycloaddition reaction using CO_2 and supported Salen catalysts*

Entry	Co-catalyst	Catalyst	Substrate	T (°C)	t (h)	P (bar)	Yield (%)	Ref.
1	Cr-salen (a)	-	SO	80	6	100	74	[82]
2	Cr-salen (b)	-	SO	80	6	100	59	[82]
3	Cr-salen (c)	-	PO	140	3	35	30	[81]
4	Cr-salen (d)	-	PO	140	3	35	41	[81]
5	Mn-salen (e)	Et_4NBr	SO	140	3	35	6	[83]
6	Mn-salen (f)	Et_4NBr	SO	140	3	35	95	[83]

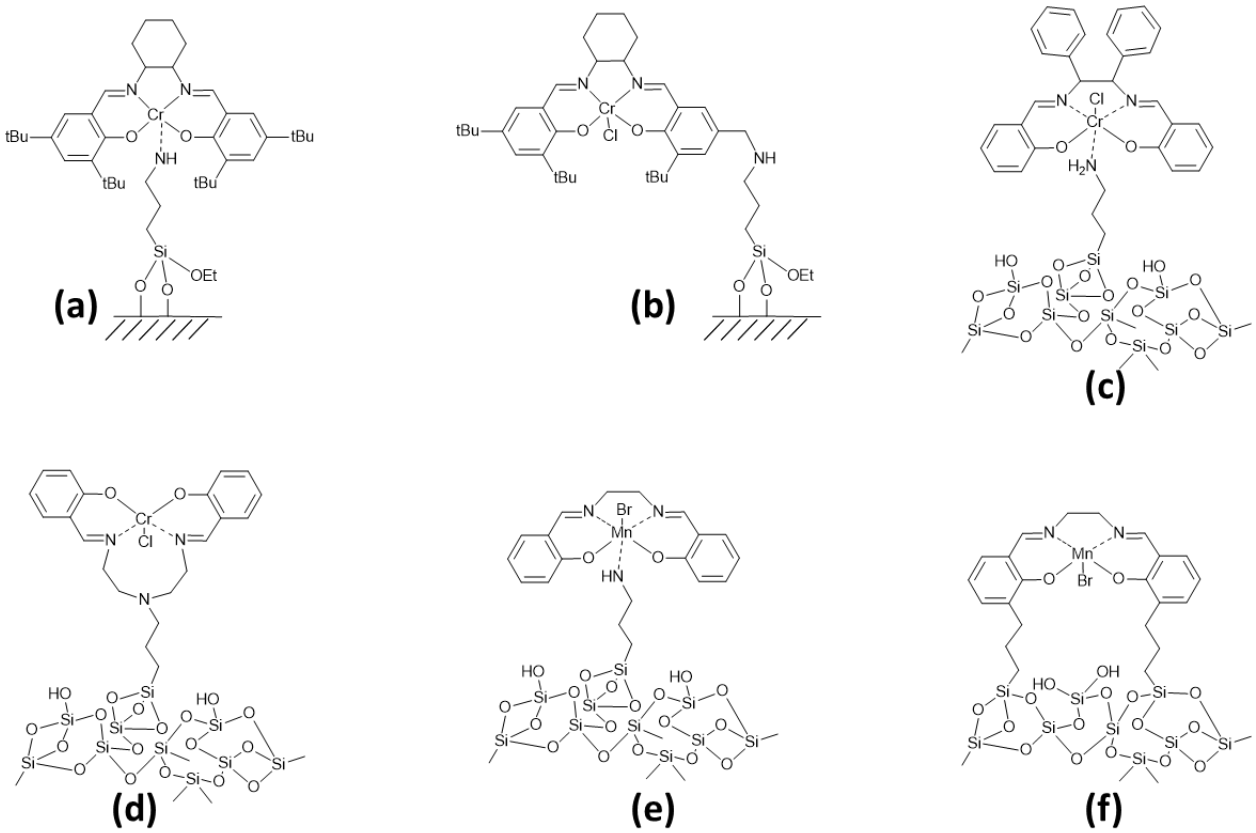

Figure 28: *Recent examples of supported Salen catalysts over functionalized silica support SBA-15*

II.4.3 Impact of hydroxy group activation

The acceleration of the cycloaddition reaction was sometimes mentioned upon immobilization of cycloaddition catalysts onto silica surface. The presence of acidic surface silanol groups interacting with the epoxide substrate could lead to the activation of this substrate before the nucleophilic attack that led to the ring opening. Sakakura *et al* thus observed the reaction acceleration of cycloaddition on propylene oxide using quaternary phosphonium salts supported on silica support.[85] As seen in **Figure 29**, supported phosphonium halide showed enhanced catalytic performance compared to their homogeneous equivalent. For example, only 4% yield of carbonate product was obtained with homogeneous Bu_4PBr catalyst after 1h reaction at 100°C under 100 bar of CO_2. Yield subsequently increased to 53% when supported catalyst has been used instead.

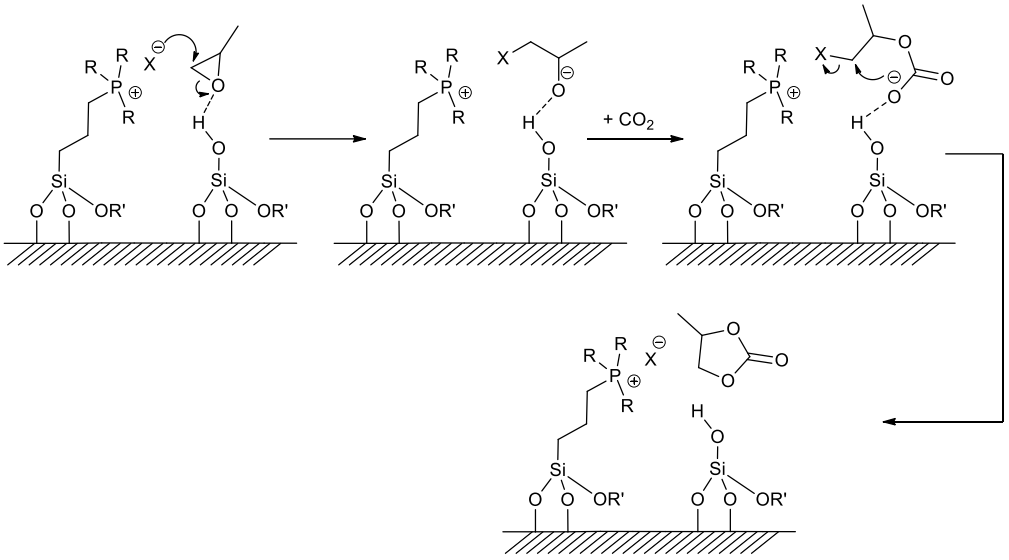

Figure 29: Possible mechanism for cycloaddition of CO2 to PO over {R_4PX}-SBA-15

Oher works were able to confirm this assumption. For instance, the catalytic activity of amine groups supported on silica support SBA-15 was investigated by Zhang et al. [60]. According to this study, the catalytic performances increased with the amine group basicity: [NH_2} < $NH(CH_2)_2NH_2$ < TBD. In the case of {TBD}-SBA-15, propylene carbonate was obtained with 99% yield after 20h reaction at 120°C under 20 bar of CO_2. Furthermore, the authors found that when the surface of the support was modified to remove the surface hydroxyl groups, the yield of carbonate severely dropped to 0.2% under the same reaction condition. According to the authors, this observation strongly suggested the implication of silanol groups in the cycloaddition reaction.

II.4.4 Impact of amines group over catalytic activity

According to Figure 30, the formation of activated CO_2 carbamate zwitterion occurred on the basic amine sites at the surface of amino-functionalized supports such as {NH_2}-SBA-15. Srivastava *et al.* showed that the carbamate formed at the surface of primary amines tends to be the most stable, followed as so by those formed with secondary and tertiary amines: primary > secondary > tertiary.[86] As seen in **Figure 30**, this is due to the formation of a neutral “carbamic acid” form, which exists in equilibrium with the corresponding zwitterionic carbamate anions in the case of the H-bearing primary and secondary amines. Such an equilibrium is therefore not possible on tertiary amines since there is no H-atom attached to

the tertiary N atom.[49,87] The presence of activated carbamate species was observed by *in situ* IR spectroscopy in the case of the H-bearing primary and secondary amines. Intensity of the corresponding peaks of bicarbonate anion HCO_3^- near 1640 and 835 cm^{-1} at depended on several parameters such as the CO_2 pressure (the higher the better) or the temperature.[88] Low temperature increased the adsorbed CO_2 concentration (T_{max} for CO_2 desorption is the lowest for tertiary amines) and the stability of the corresponding carbamate form- Hence, the lifetime of carbamate species formed on tertiary amine was found significantly shorter, making them undetected by IR spectroscopy.

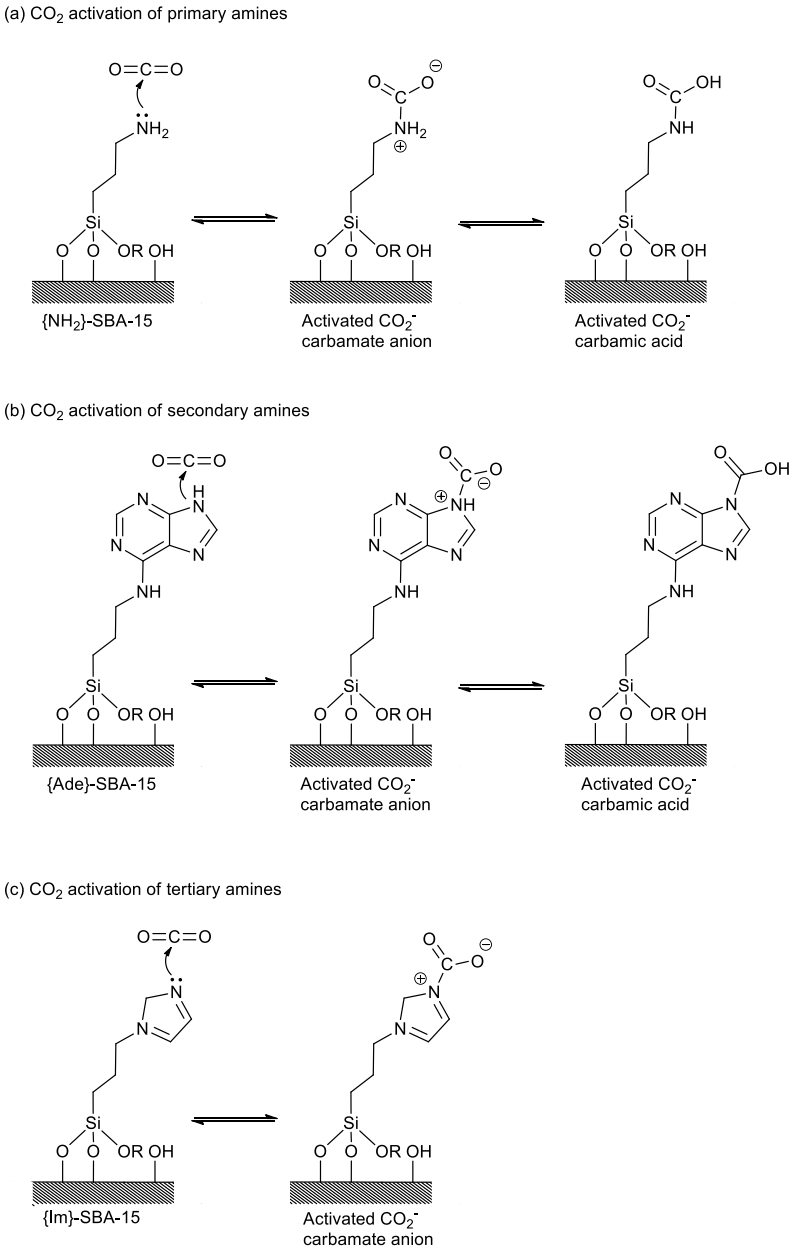

Figure 30: *CO_2 activation through primary, secondary, and tertiary amines*

II.5 Conclusion

Cyclic carbonates are an important class of organic compounds. Using CO_2 as a green substitute for the industrial utilization of phosgene constitutes a promising way for its valorization. Utilization of CO_2 as C1 material constitutes a solution to decrease its concentration in the atmosphere as well as constituting a durable way of synthesizing high-value organic compounds.

This reaction requires the use of dual catalysts systems, most seen are quaternary ammonium salt associated with various metallic complexes, in order to obtain milder experimental reaction conditions.

Among all metallic complexes, Schiff base-type salen or salophen complexes 2N2O associated with *n*-Bu_4NBr main catalyst are able to efficiently catalyse the cycloaddition reaction of styrene oxide into cyclic carbonate using CO_2. According to recent studies, the process efficiency (substrate conversion and cyclic carbonate selectivity) is controlled by several parameters: presence of a nucleophilic source, presence of a H-bond donor group, strength of the ionic interaction between the onium and halide groups, reaction conditions such as temperature, CO_2 pressure, reaction time and molar ratios. It was demonstrated that in the case of supported catalysts, active groups present at the surface (hydroxy or amine) could greatly enhance the overall reactivity.

Best catalytic systems generally involved the use of tetrabutylammonium halide *n*-Bu_4NX, with preferred halide groups being either bromide or iodine atom. A large variety of metal organic catalysts were successfully used as Lewis acid co-catalyst such as Salen and Salophen complexes. This family of complexes actually has the great advantage of being easily synthesized and functionalized. High yields of carbonates may thus be obtained in mild conditions such as room temperature or under 1 bar of CO_2 pressure, using catalyst with 5% molar concentration.

Cycloaddition reaction relies on the utilization of homogeneous quaternary onium salts in solution, which could be improved by grafting them at the surface of silica support. Dual utilization of supported catalyst and co-catalyst would play an important role in the upcoming improvement of such catalytic systems. In addition, a crucial point still to be

considered is to determine the feasibility of such system to effectively reduce CO_2 emissions: Why bother utilizing CO_2 as C1 material if the process itself reject even more CO_2? Great efforts shall be made to obtain a negative carbon balance within the implementation of a catalytic process, by lowering temperature and pressure conditions as well as the time reaction.

References

[1] D. Chareyron, H. Horsin-Molinaro, B. Multon, Concepts et chiffres de l'énergie : émissions de CO_2, http://culturesciencesphysique.ens-lyon.fr/ressource/chiffres-energie-CO2-monde.xml, *Cult. Sci. Phys.*, (**2020**),.

[2] P. Glen, How much carbon dioxide can we emit?, https://www.cicero.oslo.no/en/posts/climate-news/how-much-carbon-dioxide-can-we-emit, *CICERO.*, (**2017**),.

[3] Our world in data: https://ourworldindata.org/grapher/co2-concentration-long-term, (**2018**),.

[4] J.-M. Jancovici, Le Changement climatique expliqué à ma fille, **2009**.

[5] C. Mora, B. Dousset, I.R. Caldwell, F.E. Powell, R.C. Geronimo, C.R. Bielecki, C.W.W. Counsell, B.S. Dietrich, E.T. Johnston, L. V. Louis, M.P. Lucas, M.M. Mckenzie, A.G. Shea, H. Tseng, T.W. Giambelluca, L.R. Leon, E. Hawkins, C. Trauernicht, Global risk of deadly heat, *Nat. Clim. Chang.*, (**2017**), 7, 501–506.

[6] D. Roberts, R. Pidcock, Y. Chen, S. Connors, M. Tignor, IPCC Report 2019: Global warming of 1.5°C, *IPCC.*, (**2019**),.

[7] P. Sadorsky, Energy related CO_2 emissions before and after the financial crisis, *Sustain.*, (**2020**), 12,.

[8] J.-M. Jancovici, A quand le pic de production mondial pour le pétrole ?: https://jancovici.com/transition-energetique/petrole/a-quand-le-pic-de-production-mondial-pour-le-petrole/, (**2014**),.

[9] A. Lopez, D. Roizard, E. Favre, A. Dufour, Les procédés de capture du CO2. Cas des unités de traitement et de valorisation thermique des déchets. Etat de l'art., *ETUDE N° 11-0236/1A.*, (**2013**), 1–22.

[10] B. Durand, Captage et stockage du gaz carbonique (CSC), *NCL Collect. Store.*, (**2011**), 1–32.

[11] M. Aresta, I. Tommasi, Carbon dioxide utilization in the chemical industry, *Energy Convers. Manag.*, (**1997**), 38, 373–378.

[12] M. Aresta, A. Dibenedetto, A. Angelini, The changing paradigm in CO_2 utilization, *J. CO_2 Util.*, (**2013**), 3–4, 65–73.

[13] S.-M. Shih, C.-S. Ho, Y.-S. Song, J.-P. Lin, Kinetics of the Reaction of $Ca(OH)_2$ with CO_2 at Low Temperature, *Ind. Eng. Chem. Res.*, (**1999**), 38, 1316–1322.

[14] A. Rozhentsev, C.-C.C. Wang, Some design features of a CO_2 air conditioner, *Appl. Therm. Eng.*, (**2001**), 21, 871–880.

[15] M.J.E. van Roosmalen, M. van Diggelen, G.F. Woerlee, G.J. Witkamp, Dry-cleaning with high-pressure carbon dioxide—the influence of mechanical action on washing-results, *J. Supercrit. Fluids.*, (**2003**), 27, 97–108.

[16] J. Daniels, R. Krishnamurthi, S. Rizvi, A Review of Effects of Carbon Dioxide on Microbial Growth and Food Quality, *J. Food Prot.*, (**1985**), 48, 532–537.

[17] H. Peker, M.P. Srinivasan, J.M. Smith, B.J. McCoy, Caffeine extraction rates from coffee beans with supercritical carbon dioxide, *AIChE J.*, (**1992**), 38, 761–770.

[18] A. Aresta, Michele; Quaranta, Eugenio; Tommasi, Immacolata; Giannoccaro, Potenzo; Ciccarese, Enzymic versus chemical carbon dioxide utilization. Part I. The role of metal centers in carboxylation reactions, *Gazz. Chim. Ital.*, (**1995**), 125, 509–538.

[19] A. Abd, Nanotechnology: Science and Application, **2019**.

[20] M. Aresta, A. Dibenedetto, E. Quaranta, Reaction Mechanisms in Carbon Dioxide Conversion, **2016**.

[21] T.E. Müller, W. Leitner, CO_2 chemistry, *Beilstein J. Org. Chem.*, (**2015**), 11, 675–677.

[22] B.M. Bhanage, M. Arai, Green Chemistry and Sustainable Technology Transformation and Utilization of Carbon Dioxide, **2014**. http://www.springer.com/series/11661.
[23] M. Aresta, Carbon Dioxide as Chemical Feedstock, **2010**.
[24] W.B. Tolman, Activation of Small Molecules, **2006**.
[25] S. Fujita, M. Arai, B.M. Bhanage, Direct Transformation of Carbon Dioxide to Value-Added Products over Heterogeneous Catalysts, in: B.M. Bhanage, M. Arai (Eds.), Transform. Util. Carbon Dioxide, Springer Berlin Heidelberg, Berlin, Heidelberg, **2014**: pp. 39–53.
[26] P.T. Anastas, D.G. Hammond, Inherent Safety at Chemical Sites: Reducing Vulnerability to Accidents and Terrorism Through Green Chemistry, **2015**. https://books.google.com/books?id=KqDDCQAAQBAJ&pgis=1.
[27] R.Y. WT McShea, Method of methanol production, *US Pat. 4,927,857*., (**1990**),.
[28] G. Rokicki, Aliphatic cyclic carbonates and spiroorthocarbonates as monomers, *Prog. Polym. Sci.*, (**2000**), 25, 259–342.
[29] M. Ratzenhofer, H. Kisch, Metal-Catalyzed Synthesis of Cyclic Carbonates from Carbon Dioxide and Oxiranes, *Angew. Chemie Int. Ed. English*., (**1980**), 19, 317–318.
[30] D.J. Darensbourg, M.W. Holtcamp, Catalysts for the reactions of epoxides and carbon dioxide, *Coord. Chem. Rev.*, (**1996**), 153, 155–174.
[31] J.P. Parrish, R.N. Salvatore, K.W. Jung, Perspectives on Alkyl Carbonates in Organic Synthesis, *Tetrahedron*., (**2000**), 56, 8207–8237.
[32] K.J. Zhu, R.W. Hendren, K. Jensen, C.G. Pitt, Synthesis, properties, and biodegradation of poly(1,3-trimethylene carbonate), (**1991**), 1736–1740.
[33] P. Avramova, L. Dryanovska, Y. Ilarionov, Synthesis and pharmacologic assessment of carbamic and carbonic acid esters with 1-aryl-3-dimethylamino-1-propanols. Part 3, *Pharmazie*., (**1983**), 38, 443—444. http://europepmc.org/abstract/MED/6138779.
[34] S. Fukuoka, M. Kawamura, K. Komiya, M. Tojo, H. Hachiya, K. Hasegawa, M. Aminaka, H. Okamoto, I. Fukawa, S. Konno, A novel non-phosgene polycarbonate production process using by-product CO_2 as starting material, in: Green Chem., **2003**: pp. 497–507.
[35] T. Sakakura, K. Kohno, The synthesis of organic carbonates from carbon dioxide, *Chem. Commun.*, (**2009**), 1312–1330.
[36] M. North, R. Pasquale, C. Young, Synthesis of cyclic carbonates from epoxides and CO_2, *Green Chem.*, (**2010**), 12, 1514–1539.
[37] Hans-Josef Buysch, Carbonic Esters, in: Ullmann's Encycl. Ind. Chem., **2000**: pp. 102–123.
[38] M. Kobayashi, S. Inoue, T. Tsuruta, Diethylzinc-Dihydric Phenol System as Catalyst for the Copolymerization of Carbon Dioxide with Propylene Oxide, *Macromolecules*., (**1971**), 4, 658–659.
[39] S. Inoue, H. Koinuma, T. Tsuruta, Copolymerization of carbon dioxide and epoxide, *J. Polym. Sci. Part B Polym. Lett.*, (**2004**), 7, 287–292.
[40] J. Steinbauer, C. Kubis, R. Ludwig, T. Werner, Mechanistic Study on the Addition of CO_2 to Epoxides Catalyzed by Ammonium and Phosphonium Salts: A Combined Spectroscopic and Kinetic Approach, *ACS Sustain. Chem. Eng.*, (**2018**), 6, 10778–10788.
[41] H. Büttner, L. Longwitz, J. Steinbauer, C. Wulf, T. Werner, Recent Developments in the Synthesis of Cyclic Carbonates from Epoxides and CO_2, *Top. Curr. Chem.*, (**2017**), 375, 1–37.
[42] J. Sun, L. Liang, J. Sun, Y. Jiang, K. Lin, X. Xu, R. Wang, Direct Synthetic Processes for Cyclic Carbonates from Olefins and CO_2, *Catal. Surv. from Asia*., (**2011**), 49–54.
[43] B. Zou, C. Hu, Synthesis of Cyclic Carbonates from Alkenyl and Alkynyl Substrates, *Chinese J. Chem.*, (**2017**), 35, 541–550.
[44] X.D. Lang, L.N. He, Green Catalytic Process for Cyclic Carbonate Synthesis from Carbon Dioxide under Mild Conditions, *Chem. Rec.*, (**2016**), 1337–1352.
[45] I. Karamé, S. Zaher, N. Eid, L. Christ, New zinc/tetradentate N4 ligand complexes: Efficient catalysts for solvent-free preparation of cyclic carbonates by CO_2/epoxide coupling, *Mol. Catal.*, (**2018**), 456, 87–95.
[46] J. Sun, J. Ren, S. Zhang, W. Cheng, Water as an efficient medium for the synthesis of cyclic carbonate, *Tetrahedron Lett.*, (**2009**), 50, 423–426.
[47] J. Sun, S.I. Fujita, F. Zhao, M. Arai, Synthesis of styrene carbonate from styrene oxide and carbon dioxide in the presence of zinc bromide and ionic liquid under mild conditions, *Green Chem.*, (**2004**), 6, 613–616.
[48] M.M. Dharman, J.I. Yu, J.Y. Ahn, D.W. Park, Selective production of cyclic carbonate over polycarbonate using a double metal cyanide–quaternary ammonium salt catalyst system, *Green Chem.*, (**2009**), 11, 1754–1757.
[49] R. Srivastava, D. Srinivas, P. Ratnasamy, Zeolite-based organic-inorganic hybrid catalysts for phosgene-

free and solvent-free synthesis of cyclic carbonates and carbamates at mild conditions utilizing CO_2, *Appl. Catal. A Gen.*, (**2005**), 289, 128–134.
[50] S. H., Die technische Herstellung von Äthylencarbonat, *Fette, Seifen, Anstrichm.*, (**1971**), 73, 396–399.
[51] W.J. Peppel, Preparation and Properties of the Alkylene Carbonates, *Ind. Eng. Chem.*, (**1958**), 50, 767–770.
[52] P. Lozano, J.M. Bernal, E. Garcia-Verdugo, G. Sanchez-Gomez, M. Vaultier, M.I. Burguete, S. V. Luis, Sponge-like ionic liquids: a new platform for green biocatalytic chemical processes, *Green Chem.*, (**2015**), 17, 3706–3717.
[53] E. García-Verdugo, B. Altava, M.I. Burguete, P. Lozano, S. V. Luis, Ionic liquids and continuous flow processes: a good marriage to design sustainable processes, *Green Chem.*, (**2015**), 17, 2693–2713.
[54] P.T. Anastas, P. Wasserscheid, A. Strak, Handbook of Green Chemistry: Vol. 6 Green Solvents: Ionic Liquids, Wiley-VCH, Wiley-VCH, **2010**.
[55] R.D. Rogers, K.R. Seddon, Ionic Liquids--Solvents of the Future?, *Science (80-.).*, (**2003**), 302, 792–793.
[56] Q. Zhang, K. De Oliveira Vigier, S. Royer, F. Jérôme, Deep eutectic solvents: syntheses, properties and applications, *Chem. Soc. Rev.*, (**2012**), 41, 7108.
[57] T. Welton, Room-Temperature Ionic Liquids. Solvents for Synthesis and Catalysis, *Chem. Rev.*, (**1999**), 99, 2071–2084.
[58] K. Yamaguchi, K. Ebitani, T. Yoshida, H. Yoshida, K. Kaneda, Mg-Al mixed oxides as highly active acid-base catalysts for cycloaddition of carbon dioxide to epoxides, *J. Am. Chem. Soc.*, (**1999**), 121, 4526–4527.
[59] Y. Shen, W. Duan, M. Shi, Phenol and Organic Bases Co-Catalyzed Chemical Fixation of Carbon Dioxide with Terminal Epoxides to Form Cyclic Carbonates, *Adv. Synth. Catal.*, (**2003**), 345, 337–340.
[60] K. Kossev, N. Koseva, K. Troev, Calcium chloride as co-catalyst of onium halides in the cycloaddition of carbon dioxide to oxiranes, *J. Mol. Catal. A Chem.*, (**2003**), 194, 29–37.
[61] T. Yano, H. Matsui, T. Koike, H. Ishiguro, H. Fujihara, M. Yoshihara, T. Maeshima, Magnesium oxide-catalysed reaction of carbon dioxide with an epoxide with retention of stereochemistry, *Chem. Commun.*, (**1997**), 1129–1130.
[62] C. Villiers, J.-P. Dognon, R. Pollet, P. Thuéry, M. Ephritikhine, An Isolated CO_2 Adduct of a Nitrogen Base: Crystal and Electronic Structures, *Angew. Chemie*., (**2010**), 122, 3543–3546.
[63] E.R. Pérez, R.H.A. Santos, M.T.P. Gambardella, L.G.M. De Macedo, U.P. Rodrigues-Filho, J.C. Launay, D.W. Franco, Activation of carbon dioxide by bicyclic amidines, *J. Org. Chem.*, (**2004**), 69, 8005–8011.
[64] M. Yoshida, Y. Komatsuzaki, M. Ihara, Synthesis of 5-vinylideneoxazolidin-2-ones by DBU-mediated CO_2-fixation reaction of 4-(benzylamino)-2-butynyl carbonates and benzoates, *Org. Lett.*, (**2008**), 10, 2083–2086.
[65] H.A. Duong, T.N. Tekavec, J. Louie, Reversible carboxylation of N-heterocyclic carbenes, *Chem. Commun.*, (**2004**), 4, 112–113.
[66] L. Wang, G. Zhang, K. Kodama, T. Hirose, An efficient metal- and solvent-free organocatalytic system for chemical fixation of CO_2 into cyclic carbonates under mild conditions, *Green Chem.*, (**2016**), 18, 1229–1233.
[67] J.A. Castro-Osma, K.J. Lamb, M. North, Cr(salophen) Complex Catalyzed Cyclic Carbonate Synthesis at Ambient Temperature And Pressure, *ACS Catal.*, (**2016**), 6, 5012–5025.
[68] T.-T. Wang, Y. Xie, W.-Q. Deng, Reaction Mechanism of Epoxide Cycloaddition to CO_2 Catalyzed by Salen-M (M = Co, Al, Zn), *J. Phys. Chem. A*., (**2014**), 118, 9239–9243.
[69] C. Maeda, J. Shimonishi, R. Miyazaki, J. Hasegawa, T. Ema, Highly Active and Robust Metalloporphyrin Catalysts for the Synthesis of Cyclic Carbonates from a Broad Range of Epoxides and Carbon Dioxide, *Chem. – A Eur. J.*, (**2016**), 22, 6556–6563.
[70] D. De, A. Bhattacharyya, P.K. Bharadwaj, Enantioselective Aldol Reactions in Water by a Proline-Derived Cryptand and Fixation of CO_2 by Its Exocyclic Co(II) Complex, *Inorg. Chem.*, (**2017**), 56, 11443–11449.
[71] J.A. Castro-Osma, C. Alonso-Moreno, A. Lara-Sánchez, J. Martínez, M. North, A. Otero, Synthesis of cyclic carbonates catalysed by aluminium heteroscorpionate complexes, *Catal. Sci. Technol.*, (**2014**), 4, 1674–1684.
[72] C.Y. Li, Y.C. Su, C.H. Lin, H.Y. Huang, C.Y. Tsai, T.Y. Lee, B.T. Ko, Synthesis and characterization of trimetallic cobalt, zinc and nickel complexes containing amine-bis(benzotriazole phenolate) ligands: Efficient catalysts for coupling of carbon dioxide with epoxides, *Dalt. Trans.*, (**2017**), 46, 15399–15406.
[73] J. Sun, S.I. Fujita, B.M. Bhanage, M. Arai, One-pot synthesis of styrene carbonate from styrene in tetrabutylammonium bromide, in: Catal. Today, **2004**: pp. 383–388.
[74] H. Xie, S. Li, S. Zhang, Highly active , hexabutylguanidinium salt / zinc bromide binary catalyst for the coupling reaction of carbon dioxide and epoxides, *J. Mol. Catal. A Chem.*, (**2006**), 250, 30–34.

[75] M. Alves, B. Grignard, R. Mereau, C. Jerome, T. Tassaing, C. Detrembleur, Organocatalyzed coupling of carbon dioxide with epoxides for the synthesis of cyclic carbonates: Catalyst design and mechanistic studies, *Catal. Sci. Technol.*, (**2017**), 7, 2651–2684.

[76] Y. Xie, Z. Zhang, T. Jiang, J. He, B. Han, T. Wu, K. Ding, CO_2 cycloaddition reactions catalyzed by an ionic liquid grafted onto a highly cross-linked polymer matrix, *Angew. Chemie - Int. Ed.*, (**2007**), 46, 7255–7258.

[77] S. Ghazali-Esfahani, H. Song, E. Păunescu, F.D. Bobbink, H. Liu, Z. Fei, G. Laurenczy, M. Bagherzadeh, N. Yan, P.J. Dyson, Cycloaddition of CO_2 to epoxides catalyzed by imidazolium-based polymeric ionic liquids, *Green Chem.*, (**2013**), 15, 1584–1589.

[78] S. Udayakumar, M.K. Lee, H.L. Shim, S.W. Park, D.W. Park, Imidazolium derivatives functionalized MCM-41 for catalytic conversion of carbon dioxide to cyclic carbonate, *Catal. Commun.*, (**2009**), 10, 659–664.

[79] W. Cheng, X. Chen, J. Sun, J. Wang, S. Zhang, SBA-15 supported triazolium-based ionic liquids as highly efficient and recyclable catalysts for fixation of CO_2 with epoxides, *Catal. Today*., (**2013**), 200, 117–124.

[80] C. Baleizão, B. Gigante, M.J. Sabater, H. Garcia, A. Corma, On the activity of chiral chromium salen complexes covalently bound to solid silicates for the enantioselective epoxide ring opening, *Appl. Catal. A Gen.*, (**2002**), 228, 279–288.

[81] M. Ramin, F. Jutz, J.-D.D. Grunwaldt, A. Baiker, Solventless synthesis of propylene carbonate catalysed by chromium-salen complexes: Bridging homogeneous and heterogeneous catalysis, *J. Mol. Catal. A Chem.*, (**2005**), 242, 32–39.

[82] M. Alvaro, C. Baleizao, D. Das, E. Carbonell, H. García, CO_2 fixation using recoverable chromium salen catalysts: use of ionic liquids as cosolvent or high-surface-area silicates as supports, *J. Catal.*, (**2004**), 228, 254–258.

[83] F. Jutz, J.D. Grunwaldt, A. Baiker, Mn(III)(salen)-catalyzed synthesis of cyclic organic carbonates from propylene and styrene oxide in "supercritical" CO_2, *J. Mol. Catal. A Chem.*, (**2008**), 279, 94–103.

[84] X.B. Lu, J.H. Xiu, R. He, K. Jin, L.M. Luo, X.J. Feng, Chemical fixation of CO_2 to ethylene carbonate under supercritical conditions: Continuous and selective, *Appl. Catal. A Gen.*, (**2004**), 275, 73–78.

[85] T. Takahashi, T. Watahiki, S. Kitazume, H. Yasuda, T. Sakakura, Synergistic hybrid catalyst for cyclic carbonate synthesis: Remarkable acceleration caused by immobilization of homogeneous catalyst on silica, *Chem. Commun.*, (**2006**), 1664–1666.

[86] R. Srivastava, D. Srinivas, P. Ratnasamy, Sites for CO_2 activation over amine-functionalized mesoporous Ti(Al)-SBA-15 catalysts, *Microporous Mesoporous Mater.*, (**2006**), 90, 314–326.

[87] R. Srivastava, D. Srinivas, P. Ratnasamy, Syntheses of polycarbonate and polyurethane precursors utilizing CO_2 over highly efficient, solid as-synthesized MCM-41 catalyst, *Tetrahedron Lett.*, (**2006**), 47, 4213–4217.

[88] D.J. Heldebrant, P.G. Jessop, C.A. Thomas, C.A. Eckert, C.L. Liotta, The reaction of 1,8-diazabicyclo[5.4.0]undec-7-ene (DBU) with carbon dioxide, *J. Org. Chem.*, (**2005**), 70, 5335–5338.

CHAPTER III

Bibliographic survey of the strategies implemented for the one-pot synthesis of cyclic carbonates from alkenes using CO_2 and green oxidants (part of the review to be submitted)

Bibliographic survey of the strategies implemented for the one-pot synthesis of cyclic carbonates from alkenes using CO_2 and green oxidants

Matthieu Balas,[†,‡] Richard Villanneau,[‡] Franck Launay[†*]

[†] *Sorbonne Université, CNRS UMR 7197, Laboratoire de Réactivité de Surface, Campus Pierre et Marie Curie, 4 Place Jussieu, F-75005, Paris, France*

[‡] *Sorbonne Université, CNRS UMR 8232, Institut Parisien de Chimie Moléculaire, Campus Pierre et Marie Curie, 4 Place Jussieu, F-75005, Paris, France*

ABSTRACT

Cyclic carbonates are key compounds with a large scope of applications. Their one-pot synthesis from cheap and available alkenes using CO_2 and oxidants has gained great attention from an economic perspective. Furthermore, their synthesis under relatively low temperature and CO_2 pressure with oxidants such O_2 and H_2O_2 could lead to a very sustainable preparation route. Over the last two decades, some advances have been made in the development of catalytic systems affording the reaction of CO_2 with epoxides under mild conditions which is a prerequisite for the whole process. This review covers the state of art of the one-pot synthesis of cyclic carbonates from alkenes, CO_2 and oxidants with a focus on catalysts working under moderate temperature and low CO_2 pressure in the presence of green reagents such as O_2 and, to a lesser extent, H_2O_2. Procedures leading to a step economic pathway will be especially emphasized. Furthermore, the interest and the implementation of the possible catalytic systems involving the two steps leading to an oxidative carboxylation of alkenes (*i.e.* auto-tandem *vs.* orthogonal catalysis or one-pot catalysis) are key issues that will be addressed in this review.

Keywords: Carbon dioxide; Alkenes; Dioxygen; Hydrogen peroxide; Cyclic carbonates; Epoxidation; One-pot reaction

III.1 Introduction

CO_2, which is a very stable molecule ($\Delta_f G^\circ$ = -396 kJ/mol)[1] and has long been considered as a "spent" form of carbon. Nevertheless, CO_2 is utilised in nature, the most well-known reaction being photosynthesis, which converts carbon dioxide into carbohydrates and dioxygen using energy from sunlight and water. Conversions of CO_2 based on the reduction of carbon [2],[3–8] will not be discussed in this paper. Other reactions where carbon dioxide is incorporated into target chemicals without any change of its carbon oxidation state are carboxylation reactions leading to carbamates (RR'NC(O)OR"), ureas ($(RNH)_2CO$) and carbonates ($(RO)_2CO$). Important organic carbonates include dimethyl carbonate, diphenyl carbonate, ethylene carbonate, propylene carbonate as well as poly-carbonates[9,10],[11]. Cyclic carbonates, targeted by this review, are widely used in the manufacture of industrial products such as solvents, paint-strippers, lithium batteries, and biodegradable packaging[12–14]. They also have application in the medicinal chemistry, such as in controlled drug release[15], surgical implant substances[16], or even as anti-depressant.[17] With the progresses of an inherently safer green chemistry[18], CO_2 is a very interesting alternative to replace phosgene $C(O)Cl_2$, another source of C(IV) which is more reactive but which is a toxic reagent[19]. Recycling this "waste" carbon into new valuable compounds and thus, offering a much less environmentally impacting technology than the previous ones is a nice objective[20].

Cycloaddition of CO_2 to epoxides to produce cyclic carbonates catalysed by quaternary ammonium salts is a 100% atom-economical efficient process that has been industrialized for more than 40 years[21],[22]. Nowadays, new catalysts have been developed for this reaction enabling milder conditions that are compatible with the oxidation of alkenes. As the result, the present review is focused on recent works dealing with the combination of the epoxidation of alkenes and the further reaction of the oxiranes with CO_2 in the same pot (direct synthesis of cyclic carbonates from alkenes)[23–25]. Thereby, this review is divided into three main sections. First, the different strategies implemented to carry out the multi-step reaction to produce five-membered cyclic carbonate from alkenes will be fully developed. Then, the general process state-of-art involving the use of hydroperoxide as oxidant and

homogenous ammonium salt catalyst will be presented. Finally, alternative processes using O_2 as oxidant and new supported carboxylation catalyst will be detailed in the last part.

III.2 Some guides for the direct synthesis of cyclic carbonates from alkenes

Coupling of CO_2 with an epoxide, a chemical reaction known since 1969 when Inoue *et al.* combined $ZnEt_2$ (catalyst), water, CO_2 and propylene oxide[26,27], is much more environment friendly (no waste, no toxicity) than the conversion of the same epoxide into an intermediate diol that later reacts with phosgene (figure 1)[21]. In both routes, epoxides are used as starting materials but alkenes can be considered as more interesting due to their better availability[28] and so, lower price, thus encouraging the development of one-pot processes for their conversion into cyclic carbonates in the presence of CO_2 and oxidants.

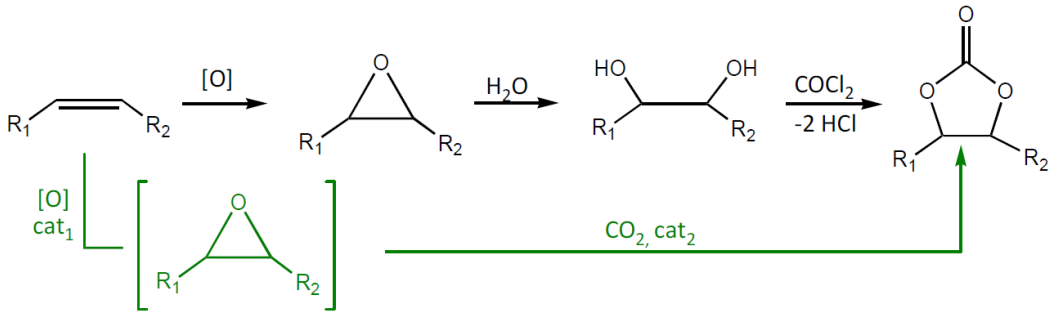

Figure 31: *Initial multi-step synthesis of cyclocarbonate using phosgene compared to the improved route using CO_2 as C1 source*

Therefore, the direct synthesis of cyclic carbonates from olefins using CO_2 and an oxidant can be considered as a more economic, safe and valuable process due to the lower price and better availability of alkenes[28]. From the literature, typical one-pot methodologies may be classified as a two-steps sequential epoxidation of the olefin and cycloaddition of CO_2 onto the epoxide formed (figure 2, route 1)[29] or as a simultaneous oxidative and carboxylative path (figure 2, route 2)[30–32]. In some cases (use of hypohalites as oxidants), halohydrines are formed instead of epoxides (figure 2, route 3) and transformed into cyclic carbonates by reaction with CO_2[25,33–36]. Nevertheless, due to the stoichiometric

production of HX waste (like for phosgenation), the route 3 will not be further considered in the present review[37].

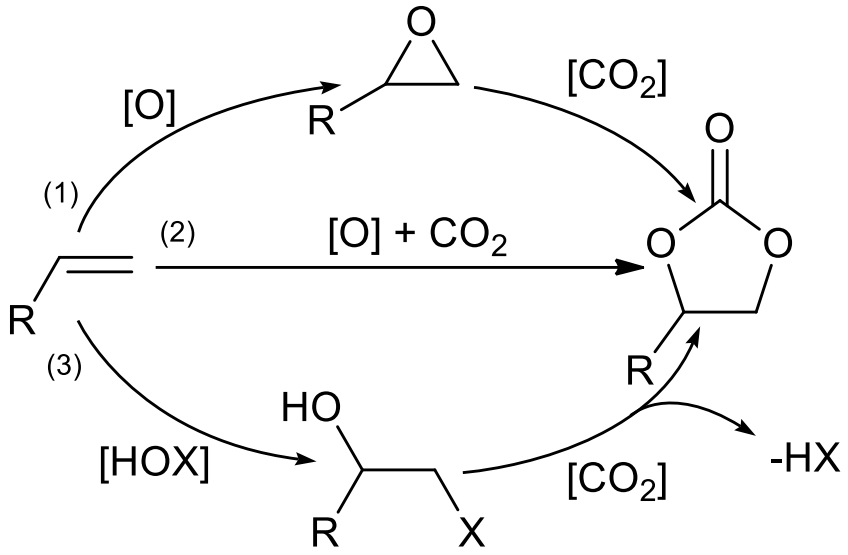

Figure 32: *Synthetic routes to cyclic carbonates from olefins and CO_2*

An overview of the different epoxidation processes will be presented in the next part, followed by the main catalytic systems found in cycloaddition reaction of epoxides. Emphasizes will be made especially on the systems favouring the use of small green molecules O_2 and H_2O_2. Finally, catalysts allowing a global reaction including both oxidation and cycloaddition steps will be presented in a third part.

III.2.1 Different catalysis options for the one-pot synthesis of carbonates from alkenes

The implementation of both oxidative and carboxylative catalytic steps, required for the synthesis of cyclic carbonates from alkenes, into an economic one-pot process, without the need for the isolation of the epoxide intermediate[38] is discussed now. Such a step economy, as defined by Wender *et al.*,[39] should lead to a reduction in the amounts of reagents and solvents, hence, in the waste generated, as well as potentially of the number of catalysts used in some cases.

The concept of “one-pot catalysed processes” comes into at least three sub-categories (Figure 4) as described by Fogg et *al.*[40] At first sight, auto tandem catalysis (**Figure**

33.a) where a single catalyst (here, defined as OxCyCat) is involved in mechanistically distinct reactions (in a single reactor), appears as the most seducing approach. Alternative options are one-pot reaction and orthogonal catalysis, both involving two catalysts, one for each step (respectively OxCat and CyCat). In orthogonal catalysis (**Figure 33.b**), OxCat and CyCat are introduced together at the beginning of the transformation but they work one after the other with a unique set of reaction conditions.[40] On the contrary, in the one-pot reaction (**Figure 33.c**), CyCat is added only once the epoxidation step catalysed by OxCat is complete. As a consequence, reaction conditions may be different for both catalysts.

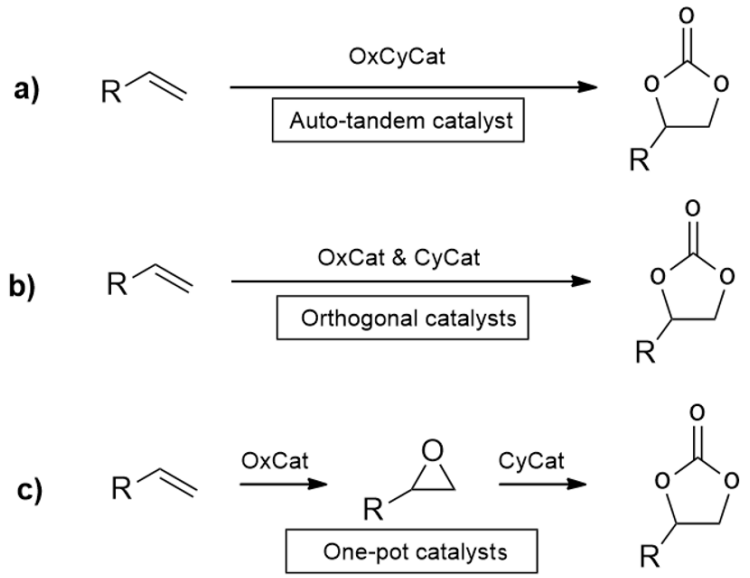

Figure 33: *"One-pot catalysed processes" for styrene carbonate synthesis from styrene via multiple catalytic transformations*

Hence, one-pot catalysis is chosen when the conditions for the optimal performance of OxCat and CyCat are significantly different. For example, the temperature can be modulated in order to improve alkene conversion and the carbonate selectivity. Advantages and disadvantages of the different options are briefly presented in **table 1** in the light of various parameters. Auto-tandem and orthogonal catalysis should be favored as much as possible for efficiency reasons because they allow working with a single set of conditions for both parts of the overall transformation, but the conditions chosen correspond to a compromise when they are very different for each single step, which implies more difficulties in controlling the cyclocarbonate selectivity.

Table 11: *Relative merits of the different classes of "One-pot* catalysed *processes"*

Criteria	Options		
	One-pot reaction	**Orthogonal**	**Auto-tandem**
Efficiency in catalyst utilization	Poor	Poor	High
Ease of catalyst recovery	Poor	Poor	Good
Interaction between catalysts	Possible	Possible	-
Process efficiency	Low	High	High
Capacity to optimize conditions for both catalyses	High	Poor	Poor
Capacity to control selectivity	High	Limited	Limited

In general, one-pot reaction allows a stepwise temperature control and the addition of the cycloaddition catalyst in a timely way, *i.e.* after an optimum formation of the epoxide. Future work on orthogonal catalysis should be encouraged because of the simpler devices required and easier operations.[41] To achieve this, it is necessary to find at once oxidation and cycloaddition catalysts capable of operating under close operating conditions (especially for the temperature).

III.3 Main strategies for the synthesis of cyclic carbonates from alkenes with green oxidants

Direct synthesis of cyclic carbonates from olefins was first described in 1962.[42],[43] As one of the most common olefins used in industry, styrene was explored as a model substrate.[42] In 1987, Aresta *et al*[44] used rhodium complexes such as $[Rh^{I}ClL_2]$ (L_2 = various phosphines or diphosphines) as unique catalysts precursors to accomplish the transformation of styrene to styrene carbonate. With a substrate-to-metal molar ratio of 100, the complete conversion of styrene with a carbonate yield of 25% could be achieved under mild conditions (CO_2/O_2 mix pressure = 0.5 bar each, temperature = 40°C) in tetrahydrofuran. It is noteworthy that this reaction occurred without the use of a quaternary ammonium salt. Styrene oxide was nevertheless obtained as well as benzaldehyde probably as the result of some competitive oxidative cleavage of the styrene double bond. The product distribution was strongly influenced by the solvent, as well as by the O_2/CO_2 pressure and reaction

temperature, with carbonate production better achieved working at low pressure and at temperature close to 40°C. Interestingly, mechanism studies showed that the *in situ* isolation of the styrene oxide intermediate was not necessary for the synthesis of the cyclocarbonate, due to the ability of the noble metal based-complex to catalyse the overall transformation (auto-tandem catalysis?). Such example involves what might be an ideal combination of reagents, *i.e.* O_2 and CO_2. However, it has to be admitted that the choice of O_2 as the oxidant for the whole oxidative carboxylation process is not the most widespread in the literature. Indeed, organic hydroperoxides or hydrogen peroxide are generally more often involved because affording a better control of the selectivity in the epoxide intermediate formation. Main catalytic systems using either organic hydroperoxides, then hydrogen peroxide will be reviewed in the following paragraphs (see also **Table 2**).

III.3.1 Synthesis of styrene carbonate using CO_2 and organic hydroperoxides

The use of CO_2 and organic hydroperoxides as reactants for the direct synthesis of cyclic carbonates (here, styrene carbonate) from alkenes (here, styrene) is obvious as the result of the progress made on the design of efficient epoxidation catalysts, the latter being combined with quaternary ammonium salts and, especially *n*-Bu_4NBr, themselves associated with a co-catalyst.

One well-known example described in 2005 deals with the combination of *n*-$Bu_4NBr/ZnBr_2$ (CyCat) with Au catalyst supported on silica[45] (**Table 12**, **entry 2**) or on $Fe(OH)_3$ (OxCat) (**Table 12**, **entry 3**) used in the presence of *tert*-butyl hydroperoxide (TBHP).[45] With Au/SiO_2 and *n*-$Bu_4NBr/ZnBr_2$ at 80°C, the CO_2 pressure was rather low (10 bar) and the overall yield of styrene carbonate modest (36%). Besides Au(0), various metal-based (Ti^{III}, Mn^{III}, Mo^{II}, Re^{III}, Cr^{III} or Fe^{II}) homogeneous or heterogeneous epoxidation catalysts (OxCat) also working with TBHP have been associated to quaternary ammonium salts (see **Table 12**). Most of them emphasized excellent styrene conversions but moderate styrene carbonate yields (between 33 and 68%). It is noteworthy that weak yields in styrene carbonate are often related to the formation of side products such as benzaldehyde, phenyl acetaldehyde and styrene glycol (see **Figure 34**). Styrene glycol would be obtained by the reaction of residual water with styrene

oxide,[46] whereas benzaldehyde would be formed from the oxidative C=C cleavage of styrene.[47,48]

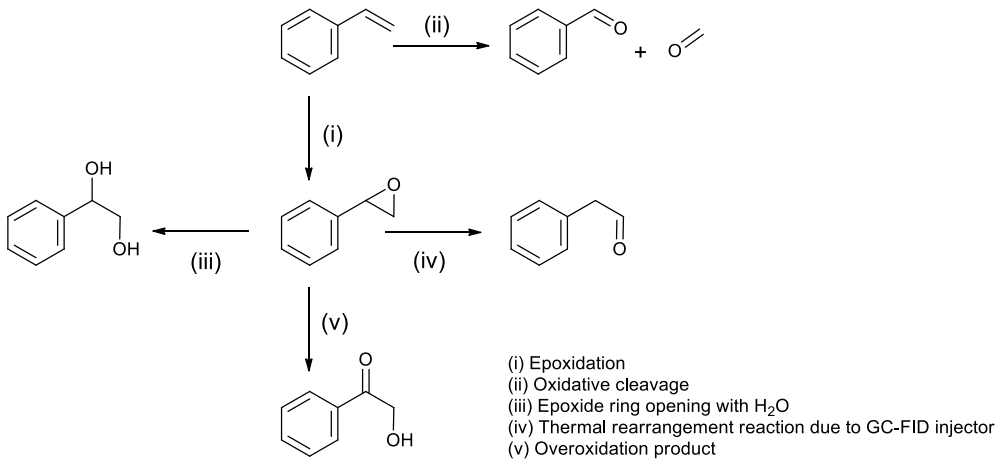

Figure 34: *Main products obtained from styrene epoxidation reaction*

Heterogeneous oxidation catalysts bearing Ti-sites on the surface of mesoporous silica known to be efficient with *tert*-butyl hydroperoxide have of course been investigated.[47,48] Using TBHP and CO_2, Srivastava, Kholdeeva and Evangelisti[29,49]′[50] (**Table 12**, **entry 4-6)** obtained styrene carbonate in the presence of a mesoporous titanium-silicate material (Ti-MCM-41[45], Ti-MMM-E[166] or Ti_nO_x-MMM-2[50]), and DMAP[45] or *n*-Bu_4NBr[166,][50] as cycloaddition catalysts in orthogonal catalysed-processes. The best yield in styrene carbonate was reached by Evangelisti *et al*. (67%) at 70°C under 8 bar of CO_2 but it has to be noted that the molar ratios of Br : Ti : styrene ratio remain pretty low 1 : 5 : 10, resulting in a poor TON_{Ti} of 1.3.

Metal complexes were also studied as homogeneous epoxidation catalysts in parallel, most of them being tested in one-pot catalysed processes. The only example of orthogonal process was described by Ramidi *et al.*[51] who used a amido-amine manganese (III)-chloro 4N-complex coupled with *n*-Bu_4NBr at 100°C under 17 bar of CO_2 for the direct oxidative carboxylation of styrene **(Table 12, entry 7)**. Detailed investigations showed that a stable manganese(V)=O was formed and capable of transferring an oxygen atom from various oxidants (such as TBHP or H_2O_2) onto styrene. TBHP was found to be the most active oxidant for the production of styrene carbonate with 34% yield (11% with H_2O_2) for 6h. Before introducing the catalysts required for the CO_2 cycloaddition, Chen[32] (**Table 12, entry 8**), then Siewniak[52] (**Table 12, entry 9**) used $[MoO_2(acac)_2]$ for the epoxidation step with TBHP at

100°C. Chen utilized *n*-Bu_4NBr alone for the cycloaddition step leading to a styrene carbonate yield of 68% with both high temperature and CO_2 pressure (140°C, P_{CO2} = 30 bar). Siewniak used instead an immobilized tributylmethylammonium chloride (TBMAC) with $ZnBr_2$ as co-catalyst and thus obtained a similar styrene carbonate yield (67%) but with milder reaction conditions (100°C, p_{CO2} = 9 bar). The example described by Siewniak[169] is indeed the first report of a supported ammonium salt, in this case using polystyrene molecular sieve as a polymeric carrier, for the direct oxidative carboxylation of styrene.

As mentioned earlier, ionic liquids such as N-butyl-N'-methylimidazolium tetrafluoroborate ([BMIm]Br can be used as both solvents and catalysts to synthesize styrene carbonate from styrene oxide in the presence of CO_2[53]. So, it was not surprising that the global reaction from styrene to styrene carbonate has also been carried out in the presence of such compounds. Girard (**Table 12, entry 10**) and Jasiak *et al.*(**Table 12, entry 11**)[54,55] obtain good yields (60-62%) of styrene carbonate at 120 °C under 6 bar of CO_2 in [BMIm]Br Due to the important amount of imidazolium, TOF values were pretty low for these systems.

Chromium terephtalate MIL-101-Cr, which is a metal-organic framework known for its high CO_2 adsorption capacity, was tested by Zalomaeva *et al.* in the presence of *n*-Bu_4NBr for the synthesis of cyclic carbonates from epoxides or olefins (**Table 12 , entry 12**).[56] MIL-101-Cr / *n*-Bu_4NBr led to very good yields of styrene carbonate (up to 82-95%) ~~direct~~ from styrene oxide under 8 bar of CO_2 at 25◦C under solvent-free mild conditions after 24h reaction. However, in the case of the direct oxidative carboxylation of styrene under 8 bar of CO_2 at 25◦C using TBHP as the oxidant and TBABr + Cr-MIL-101 as the catalyst, very poor conversion and yield of 7% (39% conversion) were obtained after 24h reaction. Ambient temperature conditions are probably too low in order to perform the epoxidation. Moreover, MIL-101-Cr, in oxidative conditions, seems to promote the formation of side products, mainly benzaldehyde, and thus reduces the carbonate selectivity. A more recent catalytic system involving the use of Zr-based MOF-892 developed by Nguyen *et al.* (**Table 12, entry 13**) [57] turned out to be very efficient for the one-pot synthesis of styrene carbonate from styrene (100 % conversion, overall yield = 80% after 9h) at 80°C and 1 bar of CO_2 using TBHP as oxidant and *n*-Bu_4NBr. The authors demonstrated the active role of Lewis acid sites on Zr units (acting as co-catalysts for *n*-Bu_4NBr) combined with the (Brønsted) carboxylic acid groups integrated within MOF-892 structure involved in the activation of the epoxide substrate.

Cumene hydroperoxide (CHP) was also tested as an alternative to TBHP. Indeed, CHP is a cheap and stable oxidant obtained from cumene in the presence of O_2 and is widely used in the industry.[37] Mixtures of CHP in excess of cumene can be utilized both as oxidant and solvent. Moreover, the reduced form of CHP, *i.e.* cumyl alcohol, can be easily back converted to cumene in two steps (dehydration, then hydrogenation).[37] Sun *et al*[45] (**Table 12, entry 14**) did replace TBHP (**Table 12, entry 2**) by CHP in order to obtain styrene carbonate in the presence of gold nanoparticles supported on SiO_2 (oxidation catalysts) and of *n*-$Bu_4NBr/ZnBr_2$ (cycloaddition catalysts) at 80°C with 10 bar of CO_2, in solvent-free conditions. Hence, the authors demonstrated that CHP was able to act as an efficient oxidant for this reaction, leading to a final styrene carbonate yield of 43%, slightly higher to the 36% yield obtained with TBHP in the same conditions.

Last but not least, it has to be reminded that *n*-Bu_4NBr can be used as a unique catalyst (tandem catalysis) for the synthesis of cyclic carbonates from alkenes in the presence of TBHP and CO_2 as shown by Sun et al[58] (**Table 12**, **entry 1**). In this case, these authors observed the *in-situ* conversion of Br^- from *n*-Bu_4NBr into hypobromite, BrO^-, by reaction with TBHP, which then affords a bromohydrin intermediate by reaction with alkenes. In a second step, a base-promoted removal of Br^- by intramolecular nucleophilic substitution (after the deprotonation of the hydroxyl group of the bromohydrin) leads to the epoxide, which is finally converted to the corresponding cyclic carbonate by reaction with CO_2. The styrene carbonate yield reached 33% using 1.5 mol% of *n*-Bu_4NBr compared to styrene, at a moderate temperature (80°C) and in solvent-free conditions. However, this reaction requires a very high pressure of CO_2 (150 bar) and generates benzaldehyde as a by-product. Using imidazolium type ionic liquids as solvents, TBHP as oxidant with no added epoxidation and cycloaddition catalysts apparently gives rise to a similar reaction pathway.

Regarding the use of organic hydroperoxides and CO_2 as reagents in the one-pot synthesis of cyclic carbonates from alkenes, the most efficient catalytic systems reported are not implemented in true tandem conditions (only one catalyst) but are involving a soluble quaternary ammonium halides for the cycloaddition and Mo^{VI}, Ti^{IV}, Zr^{IV} (d^0 metals) homogeneous or heterogeneous entities with a strong Lewis acidity for the activation of hydroperoxides that are implemented either in orthogonal (case of Ti^{IV} and Zr^{IV}) or one-pot (case of Mo^{VI}) modes. For conversions closed to 100%, yields of styrene carbonate in the order

of 62-68% and even 80% were obtained for Ti^{IV}, Mo^{VI} and Zr^{IV} (case of a MOF structure). However, these encouraging results appears in drastic conditions reaction, with temperature going from 80 to 150°C and CO_2 pressure from 5 to 30. Co-catalysts were used in small molar quantity (up to 0.1% and 0.5% for Mo and Mn co-catalysts) as seen in **Table 12 entries 7-9**. Efforts must be put to assess a good catalytic activity with low main catalyst TBABr loading which is used in high concentration of 10% in some examples (see **Table 12 entries 5, 6 and 12**). It is noteworthy that none of the reported works involved a true heterogeneous catalytic system.

Table 12: *Synthesis of cyclic carbonates from olefins and CO_2 using either organic hydroperoxides or hydrogen peroxide. DBU : 1,8-Diazabicyclo(5.4.0)undec-7-ene, EMO : Methyl oleate oxide, MO : methyl oleate, PPNCl : Bis(triphenylphosphine)iminium chloride, $ScCO_2$: Supercritical CO_2*

Entry	Reference	Epoxidation catalyst	Oxidant	Cycloaddition catalyst system	Reaction conditions	SC. Yield (conv.) %	Catalytic transformation
1	Sun *et al.*[58]	-	TBHP	*n*-Bu_4NBr	[Bu_4NBr : styrene, 1 : 9 TBHP (1.5 eq.)], 80 °C, 150 bar, 6h	33 (74)	Auto-tandem
2	Sun *et al.*[45]	Au/SiO_2	TBHP	*n*-Bu_4NBr /$ZnBr_2$	[Au : $ZnBr_2$: Bu_4NBr : styrene, 1 : 2 : 3 : 69, TBHP (1.5 eq.)], 80 °C, 10 bar, 6h	36 (90)	Orthogonal
3	Sun *et al.*[59]	$Au/Fe(OH)_3$	TBHP	*n*-$Bu_4NBr/ZnBr_2$	[Au : $ZnBr_2$: Bu_4NBr : styrene, 1 : 2 : 3 : 69, TBHP (1.5 eq.)], 80 °C, 40 bar, 4h	43 (91)	Orthogonal
4	Srivastava *et al.*[29]	TiMCM-41	TBHP	DMAP	[Ti : DMAP : styrene, 1 : 1 : 2200, TBHP (1 eq)], 140 °C, 7 bar, >10h	33 (40)	Orthogonal
5	Kholdeeva *et al.*[49]	Ti-MMM-E	TBHP	*n*-Bu_4NBr	[Ti : Bu_4NBr : styrene, 1 : 5 : 52, TBHP (1.5 eq.)], 70 °C, 80 bar, 48h	64 (92)	Orthogonal
6	Evangelisti *et al.*[50]	TinOx-MMM-2	TBHP	*n*-Bu_4NBr	[Ti : Br : styrene, 1 : 2 : 25, TBHP (1.5 eq.)], 70°C, 8 bar, 24h	67 (99)	Orthogonal
7	Ramidi *et al.*[51]	Mn complex	TBHP	*n*-Bu_4NBr	[Mn : Bu_4NBr : styrene, 1 : 2 : 500, TBHP (1.5 eq)], ACN, 100 °C, 17 bar, 6h	34 (-)	Orthogonal
8	Chen *et al.*[32]	$MoO_2(acac)_2$	TBHP	*n*-Bu_4NBr	(i) [Mo : styrene, 1 : 1000, TBHP (1.1 eq.)], 100 °C, 1 h (ii) [Bu_4NBr : styrene 1 : 20], 140 °C, 30 bar, 1h	68 (99)	One-pot
9	Siewniak *et al.*[52]	$MoO_2(acac)_2$	TBHP	PS-TBMAC/$ZnBr_2$	(i) [Mo : styrene, 1 : 1000], 100 °C, 1 h (ii) [Zn : TBMAC : styrene 1 : 4 : 362], 100 °C, 9 bar, 4h	67 (96)	One-pot
10	Girard *et al.*[54]	-	TBHP	[BMIm]Br	(a) (i) [Br : styrene 1 : 10, TBHP (1.5 eq)], 100°C, 16h (ii) 150 °C, CO_2 5 bar, 6h (b) [Br : styrene 1 : 10, TBHP (1.5 eq)], 150°C, 5 bar, 6h	(a) 62 (99) (b) 36 (90)	(a) One-pot (b) Orthogonal
11	Jasiak *et al.*[55]	Au/CNT	TBHP	[BMIm]Br-$ZnBr_2$	(i) [Au : styrene, 1 : 5], 80 °C, 4 h (ii) [[BMIm]Br : Zn : substrate 22 : 1 : 357], 120 °C, 12 bar, 2h	60 (100)	One-pot
12	Zaloemaeva *et al.*[56]	Cr-MIL-101	TBHP	*n*-Bu_4NBr	[Cr: Bu_4NBr : styrene, 1 : 2 : 20, TBHP (1.5 eq.)] in CH_2Cl_2, 25 °C, 8 bar, 5h	7 (39)	Orthogonal
13	Nguyen *et al.*[50]	MOF-89(Zr)	TBHP	MOF-89(Zr)/ Bu_4NBr	[MOF : styrene : Br : TBHP, 1 : 17 : 33 : 25], 80°C, 1 bar, 9h	80 (100)	Orthogonal
14	Sun *et al.*[45]	Au/SiO_2	CHP	*n*-Bu_4NBr /$ZnBr_2$	[Au : $ZnBr_2$: Bu_4NBr : styrene, 1 : 2 : 3 : 69, TBHP (1.5 eq.)], 80 °C, 10 bar, 6h	43 (75)	Orthogonal
15	Yokoyama *et al.*[60]	MTO [Re]	UHP	Zn[EMIm]2Br4 / [BMIm]BF4.	(i) [Re : styrene, 1 : 50, UHP (1.1 eq.)], 2h, 110°C (ii) [$Zn[EMIm]_2Br_4$], [BMIm]BF_4 solvent, 110 °C, 30 bar, 2h	83 (99)	Orthogonal

16	Srivastava *et al.*[29]	TS-1	H_2O_2 (aq.)	DMAP	[Ti : DMAP : styrene, 1 : 1 : 2200, H_2O_2 (2 eq)], 120 °C, 7 bar, >10h	6 (22)	Orthogonal
17	Doll *et al.*[61]	-	H_2O_2 (aq.) / HC(O)OOH	*n*-Bu_4NBr	(i) [MO : formic acid, 1 : 3, H_2O_2 (2 eq.)], 25 °C (ii) [Bu_4NBr : EMO 1:20], 100 °C, 103 bar, 15h	90 (-)	One-pot
18	Eghbali *et al.*[33]	-	H_2O_2 (aq.)	*n*-Bu_4NBr /DBU	[TBABr : Styrene : DBU, 1 : 10 : 1.3, H_2O_2 (6 eq.)], 50 °C, 18 bar, 15h	70 (89)	Orthogonal
19	Sathe *et al.*[62]	MTO [Re]/3-methyl pyrazole	H_2O_2 (aq.)	Al complex / Bu_4N I	(i) [Re: styrene : 3-MP, 1 : 100 : 24, H_2O_2 (2 eq.)], 40 °C, 30 min (ii) [Al: styrene : Bu_4NI 1 : 44 : 5], 100 °C, 8 bar, 0.66h	88 (98)	One-pot
20	Dias *et al.* [63]	6MnNP@SiO_2	H_2O_2 (aq.)	2CrNP@SiO_2	[Mn : styrene : NH_4OAc, 1 : 600 : 387, H_2O_2 (4 eq.)], ACN, 25°C, 0.75h (ii) [Cr : PPNCl : styrene, 1:1400:1400], 80°C, 10 bar, 24h	70 (99)	One-pot

III.3.2 Synthesis of styrene carbonate using CO_2 and H_2O_2

Much less contributions dealing with the formation of cyclic carbonates from the corresponding alkenes using CO_2 and H_2O_2 as reagents are available in the literature. The first example of styrene carbonate synthesis from styrene using aqueous H_2O_2 was reported by Srivastava et al. in 2003. (**Table 12, entry 16**).[29] In this work, the authors used TS-1 (titanosilicate-1) and DMAP respectively as epoxidation and cycloaddition catalysts. The implementation of the whole process was performed using an orthogonal catalysis approach. Very low styrene conversion (22%) and yield of styrene carbonate (6%) were obtained in these conditions (120°C, 7 bar of CO_2). According to the authors, the presence of H_2O in the reaction mixture had a negative impact on the reaction of epoxide with CO_2 because of the formation of the undesired diol (styrene glycol) as a by-product. Removal of H_2O from the reaction system by using molecular sieves[37] or for example 2,2-dimethoxy propane[37] acting as a dehydration reagent could be an option to obtain higher yield of carbonate.

Hydrogen peroxide, when combined with an organic acid (e.g. formic acid), works quite well to get cyclic carbonates from olefins. Indeed, Doll *et al.* (**Table 12, entry 17**)[61] were able to synthesize carbonated fatty methyl esters using such oxidant in the presence of *n*-Bu_4NBr alone in supercritical CO_2. The methodology implemented was sequential. First, formic acid was mixed with methyl oleate and then H_2O_2 was added leading to the RT epoxidation of the unsaturated fatty methyl ester without the assistance of a catalyst. Afterwards, the epoxide was separated from the reaction mixture and made react with CO_2 and *n*-Bu_4NBr in supercritical CO_2 (100 bar) at 100°C during 20h for the cycloaddition part, affording an excellent carbonate yield of 90%. A few other processes dealing with cycloaddition[64] only or the whole transformation from alkenes to cyclic carbonates[63] using environmentally friendly supercritical CO_2 were also described in the literature.

Although it has been claimed that the presence of water tends to alter the yield of cyclic carbonates from their corresponding olefins, some authors showed recently that H_2O could also be beneficial for an enhanced formation of the cyclic carbonate[65]. Indeed, aqueous hydrogen peroxide is not always leading to deceiving yields of cyclic carbonates as shown, for example, by Eghbali and Li[33] **(Table 12, entry 18)** in an orthogonal approach.

These authors were able to get styrene carbonate with 70% yield at 50°C by the reaction of styrene with H_2O_2 and CO_2 in the presence of *n*-Bu_4NBr and of an organic base, 1,8-diazabicyclo[5.4.0]undec-7-ene (DBU), the latter being used as a "CO_2 activator" due its ability to form an adduct with CO_2. DBU in association with *n*-Bu_4NBr worked much better than DMAP previously used by Srivastava et al. **(Table 12, entries 4 and 16)** and in milder conditions (50°C vs. 120 or 140°C). However, a relatively high CO_2 pressure (18 bar) and long reaction time (15h) were necessary. Using NBS (N-bromosuccinimide) as cycloaddition catalyst precursor instead of TBABr, an even higher yield of styrene carbonate could be reached (89%) at 60°C under 18 bar of CO_2 and in a very short period of time (3h).[33] However, hydrobromic acid was generated during the reaction requiring, in that case, the use of excess amounts of NBS and DBU in order to deprotonate the weakly acidic alcohol and to neutralize hydrobromic acid generated during the reaction. Intermediary bromohydrin specie was in-situ formed before reaction with activated CO_2.

Two-steps processes can also be implemented using fixed bed flow reactors in series as shown by Sathe et al[62] (**Table 12, entry 19**) who worked with the urea-hydrogen peroxide adduct (UHP) instead of conventional aqueous hydrogen peroxide in order to avoid the introduction of water. In that case, methyl trioxorhenium complex (MTO) was contacted first with the reaction medium at 40°C to get the epoxide, then Bu_4NI associated with an amino trisphenolate complexed aluminium[66–68] was involved for the cycloaddition step at 100°C and 8 bar in a kind of "one-pot catalytic" system. Using a membrane separator between organic and aqueous phases, a liquid-liquid separation was utilized to isolate incompatible reagents such as Lewis acid and base, oxidizer, and reductant, with only the initial olefins and corresponding products remaining. In those conditions, styrene carbonate could be produced with an overall yield of 88% after *ca.* one hour (0.5 h for the epoxidation step, and 0.66 h for the cycloaddition step). Other alkenes with higher molecular weight were also tested with a good yield in the corresponding carbonates (>80%). According to the authors, this work was the first to report an overall conversion of alkene into the corresponding cyclocarbonate in such a small period of time. Rather mild temperature conditions (100°C) were used during the cycloaddition step, as well as a moderate pressure of CO_2 (8 bar). However, the homogeneous rhenium catalyst was not easily separated from the reaction mixture, making straightforward

recycling difficult suggesting the implementation of such system with heterogenized catalysts for a better recovery and reuse.[69,70]

Other system involving MTO as oxidant was developed. Yokoyama and co-workers **(Table 12, entry 15**)[60] used the urea/hydrogen peroxide adduct (UHP) instead of aqueous hydrogen peroxide as the oxidant combined with methyltrioxorhenium (MTO, epoxidation catalyst) in [BMIm]Br Both UHP and MTO are soluble in the ionic liquid,[71] and the authors claimed that this good solubility is the key-point for the important styrene carbonate global yield reported (83%). It is noteworthy that this styrene carbonate yield is one of the highest values reported so far in that review. On the opposite, only traces of carbonates were obtained using an aqueous solution of TBHP, which is not miscible with [BMIm]BF_4.[72]

Actually, Dias *et al*[63]. (**Table 12, entry 20)** used both Mn(III) and Cr(III) porphyrin complexes either as homogeneous or immobilized catalysts for the sequential epoxidation of styrene and its derivatives by aqueous H_2O_2 followed by CO_2 cycloaddition onto their epoxides in separately optimized conditions ("one-pot catalysis"). The soluble manganese(III)-porphyrin was used for the epoxidation step while soluble bis(triphenylphosphine)iminium chloride (PPNCl) assisted by the chromium(III)-porphyrin was added in the second step. In these conditions, high olefin conversions (93 to 99% depending on the olefin) were achieved, and fairly good to good carbonate yields generally obtained (in the range 47 to 70 %), under mild conditions (25°C, 0.75 h then 80°C, 10 bar of CO_2 pressure for 24h). Alternatively, both complexes were covalently attached to core-shell silica-coated magnetite nanoparticles. The thus immobilized metalloporphyrin's were then combined and evaluated as sequential heterogeneous bimetallic nano-catalysts for the styrene conversion into styrene carbonate. Manganese MNP (Magnetic Nanoparticle) was collected at the reactor walls with an external magnet before the cycloaddition catalysts PPNCl and Cr MNP were added. Furthermore, the nano catalysts were magnetically separated and successfully reused 3 times, leading however to a slight loss of selectivity in carbonate.

Regarding the global reaction involving the use of hydrogen peroxide studies are scarcer than the ones including the use of TBHP as main oxidant. While keeping the green aspect of the oxidizer, a special effort must be made to promote this kind of system. Even though, we can clearly see encouraging results regarding the overall yield of styrene carbonate and the reaction conditions. As such, a yield of styrene carbonate as high as 70% has been

found in most of the system, with a few able to perform with 88% and higher (see **Table 12 entries 17 and 19**). Most of the systems described involve mild conditions for the oxidation step, with room temperature conditions in the systems developed by Doll (**Table 12 entries 17**) and Dias (**Table 12 entries 20**). The later developed a fully heterogenized system involving Mn and Cr silica nanoparticles. Though, improvement can be made to prevent the use of homogeneous additives NH_4OAc and main catalyst PPNCl. Following cycloaddition step leads then to an increase of the temperature up to 80°C in most system. This binary conditions system found in one-pot catalytic process allow a better optimisation and an overall improvement of the styrene carbonate yield. Somehow, system developed by Eghbali stands out by its relatively mild temperature condition of 50°C found in both steps, still affording an excellent yield of 70%. Overall improvement of the system includes the use of H_2O_2 lower molar equivalents (most of them being 2 or higher) and by the development of a fully heterogenized auto-tandem system able to perform well in both oxidation and cycloaddition steps.

III.3.3 Scope of the olefins tested with H_2O_2 and organic hydroperoxides

Styrene is often considered as a reference in catalytic cycloaddition tests and by extension in the overall transformation of alkenes to cyclic carbonates due to its reasonable activity and the easy quantification of its products by GC, ^{1}H NMR or HPLC with a UV detector. However, styrene is a particular alkene because of the conjugation of its double bond with the aromatic ring and styrene carbonate is not necessarily a compound of strategic interest. New catalytic systems should be evaluated on a wider range of alkenes[63] but such studies are not systematically undertaken. When the scope of olefins is investigated, authors are working either with linear (generally inactivated and terminal) alkenes (1-pentene, 1-hexene, 1-octene), internal[61] or even endocyclic alkenes such as cyclohexene or cyclooctene, the latter being often used as a reference substrate in studies dealing with the development of catalytic oxidation systems.

In general, linear terminal alkenes were found to be less reactive than styrene. In their work with H_2O_2 using an orthogonal approach, Eghbali and Li[33] have compared the reactivity of styrene, hexene and octene using N-bromosuccinimide (NBS) associated to 1,8-

diazabicyclo[5.4.0]undecenc-7-ene (DBU). The respective yields of styrene, hexene and octene carbonates at 50°C under 18 bar of CO_2 were 70%, 47% and 27% (alkene conversion in the range 89% to 72%). Such order of reactivity was confirmed by Ramidi *et al*.[51] who also used an orthogonal approach (17 bar, 100°C) involving a Mn(III) complex, *n*-Bu_4NBr and TBHP. In that case, the styrene, 1-pentene, 1-hexene and 1-octene cyclic carbonates yields reported were 43%, 48%, 47% and 31%, respectively.

Similar alkenes, including also cyclooctene and allyl chloride, were studied by Chen *et al.* in a one-pot approach using CO_2 and TBHP with *n*-Bu_4NBr and $[MoO_2(acac)_2]$ with optimized sets of conditions for both steps (30 bar for CO_2)[32]. Thus, it could be emphasized that experimental conditions have to be adapted depending on the substrates investigated. For example, better yield was obtained for cyclohexene was obtained when the cycloaddition reaction time were set to 6h instead of 1h, leading to an increase from 33 to 84% yield in the corresponding carbonate. In the case of the allyl chloride alkene, it was the epoxidation temperature set at 70°C instead of 100°C that led to an increase of yield from 45 to 80% after 2h reaction. With this approach, excellent overall yields were obtained for 1-octene (83%) and cyclohexene (84%). In the case of cyclohexene, best yield was obtained 1h epoxidation followed by 6h cycloaddition (instead of 1h originally) at 140°C at 30 bar CO_2. Siewniak and co-workers,[52] (**Table 12, entry 9**) who also used $[MoO_2(acac)_2]$ but in combination with a quaternary ammonium salt supported on polystyrene (PS-TBMAC) associated with $ZnBr_2$ did not only test styrene as discussed before **(Table 12, entry 9)** but also linear C_6 and C_8 alkenes and cyclohexene. Yields of cyclic carbonates were in the range of 50% obtained for hexene carbonate or 67% for styrene carbonate i.e. slightly lower than those obtained by Chen *et al.*[48], probably as the result of lower CO_2 pressure and temperature in the second step (9 bar for Siewniak and co-workers[169], 30 bar for Chen *et al.*[48]). Very low yield in cyclohexene carbonate (4%) was obtained despite a cyclohexene conversion of 87%. According to the authors, it could be due to the formation of polycarbonates (by reaction of CO_2 with cyclohexene epoxide) which cannot be detected by conventional gas chromatography analysis.[73] It is noteworthy that Ramidi et al[51] also reported very low yields of cyclohexene and cyclooctene carbonates (respectively 11 and 10 %) compared to those of linear carbonates with similar reaction conditions (yields in the range 31 to 48 %, see

above). According to the authors, the weak performances of their catalytic system towards endocyclic strained alkenes could be related to steric factors.

Using a recyclable mesoporous titanium-silicate Ti-MMM-E and *n*-Bu_4NBr, in an orthogonal approach, Kholdeeva and co-workers[49] (see **Table 12 entry 5**) managed to get styrene carbonate with a yield of 64% under a unified set of conditions. However, using these optimized conditions (oxidant = TBHP, T = 70°C, P_{CO2} = 80 bar, 48h), they were not able to obtain cyclic carbonates from cyclohexene and 1-hexene at all, thus showing the importance of the activation of the double bond by the aromatic ring in styrene. Main products were epoxides and other oxidation or bromination by-products. On the other hand, all styrene derivatives tested were converted to the expected cyclic carbonates with yields in the range of 27% (for 4-chlorostyrene) to 68% (for 4-methylstyrene). As shown in previous studies,[32,74] 4-chlorostyrene and, in a lesser extent, 4-methoxystyrene appear thus to be less prone to oxidative carboxylation. No explanation was given by the authors though. Such differences between styrene derivatives and linear aliphatic alkenes (here 1-heptene), were not always observed. Hence, using MTO, Bu_4NI assisted by a Al complex in a one-pot catalyzed approach (with optimized conditions for both steps), Sathe *et al.*[62] reported very good yields for 1-heptene (90 %), as well as styrene derivatives such as 4-chlorostyrene (90 %), 4-fluorostyrene (91 %), or 4-*tert*-butylstyrene (86 %) carbonates in similar reaction conditions used with styrene (40°C, then 100°C, 8 bar of CO_2). Authors also indicated that the one-pot protocol implemented in this case was optimized for weakly polar olefins with a rather high molecular weight since their non-miscibility with water allowed an easy separation of H_2O_2 at the end of the epoxidation step, thus avoiding the oxidation of I^- from Bu_4NI in the next step.

III.4 Future directions for the synthesis of cyclic carbonates from alkenes

It is noteworthy that Mukaiyama-type conditions (under O_2, using isobutyraldehyde as a co-reductant) were also tested for the homogeneous oxidation step. Despite a good conversion of the alkene using this methodology, the authors pointed out that no trace of carbonates was evidenced in the final mixture.

III.4.1 Use of molecular oxygen with carbon dioxide

As mentioned before, Aresta and co-workers showed that Rh(I) phosphines-based complexes are able to facilitate the conversion of styrene into styrene carbonate using O_2 as the oxidant in an auto-tandem catalysis process.[75]Styrene carbonate was obtained with a maximum yield of 25% at 40 °C with a 50/50 1 bar mix of O_2/CO_2. However, due to the low lifetimes of these Rh(I) complexes (< few hours) and their rather low efficiency, metal oxides such as Ag_2O, MgO, Fe_2O_3, MoO_3, Ta_2O_5, La_2O_3, etc were also tested as catalysts by the same authors (**Table 13, entry 1**).[76] Indeed, such heterogeneous materials have previously shown interesting performance either for epoxidation (e.g. Ag_2O for the aerobic formation of ethylene epoxide)[77–79] or for CO_2 cycloaddition (e.g. MgO for the formation of styrene carbonate from styrene oxide).[80] As indicated in **Table 13**, the highest styrene carbonate yield obtained by Aresta and co-workers, using Nb_2O_5 (the best oxide of the series), was only 4% (for 27% conversion) at 120°C at 45 bar of CO_2 and 5 bar of O_2 , which is rather low. Seemingly, due to high temperature conditions, the formation of styrene carbonate was accompanied by other by-products, such as benzaldehyde and benzoic acid. Later, these authors used a $Nb_2O_5/NbCl_5$ mixture (**Table 13, entry 2**) leading to some improvement of the yield of styrene carbonate up to 11% in DMF,[30] thus confirming if necessary the particular role of halide ions in the CO_2 cycloaddition.[81] According to the authors, an acid-base catalysis operates in the synthesis of carbonate generated from in in-situ $NbOCl_3$ specie obtained from moist in the air (see **Figure 35**).

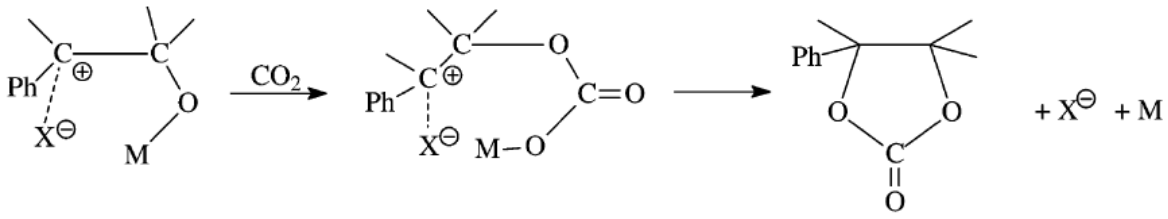

Figure 35: *Acid–base catalysis in the formation of carbonate*

However, in all cases, benzaldehyde was found as the major reaction product. Results were not much better (26% SC yield at 150°C, 5 bar of O_2 and 35 bar of CO_2) for another heterogeneous catalyst based on Fe^{3+}-doped polymeric graphitic carbon nitride g-C_3N_4 nanophases immobilized in the channels of a mesoporous silica SBA-15 developed by Yuan *et al in* 2013 (**Table 13, entry 3**).[82] Both reactions (epoxidation and cycloaddition) seemed to be promoted by Fe^{3+} and the solvent used (dioxane) may have a role in the epoxidation

process due to its reactivity with O_2 that may be responsible for the in-situ generation of some hydroperoxides. No halide or ammonium specie were necessary to conduct the cycloaddition reaction. The authors suggest that CO_2 was used as a mild oxidant coupled with O_2. Since CO_2 is a poor electron donor has a more tendency to accept electron than donation. It is then reduced to CO, oxidizing the target molecule. As seen in other study, in the case of a mix O_2/CO_2, an oxygen transfer can be seen from the peroxocarbonate metal complex to the oxophile substrate, leading to an increase in the formation of phenylacetaldehyde and epoxide (see **Figure 36**).[83]

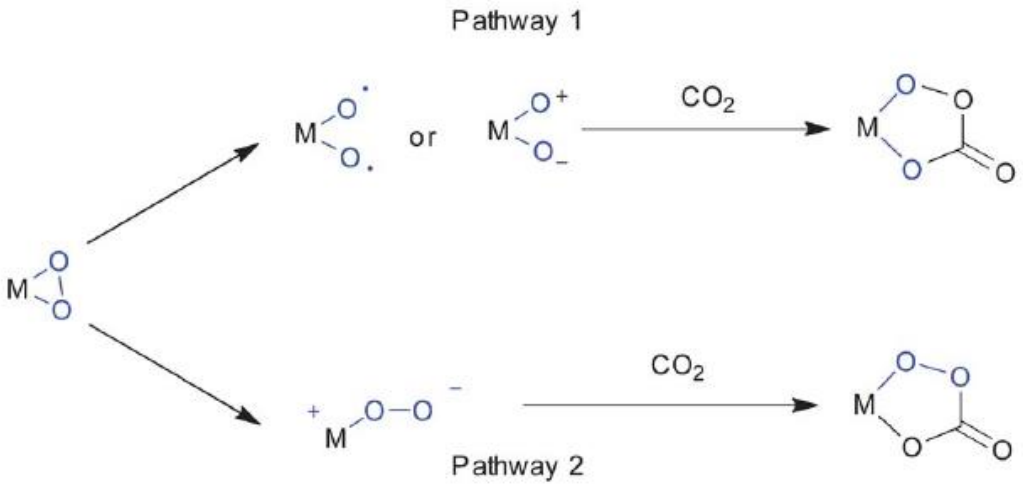

Figure 36: *Mechanistic pathways for the formation of metal*

Homogeneous catalytic systems using both O_2 and CO_2 are not numerous in the literature. We actually found a paper of Bai et Jing[31] describing the use of the combination of soluble dioxo(tetraphenylporphyrinato)Ru(VI) and quaternary ammonium salts for the direct oxidative carboxylation of various olefins (**Table 13, entry 4**). Varying the experimental conditions (nature of the catalyst, its molar equivalent or the time reaction) led to high yields of styrene carbonates up to 76 after 48h (p_{O2} = 5 bar, p_{CO2} = 11 bar, 30°C in the presence of Bu_4NI, in ethanol). Interestingly, the authors reached a 100% selectivity of styrene carbonate at ambient temperature and under relatively low pressures of CO_2 and dioxygen. As the result of the absence of benzaldehyde among the products, the authors have proposed a concerted mechanism in which the epoxide intermediate would remain tied to the Ru centre, during the attack by CO_2, preliminary activated by I^- (see **Figure 37**).

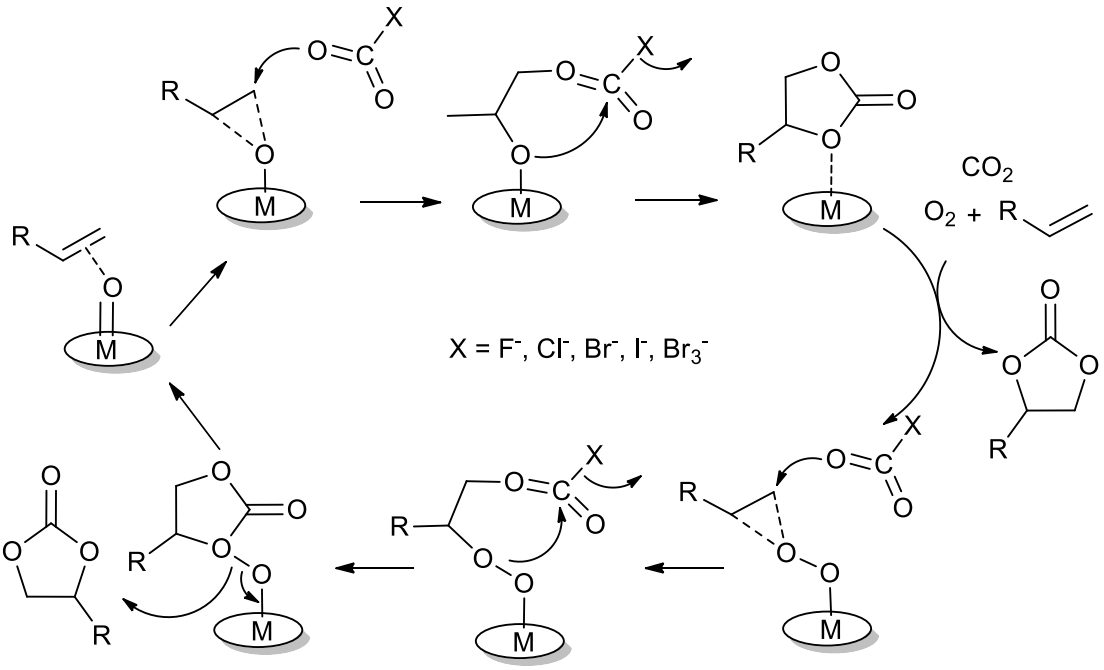

Figure 37: *Proposed mechanism for the cycloaddition reaction involving the nucleophilic attack on CO_2 instead of epoxide*

III.4.2 Use of supported halides for the design of fully heterogeneous catalytic systems

Due to their reasonable catalytic activity and a large range of available compounds, soluble halide reagents, especially quaternary onium salts have been overwhelmingly utilized in the synthetic schemes described for the cycloaddition of CO_2 onto epoxides. However, these reagents used as homogeneous catalysts, are handicapped by their difficult recovery. Indeed, some halides maybe lost and contaminate the reaction products. One of the reported methods to get rid of the *n*-Bu_4NBr catalyst consists to heat the crude reaction mixture up to 190°C, taking advantage of the Hofmann-type elimination which decomposes the above-cited TBABr ammonium into volatile products. However, the authors also suggested the loss of product carbonated oleate due to it decomposition or volatilization at such high temperature.[61] In order to come up with a more economically viable and more environmental friendly process, the covalent immobilization of the halide reagent onto a solid support appears a more elegant option.

Supported quaternary ammonium salts are either commercially available or maybe synthesized on purpose. Amberlite IRA-400, an anion exchange resin made of polystyrene

functionalized with $–NR_3^+/Cl^-$, is one example of commercially available material. This was used by Sun and co-workers[45] to design a catalytic system for the conversion of styrene into styrene carbonate in the presence of TBHP and CO_2. Amberlite IRA-400 allowed the generation of supported Au^0 nanoparticles stabilized by the polymeric support that are catalytically active for the epoxidation step in the presence of TBHP while NR_3^+/Cl^- in excess are responsible for the cycloaddition of CO_2. Styrene carbonate was thus obtained at high temperature (150°C) and CO_2 pressure (40 bar) at once with a maximum yield of 50 % (**Table 13, entry 6**). The reusability of Au/R201 catalyst was examined and the catalyst was readily separated and reused for a second run without any loss of activity. Interestingly, it has been noted that the authors showed that a too high CO_2 pressure has a negative effect on the epoxidation step. On their side, Liu and co-workers[84] (**Table 13, entry 7**) have designed a catalytic system involving a delaminated titanosilicate with an open external surface providing support for the immobilization of quaternary ammonium salts. Oxidation step was conducted at 40 °C for 1h, then the temperature was increased to 140°C during 6h for the cycloaddition step under 20 bar of CO_2. This bi-functional catalyst was obtained by reaction of the delaminated titanosilicate (Del-Ti-MWW) with $(OEt)_3Si(CH_2)_3NBu_3Br$ and its performances were evaluated in, an orthogonal mode, for the one-pot synthesis of propylene carbonate in the presence of H_2O_2, giving rise to an overall yield of 48%. According to the authors, the oxidation step was enhanced by the titanosilicate support bearing quaternary ammonium groups, i.e., the active sites for the carbonation. A first reuse of the catalyst led to a *ca.* 50% decrease of activity (yield = 28%), mainly due to the pore blocking by the heavy by-products formed at high temperature (140°C). However, thereafter, the catalyst displayed comparable propylene conversions and propylene carbonates yields for the other catalytic runs.

Among the other supports used, one can mentioned chitosan, a natural polymer that has found extensive applications as a catalyst support in diverse applications, owing to its low cost, non-toxicity, and multifunctional properties.[85–89] Jain and co-workers (**Table 13, entry 8**)[90], hence prepared a dual catalytic system starting from magnetic chitosan (MCS), a material made of magnetic Fe_3O_4 nanoparticles dispersed and stabilized by chitosan.[91] MCS was subsequently used as a durable and sustainable support for the covalent immobilisation of the epoxidation ($[Co(acac)_2]$) and the cycloaddition catalysts (a quaternary phosphonium bromide (QPB)) at once. Such bifunctional material was tested in the orthogonal catalyzed

synthesis of styrene carbonate with a 67% yield (at 95% conversion) from O_2/CO_2 and styrene, using acetonitrile as a solvent at 100 °C, and relatively heavy pressure condition (5 bar O_2 and 30 bar CO_2). The aerobic epoxidation of styrene required the use of isobutyraldehyde as a sacrificial reducing agent (Mukaiyama reaction).[92]. In such oxidation process, peroxide intermediates derived from the aldehyde are supposedly generated in-situ and are responsible for the formation of the expected epoxide (styrene oxide) but also of benzaldehyde that is issued from the undesired C=C oxidative cleavage. In addition, hexene, cyclohexene and propene carbonates could be prepared with yields of 85%, 78% and 85%, respectively, using similar experimental conditions. Last but not least, the catalyst was successfully used several times without observing a significant decrease of the styrene carbonate yield, showing a rather high stability. No leaching was observed too.

MOFs are solids that present some substantial advantages since, in theory, they have an easily tuneable composition and can be functionalised with one or multiple active centers while maintaining their crystallinity and surface area. [206–210] As the result, they have already been used as catalysts both for the epoxidation of alkenes[98,99] and for the cycloaddition of CO_2 onto epoxides[100–103], but not so much for the direct conversion of styrene into styrene carbonate in the presence of CO_2. One interesting example is given by Han et al.[104] (**Table 13, entry 9**) who have designed a POMOF including Keggin type polyoxometalates (POMs) $[ZnW_{12}O_{40}]^{6-}$ entities, known for their catalytic activity in epoxidation[105–107] with cationic $[Zn_2(NH_2\text{-Bipy})_2(HPYI)_2(H_2O)(CH_3CN)]^{6+}$ units (NH_2-Bipy = NH_2-functionalized bipyridine, HPY = pyrrolidine-2-yl-imidazole) whose basic amino bipyridine ligands are expected to contribute to CO_2 capture. Such material was used in the presence of *n*-Bu_4NBr and TBHP as the oxidant searching for some synergy effects[108–110] induced by the proximity of the different catalytically active centers. Under mild conditions (50°C and 5 bar of CO_2), styrene carbonate was synthesized with a 92% yield after a long reaction time of 96h. Furthermore, the catalyst could be reused with moderate loss of activity and selectivity after 3 runs.

Table 13: *Aerobic and supported reagent synthesis of cyclic carbonate from olefin and CO_2*

entry	Reference	Epoxidation catalyst	Oxidant	Cycloaddition catalyst	Reaction conditions	SC. Yield (conv.) %	Catalytic transformation
1	Aresta *et al.*[76]	Nb_2O_5	O_2	-	[Nb_2O_5 : styrene, 1 : 25, DMF (10 mL)], O_2 5 bar, 120 °C, CO_2 45 bar, 5h	4 (27)	Auto-tandem
2	Aresta *et al.*[30]	Nb_2O_5/$NbCl_5$	O_2	Nb_2O_5/$NbCl_5$	[Nb_2O_5 : $NbCl_5$: styrene, 2 : 1 : 80], DMF (10 mL), O_2 1 bar, 135 °C, CO_2 49 bar, 12h	11 (-)	Auto-tandem
3	Yuan *et al.*[82]	(Fe^{3+})g-C_3N_4/SBA-15	O_2	(Fe^{3+})g-C_3N_4/ SBA-15	[Fe : styrene, 1 : 200], 1,4-dioxane (3 mL), O_2 5 bar, 150°C, CO_2 30 bar, 5h	26 (58)	Auto-tandem
4	Bai *and Jing.*[31]	Ru(TPP)(O)2	O_2	Bu_4NI	[Ru : Bu_4NI : styrene, 1 : 2 : 25], in CH_2Cl_2, O_2 5 bar, 30 °C, CO_2 11 bar, 48h	76 (76)	Orthogonal
5	D Dias *et al.*	8MnNP@SiO_2	O_2 + IBA	4CrNP@SiO_2	(i) [Mn : styrene : IBA : chlorobenzene, 1 : 10 650 : 53 200 : 4 100], CH_2Cl_2 (2 mL), 2h, O_2 bubbling, 25°C (ii) [Cr : PPNCl : styrene, 1 : 1 400 : 1 400], 80°C, CO_2 10 bar, 24h	52 (100)	One-pot
6	Sun *et al.*[111]	Au/R201	TBHP	Au/R201	(i) [Au : styrene, 1 : 173 000, TBHP (1.5 eq)], 80 °C, 3 h (ii) 150 °C, CO_2 40 bar, 4h	51 (98)	Auto-tandem
7	Liu *et al.*[84]	Del-Ti-MWW-NBu_3Br	H_2O_2	Del-Ti-MWW-NBu_3Br	Catalyst : styrene, 1 : 4, H_2O_2 (2 eq.), ACN, (i) 40 °C, 1h (ii) 140 °C, CO_2 20 bar, 6h	48 (81)	Orthogonal
8	Jain *et al.*[90]	$Co(acac)_2$-QPB@MCS	O_2	$Co(acac)_2$-QPB@MCS	(i) [Co : styrene : IBA, 1 : 130 : 160], ACN (10mL), O_2 5 bar, 100 °C, CO_2 30 bar, 10h	67 (95)	Orthogonal
9	Han *et al.*[104]	POMOF ZnW-PYI	TBHP	POMOF ZnW-PYI	[ZnW : Olefin, 1 : 1000, TBHP (2 eq.)], 50 °C, CO_2 5 bar, 96h	92 (ee 80)	Auto-tandem

III.4.3 Discussion

From all the catalytic systems reviewed here, it seems to us that the most successful in terms of carbonate formation but also in terms of sustainability are those gathered in table 4. Our criteria were the yield of styrene carbonate (used as a model substrate), the reaction time, the temperature, the CO_2 pressure, the catalyst efficiency as well as the oxidant used.

Table 14: *Best systems reported so far for the direct synthesis of cyclic carbonate from olefins and CO_2*

	Sathe *et al.* *2017*[62]	**Han *et al.* 2015**[104]	**Jing *et al.* *2010*[31]**	**Yokoyama *et al.* 2007**[60]	**Jain *et al.* 2015**[90]	**Siewniak *et al.* 2017**[52]	**Sun *et al.* 2009**[111]
Conditions	**H_2O_2 / MTO (40°C, 0.5h) Bu_4NI / « Al » (100°C, 8 bar, 0,75 h)**	**TBHP/ POMOF (50°C, 5 bar, 96 h)**	**O_2 / Ru(TPP)$(O)_2$ Bu_4NI (30°C, 5 bar O_2, 11 bar CO_2, 40 h)**	**H_2O_2 / MTO (110°C, 2h) / Zn-ILs (110°C, 30 bar, 2h)**	**O_2 / Co-QPB@MCS (100°C, 10h, 35 bar)**	**TBHP / $MoO_2(acac)_2$ (100°C, 1h) Bu_3MeNCl / « Zn » (100°C, 9 bar, 4 h)**	**TBHP / Au/R201 (80°C, 3h) (80-140°C, 40 bar, 7 h)**
Green Oxidant	++	-	+++	+	+++	-	-
Low CO_2 pressure	++	+++	+	-	-	++	-
Mild Temp.	+++	+++	+++	++	-	+	-
Short reaction time	+++	- -	-	++	+	++	+
High yield	+++	+++	++	+++	+	+	+
Catalyst efficiently	+	+++	++	++	+++	+	++

Among, these studies, three deserve particular consideration. In the first, Sathe et al[62] used a well-known selective epoxidation catalyst (MTO),[112,113] H_2O_2, and the combination of Bu_4NI with an Al complex known as an efficient catalytic system for CO_2 cycloaddition affording a 88% yield of styrene carbonate at 98% conversion. The strengths of this system operating under one-pot catalysis conditions are the use of gentle reaction temperatures (40°C, then 100°C), short reaction times (0.5h, then 0.66h) for each step and the use of H_2O_2, a rather green oxidant. No benzaldehyde (oxidative cleavage product) was formed as a by-product. However, it seems that the protocol implemented is limited by the use of alkenes with heavy molecular weight or low polar substituents, as they are easily separated using the membrane separator between organic and aqueous phases. Therefore, the authors concluded their article by suggesting that the design of supported catalysts would be an improvement for the overall transformation. In the second selected example, Yokoyama

et al [60] developed a fast (2h, then 2h) one-pot catalytic process involving MTO and "anhydrous" H_2O_2 (UHP), and a mixture of ionic liquids [BMIm]BF_4 Zn[EMIm]$_2Br_4$ working at rather low temperatures, 30°C for the epoxidation and 110°C for the cycloaddition. Urea hydrogen peroxide was used as the oxidant due to its good solubility in the ionic liquid. Despite the use of a high CO_2 pressure (30 bar), this system represents, according to the authors, an improvement over other existing systems because it leads to a good styrene carbonate yield (83% in 4h), a better use of the oxidant and because the separation/recycling of the ionic liquid is easy. The last system with many favourable criteria is the one developed by Siewniak et al. (one-pot)[52] involving $MoO_2(acac)_2$ and a supported quaternary ammonium coupled with a Zn(II) salt. Working with TPHP (the less green oxidant of the O_2, H_2O_2 and TBHP series) and CO_2, the authors achieved the oxidative carboxylation of alkenes at 100°C with important carbonate yields (up to 77%, depending on the substrate, 67% for SC) in 4h, but no reusability test was performed.

With regard to the possibilities of catalyst recycling, two other works dealing with fully heterogenized systems can be pointed out. Among them, POMOF developed by Han and co-workers[104] is a true auto-tandem heterogeneous catalytic system, that fulfils a lot of the above criteria such as a high yield of styrene carbonate of 92%, the use of mild temperature (50°C) and CO_2 pressure (5 bar). The catalysts could be reused at least three times with moderate loss of activity (from 92 to 88% yield). However, hydroperoxides such as TBHP and excessive reaction times (in the present case, 96 h) are prohibitive conditions for a large-scale industrial use. Orthogonal catalytic system designed by Sun and co-workers[111] in which gold nanoparticles and ammonium in excess co-exist on a single polymer support. In that case, the reaction times were satisfying (3h) but the process was handicapped by the high temperature (150°C) and the high CO_2 pressure (40 bar) required for cycloaddition and, again, the use of an organic hyperoxide to achieve the formation of styrene carbonate in a reasonable yield 51 % but with 98% conversion.

Finally, it is tempting to turn to one last criterion, namely the use of the "greenest" oxidant possible, i.e. O_2, thus avoiding organic hydroperoxides or even H_2O_2 itself coming from O_2 in a non-environment-friendly pathway. In this respect, Jing[31] and Jain[90] both developed catalytic processes involving O_2 as oxidant affording relatively high yields of styrene carbonate (76% (100% selectivity) and 67%, respectively). The orthogonal process

based on $Ru(TPP)O_2$ and Bu_4NI introduced by Jing et al.[31], which does not require the assistance of a sacrificial reducing agent was tested successfully for the synthesis of various cyclic carbonates in mild conditions (T = 30°C, p_{CO2} = 11 bar, p_{O2} = 5 bar). However, such system is limited by a long reaction time (48h), the use of dichloromethane as the solvent and the impossibility of catalysts recovery (homogeneous catalysis). On the other hand, the catalyst system implemented by Jain and co-workers[90] is fully heterogeneous owing to the use of a natural polymer doped with magnetite nanoparticles. The latter functionalized by $Co(acac)_2$ and a quaternary phosphonium bromide allowed 67% yield of styrene carbonate (95% conversion) at 100°C and at a relatively high pressure of CO_2 (35 bar). After the reaction, the catalyst was recovered by applying an external magnet and reused for several runs without significant loss in catalytic activity and no leaching was observed during this course. Moreover, a stoichiometric amount of a sacrificial aldehyde has to be engaged in order to promote the epoxidation.

This bibliographic review has shown that significant progress in the field of CO_2 cycloaddition and epoxidation catalysts has been made over the last two decades, thus encouraging different teams to study the catalysis of the direct transformation of alkenes into cyclocarbonates in the presence of CO_2 and oxidants, especially with green reagents. Through the given examples, one can note that it is now possible to work with relatively low temperatures, CO_2 pressure, and, sometimes, with very short reaction times. However, works with O_2, the greenest oxidant are scarcer but they should be strongly encouraged. Various strategies for the recycling (in particular by immobilization on support) have been mentioned and successfully tested, but one can wonder why very efficient soluble catalysts systems were not tested after deposition onto inorganic or organic supports. Last but not least, no system described up to now uses a CO_2 pressure equivalent to that found in the fumes of industrial effluents that also contain molecular oxygen, thus avoiding the pre-concentration of CO_2. These are the two points on which it is necessary to focus in order to obtain more and more effective catalyst.

III.5 Conclusion

For the last two decades, there has been a growing interest for the direct oxidative carboxylation of olefins to corresponding cyclic carbonates. The current review shows prominent results for the study of alternative methods involving the use of CO_2 as raw material and green oxidants. There is a lot of interest in implementing one-pot reactions instead of conducting them separately. Indeed, economies and an improvement of environmental impacts can be expected compared to the two separate reactions through the suppression of separation protocols between steps. Catalytic systems which allow this transformation at reaction temperature ≤ 100°C and/or relatively low carbon dioxide pressures were specially emphasized. The oxycarboxylation reaction of an olefin in the presence of CO_2 and an oxidant by a one-pot route (direct synthesis of cyclic carbonate) under single reaction conditions throughout the process is feasible due to the good compatibility between CO_2 and oxidants such as O_2, H_2O_2 and organic hydroperoxides. However, the direct synthesis of cyclic carbonates is not always easy to implement because of the relatively large differences between the optimal conditions required for each of the reactions considered separately.

This review has allowed to assess the important progress made to approach the conditions for carrying out epoxidation on the one hand and the cycloaddition of CO_2 on the epoxide on the other hand, thus enabling interesting yields of cyclocarbonates from alkenes. Two strategies can be adopted: either unique reaction conditions are used (a kind of compromise between the conditions of the separate reactions), or the conditions are modified during the overall transformation from conditions favorable to epoxidation to conditions more favorable to cycloaddition. For this purpose, carbon dioxide can be added, and the temperature conditions hardened as soon as the optimum epoxide yield has been obtained, allowing the formation of the cyclic carbonate.

This review focused on the handling of the catalyst(s). It can be stated that organocatalysts, *e.g*. ammonium and imidazolium salts, are the most used for the cycloaddition step. Furthermore, the addition of catalytic amount of metal complexes or Lewis acid metal sites leads generally to a significant higher activity. The overall reaction may indeed involve a single catalyst, but this simple case is rare (**Table 3, entry 6-9).** More often, two catalysts are required, even often three if one considers the co-catalyst for the CO_2

cycloaddition reaction on the intermediate epoxide. Catalysts are most often introduced at the beginning of the overall reaction. It should be noted that the majority of catalytic systems designed involve homogeneous or even mixed catalysts, homogeneous for one step and heterogeneous for the other, with the result that all or part of the catalysts used are lost at the end of the transformation. The number of completely heterogeneous catalytic systems is in the minority. We believe that it is at this level that an effort must be made because the heterogenisation of active phases with complementary activities is also a tool to lead to interesting synergies in connection with the control of their respective positioning on the support. Interesting work with MOFs, which are solids with properties that can be very finely adjusted, since at the molecular scale, has led to catalytic systems that are among the best we have been able to identify in the review.

Another important issue concerns the choice of the cleanest possible oxidants. TBHP remains unfortunately the most used one for the epoxidation step, despite the low carbon efficiency linked to its utilization. Molecular oxygen should be preferred for many reasons. One of them, is its availability, with CO_2, in industrial emissions, allowing to imagine later a direct use of the latter without having to separate CO_2 from the other gases. In our opinion, still too little work has been reported for the synthesis of cyclic carbonates from alkenes using O_2 and CO_2 as reagents. It is true that the use of O_2 is handicapped by its association in most cases with sacrificial reductants (but not always) which generate waste, but it is perhaps possible to use certain sacrificial reductants whose oxidation could lead to a co-production of compounds that can be recovered on the fringes of the formation of cyclic carbonates.

To date, the increase of the number of publications dealing with oxidative cycloaddition remains relatively modest. This is all the more surprising regarding the quantity of available alkene substrates and the potential interest of cyclic carbonates at once. The authors hope that the readers will consider this review as a valuable contribution to this field.

References

[1] M. Aresta, A. Dibenedetto, A. Angelini, The changing paradigm in CO_2 utilization, *J. CO_2 Util.*, (**2013**), 3–4, 65–73.

[2] A. Aresta, Michele; Quaranta, Eugenio; Tommasi, Immacolata; Giannoccaro, Potenzo; Ciccarese, Enzymic versus chemical carbon dioxide utilization. Part I. The role of metal centers in carboxylation reactions, *Gazz. Chim. Ital.*, (**1995**), 125, 509–538.

[3] A. Abd, Nanotechnology: Science and Application, **2019**.

[4] M. Aresta, A. Dibenedetto, E. Quaranta, Reaction Mechanisms in Carbon Dioxide Conversion, **2016**.

[5] T.E. Müller, W. Leitner, CO_2 chemistry, *Beilstein J. Org. Chem.*, (**2015**), 11, 675–677.

[6] B.M. Bhanage, M. Arai, Green Chemistry and Sustainable Technology Transformation and Utilization of Carbon Dioxide, **2014**. http://www.springer.com/series/11661.

[7] M. Aresta, Carbon Dioxide as Chemical Feedstock, **2010**.

[8] W.B. Tolman, Activation of Small Molecules, **2006**.

[9] S. Fukuoka, M. Kawamura, K. Komiya, M. Tojo, H. Hachiya, K. Hasegawa, M. Aminaka, H. Okamoto, I. Fukawa, S. Konno, A novel non-phosgene polycarbonate production process using by-product CO_2 as starting material, in: Green Chem., **2003**: pp. 497–507.

[10] T. Sakakura, K. Kohno, The synthesis of organic carbonates from carbon dioxide, *Chem. Commun.*, (**2009**), 1312–1330.

[11] M. North, R. Pasquale, C. Young, Synthesis of cyclic carbonates from epoxides and CO_2, *Green Chem.*, (**2010**), 12, 1514–1539.

[12] G. Rokicki, Aliphatic cyclic carbonates and spiroorthocarbonates as monomers, *Prog. Polym. Sci.*, (**2000**), 25, 259–342.

[13] M. Ratzenhofer, H. Kisch, Metal-Catalyzed Synthesis of Cyclic Carbonates from Carbon Dioxide and Oxiranes, *Angew. Chemie Int. Ed. English*., (**1980**), 19, 317–318.

[14] D.J. Darensbourg, M.W. Holtcamp, Catalysts for the reactions of epoxides and carbon dioxide, *Coord. Chem. Rev.*, (**1996**), 153, 155–174.

[15] J.P. Parrish, R.N. Salvatore, K.W. Jung, Perspectives on Alkyl Carbonates in Organic Synthesis, *Tetrahedron*., (**2000**), 56, 8207–8237.

[16] K.J. Zhu, R.W. Hendren, K. Jensen, C.G. Pitt, Synthesis, properties, and biodegradation of poly(1,3-trimethylene carbonate), (**1991**), 1736–1740.

[17] P. Avramova, L. Dryanovska, Y. Ilarionov, Synthesis and pharmacologic assessment of carbamic and carbonic acid esters with 1-aryl-3-dimethylamino-1-propanols. Part 3, *Pharmazie*., (**1983**), 38, 443—444. http://europepmc.org/abstract/MED/6138779.

[18] P.T. Anastas, D.G. Hammond, Inherent Safety at Chemical Sites: Reducing Vulnerability to Accidents and Terrorism Through Green Chemistry, **2015**. https://books.google.com/books?id=KqDDCQAAQBAJ&pgis=1.

[19] S. Fujita, M. Arai, B.M. Bhanage, Direct Transformation of Carbon Dioxide to Value-Added Products over Heterogeneous Catalysts, in: B.M. Bhanage, M. Arai (Eds.), Transform. Util. Carbon Dioxide, Springer Berlin Heidelberg, Berlin, Heidelberg, **2014**: pp. 39–53.

[20] H.C. Erythropel, J.B. Zimmerman, T.M. De Winter, L. Petitjean, F. Melnikov, C.H. Lam, A.W. Lounsbury, K.E. Mellor, N.Z. Janković, Q. Tu, L.N. Pincus, M.M. Falinski, W. Shi, P. Coish, D.L. Plata, P.T. Anastas, The Green ChemisTREE: 20 years after taking root with the 12 principles, *Green Chem.*, (**2018**), 20, 1929–1961.

[21] Hans-Josef Buysch, Carbonic Esters, in: Ullmann's Encycl. Ind. Chem., **2000**: pp. 102–123.

[22] R.Y. WT McShea, Method of methanol production, *US Pat. 4,927,857*., (**1990**),.

[23] X.D. Lang, L.N. He, Green Catalytic Process for Cyclic Carbonate Synthesis from Carbon Dioxide under Mild Conditions, *Chem. Rec.*, (**2016**), 1337–1352.

[24] M. Peters, B. Köhler, W. Kuckshinrichs, W. Leitner, P. Markewitz, T.E. Müller, Chemical technologies for exploiting and recycling carbon dioxide into the value chain, *ChemSusChem*., (**2011**), 4, 1216–1240.

[25] J. Sun, L. Liang, J. Sun, Y. Jiang, K. Lin, X. Xu, R. Wang, Direct Synthetic Processes for Cyclic Carbonates from Olefins and CO_2, *Catal. Surv. from Asia*., (**2011**), 49–54.

[26] M. Kobayashi, S. Inoue, T. Tsuruta, Diethylzinc-Dihydric Phenol System as Catalyst for the Copolymerization of Carbon Dioxide with Propylene Oxide, *Macromolecules*., (**1971**), 4, 658–659.

[27] S. Inoue, H. Koinuma, T. Tsuruta, Copolymerization of carbon dioxide and epoxide, *J. Polym. Sci. Part B Polym. Lett.*, (**2004**), 7, 287–292.

[28] V.M. Muzalevskiy, A. V Shastin, N.G. Shikhaliev, A.M. Magerramov, A.N. Teymurova, V.G. Nenajdenko, Ionic liquids as a reusable media for copper catalysis. Green access to alkenes using catalytic olefination reaction, *Tetrahedron*., (**2016**), 72, 7159–7163.
[29] R. Srivastava, D. Srinivas, P. Ratnasamy, Synthesis of polycarbonate precursors over titanosilicate molecular sieves, *Catal. Letters*., (**2003**), 91, 133–139.
[30] M. Aresta, A. Dibenedetto, Carbon dioxide as building block for the synthesis of organic carbonates behavior of homogeneous and heterogeneous catalysts in the oxidative carboxylation of olefins, *J. Mol. Catal. A Chem.*, (**2002**), 182–183, 399–409.
[31] D. Bai, H. Jing, Aerobic oxidative carboxylation of olefins with metalloporphyrin catalysts, *Green Chem.*, (**2010**), 12, 39–41.
[32] F. Chen, T. Dong, T. Xu, X. Li, C. Hu, Direct synthesis of cyclic carbonates from olefins and CO_2 catalyzed by a $MoO_2(acac)^{2-}$ quaternary ammonium salt system, *Green Chem.*, (**2011**), 13, 2518–2524.
[33] N. Eghbali, C.J. Li, Conversion of carbon dioxide and olefins into cyclic carbonates in water, *Green Chem.*, (**2007**), 9, 213–21.
[34] J.L. Wang, J.Q. Wang, L.N. He, X.Y. Dou, F. Wu, A CO_2/H_2O_2-tunable reaction: Direct conversion of styrene into styrene carbonate catalyzed by sodium phosphotungstate/n-Bu_4NBr, *Green Chem.*, (**2008**), 10, 1218–1223.
[35] J. Wu, J.A. Kozak, F. Simeon, T.A. Hatton, T.F. Jamison, Mechanism-guided design of flow systems for multicomponent reactions: conversion of CO_2 and olefins to cyclic carbonates, *Chem. Sci.*, (**2014**), 1227–1231.
[36] Y. Li, X. Zhou, S. Chen, R. Luo, J. Jiang, Z. Liang, H. Ji, Direct aerobic liquid phase epoxidation of propylene catalyzed by Mn(III) porphyrin under mild conditions: Evidence for the existence of both peroxide and Mn(IV)-oxo species from in situ characterizations, *RSC Adv.*, (**2015**), 5, 30014–30020.
[37] L. Sumitomo Chemical Co., Development of New Propylene, *R&D Rep.*, (**2010**), 1–8.
[38] A. Bruggink, R. Schoevaart, T. Kieboom, Concepts of nature in organic synthesis: Cascade catalysis and multistep conversions in concert, *Org. Process Res. Dev.*, (**2003**), 7, 622–640.
[39] P.A. Wender, M.P. Croatt, B. Witulski, New reactions and step economy: the total synthesis of (±)-salsolene oxide based on the type II transition metal-catalyzed intramolecular [4+4] cycloaddition, *Tetrahedron*., (**2006**), 62, 7505–7511.
[40] D.E. Fogg, E.N. dos Santos, Tandem catalysis: a taxonomy and illustrative review, *Coord. Chem. Rev.*, (**2004**), 248, 2365–2379.
[41] S. Abou-Shehada, J.M.J. Williams, Separated tandem catalysis: It's about time, *Nat. Chem.*, (**2014**), 6, 12–13.
[42] Patol, J. A., *US Pat 3 205 305*., (**1962**),.
[43] F.J. Primus, M.D. Goldenberg, S. Hills, United States Patent (19), (**1991**), 25–28.
[44] M. Aresta, E. Quaranta, A. Ciccarese, Direct synthesis of 1,3-benzodioxol-2-one from styrene, dioxygen and carbon dioxide promoted by Rh(I), *J. Mol. Catal.*, (**1987**), 41, 355–359.
[45] J. Sun, S.I. Fujita, F. Zhao, M. Hasegawa, M. Arai, A direct synthesis of styrene carbonate from styrene with the Au/SiO_2-$ZnBr_2/Bu_4NBr$ catalyst system, *J. Catal.*, (**2005**), 230, 398–405.
[46] G.-J. Kim, D.-W. Park, The catalytic activity of new chiral salen complexes immobilized on MCM-41 in the asymmetric hydrolysis of epoxides to diols, *Catal. Today*., (**2000**), 63, 537–547.
[47] V. Hulea, E. Dumitriu, Styrene oxidation with H_2O_2 over Ti-containing molecular sieves with MFI, BEA and MCM-41 topologies, *Appl. Catal. A Gen.*, (**2004**), 277, 99–106.
[48] M.A. Uguina, D.P. Serrano, R. Sanz, J.L.G. Fierro, M. López-Granados, R. Mariscal, Preliminary study on the TS-1 deactivation during styrene oxidation with H_2O_2, *Catal. Today*., (**2000**), 61, 263–270.
[49] N. V. Maksimchuk, I.D. Ivanchikova, A.B. Ayupov, O.A. Kholdeeva, One-step solvent-free synthesis of cyclic carbonates by oxidative carboxylation of styrenes over a recyclable Ti-containing catalyst, *Appl. Catal. B Environ.*, (**2016**), 181, 363–370.
[50] C. Evangelisti, M. Guidotti, C. Tiozzo, R. Psaro, N. Maksimchuk, I. Ivanchikova, A.N. Shmakov, O. Kholdeeva, Titanium-silica catalyst derived from defined metallic titanium cluster precursor: Synthesis and catalytic properties in selective oxidations, *Inorganica Chim. Acta*., (**2018**), 470, 393–401.
[51] P. Ramidi, C.M. Felton, B.P. Subedi, H. Zhou, Z.R. Tian, Y. Gartia, B.S. Pierce, A. Ghosh, Synthesis and characterization of manganese(III) and high-valent manganese-oxo complexes and their roles in conversion of alkenes to cyclic carbonates, *J. CO_2 Util.*, (**2015**), 9, 48–57.
[52] A. Siewniak, K. Jasiak-Jaroń, Ł. Kotyrba, S. Baj, Efficient Catalytic System Involving Molybdenyl Acetylacetonate and Immobilized Tributylammonium Chloride for the Direct Synthesis of Cyclic Carbonates from Carbon Dioxide and Olefins, *Catal. Letters*., (**2017**), 147, 1567–1573.

[53] W.H. Zhang, P.P. He, S. Wu, J. Xu, Y. Li, G. Zhang, X.Y. Wei, Graphene oxide grafted hydroxyl-functionalized ionic liquid: A highly efficient catalyst for cycloaddition of CO_2 with epoxides, *Appl. Catal. A Gen.*, (**2016**), 509, 111–117.

[54] A.L. Girard, N. Simon, M. Zanatta, S. Marmitt, P. Gonçalves, J. Dupont, Insights on recyclable catalytic system composed of task-specific ionic liquids for the chemical fixation of carbon dioxide, *Green Chem.*, (**2014**), 16, 2815–2825.

[55] K. Jasiak, T. Krawczyk, M. Pawlyta, A. Jakóbik-Kolon, S. Baj, One-Pot Synthesis of Styrene Carbonate from Styrene and CO_2 over the Nanogold-Ionic Liquid Catalyst, *Catal. Letters*., (**2016**), 146, 893–901.

[56] O. V. Zalomaeva, N. V. Maksimchuk, A.M. Chibiryaev, K.A. Kovalenko, V.P. Fedin, B.S. Balzhinimaev, Synthesis of cyclic carbonates from epoxides or olefins and CO_2 catalyzed by metal-organic frameworks and quaternary ammonium salts, *J. Energy Chem.*, (**2013**), 22, 130–135.

[57] P.T.K. Nguyen, H.T.D. Nguyen, H.N. Nguyen, C.A. Trickett, Q.T. Ton, E. Gutiérrez-Puebla, M.A. Monge, K.E. Cordova, F. Gándara, New Metal-Organic Frameworks for Chemical Fixation of CO_2, *ACS Appl. Mater. Interfaces*., (**2018**), 10, 733–744.

[58] J. Sun, S.I. Fujita, B.M. Bhanage, M. Arai, One-pot synthesis of styrene carbonate from styrene in tetrabutylammonium bromide, in: Catal. Today, **2004**: pp. 383–388.

[59] J. Sun, Y. Wang, J. Son, D. Xiang, L. Wang, F.S. Xiao, A facile, direct synthesis of styrene carbonate from styrene and CO_2 Catalyzed by Au/Fe$(OH)^{3-}$/$ZnBr_2$/Bu_4NBr system, *Catal. Letters*., (**2009**), 129, 437–443.

[60] F. Ono, K. Qiao, D. Tomida, C. Yokoyama, Direct preparation of styrene carbonates from styrene using an ionic-liquid-based one-pot multistep synthetic process, *Appl. Catal. A Gen.*, (**2007**), 333, 107–113.

[61] K.M. Doll, S.Z. Erhan, Synthesis of carbonated fatty methyl esters using supercritical carbon dioxide, *J. Agric. Food Chem.*, (**2005**), 53, 9608–9614.

[62] A.A. Sathe, A.M.K. Nambiar, R.M. Rioux, Synthesis of cyclic organic carbonates via catalytic oxidative carboxylation of olefins in flow reactors, *Catal. Sci. Technol.*, (**2017**), 7, 84–89.

[63] L.D. Dias, R.M.B. Carrilho, C.A. Henriques, M.J.F. Calvete, A.M. Masdeu-Bultó, C. Claver, L.M. Rossi, M.M. Pereira, Hybrid Metalloporphyrin Magnetic Nanoparticles as Catalysts for Sequential Transformation of Alkenes and CO_2 into Cyclic Carbonates, *ChemCatChem*., (**2018**), 10, 2792–2803.

[64] L. Cuesta-Aluja, M. Djoufak, A. Aghmiz, R. Rivas, L. Christ, A.M. Masdeu-Bultó, Novel chromium (III) complexes with N4-donor ligands as catalysts for the coupling of CO_2 and epoxides in supercritical CO_2, *J. Mol. Catal. A Chem.*, (**2014**), 381, 161–170.

[65] Y.A. Alassmy, P.P. Pescarmona, The Role of Water Revisited and Enhanced : A Sustainable Catalytic System for the Conversion of CO_2 into Cyclic Carbonates under Mild Conditions, (**2019**), 3856–3863.

[66] C.J. Whiteoak, N. Kielland, V. Laserna, E.C. Escudero-Adán, E. Martin, A.W. Kleij, A powerful aluminum catalyst for the synthesis of highly functional organic carbonates, *J. Am. Chem. Soc.*, (**2013**), 135, 1228—1231.

[67] and X.-B.L. Wei-Min Ren*, Ye Liu, Bifunctional Aluminum Catalyst for CO_2 Fixation: Regioselective Ring Opening of Three-Membered Heterocyclic Compounds, *J. Org. Chem.*, (**2014**), 79, 9771–9777.

[68] W. Clegg, R.W. Harrington, M. North, R. Pasquale, Cyclic Carbonate Synthesis Catalysed by Bimetallic Aluminium–Salen Complexes, *Chem. – A Eur. J.*, (**2010**), 16, 6828–6843.

[69] J. Meléndez, M. North, P. Villuendas, One-component catalysts for cyclic carbonate synthesis, *Chem. Commun.*, (**2009**), 2577–2579.

[70] M. North, P. Villuendas, C. Young, A gas-phase flow reactor for ethylene carbonate synthesis from waste carbon dioxide, *Chem. - A Eur. J.*, (**2009**), 15, 11454–11457.

[71] N.W. A. Holleman, Inorganic Chemistry, Academic p, Academic press, **2001**.

[72] J. Sun, S.I. Fujita, B.M. Bhanage, M. Arai, Direct oxidative carboxylation of styrene to styrene carbonate in the presence of ionic liquids, *Catal. Commun.*, (**2004**), 5 2, 83–87.

[73] M. Super, E. Berluche, C. Costello, E. Beckman, Copolymerization of 1,2-Epoxycyclohexane and Carbon Dioxide Using Carbon Dioxide as Both Reactant and Solvent, *Macromolecules*., (**1997**), 30, 368–372.

[74] X. Yang, J. Wu, X. Mao, T.F. Jamison, T.A. Hatton, Microwave assisted synthesis of cyclic carbonates from olefins with sodium bicarbonates as the C1 source, *Chem. Commun.*, (**2014**), 50, 3245.

[75] M. Aresta, E. Quaranta, A. Ciccarese, Letter Direct Synthesis of 1,3-Benzodioxol-a-one from Styrene, Dioxygen and Carbon Dioxide Promoted by Rh(1), *J. Mol. Catal.*, (**1987**), 41, 355–359.

[76] M. Aresta, A. Dibenedetto, I. Tommasi, Direct synthesis of organic carbonates by oxidative carboxylation of olefins catalyzed by metal oxides: Developing green chemistry based on carbon dioxide, in: Appl. Organomet. Chem., **2000**: pp. 799–802.

[77] Union Carbide and Carbon, Union Carbide and Carbon, *US Patent, 2.238.474*., (**1941**),.

[78] Shell Devel, *US Patent, 2.404.438*., (**1946**),.

[79] Celanese Corp. of America, *US Patent, 2.578.841*., (**1951**),.
[80] T. Yano, H. Matsui, T. Koike, H. Ishiguro, H. Fujihara, M. Yoshihara, T. Maeshima, Magnesium oxide-catalysed reaction of carbon dioxide with an epoxide with retention of stereochemistry, *Chem. Commun.*, (**1997**), 1129–1130.
[81] A.K. F.J. Mais, H.J. Buysch, C. Mendoza-Frohn, F.J. Mais, H.J. Buysch, C. Mendoza-Frohn, A. Klausener, *EP Pat. 543 249, Bayer*., (**1993**),.
[82] Z. Huang, F. Li, B. Chen, T. Lu, Y. Yuan, G. Yuan, Well-dispersed g-C_3N_4 nanophases in mesoporous silica channels and their catalytic activity for carbon dioxide activation and conversion, *Appl. Catal. B Environ.*, (**2013**), 136–137, 269–277.
[83] M.B. Ansari, S.E. Park, Carbon dioxide utilization as a soft oxidant and promoter in catalysis, *Energy Environ. Sci.*, (**2012**), 5, 9419–9437.
[84] J. Zhang, Y. Liu, N. Li, H. Wu, X. Li, W. XIE, Z. Zhao, P. Wu, M. He, Synthesis of Propylene Carbonate on a Bifunctional Titanosilicate Modified with Quaternary Ammonium Halides, *Chinese J. Catal.*, (**2008**), 29, 589–591.
[85] D.J. Macquarrie, J.J.E. Hardy, Applications of Functionalized Chitosan in Catalysis, *Ind. Eng. Chem. Res.*, (**2005**), 44, 8499–8520.
[86] P. Kaur, B. Kumar, V. Kumar, R. Kumar, Chitosan-supported copper as an efficient and recyclable heterogeneous catalyst for A3/decarboxylative A3-coupling reaction, *Tetrahedron Lett.*, (**2018**), 59, 1986–1991.
[87] L. Zhu, B. Li, S. Wang, W. Wang, L. Wang, L. Ding, C. Qin, Recyclable heterogeneous chitosan supported copper catalyst for silyl conjugate addition to α, β-unsaturated acceptors in water, *Polymers (Basel).*, (**2018**), 10, 385–394.
[88] B. Sakthivel, A. Dhakshinamoorthy, Chitosan as a reusable solid base catalyst for Knoevenagel condensation reaction, *J. Colloid Interface Sci.*, (**2017**), 485, 75–80.
[89] S. Kumar, M.Y. Wani, J. Koh, J.M. Gil, A.J.F.N. Sobral, Carbon dioxide adsorption and cycloaddition reaction of epoxides using chitosan–graphene oxide nanocomposite as a catalyst, *J. Environ. Sci.*, (**2017**), 69, 77–84.
[90] S. Kumar, N. Singhal, R.K. Singh, P. Gupta, R. Singh, S.L. Jain, Dual catalysis with magnetic chitosan: Direct synthesis of cyclic carbonates from olefins with carbon dioxide using isobutyraldehyde as the sacrificial reductant, *Dalt. Trans.*, (**2015**), 44, 11860–11866.
[91] Y. Zhu, L.P. Stubbs, F. Ho, R. Liu, C.P. Ship, J.A. Maguire, N.S. Hosmane, Magnetic Nanocomposites: A New Perspective in Catalysis, *ChemCatChem*., (**2010**), 2, 365–374.
[92] Z. Li, S. Wu, H. Ding, D. Zheng, J. Hu, X. Wang, Q. Huo, J. Guan, Q. Kan, Immobilized Cu(II) and Co(II) salen complexes on graphene oxide and their catalytic activity for aerobic epoxidation of styrene, *New J. Chem.*, (**2013**), 37, 1561.
[93] M.-L. Hu, V. Safarifard, E. Doustkhah, S. Rostamnia, A. Morsali, N. Nouruzi, S. Beheshti, K. Akhbari, Taking organic reactions over metal-organic frameworks as heterogeneous catalysis, *Microporous Mesoporous Mater.*, (**2018**), 256, 111–127.
[94] S.-N. Zhao, X.-Z. Song, S.-Y. Song, H. Zhang, Highly efficient heterogeneous catalytic materials derived from metal-organic framework supports/precursors, *Coord. Chem. Rev.*, (**2017**), 337, 80–96.
[95] Z. Yin, S. Wan, J. Yang, M. Kurmoo, M.-H. Zeng, Recent advances in post-synthetic modification of metal–organic frameworks: New types and tandem reactions, *Coord. Chem. Rev.*, (**2017**), 378, 500–512.
[96] J.L.C. Rowsell, O.M. Yaghi, Effects of Functionalization, Catenation, and Variation of the Metal Oxide and Organic Linking Units on the Low-Pressure Hydrogen Adsorption Properties of Metal−Organic Frameworks, *J. Am. Chem. Soc.*, (**2006**), 128, 1304–1315.
[97] Q. Yang, Q. Xu, H.-L. Jiang, Metal–organic frameworks meet metal nanoparticles: synergistic effect for enhanced catalysis, *Chem. Soc. Rev.*, (**2017**), 46, 4774–4808.
[98] J.W. Brown, Q.T. Nguyen, T. Otto, N.N. Jarenwattananon, S. Glöggler, L.S. Bouchard, Epoxidation of alkenes with molecular oxygen catalyzed by a manganese porphyrin-based metal-organic framework, *Catal. Commun.*, (**2015**), 59, 50–54.
[99] K. Leus, Y.Y. Liu, P. Van Der Voort, Metal-organic frameworks as selective or chiral oxidation catalysts, *Catal. Rev. - Sci. Eng.*, (**2014**), 56, 1–56.
[100] J. Kim, S.-N.N. Kim, H.-G.G. Jang, G. Seo, W.-S.S. Ahn, CO_2 cycloaddition of styrene oxide over MOF catalysts, *Appl. Catal. A Gen.*, (**2013**), 453, 175–180.
[101] Z. Zhou, C. He, J. Xiu, L. Yang, C. Duan, Metal–Organic Polymers Containing Discrete Single-Walled Nanotube as a Heterogeneous Catalyst for the Cycloaddition of Carbon Dioxide to Epoxides, *J. Am. Chem. Soc.*, (**2015**), 137, 15066–15069.

[102] Y. Ren, Y. Shi, J. Chen, S. Yang, C. Qi, H. Jiang, Ni(salphen)-based metal–organic framework for the synthesis of cyclic carbonates by cycloaddition of CO_2 to epoxides, *RSC Adv.*, (**2013**), 3, 2167.

[103] J. Song, Z. Zhang, S. Hu, T. Wu, T. Jiang, B. Han, MOF-5/n-Bu_4NBr: an efficient catalyst system for the synthesis of cyclic carbonates from epoxides and CO_2 under mild conditions, *Green Chem.*, (**2009**), 11, 1031.

[104] Q. Han, B. Qi, W. Ren, C. He, J. Niu, C. Duan, Polyoxometalate-based homochiral metal-organic frameworks for tandem asymmetric transformation of cyclic carbonates from olefins, *Nat. Commun.*, (**2015**), 6,.

[105] Z. Hu, X. Fu, Y. Li, X. Tu, Highly efficient and excellent reusable catalysts of molybdenum(VI) complexes grafted on ZPS-PVPA for epoxidation of olefins with tert-BuOOH, *Appl. Organomet. Chem.*, (**2011**), 25, 128–132.

[106] D.Y. Du, J.S. Qin, S.L. Li, Z.M. Su, Y.Q. Lan, Recent advances in porous polyoxometalate-based metal-organic framework materials, *Chem. Soc. Rev.*, (**2014**), 43, 4615–4632.

[107] N. Mizuno, K. Kamata, Catalytic oxidation of hydrocarbons with hydrogen peroxide by vanadium-based polyoxometalates, *Coord. Chem. Rev.*, (**2011**), 255, 2358–2370.

[108] Y.-B. Huang, J. Liang, X.-S. Wang, R. Cao, Multifunctional metal–organic framework catalysts: synergistic catalysis and tandem reactions, *Chem. Soc. Rev.*, (**2017**), 46, 126–157.

[109] L. Bromberg, X. Su, T.A. Hatton, Heteropolyacid-Functionalized Aluminum 2-Aminoterephthalate Metal-Organic Frameworks As Reactive Aldehyde Sorbents and Catalysts, *ACS Appl. Mater. Interfaces*., (**2013**), 5, 5468–5477.

[110] Z.-M. Zhang, T. Zhang, C. Wang, Z. Lin, L.-S. Long, W. Lin, Photosensitizing Metal–Organic Framework Enabling Visible-Light-Driven Proton Reduction by a Wells–Dawson-Type Polyoxometalate, *J. Am. Chem. Soc.*, (**2015**), 137, 3197–3200.

[111] D. Xiang, X. Liu, J. Sun, F.S. Xiao, J. Sun, A novel route for synthesis of styrene carbonate using styrene and CO_2 as substrates over basic resin R201 supported Au catalyst, *Catal. Today*., (**2009**), 148, 383–388.

[112] A.L.P. de Villa, D.E. De Vos, C.C. de Montes, P.A. Jacobs, Selective epoxidation of monoterpenes with methyltrioxorhenium and H_2O_2, *Tetrahedron Lett.*, (**1998**), 39, 8521–8524.

[113] A.E. Gerbase, J.R. Gregório, M. Martinelli, M.C. Brasil, A.N.F. Mendes, Epoxidation of soybean oil by the methyltrioxorhenium-CH_2Cl_2/H_2O_2 catalytic biphasic system, *J. Am. Oil Chem. Soc.*, (**2002**), 79, 179–181.

PART II : EXPERIMENTAL SECTION

CHAPTER IV

OPTIMISATION OF THE CYCLOADDITION STEP

CHAPTER IV.1

Advantages of covalent immobilization of metal-Salophen by amide linkage on amino-functionalized mesoporous silica in terms of recycling and catalytic activity for the CO_2 cycloaddition onto epoxides (publication in progress)

(Work carried out in collaboration with Sebastien Beaudoin (M2))

Advantages of covalent immobilization of metal-Salophen by amide linkage on amino-functionalized mesoporous silica in terms of recycling and catalytic activity for the CO_2 cycloaddition onto epoxides

Matthieu Balas,[a,b] Sébastien Beaudoin,[a,b] Anna Proust,[a] Franck Launay*[b], Richard Villanneau*[a]

[a] *Sorbonne Université, CNRS UMR 8232, Institut Parisien de Chimie Moléculaire, IPCM, Campus Pierre et Marie Curie, 4 Place Jussieu, F-75005 Paris, France. richard.villanneau@sorbonne-universite.fr*

[b] *Sorbonne Université, CNRS UMR 7197, Laboratoire de Réactivité de Surface, LRS, Campus Pierre et Marie Curie, 4 Place Jussieu, F-75005 Paris, France*

Abstract:

Ni^{II} and Mn^{III} Schiff base complexes (Salophen-tBu-Ni and Salophen-tBu-MnCl) bearing a pending carboxylic group were prepared and characterized. Both complexes were grafted onto a mesoporous amino-functionalized SBA-15 silica, by formation of an amide function between the propylamine groups of the support and the carboxylic acid functions of the salophen ligand. The co-catalytic behaviour of the free and grafted complexes was then evaluated in the CO_2 cycloaddition reaction onto styrene oxide, using tetra-butylammonium bromide (^{n}-Bu_4NBr) as the main catalyst. In homogeneous conditions, the Mn^{III} Schiff base complex and the Ni^{II} one, to a lesser extent, behave as efficient co-catalysts for this reaction. Upon immobilization at the surface of the amino-functionalized SBA-15, we showed that the co-catalytic activity of the less efficient one, i.e. Ni^{2+} salophen complex, could be enhanced, hence highlighting a potential synergistic effect between the unused amine functions of the support and the Ni^{2+} salophen co-catalyst. Both salophen complexes were successfully re-used in homogeneous conditions or after their immobilization without any appreciable loss of activity.

Keywords: Salen derivatives; hybrid catalysts; mesoporous materials; CO_2 valorization; cyloaddition reaction.

IV.1.1 Introduction

The large amounts of carbon dioxide released in atmosphere by human activities significantly contribute to the greenhouse effect. In this context, methods using CO_2 as a renewable, abundant C1-source to produce valuable chemicals are regarded with large interest and research concerning CO_2 transformation has led to significant progress [1-10]. In this context, CO_2 coupling reactions with epoxides leading to useful cyclic carbonates [8-14] have attracted particular attention in the community. CO_2 industrial applications already exist but need to be much more developed. Valuable products such as carboxylic acids, carbamates and carbonates can be obtained [15]. In such synthesis, carbon dioxide behaves as a green reagent as the result of its direct reaction with epoxides avoiding the use of phosgene, an extremely toxic reagent, and the formation of by-products [16]. Ethylene and propylene carbonates are already obtained at industrial scale by the reaction of CO_2 with epoxides in the presence of organocatalysts such as quaternary ammonium (NR_4^+, X^-) or phosphonium (PR_4^+, X^-) salts (mainly halogenated ones). Reaction conditions are however severe with temperatures and pressures of 120°C and 40 bar, respectively [17]. According to recent studies, milder conditions can be used when quaternary ammonium salts (QAS) are combined with co-catalysts [8-14, 18-27], generally hydrogen bond donor compounds [8-10] or metal complexes [11-14]. The latter provide Lewis acidity and thus, facilitate the nucleophilic attack of the activated epoxide by counter-anions of QAS. In this regard, transition metal complexes (especially Schiff bases and porphyrins complexes) are particularly promising [28-29]. Salen-type compounds have been introduced very early by North [18] and Zhang [19], then porphyrins by Ema [30] and, more recently, Schiff bases with 4 nitrogen atoms (BS4N) by Christ and Masdeu-Bulto [28]. Some of the systems involving metal complexes and QAS operate at room temperature and at atmospheric pressure [31]. In recent years, significant advances have led to a great reduction of the catalyst loading, particularly of the QAS. In parallel, several studies on the use of efficient co-catalysts immobilized on supports using a more or less sophisticated pathway have emerged in the literature [32-39]. In the light of our recent studies dealing with the immobilization of polyoxometalates on mesoporous supports [40-41], the present work focuses on the covalent grafting of Ni and Mn metal-salophen complexes bearing a carboxylic acid group onto propylamine-functionalized mesoporous silica of the SBA-15 type (**Figure 38**). In particular, the strategy developed allowed the straightforward

immobilization of the metal-salophen co-catalysts onto the inorganic support, and, the comparison of their reactivity for the CO_2 cycloaddition onto styrene oxide, in homogeneous and heterogeneous conditions.

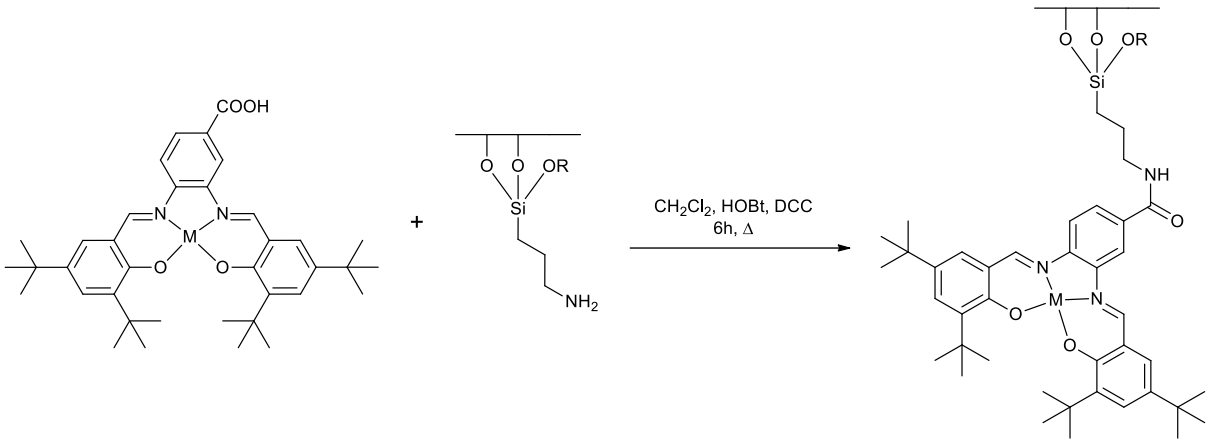

Figure 38: *Covalent grafting strategy to anchor metal-salophen complexes onto propylamine-functionalized SBA-15 silica.*

IV.1.2 Experimental part

IV.1.2.1 Synthesis and heterogenization of the precursor complexes

Preparation of *N,N'*-bis(3,5-di-*tert*-butylsalicylidene)-1-carboxy-3,4-phenylene-diamine (H_2Salophen-tBu). Diaminobenzoic acid (0.973 g, 6.40 mmol) was introduced in a two-neck round-bottom flask connected to a condenser under argon and dispersed in 20 mL of freshly distilled tetrahydrofuran (THF). In parallel, a solution of 3,5-di-tertiobutyl-2-hydroxy-benzaldehyde (3.002 g, 12.80 mmol) in 20 mL of freshly distilled THF was prepared under argon. This solution was then added dropwise using a syringe to the suspension of diaminobenzoic acid over a period of 20 min. After the addition was completed, 9.3 mL of a solution of $ZnCl_2$ in THF (0.7 mol·L^{-1}, corresponding to 6.41 mmol) was added to the resulting brown suspension. The mixture was refluxed 45 min during which the suspension turned progressively to a yellow solid in a brown solution. The yellow solid (compound 1) was then filtered on glass frit (n°4) then rinsed twice with 20 mL of freshly distilled methanol and dried at air, yielding 3.543 g (95 %). IR (KBr, cm^{-1}): 3425 (w), 2958 (s), 1686 (m), 1615 (s), 1574 (s), 1438 (m), 1361 (m), 1252 (m), 1172 (s), 1132 (w), 1026 (w), 771 (m) cm^{-1}. ^{1}H NMR ([D6]dmso, **Figure 39**, ppm): δH 13.69 (1H, s, C(2)OH), 13.61 (1H, s, C(2')OH), 9.08 (1H, s, C(7)H=N), 9.02 (1H, s, C(7')H=N), 8.05 (1H, s, C(12)H), 7.95 (1H, d, $^3J_{HH}$ = 8.0 Hz, C(9)H), 7.61 (1H, d, $^3J_{HH}$ = 8.0

Hz, C(10)H), 7.59 (1H, s, C(6)H), 7.53 (1H, s, C(6')H), 7.42 (1H, s, C(4)H), 7.41 (1H, s, C(4')H), 1.39 (18H, s, C(3)C(CH_3)$_3$ + C(3')C(CH_3)$_3$), 1.29 (18H, s, C(5)C(CH_3)$_3$ + C(5')C(CH_3)$_3$), HRMS $[1+H]^+$ (ESI, **Figure 40**) : m/z = 585.37.

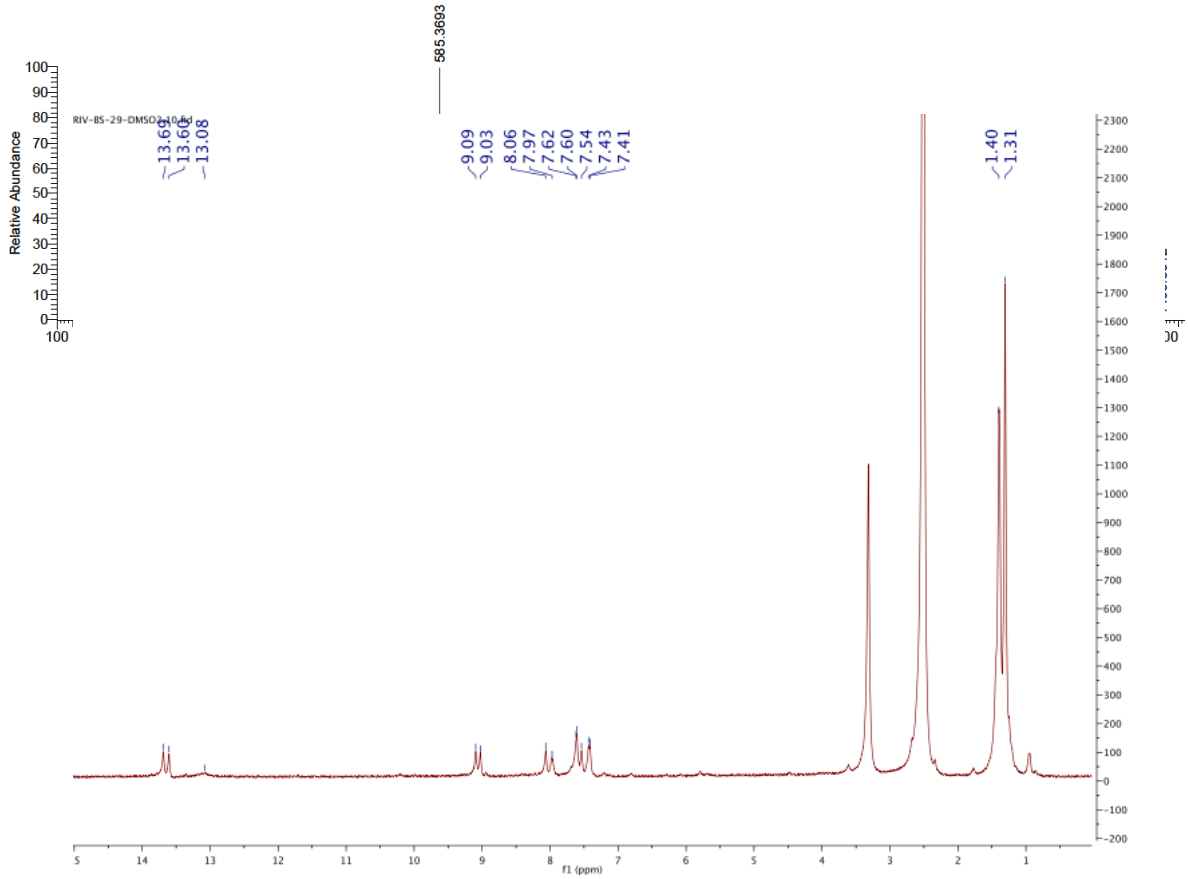

Figure 39. *^{1}H NMR spectrum ([D6]dmso) of N,N'-bis(3,5-di-tert-butylsalicylidene)-1-carboxy-3,4-phenylene-diamine (H2Salophen).*

Preparation of *N,N'*-bis(3,5-di-*tert*-butylsalicylidene)-1-carboxy-3,4-phenylene-diamine-nickel(II) (Salophen-tBu-Ni). H_2Salophen-tBu ligand (1.000 g, 1.70 mmol, was dissolved in 50 mL of dry methanol under argon in a two-neck round-bottom flask connected to a condenser. A solution of $NiCl_2.6H_2O$ (1.069 g, 4.50 mmol) dissolved in 30 mL of dry methanol was then added and the mixture was refluxed for one hour under argon. The volume of the solution was then reduced until 20 mL under vacuum and allowed to stand at room temperature overnight. The dark red solid (Salophen-tBu-Ni) that appeared during this time was then filtered at air on a frit glass (n°4) and washed quickly with small portions of methanol, yielding 0.550 g (51 %). ^{1}H NMR ([D_6]dmso, ppm, **Figure 41**): δH 8.98 (1H, s, C(7)H=N), 8.91 (1H, s, C(7')H=N), 8.72 (1H, s, C(12)H), 8.27 (1H, d, $^3J_{HH}$ = 12.0 Hz, C(9)H), 7.84 (1H, d, $^3J_{HH}$ = 12.0 Hz, C(10)H), 7.63 (1H, d, $^4J_{HH}$ = 3.3 Hz, C(6)H), 7.49 (1H, d, ^{4}JHH = 2.6 Hz, C(6')H), 7.38 (1H, d, ^{4}JHH = 3.3 Hz, C(4)H), 7.35 (1H, d, ^{4}JHH = 2.6 Hz, C(4')H), 1.41 (18H, s, C(3)C$(CH_3)_3$ + C(3')C$(CH_3)_3$), 1.30 (18H, s, C(5)C$(CH_3)_3$) + C(5')C$(CH_3)_3$); IR (KBr, cm^{-1}): 3422 (m), 3054(m), 2959 (s), 1729 (s), 1686 (m), 1619 (s), 1579 (s), 1523 (s), 1458 (m), 1426 (s), 1386 (s), 1359 (s), 1260 (m), 1200 (s), 1180 (s), 1130 (m), 1026 (m), 788 (m), 541 (m). HRMS [**2**-H]$^-$ (ESI): m/z = 639.27 (**Figure 42**).

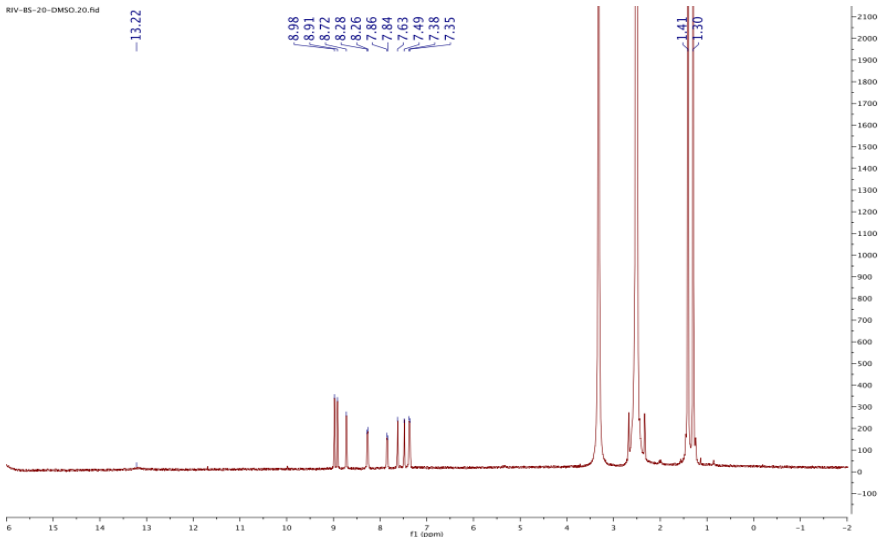

Figure 41. *^{1}H NMR spectrum ([D6]dmso) of Salophen-tBu-Ni*

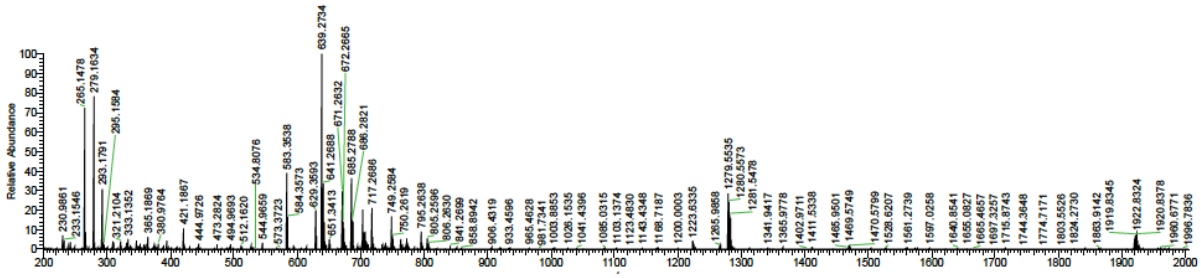

Figure 42. *HRMS (ESI) spectrum for Salophen-tBu-Ni calculated for $C_{37}H_{45}N_2NiO_4$ (m/z ($[M^-H]^-$) = 639.27).*

Preparation of *N,N'*-bis(3,5-di-*tert*-butylsalicylidene)-1-carboxy-3,4-phenylene-diamine-chloro-Manganese(III) (Salophen-tBu-MnCl). H_2Salophen-tBu ligand (0.347 g, 0.60 mmol) was dissolved in 20 mL of dry THF under argon in a two-neck round-bottom flask connected to a condenser. [$MnCl_2(THF)_2$] (0.160 g, 0.60 mmol) was then added to the solution and the mixture was stirred at room temperature for 1 h, then refluxed for 20 min. After cooling at room temperature, triethylamine (0,12 g, 1.20 mmol, 0,17 mL) was then added and the mixture stirred for another 45 min. The volume of the solution was then reduced up to 10 mL under vacuum and allowed to stand at room temperature overnight. After this period, a white powder (triethylammonium chloride) was filtered and discarded. The brown solution was evaporated, leading to a brown solid (Salophen-tBu-MnCl) that can be recrystallized in THF (yield: 0.350 g, 0,50 mmol, 88 %). IR (KBr, cm^{-1}): 3416 (m), 2958 (m), 1680 (sh), 1610 (s), 1573 (s), 1466 (s), 1392 (s), 1361 (s), 1325 (s), 1249 (s), 1198 (s), 1178 (s), 1097 (s), 1026 (s), 807 (s), 781 (s), 548 (m). HRMS [**3**-Cl]$^+$ (ESI) : m/z = 637.28 (**Figure 43**).

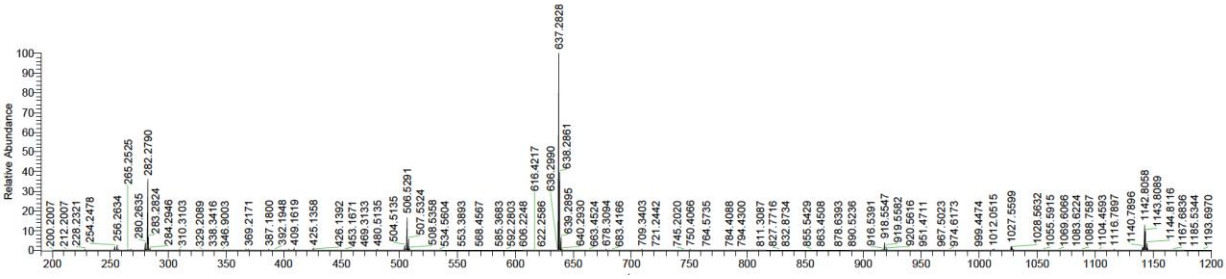

Figure 43. *HRMS (ESI) spectrum for Salophen-tBu-MnCl calculated for $C_{37}H_{47}MnN_2O_4$ (m/z ([M-Cl]$^+$) = 637.28.*

Covalent grafting of Salophen-tBu-Ni onto {NH_2}-SBA-15. {NH_2}-SBA-15 (0.30 g, [-RNH_2] = 2.2 mmol g^{-1}, corresponding to 0.66 mmol of {-RNH_2} functions, see synthesis in SI) and Salophen-tBu-Ni (0.105 g, 0.16 mmol) were dried under vacuum overnight in two schlenk tubes. Then, Salophen-tBu-Ni was dissolved in dichloromethane (DCM, 3 mL). In parallel, 1-hydroxy-1H-benzotriazole (HOBT, 0.007 g, 0.05 mmol) and *N,N'*-dicyclohexylcarbodiimide (DCC, 0.05 g, 0.22 mmol) were dissolved in 2 mL of DCM and the resulting solution was added to the solution of Salophen-tBu-Ni. The mixture was stirred for 40 min at room temperature. Meanwhile, 10 mL of DCM were added to {NH_2}-SBA-15. After 40 min, the previous mixture of **2**, HOBT and DCC was transferred to the suspension of {NH_2}-SBA-15 and refluxed for 6 h under N_2. Then, the solvent was evaporated until dryness and the resulting red powder was washed successively with refluxing methanol and acetone using a Soxhlet, respectively for 3 days and

24 h. Salophen-tBu-Ni@{NH_2}-SBA-15 (0.32 g) was thus obtained as a dark red purple powder (Ni $\%_{weight}$ = 1.30 % determined by TGA (10.8% mol Ni/mol –NH_2) corresponding to a Ni grafting yield of 52 %).

Covalent grafting of Salophen-tBu-MnCl onto {NH_2}-SBA-15. {NH_2}-SBA-15 (1.5 g, [-RNH_2] = 2.2 mmol g^{-1}, corresponding to 3.45 mmol of {-RNH_2} functions) and Salophen-tBu-MnCl (0.30 g, 0.45 mmol) were dried under vacuum overnight in two schlenk tubes. Then, Salophen-tBu-MnCl was dissolved in DCM, 6 mL, and 1-hydroxy-1H-benzotriazole (0.021g, 0.138 mmol) and N,N'-dicyclohexylcarbodiimide (DCC, 0.135 g, 0.66 mmol) were added to this solution. The mixture was stirred for 40 min at room temperature. Meanwhile, 10 mL of DCM were added to {NH_2}-SBA-15. After 40 min, the previous mixture of **3**, HOBT and DCC was transferred to the suspension of {NH_2}-SBA-15 and refluxed for 6 h under N_2. The solvent was then evaporated until dryness and the resulting brown powder was washed successively with refluxing methanol and acetone using a Soxhlet, respectively for 3 days and 24 h. Salophen-tBu-MnCl@{NH_2}-SBA-15 (1.44 g) was thus obtained as a dark brown powder (Mn $\%_{weight}$ = 1.03 % determined by TGA (8.6 % mol Mn/mol –NH_2) corresponding to a Mn grafting yield of 68 %).

IV.1.2.2 Protocols for the catalysis tests

After each catalytic test, the resulting solutions or suspensions were analysed by gas chromatography (GC, see details in **Appendix**) after dilution (samples of 25 µL diluted in 10 mL of CH_2Cl_2).

Experiments in homogeneous conditions (including stability test). In a 50 mL Teflon container, 0.7 mL of styrene oxide (5.6 mmol) and 0.031 g (0.100 mmol) of $^{n-}Bu_4NBr$ were dissolved in 13.3 mL of benzonitrile. Except for the tests performed in the absence of co-catalysts, 0.031 g of Salophen-tBu-Ni (or 0.033 g Salophen-tBu-MnCl) (0.05 mmol)) was added and the resulting mixture was stirred for 5 min at room temperature. Then, the autoclave was pressurized at 11 bar of CO_2 (corresponding to 41 mmol). The temperature was then increased up to 120°C in 40 min, leading to a CO_2 pressure of 15 bar. Heating was then prolonged for 3, 7 or 23 h and the reaction was quenched by cooling the autoclave into a water-ice mixture.

For the stability test, the reaction was carried out for 3 h, then quenched as described above. After analysis by GC, a new batch of styrene oxide (0.7 mL, 6.1 mmol) was introduced in the recovered Teflon container and the reaction mixture was stirred for 5 min at room temperature. Then, the autoclave was pressurized as described before. This procedure was repeated 3 times.

Experiments with the supported complexes (including recyclability test). The protocols were identical with the exception of the mass of co-catalysts added. 0.218 g of Salophen-tBu-Ni@{NH_2}-SBA-15 (or 0.259 g Salophen-tBu-MnCl@{NH_2}-SBA-15), corresponding to 0.05 mmol of immobilized metal Salophen-tBu complexes, was suspended in the benzonitrile solution. Then, the autoclave was pressurized as described before. After 3, 7 or 23 h, the reaction was quenched by cooling the autoclave into a water-ice mixture, and the reaction mixture was filtered on a büchner funnel, in order to separate the supported catalyst.

For the recyclability test, the reaction was carried out for 23 h and the solid recovered after each attempt was carefully washed by acetone, dried in an oven at 50°C for 12 h and weighted to check the mass after each run. This procedure was repeated three times.

IV.1.3 Results and Discussion

Here, in continuity with our previous work [40-41] on metal complexes immobilization, the strategy used consisted in the coupling of complementary functions, one (amino group) at the oxide support (amino group) and the second at the termination of the organic Salophen ligand. To do so, two different metal complexes (with either Ni^{II} or $\{Mn^{III}\text{-}Cl\}^{2+}$) were prepared with a Salophen ligand bearing a remote carboxylic acid function. Comparison of the co-catalytic reactivity of the two complexes in solution and after their immobilization was performed for the cycloaddition of CO_2 onto styrene oxide in the presence of $^{n}Bu_4NBr$ for the preparation of styrene carbonate.

IV.1.3.1 Synthesis and characterization of the ligand H_2Salophen-tBu and of its Ni(II) and Mn(III) complexes.

A convenient Salophen-tBu ligand that meets all the criteria is N,N'-bis(3,5-di-tert-butylsalicylidene)-1-carboxy-3,4-phenylene-diamine, denoted H_2Salophen-tBu (**Figure 44**) whose synthesis, in the present study, was adapted from the literature.[42] Hence, the Schiff-base ligand was synthesized with 95% yield using a classical condensation reaction of 1,2-diamino-4-carboxybenzene with 2 equivalents of 3,5-di-*tert*-butyl-2-hydroxybenzaldehyde (3,5-di-*tert*-butylsalicylaldehyde). It has to be noted that this reaction required the presence of Zn^{2+} that played the dual role of a templating agent and a Lewis acid that was not recovered in the final product. The ligand was characterized in mass spectrometry (HRMS) by a molecular peak at m/z ($[M+H]^+$) = 585.37 (**Figure 40**). The ^{1}H NMR spectrum (**Figure 39**) was consistent with the literature [42-43] showing several characteristic peaks, among which two groups of singlets were attributed respectively to the imine functions (-HC=N- at 9.08 and 9.02 ppm) and the phenol groups (13.69 and 13.61 ppm).

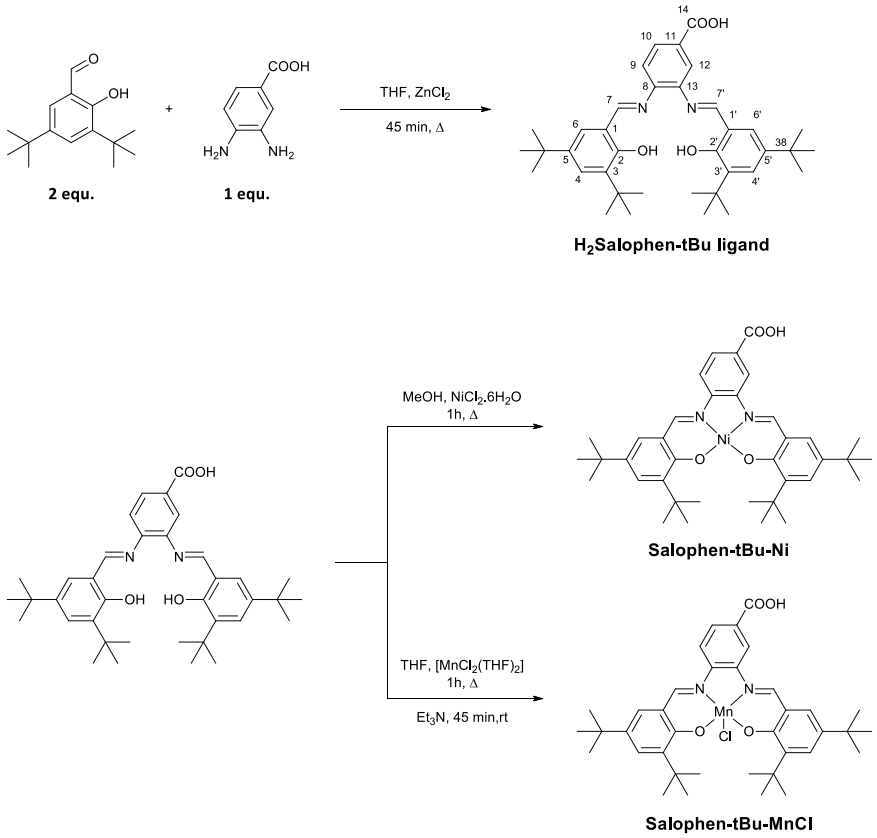

Figure 44: *Routes synthesis of N,N'-bis(3,5-di-tert-butylsalicylidene)-1-carboxy-3,4-phenylene-diamine (H_2Salophen-tBu, top) and its complexation leading to Salophen-tBu-Ni and Salophen-tBu -MnCl.*

The formation of the imine functions was also attested in IR spectroscopy by the absence of the $\nu_{(NH2)}$ bands of the initial 1,2-diamino-4-carboxybenzene at 3400 and 3487 cm^{-1} and by the occurrence of the $\nu_{(-HC=N-)}$ band at 1686 cm^{-1}.

Many transition metal complexes with Schiff-Base ligands were used in the literature for the CO_2 cycloaddition onto epoxides. In the present work, we focused our attention on Ni^{2+} and Mn^{3+} complexes. While many examples of co-catalysts based on Mn^{3+} salen/Salophen/porphyrin complexes have been reported [44-47], those based on Ni^{2+} are scarce [48]. Furthermore, the Salophen-tBu-Ni complex obtained by reaction of ligand with $NiCl_2.6H_2O$ displays a square planar geometry [42] in which the Ni^{2+} ion was found diamagnetic. It was thus possible to characterize the complex, in contrast to the Mn one, by ^1H NMR spectroscopy in solution, but also by ^{13}C CP-MAS NMR spectroscopy in view of its subsequent immobilization.

In the case of the Salophen-tBu-Ni complex synthesis, the procedure described in the literature had to be modified . Indeed, the synthesis reported by Hey-Hawkins and co-workers was a *one-pot* reaction from the starting reagents (1,2-diamino-4-carboxybenzene and 3,5-di-*tert*-butylsalicylaldehyde) in the presence of a Ni^{2+} source replacing the templating Zn^{2+} ion [42]. However, we found that his procedure led to low yields and to mixtures of different reaction products. We thus turned to the direct complexation of Ni^{2+} ions by the non-metallated ligand in dry methanol. This procedure, which was also used for the complexation of Mn^{3+}, finally led to 51 and 88% yield of Salophen-tBu-Ni and Salophen-tBu-MnCl, respectively with high purity, as attested by HRMS (**Figure 42 and Figure 43**) and ^1H NMR (for the salophen-tBu-Ni, **Figure 41**). In the Salophen-tBu-MnCl complex, the Mn^{3+} displays a square pyramid five-coordination, the coordination sphere being completed with a chloride anion. Both complexes were characterized in mass spectrometry (HRMS) by a molecular peak respectively at m/z ($[M-H]^-$) = 639.27 for the Salophen-tBu-Ni (**Figure 42**) and at m/z ($[M-Cl]^+$) = 637.28 for the Salophen-tBu-MnCl (**Figure 43**), in accordance with the literature [42].

The ^1H NMR spectrum of Salophen-tBu-Ni (**Figure 41**) confirmed its diamagnetism. We did not observe any broadening of the peaks, as expected in the case of a paramagnetic system. It is noteworthy that the two singlets assigned to the -OH groups of Salophen ligand were not found in the spectrum of Ni complex, thus confirming the complexation of Ni^{2+} by the oxygen of the two phenol groups. Furthermore, the Ni

complexation was emphasized by the shift of all the peaks of the salophen ligand in comparison with those of the free ligand.

IV.1.3.2 Synthesis and characterization of {NH_2}-SBA-15 and of the covalently immobilized Ni^{2+} and Mn^{3+} catalysts.

The amino-functionalized SBA-15 (for short {NH_2}-SBA-15) was obtained by the functionalization of a pre-formed SBA-15 silica (see **Figure 45**) [49] with 3-aminopropyltriethoxysilane, as described previously, targeting 4 mmol g^{-1} [50-51]. The thermogravimetric curve of {NH_2}-SBA-15 (**Figure 46**) obtained under air from room temperature up to 700°C shows two weight losses. The first one (*ca.* 3%), under 100°C (not shown here), can be attributed to the loss of water molecules weakly adsorbed on the silica surface whereas the second one (13%, 100-600°C) was assigned to the loss of aminopropyl functions. This analysis demonstrated that {NH_2}-SBA-15 is functionalized with 2.3 mmol of {NH_2} g^{-1} (*c.a.* 55 % incorporation yield). The general formula of {NH_2}-SBA-15 is then $H_2N(CH_2)_3Si/5.8SiO_2$.

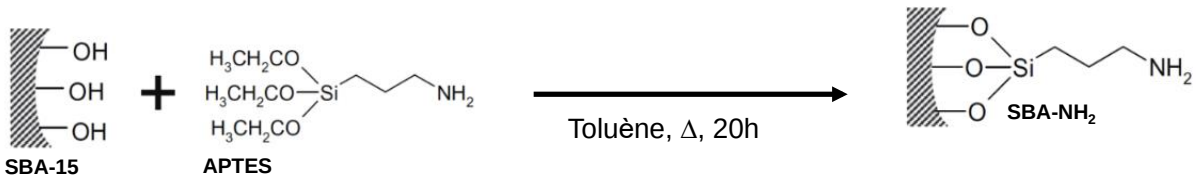

***Figure 45**: Synthetic procedure for the preparation of {NH_2}-SBA-15.*

The covalent immobilization of Mn^{3+} Salen complexes onto an organically modified silica surface was previously described in the literature [42-47, 52]. However, the grafting procedures in all these examples generally required a multistep functionalization of the hybrid support and/or of the salen ligands, which does not meet the criteria for the development of sustainable catalytic processes. The grafting procedure of the two complexes in the present study was inspired by the work of Luts and Papp [43] and by our previous studies on the heterogenization of hybrid derivatives of polyoxometalates onto {NH_2}-SBA-15 [41]. In these two examples, the strategy of linkage was built on the functionalization of both the catalyst and the mesoporous silica support by complementary organic functions leading to the

formation of robust and non-hydrolyzable amide groups. This choice is justified both by the efficiency and convenience of grafting aminopropyl synthons onto the SiO_2 support and by the one-step preparation of the Salophen ligand from commercial reagents. In the present work, the formation of an amide function by reaction between the carboxylic acid of the Salophen-tBu ligand in both complexes and the aminopropyl functions of the {NH_2}-SBA-15 support was realized using N,N'-dicyclohexylcarbodiimide (DCC) and 1-hydroxy-1H-benzotriazole (HOBT), in dichloromethane under refluxing conditions (-CO_2H : 1, HOBT : 0.3, DCC : 1.4 and -NH_2 4.3 for Salophen-tBu-Ni@{NH_2}-SBA-15 or 7.7 for Salophen-tBu-MnCl@{NH_2}-SBA-15). After each synthesis, the two materials thus obtained (Salophen-tBu-Ni@{NH_2}-SBA-15 and Salophen-tBu-MnCl@{NH_2}-SBA-15) were then extracted in a soxhlet and washed for 3 days successively with methanol and acetone to remove all the physisorbed complexes. It is noteworthy that these grafting and washing protocols were optimized in our previous work with polyoxometalates [41]. Indeed, our past studies showed that these steps are crucial to obtain materials in which the active phases are effectively covalently grafted in order to avoid later any leaching/lixiviation phenomenon. Finally, it should be noted that, after the soxhlet treatment, the color of the samples remained dark (dark brown with Mn and red/purple for Ni).

The weight percentages of Ni and Mn in Salophen-tBu-Ni@{NH_2}-SBA-15 and Salophen-tBu-MnCl@{NH_2}-SBA-15, respectively were determined by Atomic Absorption measurements (see details in SI). These amounts are important and comparable in both materials, 1.30 wt.% of Ni in Salophen-tBu-Ni@{NH_2}-SBA-15 and 1.06 wt.% of Mn in Salophen-tBu-MnCl@{NH_2}-SBA-15, corresponding to grafting yields respectively equal to 52 % (Ni) and 68 % (Mn) regarding the initial Ni or Mn loadings. Such values were confirmed indirectly by thermogravimetric analyses (TGA, **Figure 46**). Indeed, it was possible to get a reasonable estimation of the effective amount of Salophen-tBu-Ni/Mn in the final materials by subtracting the loss weight of the propylamine functions present in the starting {NH_2}-SBA-15 (see details in SI). The wt.% of Ni or Mn in the materials was estimated to 1.30 and 1.03% respectively, in good accordance with the results of the atomic absorption measurements. This corresponds to 0.22 mmol of Ni^{2+} per gram of Salophen-tBu-Ni@{NH_2}-SBA-15 and 0.19 mmol of $\{MnCl\}^{2+}$ per gram of Salophen-tBu-MnCl@{NH_2}-SBA-15. It is noteworthy that the initial Ni^{2+}/{-NH_2} functions and $\{MnCl\}^{2+}$/{-NH_2} functions ratios described in the experimental

part correspond to optimized conditions for both systems. In other words, an increase or a decrease of these ratios did not allow an increase of Ni^{2+} or $\{MnCl\}^{2+}$ loadings in the final materials.

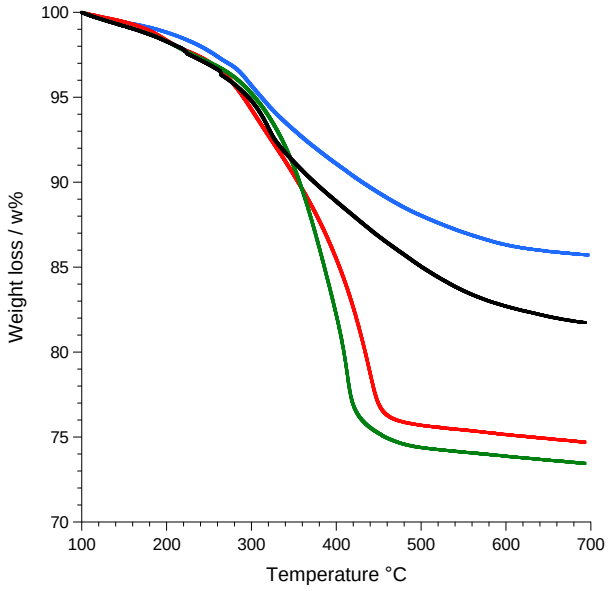

Figure 46: *Weight loss % (thermogravimetric analysis, TGA) for {NH_2}-SBA-15 (blue), Salophen-tBu-Ni/{NH_2}-SBA-15 (sample without coupling agent) (black), Salophen-tBu-Ni@{NH_2}-SBA-15 (green), Salophen-tBu-MnCl@{NH_2}-SBA-15 (red). All the curves were normalized at 100°C.*

In order to evaluate the efficiency of the covalent grafting of the complexes onto the surface, a blank test was done in which the deposition of the Salophen-tBu-Ni was carried out in the absence of a coupling agent (DCC and HOBT). This test was performed with experimental conditions (concentrations, temperature, duration of the experiment and work up) similar to those used in the presence of the coupling agent. After the washing step (4 days using a soxhlet in methanol and acetone), this control sample was visually different as the resulting solid had a light red color. TGA analyses, displayed on **Figure 46**, were also performed on this sample for sake of comparison. As expected, the amount of Salophen-tBu-Ni was found significantly lower in the absence of the coupling agents (Ni $\%_{weight}$ = 0.40 %). When DCC and HOBT are used, all these data led us to envisage a strong linkage of the Salophen-tBu-Ni/MnCl complexes with silica in Salophen-tBu-Ni@{NH_2}-SBA-15 and Salophen-tBu-MnCl@{NH_2}-SBA-15 that differs clearly from a simple physical adsorption. This also shows that this protocol is relevant as regards the immobilization of this type of co-catalyst. Therefore, it validates in a more general way our covalent grafting strategy on mesoporous support 1) to limit the

lixiviation phenomena during subsequent catalytic tests and 2) to increase the loading rate of the metal-Salophen complexes in the catalytic materials.

The ^{13}C CP-MAS NMR spectrum of Ni complex in its solid state showed a large number of peaks (**Figure 47**) due to its low symmetry and the absence of free rotation of the methyl groups of the ^{t}-butyl functions (up to 37 non-equivalent carbon atoms). Despite a lower resolution of the spectrum of Salophen-tBu-Ni@{NH_2}-SBA-15 compared to the spectrum of Ni complex, similar patterns were observed for both samples (**Figure 47**). In particular, the most intense peak at 31.2 ppm (assigned to some methyl of the ^{t}-butyl groups of the salophen) was clearly observed in both samples. In addition, it is noteworthy that the spectrum of

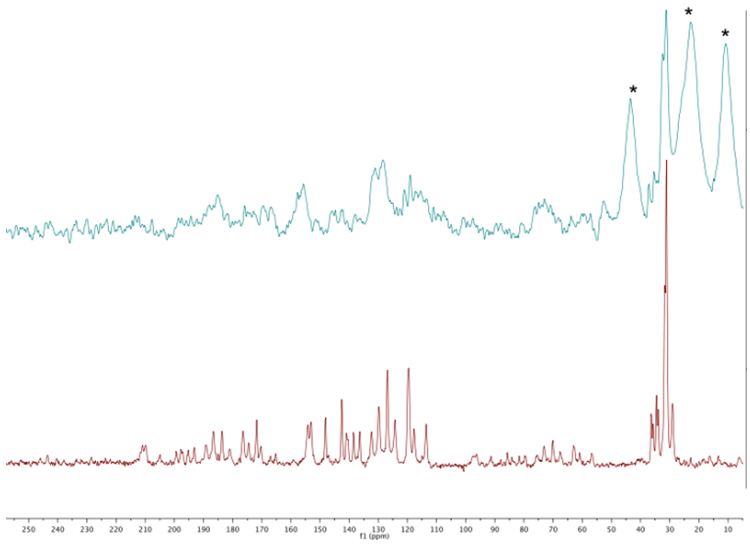

Figure 47: *^{13}C CP-MAS NMR spectra of Salophen-tBu-Ni (in red) and Salophen-tBu-Ni@{NH2}-SBA-15 (in blue). The 3 peaks with the asterisk correspond to the {CH_2} of the propylamine groups of {NH_2}-SBA-15.*

Salophen-tBu-Ni@{NH_2}-SBA-15 was dominated by the three peaks (topped with an asterisk) attributed to the carbon atoms of the propylamine functions of the support.

The Raman spectra of the Salophen-tBu-Ni and Salophen-tBu-MnCl complexes in solid state were also compared to those of Salophen-tBu-Ni@{NH_2}-SBA-15 and Salophen-tBu-MnCl@{NH_2}-SBA-15, respectively (**Figure 48**). In both cases, the two datasets clearly indicated that the spectroscopic footprints of the supported complexes are identical to those of the pure complexes in the solid state. This confirmed that the integrity of both complexes

was maintained after surface grafting, even though the spectrum of Salophen-tBu-MnCl@{NH_2}-SBA-15 was less well defined, probably due to fluorescence phenomena under Raman beam. It is noteworthy that Raman spectra of Base-Schiff compounds are complex, displaying many bands and consequently are difficult to index in details. However, by comparison with the data obtained on the parent complex without ^{t}-Butyl and carboxylic groups (*i.e.* N,N'-bis(salicylaldehyde)-1,2-phenylenediamine-nickel(II)) [53-54], it was possible to identify and assign the most intense bands at 1412 ($\delta_{HC=N}$) and 1573 cm^{-1} ($\nu_{C=C}$ aromatic) on the spectra of both the Salophen-tBu-Ni and the Salophen-tBu-MnCl complexes.

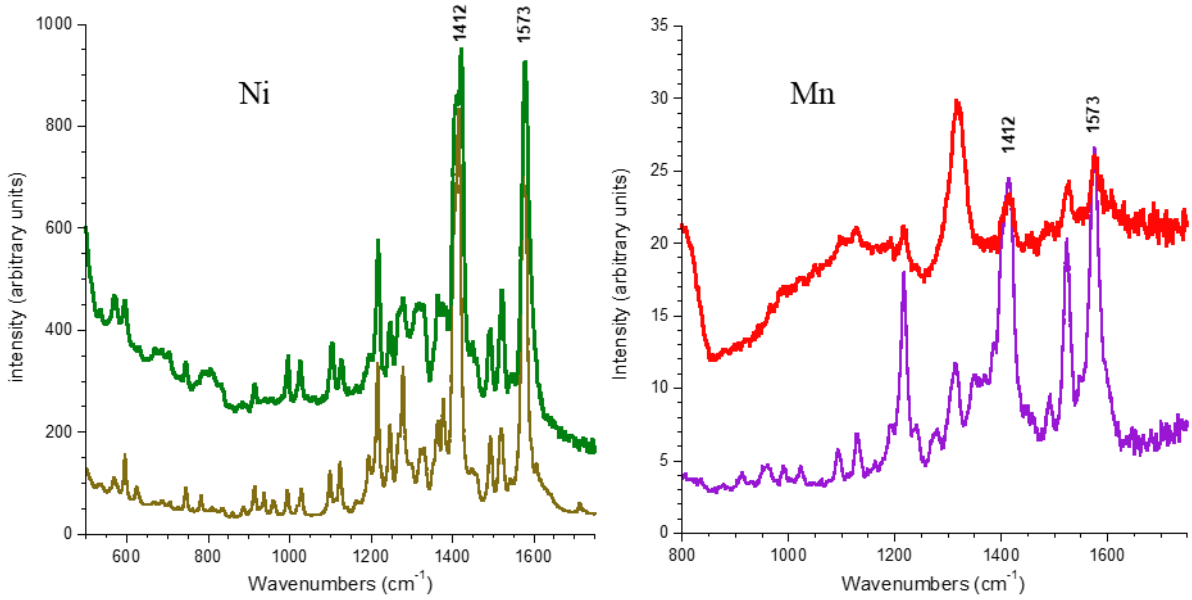

Figure 48: *Raman spectra (left) of Salophen-tBu-Ni (in brown) and Salophen-tBu-Ni@{NH_2}-SBA-15 (in green) and (right) Salophen-MnCl (in purple) and Salophen-tBu-MnCl@{NH_2}-SBA-15 (in red).*

The Salophen-tBu-Ni@{NH_2}-SBA-15 and Salophen-tBu-MnCl@{NH_2}-SBA-15 materials were also characterized by High-Resolution Transmission Electronic Microscopy (HR-TEM), after microtome cutting (**Figure 49**). For both samples, the micrographs showed that the grafting of the Salophen-tBu complexes did not alter the porosity of the support.

The N_2 adsorption-desorption isotherms of the SBA-15-based materials (**Figure 50**) exhibited characteristic type IV patterns with H_1 hysteresis confirming that all materials were constituted of mesoporous channels of relatively uniform diameter.

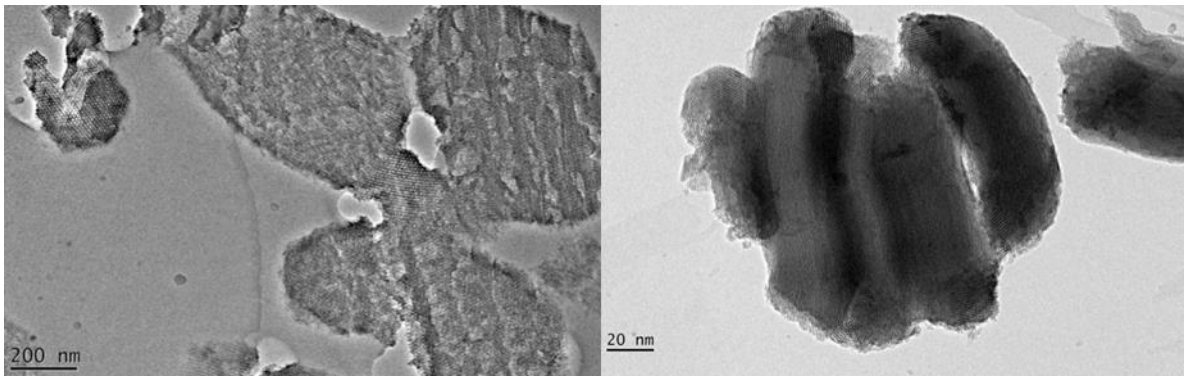

Figure 49: *HR-TEM micrograph of Salophen-tBu-Ni@{NH_2}-SBA-15 (left) and Salophen-tBu-MnCl@{NH_2}-SBA-15 after microtome cutting.*

The pore properties of the materials at the different stages of their preparation were determined from their nitrogen adsorption-desorption isotherms using the Brunauer-Emmet-Teller (BET) and the Barret-Joyner-Halenda (BJH) models (**Table 15**).

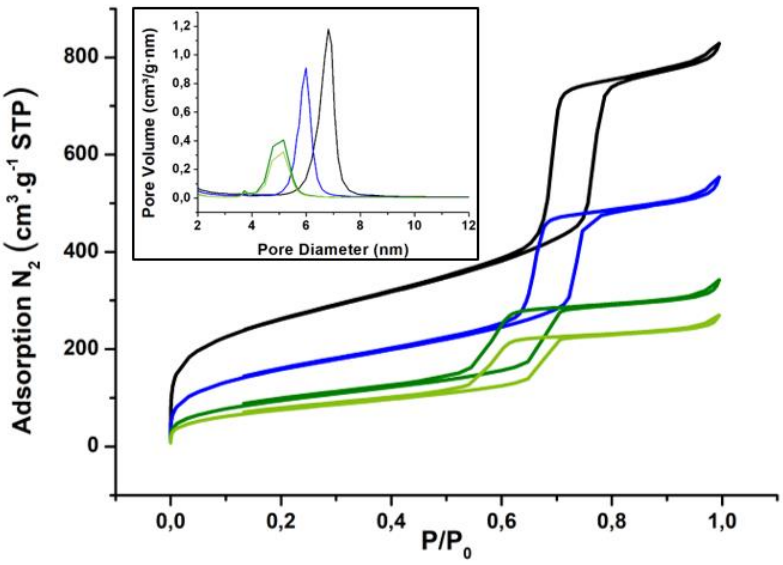

Figure 50: *Nitrogen adsorption-desorption isotherms (77K) of SBA-15 (black), {NH_2}-SBA-15 (blue), and Salophen-tBu-Ni@{NH_2}-SBA-15 before (dark green) and after 4 catalytic cycles (light green) with pores size distribution curves (inset).*

As expected, the textural parameters of the mesoporous materials significantly decreased after each functionalization step: the final BET specific surface areas were

respectively 350 $m^2.g^{-1}$ for Salophen-tBu-Ni@{NH_2}-SBA-15 and 300 $m^2.g^{-1}$ for Salophen-tBu-MnCl@{NH_2}-SBA-15 (**Figure 51**). However, this remains compatible with their utilization in anchored homogeneous catalysis.

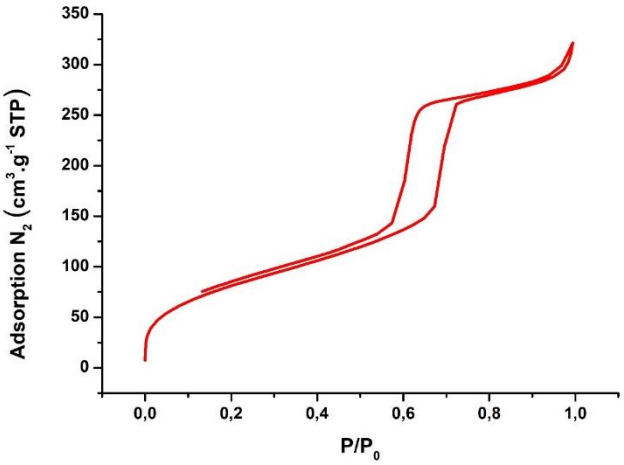

Figure 51: *Nitrogen adsorption-desorption isotherm of Salophen-tBu-MnCl@{NH_2}-SBA-15*

Table 15: *Evolution of the textural properties of the materials upon their functionalization*

Sample	S_{BET}[a] ($m^2\ g^{-1}$)	Pore Vol.[b] ($cm^3\ g^{-1}$)	Average Pore diameter[b] (nm)
SBA-15	900	1.12	6.2
{NH_2}-SBA-15	530	0.63	5.7
Salophen-tBu-MnCl @{NH_2}-SBA-15	300	0.45	5.4
Salophen-tBu-Ni@{NH_2}-SBA-15	350	0.48	5.1
Salophen-tBu-Ni@{NH_2}-SBA-15 (after 4 catalytic cycles)	280	0.38	5.0

[a] Use of the BET model for $P/P^0 < 0.25$; [b] Use of the BJH model for the treatment of the desorption branch with 2 < pore range < 26 nm.

IV.1.3.3 Comparison of the co-catalytic activity of the Salophen-type complexes in the styrene oxide conversion into styrene carbonate in homogeneous and heterogeneous conditions

Homogeneous conditions. The formation of styrene carbonate from styrene epoxide and CO_2 (Scheme 1) was firstly studied in homogeneous conditions. We thus used for this ^{n}-Bu_4NBr and the Ni/Mn-Cl Salophen complexes respectively as the catalyst and co-catalysts in benzonitrile. The reaction was performed in an autoclave under 15 bar of CO_2 at 120°C and monitored by Gas-Chromatography and ^{1}H NMR spectroscopy after 3 h, 7 h and 23 h.

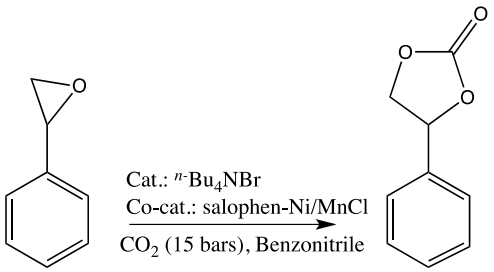

Scheme 1: *CO_2 cycloaddition onto styrene oxide.*

As already reported [55], a fairly good conversion of styrene oxide was observed with ^{n}-Bu_4NBr alone (no metal co-catalysts) after 7 h (81%, see **entry 1 Table 16**) using a styrene oxide: ^{n}-Bu_4NBr molar ratio of 60. However, the reaction slowed considerably afterwards (84% after 23 h). Typical experiments were performed with a total volume of liquid phase equal to 14 mL (13.3 mL of benzonitrile and 0.7 mL of styrene oxide) in the 100 mL vessel. It is noteworthy that this corresponds to the optimized reaction conditions, since the yield in styrene carbonate was shown to be significantly dependent on the CO_2 pressure but also on the number of moles of CO_2 available in the vessel. Thus, using the same styrene oxide concentration (0.44 mol.L^{-1}) and the same styrene oxide: ^{n}-Bu_4NBr (60:1) molar ratio, but tripling the volume of the solution in the closed vessel, led to a significant decrease in styrene oxide conversion from 81% to 40% after 7 h due to the reduction of the molar excess of CO_2 from 7 to 1.5.

In all experiments, the possible presence of polycarbonates (potentially obtained by co-polymerization of styrene oxide with styrene carbonate) was checked by ^{1}H and ^{13}C NMR spectroscopy. In any cases, no trace of polymers was detected. This was confirmed by the mass balance determination by GC using mesitylene as an internal standard. Thereafter, considering a selectivity of 100%, the total yield in styrene carbonate was assimilated to the conversion of styrene oxide.

Keeping similar reaction conditions (15 bar of CO_2 at 120°C and CO_2: epoxide = 7: 1) and using metal Salophen-tBu complexes Ni or Mn as co-catalysts with a co-catalyst: catalyst ratio of 1:2 (**Table 16**, **entries 2 and 3**), a complete conversion of styrene oxide could be reached. We have checked that both complexes were not able to catalyse alone the CO_2 cycloaddition onto styrene oxide (**Table 2**, **entries 4 and 5**). The rate increase in the presence of Salophen-tBu complexes was found to be strongly metal dependent. While the gain in the styrene oxide conversion was relatively modest with the Salophen-tBu-Ni (conversion of 65

and 85 % after respectively 3 and 7 h), it was significant after 3 h (100 % conversion) in the case of the Mn^{III} derivative. The styrene carbonate yield obtained with the latter was found to be identical to that obtained with the commercial Mn Jacobsen catalyst (**Table 16**, **entry 6**) under the same conditions, which means that the diamine used in the synthesis of the Salophen-tBu was less critical than the metal. An additional test performed with **3** and ^{n}-Bu_4NBr showed actually that, after one hour at 120°C, the styrene oxide conversion was 96%. Even if the catalytic activity of the *n*-Bu_4NBr / Salophen-tBu-Ni system in homogeneous conditions is slightly lower than that obtained with *n*-Bu_4NBr / Salophen-tBu-MnCl, it is noteworthy that this result deserved special emphasis since examples of Ni co-catalysts for the CO_2 cycloaddition are scarce.

Table 16: *Conversion of styrene oxide into styrene carbonate with homogeneous and supported catalysts.*

Entry	Catalyst	Co-catalyst	% styrene conv.		
			3 h	7 h	23 h
1	^{n}-Bu_4NBr	-	62	81	84
2	^{n}-Bu_4NBr	Salophen-tBu-Ni	65	85	100
3	^{n}-Bu_4NBr	Salophen-tBu-MnCl	100	100	100
4	-	Salophen-tBu-Ni	/	/	0
5	-	Salophen-tBu-MnCl	/	/	2
6	^{n}-Bu_4NBr	Jacobsen catalyst (commercial)	100	100	100
7	^{n}-Bu_4NBr	Salophen-tBu-Ni@{NH_2}-SBA-15	80	98	100
8	^{n}-Bu_4NBr	Salophen-tBu-MnCl@{NH_2}-SBA-15	80	100	100
9	^{n}-Bu_4NBr	{NH_2}-SBA-15*	81	86	98

Conditions: Styrene oxide (6.1 mmol), ^{n}-Bu_4NBr (0.1 mmol), homogeneous or supported Salophen-tBu-M (0.05 mmol of metal) in 13.3 mL of benzonitrile at 120°C under 15 bar of CO_2.

Heterogeneous conditions. The activity of the two anchored co-catalysts (Salophen-tBu-Ni@{NH_2}-SBA-15 or Salophen-tBu-MnCl@{NH_2}-SBA-15) was studied in the same reaction conditions (**Table 16**, **entries 7 and 8**) with 0.44 M styrene oxide keeping ^{n}-Bu_4NBr as a homogeneous catalyst with a styrene oxide: ^{n}-Bu_4NBr molar ratio of 60 and using amounts of supported Salophen-tBu-Ni or Salophen-tBu-MnCl rigorously analogous to those employed in **Table 2** (**entries 2 and 3**) for soluble Salophen-tBu-Ni and Salophen-tBu-MnCl, respectively. With Salophen-tBu-Ni@{NH_2}-SBA-15 and Salophen-tBu-MnCl@{NH_2}-SBA-15, the results obtained were comparable, allowing near complete conversion of styrene oxide after 7 h. As early as 3 h of reaction, supported Salophen-tBu-Ni showed much better performance than its homogeneous counterpart. With both supported complexes, the conversion was 80% after 3 h. Such conversion value for Salophen-tBu-MnCl@{NH_2}-SBA-15 corresponds to a slight decrease compared to what was observed for Salophen-tBu-MnCl tested in homogeneous conditions (80% conversion after 3 h instead of 100%). Indeed, heterogenized co-catalysts are

often less active at early stage than their homogeneous counterparts due to diffusion limitations. However, it is somewhat surprising to observe a significant increase in co-catalytic activity after supporting the nickel complex (80% conversion after 3 h instead of 65%).

In order to better understand those differences between the Ni homogeneous and supported co-catalysts, we also investigated the potential co-catalytic activity of the support itself, {NH_2}-SBA-15 keeping ^{n}-Bu_4NBr as the main catalyst (**Table 16**, **entry 9**). It is indeed necessary to have in mind that Salophen-tBu-Ni@{NH_2}-SBA-15 and Salophen-tBu-MnCl@{NH_2}-SBA-15 materials contain *c.a.* 0.2 mmol g^{-1} of salophen complex but also *c.a.* 2.0 mmol g^{-1} of free aminopropyl groups. Working with {NH_2}-SBA-15 (instead of Salophen-tBu-Ni@{NH_2}-SBA-15 or Salophen-tBu-MnCl@{NH_2}-SBA-15) and ^{n}-Bu_4NBr alone, all other reaction parameters being unchanged (especially the amount of amino groups), also led to a nearly complete conversion after 24 h. In the details, the effect of the presence of the metal complexes in Salophen-tBu-Ni@{NH_2}-SBA-15 and Salophen-tBu-MnCl@{NH_2}-SBA-15 was significantly observed after the first 3 h, since a complete conversion was obtained after 7 h of reaction with these last two co-catalysts. As a comparison, in their absence, the conversion was equal to 86 % (**Table 16**, **entry 9**). Such blank test emphasized the non-innocent character of those grafted amino groups in Salophen-tBu-Ni@{NH_2}-SBA-15 and Salophen-tBu-MnCl@{NH_2}-SBA-15 materials since the results with ^{n}-Bu_4NBr /{NH_2}-SBA-15 (**Table 16**, **entry 8**) turned out to be systematically better than those obtained with ^{n}-Bu_4NBr alone (**Table 16**, **entry 1**). Such positive influence was more easily observed when using Salophen-tBu-Ni due to its lower intrinsic efficiency shown in homogeneous conditions (**Table 2**, **Table 16**). Improvement of the catalytic activity of silica-supported compared to soluble phosphonium halides in CO_2 cycloaddition was already observed [56]. The proposed mechanism invoked in that case a possible activation of the epoxide by hydrogen bonding with the surface silanol groups of the support thus playing the role of electrophilic sites. At first glance, one explanation in our case would be that similar activation of the epoxide could also occur through hydrogen bonding between the free aminopropyl groups of the support and styrene oxide. However, the N-H bond in -$(CH_2)_3$-NH_2 is less polar than the O-H bond in ≡Si-OH. As a matter of fact, the N-H---$O_{epoxide}$ hydrogen bond with the epoxide should be weaker than the aforementioned O-H---$O_{epoxide}$ hydrogen bond. So, a more plausible explanation would be that CO_2 itself is activated by the primary amine of the free aminopropyl groups of {NH_2}-SBA-15,

Salophen-tBu-Ni@{NH_2}-SBA-15 or Salophen-tBu-MnCl@{NH_2}-SBA-15 even if the resulting carbamate is not the most prompt to transfer CO_2 to the anionic intermediate obtained from the attack of styrene oxide by bromide [57]. Usually activated carbamates issued from tertiary amines are preferred as exemplified in the work of J. Gao *et al* [58] who reported a significant cyclocarbonate yield increase upon the addition of triethylamine. Nevertheless, some groups have reported the beneficial impact of primary amine auxiliaries in the design of homogeneous [59] or even heterogeneous catalysts ([57, 60]) for the CO_2 addition onto epoxides.

Stability of the catalysts. Finally, the stability of the co-catalysts was investigated in homogeneous conditions with Salophen-tBu-MnCl (4 runs of 3 h with styrene oxide and CO_2 replenishment without any work-up) and in heterogeneous conditions with Salophen-tBu-Ni@{NH_2}-SBA-15 (4 runs of 23 h separated by filtration and drying steps). The detailed operating protocols for both experiments were based on the optimized experimental conditions described in the experimental part and in **Table 16**, and the results are displayed in **Figure 52**.

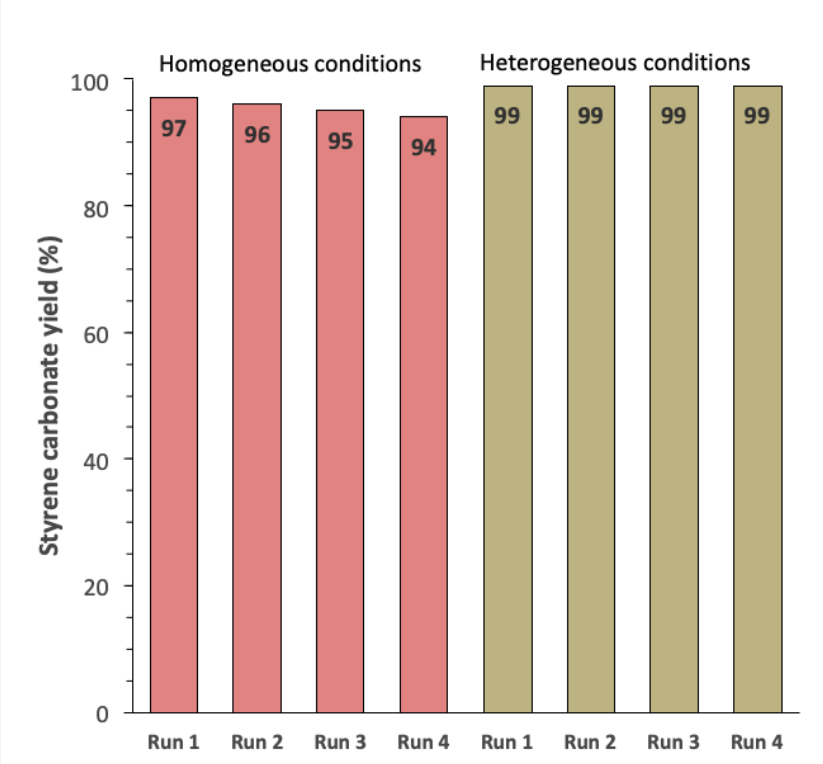

Figure 52: *Styrene carbonate yield (%) for Salophen-tBu-MnCl (homogeneous conditions, in light red) after 1 to 4 runs of 3 h and for Salophen-tBu-Ni@{NH_2}-SBA-15 (heterogeneous conditions, in light green) after 1 to 4 runs of 23 h. Conditions: Styrene oxide (6.1 mmol), $^{n}Bu_4NBr$ (0.1 mmol), homogeneous or supported Salophen-tBu-M (0,05 mmol) in 13.3 mL of benzonitrile at 120°C under 15 bar of CO_2.*

In these experiments, both co-catalysts were successfully re-used without any appreciable loss of performance after respectively four cycles, leading to a nearly complete styrene conversion (from 94 to 99%) in all cases, thus indicating an excellent stability in homogeneous and heterogeneous conditions.

Furthermore, the supported catalyst Salophen-tBu-Ni@{NH_2}-SBA-15 could be characterized after the catalytic process in order to verify that the integrity of the metal complexe is maintained. For sake of illustration, the Raman spectra of Salophen-tBu-Ni@{NH_2}-SBA-15 were compared before and after 4 catalytic cycles (**Figure 53**), showing the same patterns in both cases. In addition, the comparison of the textural parameters of Salophen-tBu-Ni@{NH_2}-SBA-15 before and after 4 catalytic cycles (**Figure 52** and **Table 16**) also demonstrated that the catalytic materials were also not altered at the microscale level. Indeed, mean pore diameter values before and after catalysis were shown to be almost unchanged while the BET surface areas and pore volumes turned out to be equivalent.

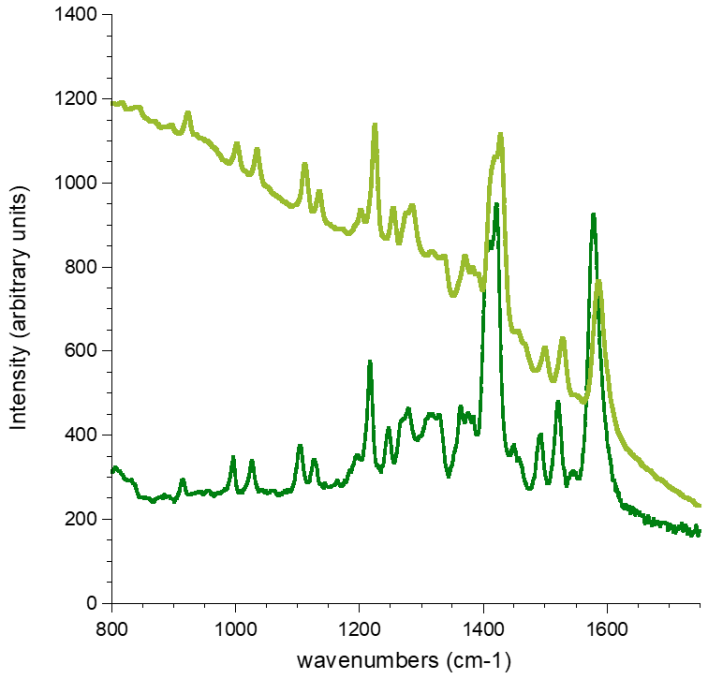

Figure 53: *Raman spectra of Salophen-tBu-Ni@{NH_2}-SBA-15 before (in dark green) and after 4 catalytic cycles (light green).*

IV.1.4 Conclusion

In this study, nickel(II) and manganese (III) complexes with the *N,N'*-bis(3,5-di-*tert*-butylsalicylidene)-1-carboxy-3,4-phenylene-diamine (Salophen-tBu-MnCl and Salophen-tBu-Ni), bearing carboxylic acid groups on their ligands, were synthesized and fully characterized. Both were shown to work as n-Bu_4NBr co-catalyst for the cycloaddition of CO_2 onto styrene oxide, thus affording a real added value in terms of epoxide conversion (100% after 3 h of reaction at 120°C under 15 bar of CO_2 with Salophen-tBu-MnCl instead of 62% without). In addition, the soluble Salophen-tBu-MnCl/ n-Bu_4NBr system proved to be stable after 3 successive replenishments of the consumed styrene oxide.

Using DCC as a convenient and efficient coupling agent, Salophen-tBu-MnCl and Salophen-tBu-Ni were easily heterogenized, with up to 1 wt.% of metal at once, by amide linkage onto a SBA-15 silica bearing propylamine groups, thus affording recoverable co-catalysts. Immobilization of the less active complex in solution, Salophen-tBu-Ni, even resulted in an enhanced co-catalytic activity (100% conversion of styrene oxide after 7 h instead of 85% in solution). This particular result paves thus the way to the utilization of (rarely used in the literature) Ni^{2+} catalysts for the CO_2 cycloaddition onto epoxides. Furthermore, the heterogenized form of Salophen-tBu-Ni was successfully re-used without any appreciable loss of activity over 4 runs. In addition, the preservation of the integrity of this co-catalyst, after the catalytic process, was demonstrated by Raman spectroscopy as well as by the measurement of the N_2 desorption/absorption isotherms.

More important, this study also showed that propylamine functions at the surface of the {NH_2}-SBA-15 support alone play also a co-catalytic role for the CO_2 cycloaddition reaction in the presence of $^{n-}Bu_4Br$ and give rise to some synergy when using covalently grafted Salophen-tBu-Ni and $^{n-}Bu_4Br$. In both cases, the origin of this effect would be due to the activation of the epoxide and/or of CO_2. Further work is in progress in order to get both the catalyst and the co-catalyst grafted on the silica support.

References

[1] A. W. Kleij, M. North, A. Urakawa, CO_2 catalysis, ChemSusChem 10 (2017) 1036-1038.

[2] M. North, Michael North, On carbon dioxide biorefinery, ChemSusChem 12 (2019) 1763-1765.

[3] M. Aresta, My journey in the CO_2-chemistry Wonderland, Coord. Chem. Rev. 334 (2017) 150-183.

[4] M. Peters, B. Köhler, W. Kuckshinrichs, W. Leitner, P. Markewitz, T. E. Müller, Chemical technologies for exploiting and recycling carbon dioxide into the value chain, ChemSusChem 9 (2011), 1216-1240.

[5] G. Laugel, C. Carvalho Rocha, P. Massiani, T. Onfroy, F. Launay, Homogeneous and heterogeneous catalysis for the synthesis of cyclic and polymeric carbonates from CO_2 and epoxides: a mechanistic overview, Adv. Chem. Lett. 1 (2013) 195-214.

[6] Special Issue: Catalysis for CO_2 conversion, ChemSusChem 10 (2017) 1034-1297.

[7] C. Chauvier, T. Cantat, A Viewpoint on chemical reductions of carbon–oxygen bonds in renewable feedstocks including CO_2 and biomass, ACS Catal. 7 (2017) 2107-2115.

[8] S. Sopeña, G. Fiorani, C. Martín, A.W. Kleij, Highly efficient organocatalyzed conversion of oxiranes and CO_2 into organic carbonates, ChemSusChem 8 (2015) 3248-3254.

[9] M. Cokoja, M.E. Wilhelm, M.H. Anthofer, W.A. Herrmann, F.E. Kühn, Synthesis of cyclic carbonates from epoxides and carbon dioxide by using organocatalysts, ChemSusChem 8 (2015) 2436-2454.

[10] M. Alves, B. Grignard, S. Gennen, C. Detrembleur, C. Jerome, T. Tassaing, Organocatalytic synthesis of bio-based cyclic carbonates from CO_2 and vegetable oils, RSC Adv. 5 (2015) 53629-53636.

[11] Z.Z. Yang, L.N. He, C.X. Miao, S. Chanfreau, Lewis basic ionic liquids-catalyzed conversion of carbon dioxide to cyclic carbonates, Adv. Synth. Catal. 352 (2010) 2233-2240.

[12] Y. Zhou, S. Hu, X. Ma, S. Liang, T. Jiang, B. Han, Synthesis of cyclic carbonates from carbon dioxide and epoxides over betaine-based catalysts, J. Mol. Catal. A: Chem 284 (2008) 52-57.

[13] B. Chatelet, L. Joucla, J.P. Dutasta, A. Martinez, K.C. Szeto, V. Dufaud, Azaphosphatranes as structurally tunable organocatalysts for carbonate synthesis from CO_2 and epoxides, J. Am. Chem. Soc. 135 (2013) 5348-5351.

[14] C. Miceli, J. Rintjema, E. Martin, E.C. Escudero-Adán, C. Zonta, G. Licini, A.W. Kleij, Vanadium(V) catalysts with high activity for the coupling of epoxides and CO_2: characterization of a putative catalytic intermediate, ACS Catal. 7 (2017) 2367-2373.

[15] D. Darensbourg, Making plastics from carbon dioxide: salen metal complexes as catalysts for the production of polycarbonates from epoxides and CO_2**,** Chem. Rev. 107 (2007) 2388-2410.

[16] P. Lan, L.E. White, E.S. Taher, P.E. Guest, M.G. Banwell, A.C. Willis, Chemoenzymatic synthesis of (+)-asperpentyn and the enantiomer of the structure assigned to Aspergillusol A, J. Nat. Prod. 78 (2015) 1963-1968.

[17] X. Xiaoding, J.A. Moulijn, Mitigation of CO_2 by chemical conversion: plausible chemical reactions and promising products, energy & fuels 10 (1996) 305-325.

[18] J. Melendez, M. North, R. Pasquale, Synthesis of cyclic carbonates from atmospheric pressure carbon dioxide using exceptionally active aluminium(salen) complexes as catalysts, Eur. J. Inorg. Chem. (2007) 3323-3326.

[19] X. Zhang, Y.B. Jia, X.B. Lu, B. Li, H. Wang, L.C. Sun, Intramolecularly two-centered cooperation catalysis for the synthesis of cyclic carbonates from CO_2 and epoxides, Tetrahedron Lett. 49 (2008) 6589-6592.

[20] J. Rintjema, L. P. Carrodeguas, V. Laserna, S. Sopena, A. W. Kleij, Metal complexes catalyzed cyclization with CO_2, Top. Organomet. Chem. 53 (2016) 39-71.

[21] L. Cuesta-Aluja, A. Campos-Carrasco, J. Castilla, M. Reguero, A. M. Masdeu-Bulto, A. Aghmiz, Highly active and selective Zn(II)-NN O Schiff base catalysts for the cycloaddition of CO_2 to epoxides, J. CO_2 Util. 14 (2016) 10-22.

[22] J.W. Comerford, I.D.V. Ingram, M. North, X. Wu, Sustainable metal-based catalysts for the synthesis of cyclic carbonates containing five-membered rings, Green Chem. 17 (2015) 1966-1987.

[23] M. Aresta, A. Dibenedetto, Utilization of CO_2 as a chemical feedstock: opportunities and challenges, Dalton Trans. (2007) 2975-2992.

[24] A. Kamphuis, F. Picchioni, P. P. Pescarmona, CO_2-fixation into cyclic and polymeric carbonates: principles and applications, Green Chem. 21 (2019) 406-448.

[25] M. Alves, B. Grignard, R. Mereau, C. Jerome, T. Tassaing, C. Detrembleur, Organocatalyzed coupling of carbon dioxide with epoxides for the synthesis of cyclic carbonates: catalyst design and mechanistic studies, Catal. Sci. Technol. 7 (2017) 2651-2684.

[26] A. Mirabaud, J.-C. Mulatier, A. Martinez, J.-P. Dutasta, V. Dufaud, Merging host-guest chemistry and organocatalysis for the chemical valorization of CO_2, Catal.Today 281 (2017) 387-391.

[27] C. Carvalho Rocha, T. Onfroy, J. Pilme, A. Denicourt-Nowicki, A. Roucoux, F. Launay, Experimental and theoretical evidences of the influence of hydrogen bonding on the catalytic activity of a series of 2-hydroxy substituted quaternary ammonium salts in the styrene oxide/CO_2 coupling reaction, J. Catal. 333 (2016) 29-39.

[28] L. Cuesta-Aluja, M. Djoufak, A. Aghmiz, R. Rivas, L. Christ, A. Masdeu-Bulto, Novel chromium (III) complexes with N_4-donor ligands as catalysts for the coupling of CO_2 and epoxides in supercritical CO_2, J. Mol. Catal. A: Chem. 381 (2014) 161-170.

[29] M. Djoufak, PhD thesis, dir. L. Christ, University of Lyon (2013).

[30] T. Ema, Y. Miyazaki, S. Koyama, Y. Yano, T. Sakai, A bifunctional catalyst for carbon dioxide fixation: cooperative double activation of epoxides for the synthesis of cyclic carbonates, Chem. Commun. 48 (2012) 4489-4491.

[31] J. A. Castro-Osma, K. J. Lamb, M. North, Cr(salophen) Complex catalyzed cyclic carbonate synthesis at ambient temperature and pressure, ACS Catal. 6 (2016) 5012-5025.

[32] J. Melendez, M. North, P. Villuendas, C. Young, One-component bimetallic aluminium(salen)-based catalysts for cyclic carbonate synthesis and their immobilization, Dalton Trans. 40 (2011) 3885-3902.

[33] P.A. Carvalho, J. W. Comerford, K.J. Lamb, M. North, P. S. Reiss, Influence of mesoporous silica properties on cyclic carbonate synthesis catalysed by supported aluminium(Salen) complexes, Adv. Synth. Catal. 361 (2019) 345-354.

[34] S. Wei, Y. Tang, G. Xu, X. Tang, Y. Ling, R. Li, Y. Sun, New chiral (salen)manganese(III) systems for asymmetric epoxidation of styrene, React. Kinet. Catal. Lett.97 (2009) 329-333.

[35] A. Heckel, D. Seebach, Enantioselective heterogeneous epoxidation and hetero-Diels-Alder reaction with Mn- and Cr-salen complexes immobilized on silica gel by radical grafting, Helv. Chim. Acta 85 (2002) 913-926.

[36] S. Xiang, Y. Zhang, Q. Xin C. Li, Enantioselective epoxidation of olefins catalyzed by Mn (salen)/MCM-41 synthesized with a new anchoring method, Chem. Commun. (2002) 2696-2697.

[37] H. Zhang, S. Xiang, J. Xiao, C. Li, Heterogeneous enantioselective epoxidation catalyzed by Mn(salen) complexes grafted onto mesoporous materials by phenoxy group, J. Mol. Cat. A: Chem. 238 (2005) 175-184.

[38] L. Saikia, D. Srinivas, P. Ratnasamy, Comparative catalytic activity of Mn(Salen) complexes grafted on SBA-15 functionalized with amine, thiol and sulfonic acid groups for selective aerial oxidation of limonene, Micropor. Mesopor. Mater. 104 (2007) 225-235.

[39] G. Trusso Sfrazzetto, S. Millesi, A. Pappalardo, R. M. Toscano, F. P. Ballistreri, G. A. Tomaselli A. Gulino, Olefin epoxidation by a (salen)Mn(III) catalyst covalently grafted on glass beads, Catal. Sci. Technol. (5) 2015, 673-679.

[40] F. Bentaleb, O. Makrygenni, D. Brouri, C. Coelho Diogo, A. Mehdi, A. Proust, F. Launay, R. Villanneau, Efficiency of polyoxometalate-based mesoporous hybrids as covalently anchored catalysts, Inorg. Chem. 54 (2015) 7607-7616.

[41] O. Makrygenni, D. Brouri, A. Proust, F. Launay, F. Launay, R. Villanneau, Immobilization of polyoxometalate hybrid catalysts onto mesoporous silica supports using phenylene diisothiocyanate as a cross-linking agent, Microporous Mesoporous Mater. 278 (2019) 314-321.

[42] T. Luts, R. Frank, W. Suprun, S. Fritzsche, E. Hey-Hawkins, H. Papp, Epoxidation of olefins catalyzed by novel Mn(III) and Mo(IV)-salen complexes immobilized on mesoporous silica gel, J. Mol. Catal. A: Chem. 273 (2007) 250-258.

[43] T. Luts, H. Papp, Novel Ways of Mn-Salen Complex immobilization on modified silica support and their catalytic activity in cyclooctene epoxidation, kinetics and catalysis 48 (2007), 176-182.

[44] F. Jutz, J.-D. Grunwaldt, A. Baiker, *In situ* XAS study of the Mn(III)(salen)Br catalyzed synthesis of cyclic organic carbonates from epoxides and CO_2, J. Mol. Catal. A: Chem. 297 (2009) 63-72.

[45] J. L. S. Milani, A. M. Meireles, B. N. Cabral, W. de A. Bezerra, F. T. Martins, D. Carvalho da Silva Martins, R. Pavao das Chagas, Highly active Mn (III) meso-tetrakis (2, 3-dichlorophenyl) porphyrin catalysts for the cycloaddition of CO_2 with epoxides, J. CO_2 Util. 30 (2019) 100-106.

[46] L. Cuesta-Aluja, J. Castilla, A. M. Masdeu-Bulto, C. A. Henriques, M. J. F. Calvete, M. M. Pereira, Halogenated *meso*-phenyl Mn(III) porphyrins as highly efficient catalysts for the synthesis of polycarbonates and cyclic carbonates using carbon dioxide and epoxides, J. Mol. Catal. A: Chem. 423 (2016) 489-494.

[47] R. Srivastava, T. H. Bennur, D. Srinivas, Factors affecting activation and utilization of carbon dioxide in cyclic carbonates synthesis over Cu and Mn peraza macrocyclic complexes, J. Mol. Catal. A: Chem. 226 (2005) 199-205.

[48] Y. Fan, J. Li, Y. Ren, H. Jiang, A Ni(salen)-based metal-organic framework: synthesis, structure, and catalytic performance for CO_2 cycloaddition with epoxides, Eur. J. Inorg. Chem. 43 (2017) 4982-4989.

[49] F. Chiker, F. Launay, J.P. Nogier, J.L. Bonardet, New Ti-SBA mesoporous solids functionnalized under gas phase conditions: characterisation and application to selective oxidation of alkenes, Appl. Catal., A: Gen. 243 (2003) 309-321.

[50] M. Boutros, G. Shirley, T. Onfroy, F. Launay, Dispersion and hydrogenation activity of surfactant-stabilized Rh(0) nanoparticles prepared on different mesoporous supports, Appl. Catal., A: Gen. 394 (2011) 158-165.

[51] R. Villanneau, A. Marzouk, Y. Wang, A. Ben Djamaa, G. Laugel, A. Proust, F. Launay, Covalent grafting of organic–inorganic polyoxometalates hybrids onto mesoporous SBA-15: a key step for new anchored homogeneous catalysts, Inorg. Chem. 52 (2013) 2958-2965.

[52] M. Schley, S. Fritzsche, P. Lönnecke, E. Hey-Hawkins, Soluble monometallic salen complexes derived from O-functionalised diamines as metalloligands for the synthesis of heterobimetallic complexes, Dalton Trans. 39 (2010) 4090-4106.

[53] M. Datta, D. H. Brown, W. E. Smith, The resonance Raman profile of a nickel Schiff base complex at 10 K, Spectrochim. Acta A, 39, (1983) 37-41.

[54] T.A. de Toledo, P.S. Pizani, L.E. da Silva, A.M.R. Teixeira, P.T.C. Freire, Spectroscopy studies on Schiff base N,N'-bis(salicylidene)-1,2-phenylenediamine by NMR, infrared, Raman and DFT calculations, J. Mol. Struct. 1097 (2015) 106-111.

[55] S. Foltran, J. Alsarraf, F. Robert, Y. Landais, E. Cloutet, H. Cramail, T. Tassaing, On the chemical fixation of supercritical carbon dioxide with epoxides catalyzed by ionic salts: an in situ FTIR and Raman study, Catal. Sci. Technol. 3 (2013) 1046-1055.

[56] T. Takahashi, T. Watahiki, S. Kitazume, H. Yasuda, T. Sakakura, Synergistic hybrid catalyst for cyclic carbonate synthesis: remarkable acceleration caused by immobilization of homogeneous catalyst on silica, Chem. Commun. (2006) 1664-1666.

[57] R. Srivastava, D. Srinivas, P. Ratnasamy, Sites for CO_2 activation over amine-functionalized mesoporous Ti(Al)-SBA-15 catalysts, Microporous and Mesoporous Materials 90 (2006) 314-326.

[58] J. Gao, L. li, C. Cui, M. A. Ziaee, Y. Gong, R. Sa, H. Zhong, Experimental and theoretical study for CO_2 activation and chemical fixation with epoxides, RSC Advances 9 (2019) 13122-13127.

[59] T. Werner, N. Tenhumberg, Synthesis of cyclic carbonates from epoxides and CO_2 catalyzed by potassium iodide and amino alcohol, J. CO_2 Util. 7 (2014) 39-45.

[60] Y. Li, X. Zhang, J. Lan, P. Xu, J. Sun, Porous Zn(Bmic)(AT) MOF with Abundant Amino Groups and Open Metal Sites for Efficient Capture and Transformation of CO_2, Inorg. Chem. 58 (2019) 13917-13926.

CHAPTER IV.2 :

Use of soluble or supported Chromium-salophen co-catalysts for the reaction of CO_2 with styrene oxide

(Work carried out in collaboration with Ludivine K/Bidi (M2))

IV.2.1 Introduction

To our knowledge, the formation of cyclic carbonates assisted by chromium salophen complexes was first described by Paddock and Nguyen in 2001.[1] Then, the combination of Chromium-Salophens with different Lewis bases (DMAP[2], TBABr[3] or ionic liquids [4], etc) has allowed the conversion of CO_2 under increasingly mild conditions. Recently, North and co-workers [5] described a very efficient catalytic system based on Bu_4NBr and Salophen-Cr allowing a 93% yield of styrene carbonate at room temperature and 1 bar CO_2 pressure after 24 h but it seems that these authors did not work on the implementation of a supported version of the Salophen-tBu-Cr (see **Figure 54**). These results are very interesting to us, since, in the context of our project to convert alkenes to cyclic carbonates in the presence of CO_2 and a green oxidant, it is of particular importance to ensure that the cycloaddition reaction can be carried out under mild conditions.

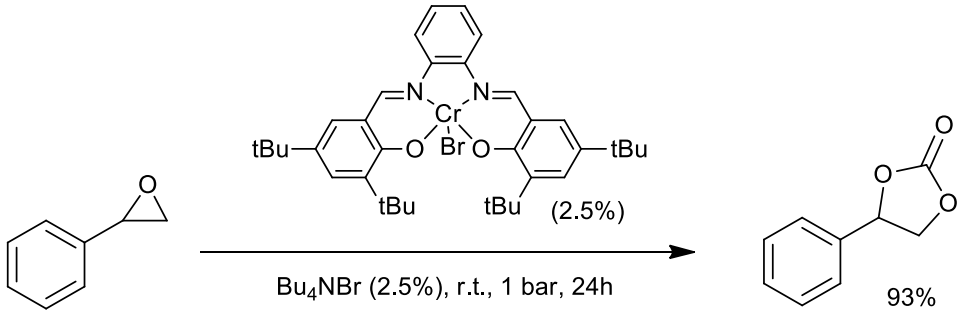

Figure 54: *Catalytic system developed by North and co-workers in the cycloaddition of styrene oxide with CO_2*

Lots of examples of Salophen complexes heterogenization have been extensively described with various kinds of supports among which zeolites or mesoporous silicas.[6,7] Here, following our previous work on Mn or Ni Salophen-tBu (see **Chapter IV.1**), we propose to investigate the use of amide bonding to get Salophen-tBu-Cr co-catalysts with good efficiency for the cycloaddition of CO_2 onto styrene oxide under mild condition.

Same Salophen-tBu used for the anchoring of Mn and Ni complexes seen in **Chapter IV.1** will be synthesized first, then Chromium centre will be added in the coordination sphere. The following part will focus first on the co-catalytic activity in solution of Salophen-tBu-Cr, a complexe that is easy to prepare, then the performances of the latter will be compared to its grafted version.

IV.2.2 Experimental part

*Only the working protocols of the syntheses that are specific to this part are described here (for the others, the reader will be referred to the corresponding parts). The same will apply to the characterisation techniques (N_2 sorption, XRD, TGA, (see **Appendix**)) in order to avoid repetition.*

IV.2.2.1 Synthesis and heterogenization of the precursor complexe

Preparation of N,N'-bis(3,5-di-tert-butylsalicylidene)-1-carboxy-3,4-phenylene-diamine-ChromiumCl (III) (Salophen-tBu-CrCl). H_2Salophen-tBu ligand (0.450 g, 1 eq, 0.67 mmol) whose synthesis and physico-chemical properties (XRD, TGA and N_2 physisorption) are described in **Chapter IV.1** was dissolved in 25 mL of dry THF under argon in a two-neck round-bottom flask connected to a condenser. Then, a solution of $[CrCl_3(THF)_3]$ (0.157 g, 1 eq, 0.68 mmol) in 25 mL of dry THF under argon was added dropwise and the resulting mixture was heated, stirred under reflux for 15 min. After cooling at room temperature, the solvent was evaporated under vacuum leading to a dark red solid (Salophen-tBu-CrCl) (yield: 0.420 g, 94%). MS (ESI): 652.296 (**Figure 55**)

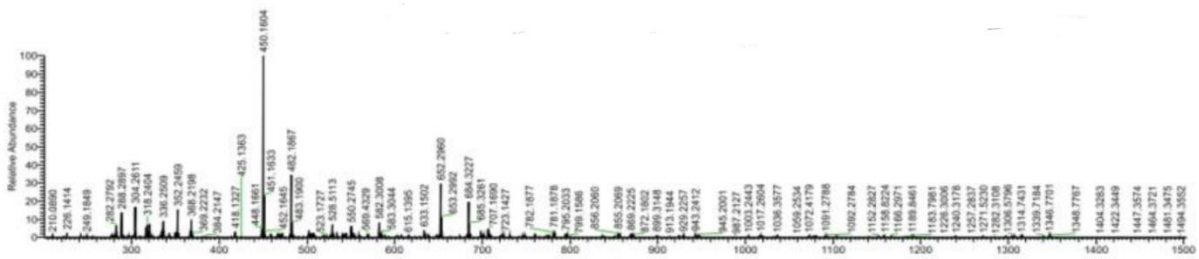

Figure 55: *HRMS spectrum of Salophen-tBu-Cr complex*

Preparation of Salophen-tBu-Cr@{NH_2}-SBA-15. {NH_2}-SBA-15 (0.30 g, [-RNH_2] = 2.2 mmol g^{-1}, corresponding to 0.66 mmol of {-RNH_2} functions, see synthesis in Chapter IV.1) and Salophen-tBu-Cr (0.105 g, 0.16 mmol) were dried under vacuum overnight in two Schlenk tubes. Then, Salophen-tBu-Cr was dissolved in dichloromethane (DCM, 3 mL). In parallel, a 2 mL solution of 1-hydroxy-1H-benzotriazole (HOBT, 0.007 g, 0.05 mmol) and *N,N'*-dicyclohexylcarbodiimide (DCC, 0.05 g, 0.34 mmol) in DCM was prepared and added to Salophen-tBu-Cr in DCM. The resulting mixture was stirred for 40 min at room temperature. Meanwhile, 10 mL of DCM were added to {NH_2}-SBA-15. After 40 min, the mixture of **2**, HOBT and DCC was transferred to the suspension of {NH_2}-SBA-15 and refluxed for 6 h under N_2.

Then, the solvent was evaporated until dryness and the resulting red powder was washed successively with refluxing methanol and acetone using a Soxhlet, respectively for 3 days and 24 h. Salophen-tBu-Cr@{NH_2}-SBA-15 (0.32 g) was thus obtained as a dark red purple powder (Cr %weight = 0.8 % determined indirectly by TGA (6.7% mol Cr/mol -NH_2) corresponding to a Cr grafting yield of 29.5%).

IV.2.2.2 Procedures for the catalysis tests and the reaction monitoring

See details for the experimental procedure used for the addition of CO_2 onto styrene oxide in **Chapter IV.1**. Here, the effect of multiple reaction parameters such has time (1 to 23 h), solvent (benzonitrile and acetonitrile) and temperature (50, 60 and 80°C) has been investigated. Tetra butyl ammonium bromide was still used as homogeneous catalyst.

IV.2.3 Results and discussion

N,N'-bis(3,5-di-tert-butylsalicylidene)-1-carboxy-3,4-phenylene-diamine-Chromium Cl (III) or Salophen-tBu-Cr was easily prepared from the salophen ligand with a 94% yield (**Figure 56.i**).

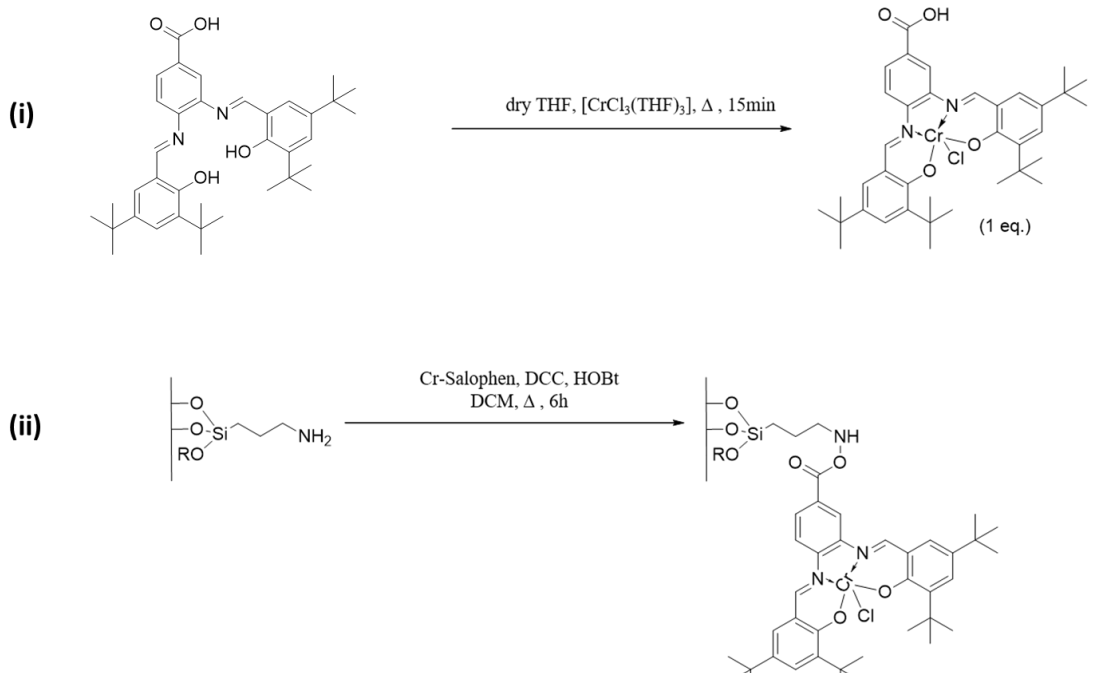

Figure 56: *Synthesis of Salophen-tBu-CrCl from ligand 1 (i) and its covalent anchoring onto SBA-15 silica bearing aminopropyl groups (ii)*

Then Salophen-tBu-Cr was grafted onto {NH_2}-SBA-15 (2.2 mmol.g^{-1} -NH_2) using the same strategy used for covalent grafting of Salophen-tBu-Mn and Ni seen in **Chapter IV.1**, which is based on the formation of strong amide bonds by the reaction of the -NH_2 groups of the support with the -COOH substituents of the Salophen-tBu (**Figure 56.ii**). N,N'-dicyclohexylcarbodiimide (DCC) and 1-hydroxy-1H-benzotriazole (HOBT) were used as coupling agents in dichloromethane under refluxing conditions affording Salophen-tBu-Cr @{NH_2}-SBA-15. The material obtained was then characterized by XRD, TGA and BET physisorption (**Figure 57**). According to the comparison of the TGA profiles of {NH_2}-SBA-15 and Salophen-tBu-Cr @{NH_2}-SBA-15, the Cr loading could be estimated to 0.8 wt.%.

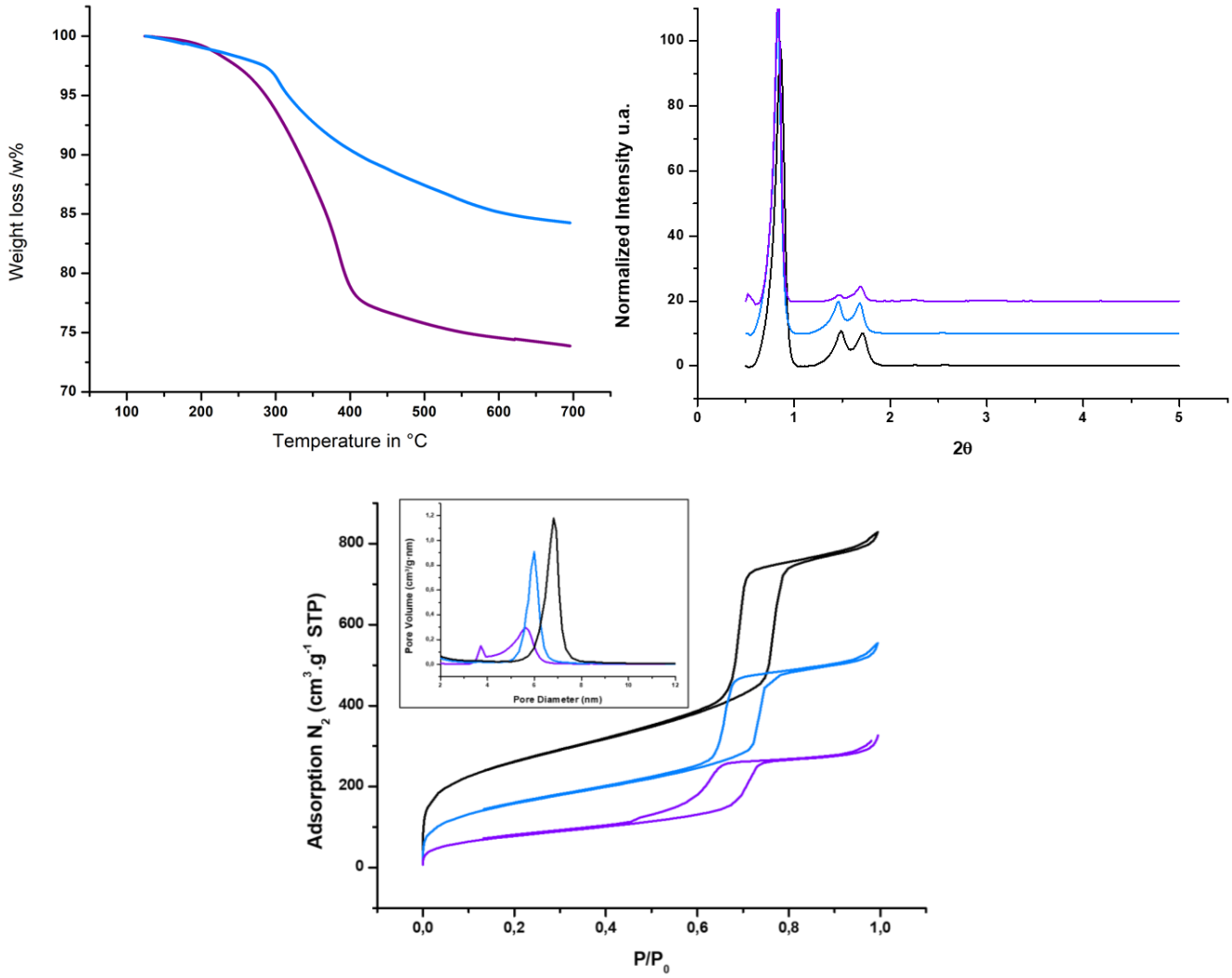

Figure 57: *(top left) Weight loss % (thermogravimetric analysis, TGA) for {NH2}-SBA-15 (blue) and Salophen-tBu-Cr@{NH_2}-SBA-15 (purple). All curves were normalized at 100°C. (top right) X-ray Diffraction patterns of SBA-15 (black), {NH_2}-SBA-15 (blue), and Salophen-tBu-Cr@{NH_2}-SBA-15 (purple). (bottom) Nitrogen adsorption-desorption isotherms (77K) of SBA-15 (black), {NH_2}-SBA-15 (blue), and Salophen-tBu-Cr@{NH_2}-SBA-15 (purple) with pore size distribution curves (inset)*

Overall, a decrease of the specific surface area was observed after grafting (see **Table 17**) (900 $m^2.g^{-1}$ to 530 then 310 $m^2.g^{-1}$ in the case of grafted Salophen-tBu-Cr), but also of the volume (1.12 $cm^3.g^{-1}$ to 0.69 {NH_2} and 0.44 $cm^3.g^{-1}$ {Salophen-tBu-Cr}-SBA-15) and of the pore diameter (6.2 nm to 5.7 nm for {NH_2}-SBA-15 and 5.2 for {Salophen-tBu-Cr}-SBA-15). These data are compatible with those observed in the case of Manganese (300 $m^2.g^{-1}$ and 5.4 nm diameter) and Nickel complexes (350 $m^2.g^{-1}$ and 5.1 nm diameter) grafted on silica SBA-15. (100), (110) and (200) reticular planes were still present, characteristic of SBA-15 (see **Figure 57**). The grafting of the organic molecules onto the SBA-15 silica does not or only slightly alter the support.

Table 17: *Sorption values for functionalized silica support*

Sample	S_{BET} ($m^2.g^{-1}$)	Pore Vol. ($cm^3.g^{-1}$)	Average Pore diameter (nm)
SBA-15	900	1.12	6.2
{NH_2}-SBA-15	530	0.69	5.7
{Salophen-tBu-Cr}-SBA-15	310	0.44	5.2

Salophen-tBu-Cr@{NH_2}-SBA-15 was prepared in a way similar to Salophen-tBu-Mn@{NH_2}-SBA-15 and Salophen-tBu-Ni@{NH_2}-SBA-15 described in the previous chapter. Chromium metal concentration estimated from thermogravimetric analysis and comparable result of metal loading (0.80%) was obtained compared to Manganese (1.03%) or Nickel (1.30%) corresponding to grafting yield of 41%.

Used alone at 80°C at a molar ration of 0.9%, without adding Bu_4NBr, we have checked that Salophen-tBu-Cr did not catalyse the CO_2 cycloaddition onto styrene oxide (**Table 18**, **entry 1**). As shown earlier in similar conditions, Bu_4NBr alone led to 12% yield of styrene carbonate in 3 h, 20% in 7 h and 99% in 23 h (**Table 18**, **entry 2**), but adding Salophen-tBu-Cr, as a co-catalyst, led to 75% yield within 3 h with 100% selectivity (**Table 18**, **entry 3**). Whatever the working temperature considered, Salophen-tBu-Cr strongly enhanced the conversion of styrene oxide, with an increase of styrene carbonate from 12 to 99% at 80°C, from 2 to 96% at 60°C and from 0 to 69% at 50°C (**Table 18**, **entries 2/3, 4/5 and 6/7**).

Working at 60°C with both Salophen-tBu-Cr, and *n*-Bu_4NBr led also to the almost consumption of styrene oxide within 23h (**Table 18**, **entry 5**, 96% yield). The results obtained at 50°C were less acceptable since the styrene carbonate yield was only 69% after 23h in this case (**Table 18**, **entry 7**).

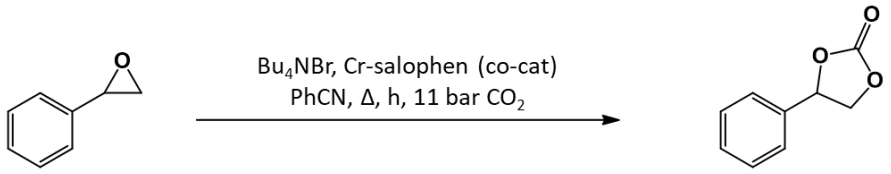

Table 18 *Yield (%) of styrene carbonate obtained with Cr- (or Mn or Ni)salophen co-catalyst as well as Salophen-tBu-Cr@{NH_2}-SBA-15*

Entry	Co-cat (Lewis acid)	cat. (Lewis base)	T (°C)	3h	7h	23h
1	Salophen-tBu-Cr	-	80			0
2	-	Bu_4NBr	80	12	20	99
3	Salophen-tBu-Cr	Bu_4NBr	80	75	92	99
4	-	Bu_4NBr	60	2	5	24
5	Salophen-tBu-Cr	Bu_4NBr	60	26	47	96
6	-	Bu_4NBr	50	0	2	11
7	Salophen-tBu-Cr	Bu_4NBr	50	12	29	69
8	Salophen-tBu-Cr@SBA	Bu_4NBr	80	58	77	99
9	Salophen-tBu-Cr@SBA	Bu_4NBr	60	10	32	79
10	Salophen-tBu-Cr@SBA	Bu_4NBr	50	5	13	47
11[(a)]	Salophen-tBu-Cr	Bu_4NBr	80	-	91	-
12 [(a)]	Salophen-tBu-Cr@SBA	Bu_4NBr	80	-	78	-
13	Salophen-tBu-Mn	Bu_4NBr	80	-	48	-
14	Salophen-tBu-Ni	Bu_4NBr	80	-	26	-

Conditions: Styrene oxide (5.6 mmol), n-Bu_4NBr (0.1 mmol), soluble and supported Salophen-tBu-Cr (0.05 mmol) in 13.3 mL of benzonitrile under 11 bar of CO_2. (a) reaction conducted I acetonitrile

Chromium(III) is clearly a better metal centre compared to Manganese(III) and Nickel(II). Indeed a significant increase of reactivity was observed in the presence of Salophen-tBu-Cr compared to Salophen-tBu-Mn (see **Table 18**, **entry 13**) and Salophen-tBu-Ni (see **Table 18**, **entry 14**) with yields of styrene carbonate of 48% for Mn, 26% for Ni and 91% for Cr.

*Then, t*he activity of the anchored co-catalyst (Salophen-tBu-Cr@{NH_2}-SBA-15) was also investigated at 50, 60 and 80°C keeping other parameters constant, especially the substrate/catalyst/co-catalyst molar ratios and working with *n*-Bu_4NBr as a homogeneous catalyst. At first sight, it is noteworthy that better results were obtained with the soluble form of Salophen-tBu-Cr, and this independently of the temperature or reaction time (see **Table 18**, **entries 8-10** vs. **entries 3, 5 and 7**). Heterogeneous results are available for reactions conducted for 3h, 7h and 23h (**Table 18, entries 8 - 10**). For a 7 h reaction time, an average loss of 15% of styrene carbonate yield could be estimated between homogeneous and heterogeneous conditions. In fact, in only one case, 23 h at 80°C, a complete transformation

of styrene oxide into styrene carbonate could be observed in heterogeneous conditions. Reactions were also conducted in acetonitrile, which is the most used solvent in epoxidation reaction (see **Chapter I**). It could be shown that, after 7h at 80°C, the yields of styrene oxide in acetonitrile were not significantly different from those obtained in benzonitrile (c.a. 92% in homogeneous *vs.* 78% in heterogeneous conditions). Similar yields of styrene carbonate were obtained at 80°C, meaning that the solvent does not impact the catalytic reactivity (see **Table 18 entries 11-12**).

Even though the loss of reactivity in the heterogeneous co-catalyst system, praised should be addressed with a significant improvement of the overall reaction with a complete conversion of styrene oxide at 80°C obtained after 23h reaction. In general, the relatively small decrease in reactivity observed in heterogeneous systems is largely offset by the advantages obtained, such as the recyclability of the catalyst compared to the homogeneous system. This difference in reactivity between homogeneous and heterogeneous systems is not found in the case of the Mn and Ni supported catalysts seen in **Chapter IV.1**. On the contrary, reactions conducted at 120°C in the presence of supported catalysts showed better results compared to those obtained in a homogeneous system. In our case, it is possible that the lower reaction temperature of 80°C does not allow the amine functions to interact as efficiently with CO_2. To confirm this hypothesis, it would be interesting to conduct cycloaddition reactions in the presence of Salophen-tBu-Mn or Ni supported on silica at temperatures of 80°C.

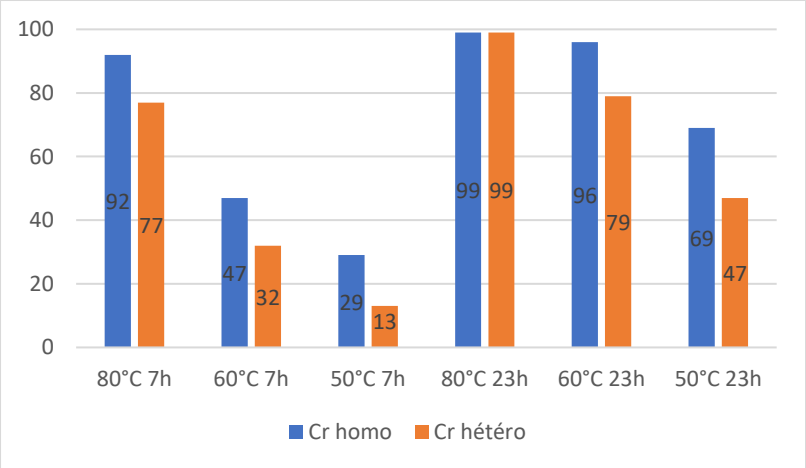

***Figure 58**: Comparison of the styrene carbonate yields obtained in homogeneous and heterogeneous condition Conditions: Styrene oxide (5.6 mmol), n-Bu_4NBr (0.1 mmol), soluble and supported Salophen-tBu-Cr (0.05 mmol) in 13.3 mL of benzonitrile under 11 bar of CO_2,* 7h 80°C

The preservation of the Cr activity has also been investigated by repeating catalysis tests in homogeneous or heterogeneous conditions. Using procedures similar to those detailed in **Chapter IV.1**, 4 runs were conducted at 80°C for 7h reactions using either Salophen-tBu-Cr (see **Table 18**, **entry 3**) or Salophen-tBu-Cr@{NH_2}-SBA-15 (see **Table 18, entry 8**). Yields of styrene carbonate in the corresponding tests are presented in **Figure 59** showing that runs in homogeneous conditions were characterized by very little loss of activity (from 92% to 90% in the fourth run). The decrease of the performances of Salophen-tBu-Cr@{NH_2}-SBA-15 seems to be more pronounced. Indeed, a progressive loss was observed after each run, with a 77% yield of styrene carbonate in the first run and 69% yield obtained in the fourth run. This difference can be explained in part by the recurrent loss of 5 wt.% of the supported co-catalyst during the work-up procedure leading to its recovery.

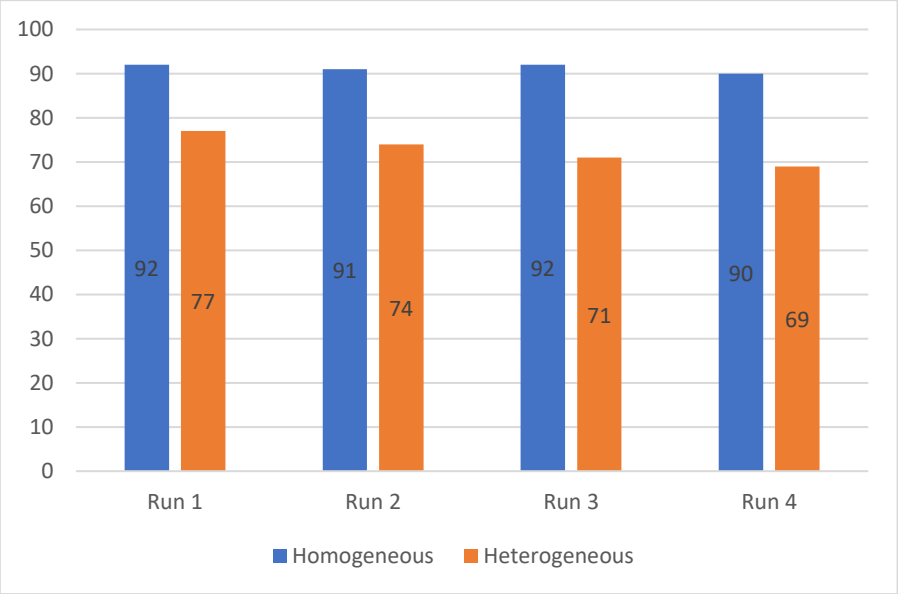

Figure 59: *Yields of styrene carbonate obtained after four runs in the presence of Salophen-tBu-Cr or Salophen-tBu-Cr@{NH_2}-SBA-15. Conditions: Styrene oxide (5.6 mmol), n-Bu_4NBr (0.1 mmol), soluble and supported Salophen-tBu-Cr (0.05 mmol) in 13.3 mL of benzonitrile under 11 bar of CO_2,* 7h 80°C

IV.2.4 Conclusion

The synthesis of N,N'-bis(3,5-di-tert-butylsalicylidene)-1-carboxy-3,4-phenylene-diamine-ChromiumCl (III) (Salophen-tBu-Cr), its grafting through an amide linkage onto SBA-15 silica and its co-catalytic activity in the cycloaddition of CO_2 onto styrene oxide have been investigated. The chromium(III) salophen complex was obtained with a 94% complexation yield and grafted onto SBA-15 bearing aminopropyl groups with a c.a. 40% yield affording a material with a Cr loading of 0.80 wt.%. The co-catalytic activity of Salophen-tBu-Cr was then

studied at several temperatures as low as 50°C in the presence of *n*-Bu_4NBr, with reaction times from 3 to 23h and tested in benzonitrile and acetonitrile. Remarkable yields of styrene carbonate were obtained with a complete conversion of styrene oxide after 7h at 80°C or 23h at 60°C but the yields were significantly lower with the heterogenized form. Nevertheless, improvement of the reactivity of homogeneous Cr was observed in comparison with Mn and Ni-Salophen-tBu (see **Chapter IV.1**), with high yields of styrene carbonate obtained at relatively mild temperature of 80 to 50°C. After grafting at the surface of silica SBA-15 using amide covalent bond, a drop of an average 15% of carbonate yield was observed compared to the homogeneous results.

References

[1] R.L. Paddock, S.T. Nguyen, Chemical CO_2 fixation: CR(III) salen complexes as highly efficient catalysts for the coupling of CO_2 and epoxides, *J. Am. Chem. Soc.*, (**2001**), 123, 11498–11499.

[2] D. Adhikari, S.B.T. Nguyen, M.H. Baik, A computational study of the mechanism of the [(salen)Cr + DMAP]-catalyzed formation of cyclic carbonates from CO_2 and epoxide, *Chem. Commun.*, (**2014**), 50, 2676–2678.

[3] M. North, S.C.Z. Quek, N.E. Pridmore, A.C. Whitwood, X. Wu, Aluminum(salen) Complexes as Catalysts for the Kinetic Resolution of Terminal Epoxides via CO_2 Coupling, *ACS Catal.*, (**2015**), 5, 3398–3402.

[4] M. Alvaro, C. Baleizao, D. Das, E. Carbonell, H. García, CO_2 fixation using recoverable chromium salen catalysts: use of ionic liquids as cosolvent or high-surface-area silicates as supports, *J. Catal.*, (**2004**), 228, 254–258.

[5] J.A. Castro-Osma, K.J. Lamb, M. North, Cr(salophen) Complex Catalyzed Cyclic Carbonate Synthesis at Ambient Temperature And Pressure, *ACS Catal.*, (**2016**), 6, 5012–5025.

[6] S. Pornpraprom, V.D. Elia, Catalytic Strategies for the Cycloaddition of Pure , Diluted , and Waste CO2 to Epoxides under Ambient Conditions, *ACS Catal.*, (**2018**), 8, 419–450.

[7] W. Dai, S. Luo, S. Yin, C. Au, The direct transformation of carbon dioxide to organic carbonates over heterogeneous catalysts, *Appl. Catal. A Gen.*, (**2009**), 366, 2–12.

CHAPTER IV.3

Impact of the nature of the ligand on the activity of Manganese and Chromium salophen 2N2O co-catalysts in CO_2 cycloaddition onto styrene oxide

IV.3.1 Introduction

Due to the easy synthesis of the N_2O_2 ligands and the wide range of possibilities to adjust their properties, Schiff base metal complexes have found a wide diversity of applications as catalysts or co-catalysts for oxidation, ring opening reactions and CO_2 cycloaddition onto epoxides. [1,2] In the latter case, Salen complexes of Mn^{III}, Cr^{III}, Ni^{II}, Al^{II}, Co^{III}, Zn^{II}, Sn^{II} and Ru^{II} have been tested.[2–7] Whatever the applications targeted, general strategies to tune the properties of such complexes are based on the introduction of substituents on the aromatic rings. Hence, bulky groups turned out to be useful to control the approach of substrates while groups with pronounced electron-withdrawing/donating properties have proved to be helpful to adjust the Lewis acidity of the metal centre. The later strategy is worth to try when Schiff base metal complexes are used as co-catalysts in the formation of cyclic carbonate that is expected to be favoured in the presence of strong Lewis acids.[8] The choice of Schiff bases substituents can also be determining to decipher on the covalent anchoring strategy of the resulting complexes onto supports.

At first sight, most of the catalytic systems using Salen complexes for CO_2 cycloaddition onto epoxides reported in the literature are based on ligands harbouring 1 or 2 bulky groups at the 3,5 positions on their aromatic cycles directly involved in the metal coordination. However, some studies focused also on the use of electron donating amino groups -R_2N (**Table 19**). The very first investigation of salen complexes bearing -Et_2N groups as co-catalyst for cycloaddition with CO_2 was described by Ulusoy and co-workers [9]. Cycloaddition was conducted with different epoxides (see **Table 19 entry 1**) in the presence of DMAP (main catalyst) and a salophen-Et_2N-Pd^{II} complex (co-catalyst). A molar ratio of 1 co-cat : 2 DMAP was used and the experiment was conducted at 100°C during 2h under 20 bar of CO_2. Other substituents were also investigated, including *tert*-butyl groups in 3,5 positions on the aromatic rings and the nature of the chain A was varied too.

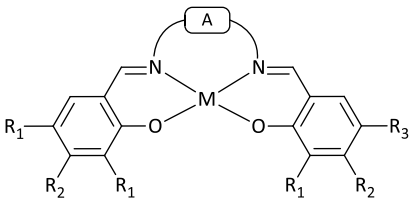

Table 19: *State of the art regarding the use of salen complexes bearing -Et_2N groups in the cycloaddition of CO_2 onto epoxides. PrClOx: Chloro-propyl oxide, StyOx: Styrene oxide*

Entry	R_1	R_2	Chain A	M	Substrate	T (°C)	t (h)	P (bar)	Catalyst	Yield (%)	TOF
1 [9]	H	Et_2N	-CH_2CH_2-	Pd	PrClOx	100	2	20	DMAP	96	48
2 [10]	H	Et_2N	-CH_2CH_2-	Cu	StyOx	100	2	10	DMAP	65	650
2' [10]	H	H	-CH_2CH_2-	Cu	StyOx	100	2	10	DMAP	72	720
3 [11]	H	Et_2N	Phenyl	Fe	StyOx	130	6	6	*n*-Bu_4NBr	68	289
4 [12]	H	Et_2N	Phenyl	Cr	StyOx	25	24	1	*n*-Bu_4NBr	86	4
5 [13]	H	Et_2N	-CH_2CH_2-	Co	StyOx	80	6	10	TBB-bpy	96	80
6 [14]	H	Et_2N	Other complex	Sm	StyOx	120	1.5	10	*n*-Bu_4NBr	97	6565

In a second study, Ulusoy investigated the use of Zn^{II} and Cu^{II} salen complexes supported on {NH_2}-SBA-15 silica using amide covalent bond.[10] Experiments were conducted with styrene oxide, at 100°C during 2h under 10 bar of CO_2. In these conditions, relatively high yields of styrene carbonate were obtained using 0.1% of co-cat and 0.6% of DMAP (**Table 19, entry 2**). Interestingly, catalytic activity was investigated in the case of Salen bearing -Et_2N or -tBu groups and a comparison of the impact of a particular group was studied. According to the authors, the yields of styrene carbonate were a little bit lower for the salen bearing -Et_2N groups in comparison with -tBu groups. They concluded that the decrease of reactivity is attributed to both steric effect and electron donor capability.

More recently, Abu-Surrah and co-workers [11] were also able to obtain a relatively good yield of 68% of styrene carbonate using an Fe^{III} salophen-Et_2N and *n*-Bu_4NBr (**Table 19, entry 3**). Both components were introduced at molar concentrations as low as 0.04%. However, reaction conditions, especially the temperature (6 bar of CO_2, 6 h, 130°C) were rather drastic. It can be noted that, in this work, the highest yields of styrene carbonate when -Et_2N was used instead of -H or -Cl substituent in the same position but nothing was no information was given about the use of -tBu groups.

North and co-workers have been involved for a while in the search of catalysts for the synthesis of cyclocarbonates using CO_2.[15,16] Very recently, this team reported high yields of styrene carbonate in very mild conditions (1 bar of CO_2, 24 h, r.t.) using a Chromium(III) salophen-Et_2N complex and *n*-Bu_4NBr (**Table 19, entry 4**).[12] Both components of the catalytic system were used with a molar ratio of 1% each, leading to a very low TOF of 6 h^{-1} compared to previous works (86% yield of styrene carbonate after 24h). Nevertheless, such results deserve the attention of the reader because, like for very few other teams, the authors used ambient temperature and 1 bar of CO_2.

As stated above, the performance of the catalytic system is influenced by the nature of the substituents on the co-catalyst. In some cases, the authors used also the reactivity of tertiary amino functions with C-X electrophilic groups to incorporate quaternary ammonium functions in close proximity to the metal centre (both catalytic and co-catalytic functions in the same molecule) or even to perform at the same time the heterogenization of those complexes onto supports bearing haloalkyl linkers.[17] Hence, Leng and co-workers managed to bind, for example, a Co salen-Et_2N complex (**Table 19, entry 5**) on microspheres of an ionic polymer bearing -CH_2-Br groups.[13] Doing so, the quaternary ammonium salt is both useful as an anchoring covalent bond and as an active phase for the cycloaddition of CO_2. Styrene carbonate could be prepared in 96% yield within 6h at 80°C under 10 bar of CO_2 with a molar ratio of cat : co-catalyst = 2 : 1). More importantly, the whole catalytic system could be recovered by filtration and reused for a total of 5 runs without any significant loss of conversion or selectivity. ICP-AES analysis confirmed the constant concentration of Co metal in the solid after five runs.

Very recently, Pan and co-workers investigated the Lewis acidity of heterogeneous organic clusters containing lanthanide metal centres (**Table 19, entry 6**).[14] Among them, the samarium metal complex was the best one with TOF values up to 6600 h^{-1} for the conversion of styrene oxide into styrene carbonate. The reaction was carried out under 10 bar of CO_2 at 120°C during 1.5h with a 0.01% co-cat and 0.75% *n*-Bu_4NBr, affording a 97% yield of styrene carbonate. The recovered catalyst was tested in 3 other runs with significant loss of conversion from 100 to 80%. According to the authors, this could be explained by the deactivation of the catalyst.

To our knowledge, there is no work describing the synthesis or use of metal complexes bearing the -Me_2N substituent. As seen in **Chapter II**, In the case of a cycloaddition reaction involving the use of amine catalysts, it was seen that better results were obtained as the basicity increased. Me_2N groups having a Lewis basicity greater than Et_2N, the development of their synthesis is therefore a strategy of choice for the cycloaddition reaction. In the light of the past bibliography review, the present work will focus on the optimization of the synthesis of salophen ligands bearing either -Et_2N or -Me_2N groups. Their catalytic activity will then be compared with previous detailed catalysts Salophen-tBu-MCl. As stated in previous studies, it is to be believed that the presence of these group could greatly enhance the catalytic activity in comparison with -tBu groups. Synthesis and characterization of these complexes will be further developed as well as their catalytic activity will be investigated in homogeneous conditions.

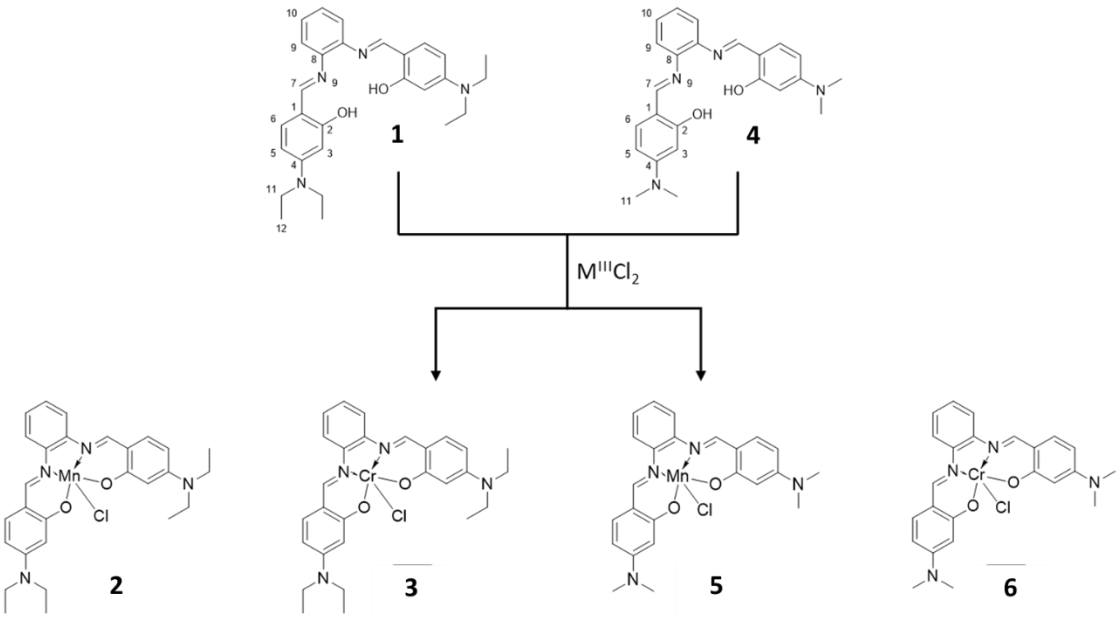

Figure 60: *Organic ligand and complexes investigated in this chapter*

IV.3.2 Experimental part

Only the working protocols of the syntheses that are specific to this part are described here (for the others, the reader will be referred to the corresponding parts).

IV.3.2.1 Catalysts synthesis and characterization

**** Salophen-Et$_2$N series***

Preparation of *N,N'-bis*(4-diethylaminosalicylidene)-1,2-phenylenediamine (Salophen-Et$_2$N ligand, 1). 1,2-phenylenediamine (0.540 g, 5 mmol) was introduced in a two-neck round-bottom flask connected to a condenser under argon and dissolved in 50 mL of pure ethanol (EtOH). In parallel, a solution of 4-(diethylamino)salicylaldehyde (1.93 g, 10 mmol) in the same solvent (50 mL) was prepared under argon. This solution was then added dropwise using a syringe to the suspension of 1,2-phenylenediamine over a period of 20 min. After the addition was completed, the mixture was stirred at room temperature for 72h. The yellow solid formed (compound 1) was then recovered by filtration on a glass frit (n°4), rinsed twice with 20 mL of pure ethanol and 30 mL of petroleum ether and dried in vacuum, yielding 0.825 g (36 % yield). IR (KBr, cm^{-1}): 3425 (w), 2958 (s), 1686 (m), 1615 (s), 1574 (s), 1438 (m), 1361 (m), 1252 (m), 1172 (s), 1132 (w), 1026 (w), 771 (m) cm^{-1}. ^{1}H NMR ([D6]dmso, **Figure 61**, ppm): δH 11.64 (2H, s, C(2)OH), 9.51 (2H, s, C(7)H=N), 7.30 (2H, s, C(10)H), 7.28 (2H, s, C(9)H), 7.27 (2H, s, C(6)H), 6.28 (2H, dd, C(5)H), 6.10 (2H, d, C(3)H), 3.44 (8H, m, C(11)(CH$_2$), 1.23 (12H, t, C(12)C(CH$_3$)$_2$,

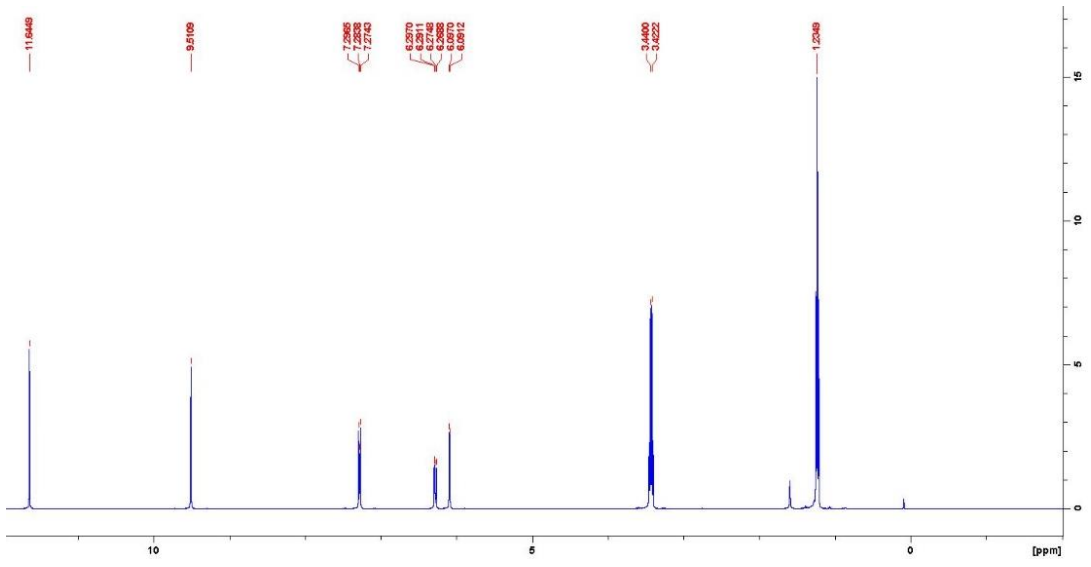

Figure 61: *^{1}H NMR spectrum of Salophen-Et$_2$N*

One-pot preparation of *N,N'*-bis(4-diethylaminosalicylidene)-1,2-phenylene-diaminechloro-Manganese(III) (Salophen-Et$_2$N-MnCl, 2). 1,2-phenylenediamine (0.065 g, 0.60 mmol) was introduced in a two-neck round-bottom flask connected to a condenser under argon and dissolved in 10 mL of dry THF. In parallel, a solution of 4-(diethylamino)salicylaldehyde (0.232 g, 1.2 mmol) in the same solvent (10 mL) was prepared under argon and later added drip by drip to the previous solution. [$MnCl_2(THF)_2$] (0.160 g, 0.60 mmol) was then added to the mixture and the resulting medium was stirred at room temperature for 1 h, then refluxed for 20 min. After cooling at room temperature, triethylamine (0,12 g, 1.20 mmol, 0,17 mL) was added and the mixture stirred for another 45 min. The volume of the solution was then reduced up to 10 mL under vacuum and the reaction mixture allowed to stand at room temperature overnight. After this period, a white powder (triethylammonium chloride) was recovered by filtration and discarded. The brown solution was submitted to evaporation, leading to a brown solid (Salophen-Et$_2$N-MnCl (**2**)) that was recrystallized in toluene (yield: 0.312 g, 0,57 mmol, 95 %). IR (KBr, cm^{-1}): 3416 (m), 2958 (m), 1680 (s), 1610 (s),1573 (s), 1466 (s), 1392 (s), 1361 (s), 1325 (s), 1249 (s), 1198 (s), 1178 (s), 1097 (s), 1026(s), 807 (s), 781 (s), 548 (m). HRMS [**2**-Cl]+ (ESI) : m/z = 511.19 **(Figure 62**).

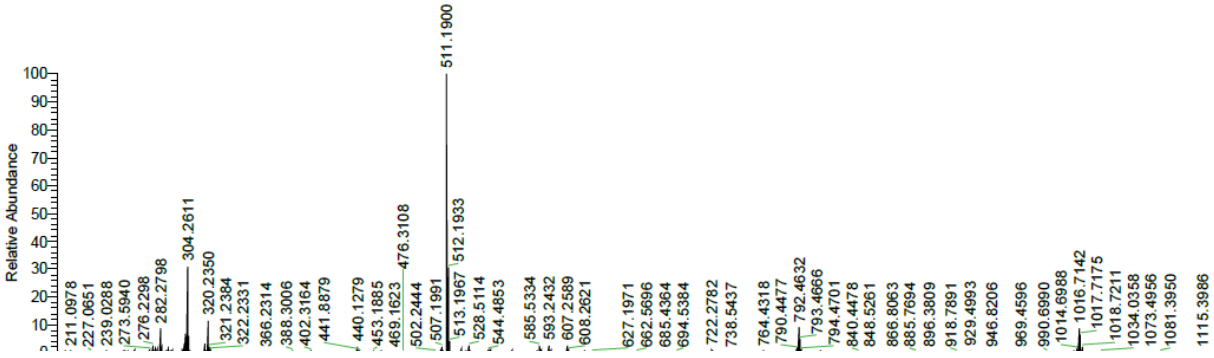

Figure 62: HR-MS spectrum of Salophen-Et$_2$N-Mn

Preparation of *N,N'*-bis(4-dimethylaminosalicylidene)-1,2-phenylene-diaminechloro -Chromium (III) (Salophen-Et$_2$N-CrCl, 3). Salophen-Et$_2$N (0.300 g, 1 eq, 0.65 mmol) was dissolved in 25 mL of dry THF under argon in a two-neck round-bottom flask connected to a condenser. Then, a solution of [$CrCl_3(THF)_3$] (0.150 g, 1 eq, 0.65 mmol) in 25 mL of dry THF was added dropwise under argon and the resulting mixture was then stirred under reflux for 15 min. After cooling at room temperature, the solution was evaporated under vacuum leading

to a dark red solid (Salophen-Et$_2$N-CrCl) (yield: 0.330 g, 94%). HRMS [**3**-Cl]+ (ESI) : m/z = 508.19 **(Figure 63**).

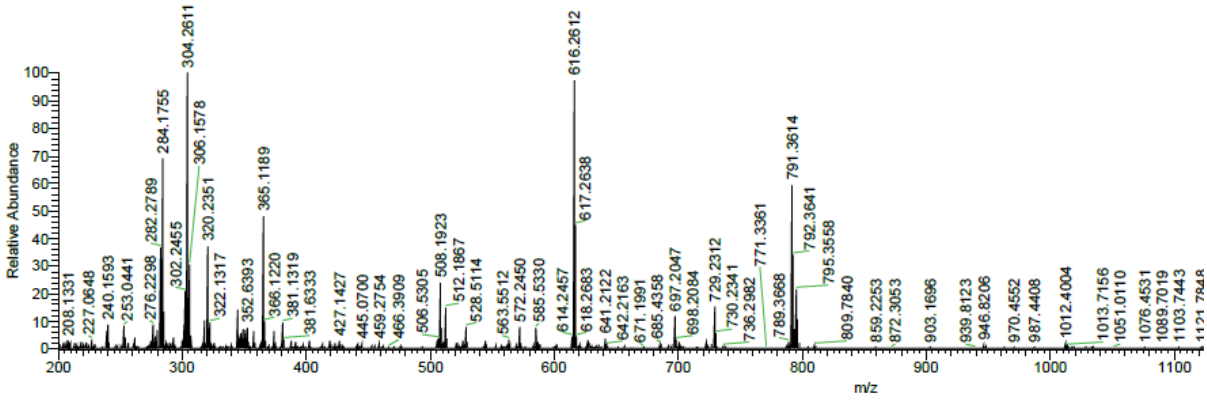

Figure 63: *HR-MS spectrum of Salophen-Et$_2$N-Cl*

**** Salophen-Me$_2$N series***

Preparation of 4-(dimethylamino)-2-hydroxy-benzaldehyde.[18]

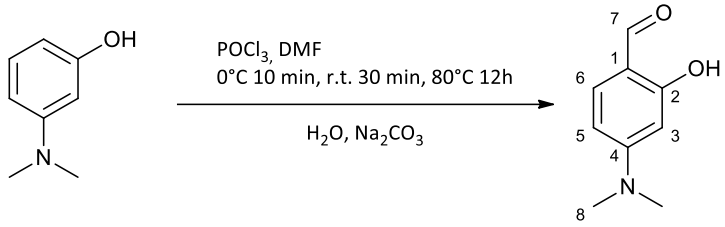

7 mL of phosphorus oxychloride ($POCl_3$) (75 mmol) was added dropwise to the solution of 3-(dimethylamino)phenol (5.00 g, 36.5 mmol) in 15 mL dry DMF at 0°C over 10 min, then the reaction mixture was stirred for 30 min at room temperature, followed for 12h at 80°C. After cooling to room temperature, 80 mL of distilled water was added and the resulting mixture was then poured into crushed ice and neutralized with 60 mL of a saturated aqueous solution of Na_2CO_3. The solid (4.1 g) was recovered by filtration, washed with water and dried in a vacuum oven at 25 °C for 4 h. Yield: 66%, m.p. 79-80 °C (lit. 80.5-81 °C).[19] Later, 4-(dimethylamino)-2-hydroxy-benzaldehyde was used without further purification. ^{1}H NMR (500 MHz, $CDCl_3$, **Figure 64**, δ =11.57 (1H, s, C(2)HO), 9.50 (1H, s, C(7)H, 7.28 (1H, d, C(6)H) 6.27 (1H, dd, C(5)H), 6.06 (1H, d, C(3)H), 3.05 (6H, s, C(8)C(CH_3)$_2$)

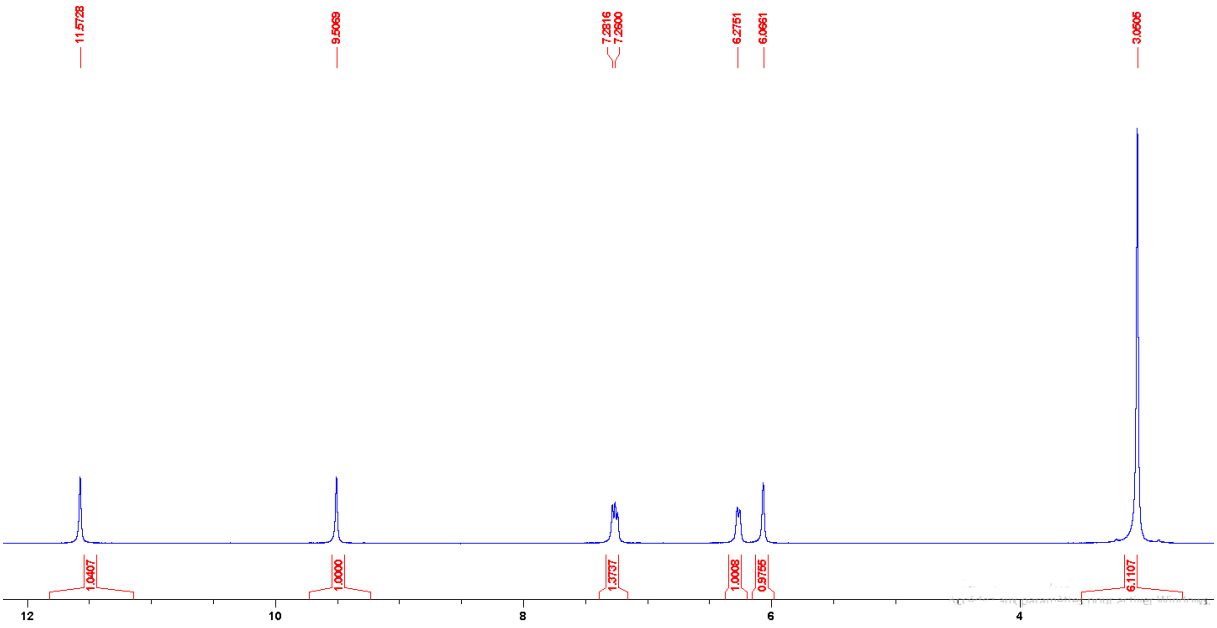

Figure 64: *1H NMR spectrum of 4-(dimethylamino)-2-hydroxy-benzaldehyde*

Preparation of *N,N'-bis*(4-dimethylaminosalicylidene)-1,2-phenylenediamine (Salophen- Me_2N ligand 4). 1,2-phenylenediamine (0.540 g, 5 mmol) was introduced in a two-neck round-bottom flask connected to a condenser under argon and dissolved in 50 mL of pure ethanol (EtOH). In parallel, a solution of 4-(dimethylamino)salicylaldehyde (1.65 g, 10 mmol) in the same solvent (50 mL) was prepared under argon. This solution was then added dropwise using a syringe to the solution of 1,2-phenylenediamine over a period of 20 min. After the addition was completed, the mixture was stirred at room temperature for 72h. The yellow solid formed (compound **4**) was recovered by filtration on a glass frit (n°4), rinsed twice with 20 mL of pure ethanol and 30 mL of petroleum ether and dried in vacuum, yielding 1.130 g (56 %). IR (KBr, cm^{-1}): 3425 (w), 2958 (s), 1686 (m), 1615 (s), 1574 (s), 1438 (m), 1361 (m), 1252 (m), 1172 (s), 1132 (w), 1026 (w), 771 (m) cm^{-1}. ^1H NMR ([D6]dmso, **Figure 65**, ppm): δH 13.50 (2H, s, C(2)OH), 8.65 (2H, s, C(7)H=N), 7.35 (2H, s, C(10)H), 7.33 (2H, s, C(9)H), 7.26 (2H, s, C(6)H), 6.35 (2H, dd, C(5)H), 6.09 (2H, d, C(3)H), 3.00 (12H, t, $C(12)C(CH_3)_3$,

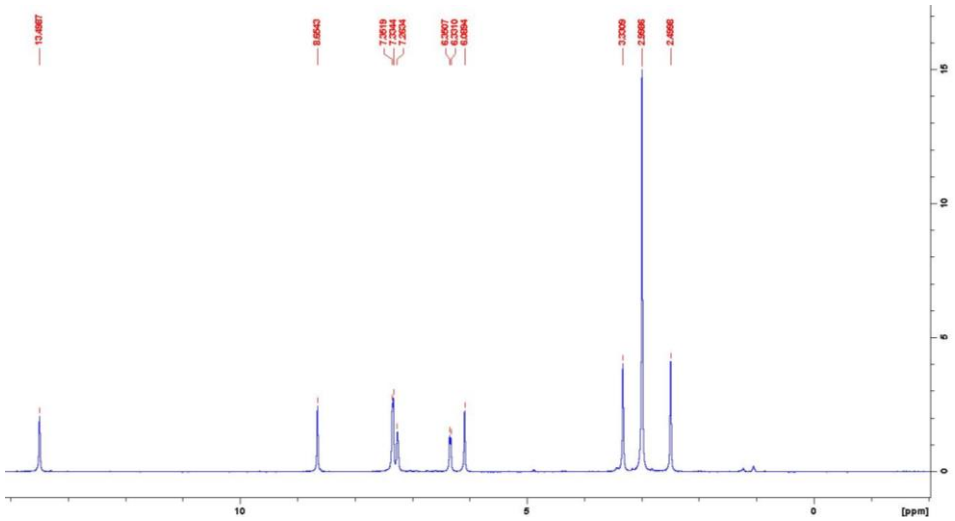

Figure 65: ^{1}H NMR spectrum of Salophen-Me$_2$N

One-pot preparation of *N,N'*-bis(4-dimethylaminosalicylidene)-1,2-phenylene-diaminechloro-Manganese(III) (Salophen-Me$_2$N-MnCl, 5). 1,2-phenylenediamine (0.065 g, 0.60 mmol) was introduced in a two-neck round-bottom flask connected to a condenser under argon and dispersed in 10 mL of dry tetrahydrofuran (THF). In parallel, a solution of 4-(diethylamino)salicylaldehyde (0.232 g, 1.2 mmol) in the same solvent (10 mL) was prepared under argon and later added drip by drip to the previous solution. [$MnCl_2(THF)_2$] (0.160 g, 0.60 mmol) was then added to the mixture and the resulting medium was stirred at room temperature for 1 h, then refluxed for 20 min. After cooling at room temperature, triethylamine (0,12 g, 1.20 mmol, 0,17 mL) was then added and the mixture stirred for another 45 min. The volume of the solution was then reduced up to 10 mL under vacuum and the reaction mixture allowed to stand at room temperature overnight. After this period, a white powder (triethylammonium chloride) was filtered and discarded. The solution was evaporated, leading to a brown solid (Salophen-Me$_2$N-MnCl (**5**)) that was recrystallized in toluene (yield: 0.279 g, 0,57 mmol, 95 %). IR (KBr, cm^{-1}): 3416 (m), 2958 (m), 1680 (s), 1610 (s),1573 (s), 1466 (s), 1392 (s), 1361 (s), 1325 (s), 1249 (s), 1198 (s), 1178 (s), 1097 (s), 1026(s), 807 (s), 781 (s), 548 (m). HRMS [**5**-Cl]+ (ESI) : m/z = 455.13 (**Figure 66**)

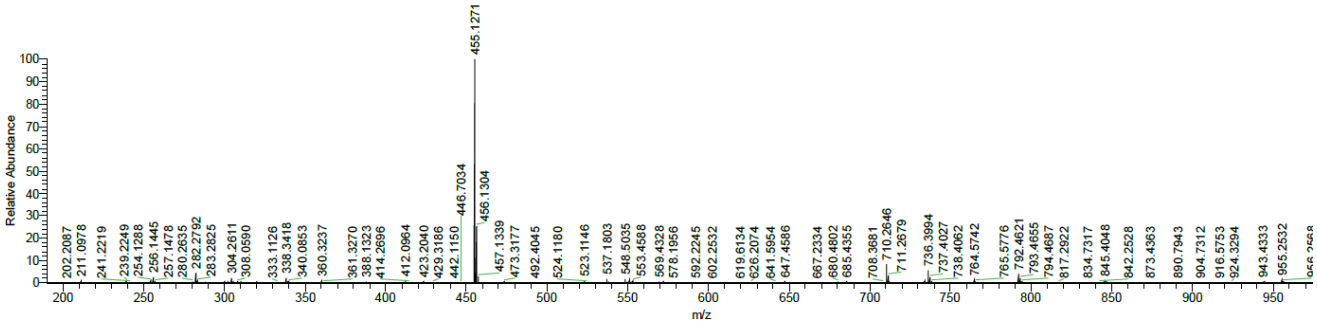

Figure 66: *HR-MS spectrum of Salophen-Me$_2$N-Mn*

Preparation of *N,N'*-bis(4-dimethylaminosalicylidene)-1,2-phenylene-diaminechloro -Chromium (III) (Salophen-Me$_2$N-CrCl, 6). Salophen-Me$_2$N ligand (0.300 g, 1 eq, 0.75 mmol) was dissolved in 25 mL of dry THF under argon in a two-neck round-bottom flask connected to a condenser, then a solution of [$CrCl_3(THF)_3$] (0.173 g, 1 eq, 0.65 mmol) in 25 mL of dry THF was added under argon dropwise and the resulting mixture was stirred under reflux for 15 min. After cooling at room temperature, the solvent was evaporated under vacuum leading to a dark red solid (Salophen-Me$_2$N-CrCl) (yield: 0.343 g, 94%). MS (ESI): 452.13(Erreur ! Source du renvoi introuvable.)

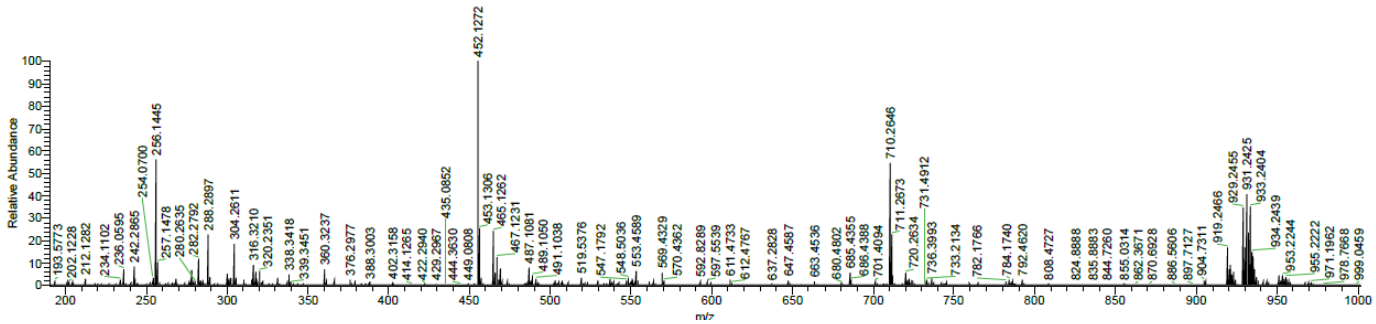

Figure 67: *HR-MS spectra of Salophen-Me$_2$N-Cr*

IV.3.2.2 Catalysts synthesis and characterization

Styrene oxide (StOx, 0.66 mL, 5.6 mmol), catalyst (Bu_4NBr, 31.1 mg, 96.2 µmol), co-catalyst (Salophen-R-M, 48.3 µmol), GC internal standard (p-xylene, 1 mL, 8.0 mmol) and benzonitrile (20 mL) were mixed into a Teflon bucket contained in a stainless-steel autoclave equipped with a magnetic stirrer and an electric heater. The autoclave was then purged with CO_2, the system was pressurized with 11 bar of CO_2 and heated at the desired temperature. The reaction mixture was stirred for several hours (see **Table 20**). After each catalytic test, the resulting solutions or suspensions were analysed by gas chromatography GC after dilution (samples of 25 µL diluted in 10 mL of CH_2Cl_2).

In all experiments, the possible presence of polycarbonates was checked by ^{1}H and ^{13}C NMR spectroscopy. In any cases, no trace of polymers was detected. This was confirmed by the mass balance determination by GC using p-xylene as an internal standard. Thereafter, styrene oxide conversion values will be considered to be equal to styrene carbonate yield values.

IV.3.3 Results and discussion

IV.3.3.1 Synthesis and characterization of the Salophen-Et_2N and -Me_2N ligands and of the corresponding Mn(III) and Cr(III) complexes

Salophen-Et_2N was synthesized according to the protocol developed by Abu-Surrah *et al*.[11] This yellow solid was obtained after a single step condensation reaction in a green solvent (ethanol). After 72h reaction at room temperature (**Figure 68**), a yield of 36% was obtained. The structure of the ligand was confirmed by ^{1}H NMR, IR and HRMS analysis. As observed in previous **Chapter IV.1** (synthesis of Salophen-tBu), the use of $ZnCl_2$ as templating agent in order to enhance the yield of the ligand was not successful, as zinc remained coordinated (formation of Salophen-Et_2N-Zn complex with 86% yield). Such behaviour could be explained by the weaker steric effect of Et_2N in position 4 compared to the two -tBu substituents in 3 and 5 positions. Here, it looks like -Et_2N groups were not bulky enough compared to -tBu substituents to prevent the zinc from staying inside the coordination sphere. The chromium complex (Salophen-Et_2N-CrCl) was then obtained in THF with a 94% yield using $CrCl_3$ as metal precursor and Salophen-Et_2N. Salophen-Et_2N-CrCl was confirmed by IR and HRMS (see **Figure 63**). Salophen-Et_2N-MnCl could be prepared in 95% yield by a one-pot synthesis starting from the ligand precursors, *i.e*. the diamine and the two aldehydes in the presence of the manganese source. To our knowledge, no one-pot synthesis of Salophen-Mn complex has yet been described before. Metal complex was characterized with IR spectra and HRMS analysis demonstrating high purity product (see **Figure 62**). A one-pot synthesis of the Chromium complex was also investigated, with $CrCl_3$ playing the role of templating agent. Unfortunately, no defined product was detected by HRMS analysis.

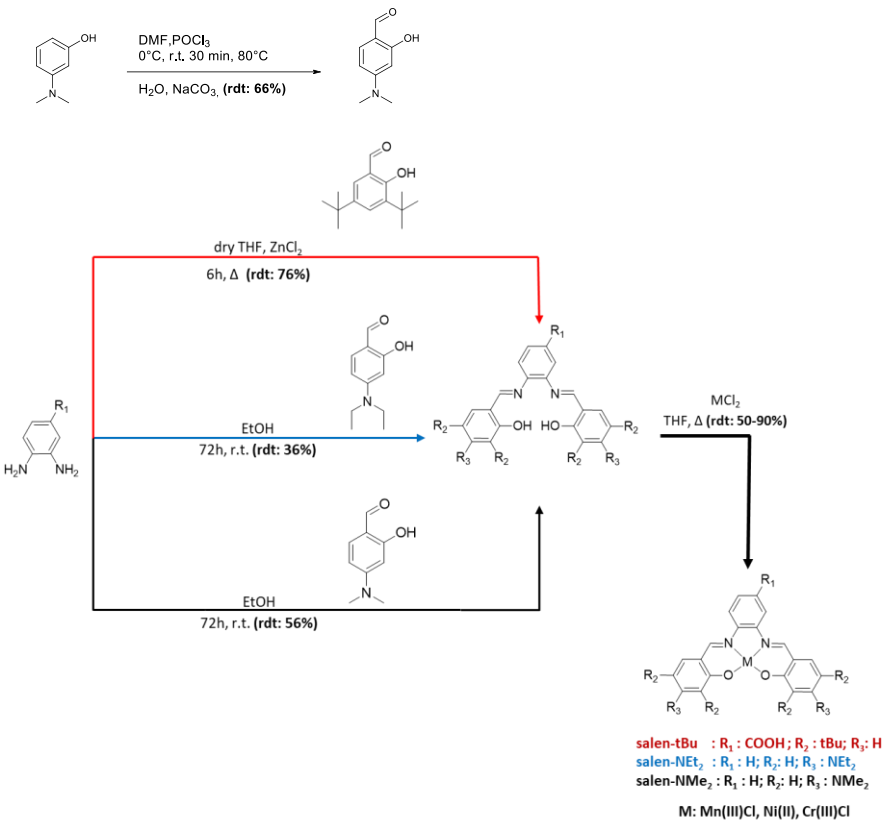

Figure 68 : *Synthesis routes of Salophen-R_2N and -tBu metal complexes*

To our knowledge, the synthesis of Salophen-Me_2N has not been reported yet in the literature although the protocol is very similar to the one implemented for Salophen-Et_2N. Commercially available but expensive, 4-(dimethylamino)-2-hydroxy-benzaldehyde was prepared in our hands before according to the protocol of Awwadi *et al.*[20] Then, Salophen-Me_2N was obtained with a higher yield compared to its Et_2N form (56% instead of 36), after 72h reaction at room temperature. Later, the Chromium and Manganese complexes were prepared following exactly the protocols used for the Salophen-Et_2N-M analogues. Regarding Manganese(III), a successful one-step procedure could also be used leading to a 98% yield of Salophen-Me_2N-Mn complex while for chromium(III), a classical complexation starting from a pre-formed ligand was necessary. Both Salophen-Me_2N-Mn and Cr were obtained in high yields of 95%.

IV.3.3.2 Comparison of the co-catalytic activity of the Salophen-type complexes in the styrene oxide conversion into styrene carbonate in homogeneous and heterogeneous conditions

The catalytic activities of both Et_2N-Cr and Me_2N-Cr complexes were investigated in homogeneous conditions. *n*-Bu_4NBr was utilized as the main catalyst and the reaction conducted under 11 bar of CO_2 (measured at r.t.) at 80, 60 and 50°C during between 1h to 23h. These new results will allow a comparison between the 3 different Salophen Chromium co-catalysts: -tBu, -Et_2N and Me_2N.

Results show that, at 80 or 60°C, a complete conversion of styrene oxide was achieved for most of the co-catalysts after 23h (**see Table 20, entries 4-9**).

***Table 20**: Yields of styrene carbonate with soluble Salophen-chromium co-catalysts*

Entry	Co-catalyst	Temperature (°C)	styrene carbonate yield (%)			
			1h	3 h	7 h	23 h
1	Salophen-Me_2N-Cr	50	20	55	75	99
2	Salophen-Et_2N-Cr	50	8	21	40	89
3	Salophen-tBu-Cr	50	5	15	29	67
4	Salophen-Me_2N-Cr	60	31	87	99	99
5	Salophen-Et_2N-Cr	60	16	42	79	99
6	Salophen-tBu-Cr	60	12	26	47	96
7	Salophen-Me_2N-Cr	80	99	99	99	99
8	Salophen-Et_2N-Cr	80	78	99	99	99
9	Salophen-tBu-Cr	80	41	75	92	99

Conditions: Styrene oxide (5.6 mmol), n-Bu_4NBr (0.1 mmol), Salophen-Cr(III) (0.05 mmol) in 13.3 mL of benzonitrile under 11 bar of CO_2.

Regarding the conversion of styrene oxide at 50 and 60°C, Cr Salophens bearing amino groups clearly stood out compared to Salophen-tBu-Cr (**Table 20**, **entries 1-3 and 4-6**). The lower the temperature, the greater the difference could be evidenced between tBu and the amino groups. Hence, the conversion was almost complete at 50°C in the case of Salophen-Et_2N and -Me_2N while -tBu led to 67% conversion after 23h at 50°C (**Table 20, entry 1-3**). In some case, the difference of co-catalytic activity is thus a factor 2 between Salophen-tBu and -Et_2N, and another factor 2 between Salophen-Et_2N and -Me_2N (**Table 20, entry 1-3)**. Of the three Cr co-catalysts tested, Salophen-Me_2N-Cr was the only one that allowed a 99% conversion of styrene oxide within 7h at 60°C (**Table 20, entry 4**). Additional tests performed with 1h showed that a complete conversion could be obtained in the case of Salophen-Me_2N-Cr at 80°C.

The co-catalytic activity of *n*-Bu_4NBr itself was also investigated in order to better emphasize the influence of the co-catalysts. A series of 3h reactions were conducted at 50, 60, 80, and 120°C in the presence or absence of the co-catalyst. As seen in **Table 21**, *n*-Bu_4NBr alone is able to catalyse the cycloaddition process without any co-catalyst with 80% yield of styrene carbonate at 3 h, but only at 120°C (**Table 21**, **entry 5**). Hence, lower reaction temperatures are better to estimate the influence of the co-catalyst. Some catalytic activity can be evidenced with *n*-Bu_4NBr alone at 80°C, with 12% yield of styrene carbonate after 3h (**Table 21**, **entry 5**). This number goes up to 75% with the addition of Salophen-tBu-Cr (**Table 21**, **entry 3**) and almost 100% yield is reached for Salophen-Cr(III) bearing tertiary amino groups (**Table 21**, **entries 1 and 2**). In comparison, Salophen-Me_2N were able to achieve 99% yield of styrene carbonate at 80°C but failed to obtained good results at lower temperatures 60°C and 50°C (see **Table 21**, **entry 4**). At 60 and 50 °C, *n*-Bu_4NBr is not active enough and co-catalysts are more than ever needed to perform the cycloaddition reaction.

***Table 21**: Influence of the co-catalyst contribution to the styrene carbonate yields obtained after 3h reaction at different temperatures*

Entry	Catalyst	Co-catalyst	Styrene carbonate yield (%)			
			50 °C	60 °C	80 °C	120 °C
1	*n*-Bu_4Br	Salophen-Me_2N-Cr	55	87	99	99
2	*n*-Bu_4Br	Salophen-Et_2N-Cr	21	42	99	99
3	*n*-Bu_4Br	Salophen-tBu-Cr	15	26	75	99
4	*n*-Bu_4Br	Salophen-Me_2N-Mn	24	49	99	99
5	*n*-Bu_4Br	-	02	21	12	80

Conditions: Styrene oxide (5.6 mmol), n-Bu_4NBr (0.1 mmol), soluble Salophen-M (0.05 mmol) in 13.3 mL of benzonitrile under 11 bar of CO_2, 3h

All these results were plotted in **Figure 69** in order to better emphasize the difference of co-catalytic activity of the three Salophen-Cr(III) complexes resulting from the switch of the organic substituent localised on the aromatic cycle, either **-tBu**, **-Et_2N**, **-Me_2N** and also to point out the requirement of co-catalysts to get acceptable results within 3 h at 80°C (see ***n*-Bu_4NBr alone)**.

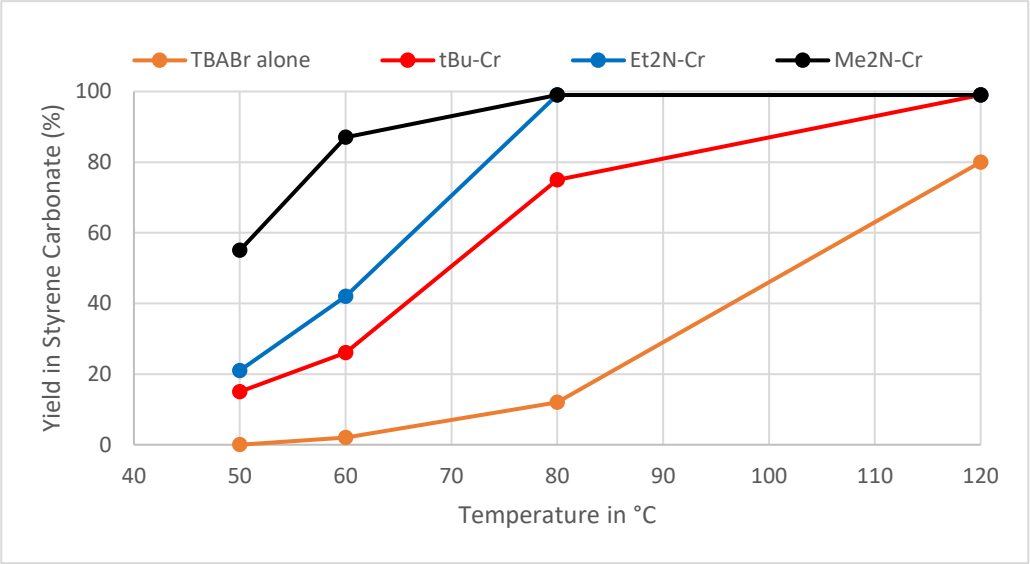

Figure 69: *Comparative results obtained with different Salophen-R-Cr after 3h cycloaddition at 80°C*

Salophen-Me_2N-Mn was logically tested to be compared to Salophen-Me_2N-Cr showing definitively the superiority of Cr(III) over Mn(III). Even though a total conversion was asserted at 80°C after 3h reaction, almost no styrene carbonate was noticed at 50 and 60°C (**Table 21**, **entry 4**). This comforted us in the choice of Chromium as a preferable metal centre for the cycloaddition reaction of styrene oxide.

Our results lead to the following ranking of desirable substituent inside the structure of Salophen ligand: -Me_2N in position 4 > -Et_2N in position 4 > -tBu in positions 3,5. Different explanations can be proposed for this variation of reactivity. Previous DFT studies suggested that the co-catalyst environment plays an important role in its ability to offer an optimal space in which the reaction can take place, specifically steric factors.[21] In the present case, tertiary amine groups could potentially offer less steric hindrance compared to -tBu groups, thus affording better interactions of CO_2 with the epoxide.

Another explanation is related to the chemical reactivity of -Me_2N and -Et_2N groups. Both can react with CO_2 in the presence of water, affording hydrogen carbonate species. A positive influence of the reaction of water with amines was described by Gao and co-workers who obtained better yields of epichlorohydrin carbonate in the presence of water (from 50% without water to 70% with an optimum water concentration of 0.4 mol% based on the epoxide).[22] According to the authors, further addition of water led to a significant decrease of the yield of carbonate, below 50% at 1 mol% of water. As represented in **Figure 70**, the tertiary amine added as a co-catalyst in the work of Gao and co-workers would react with CO_2 and H_2O leading to the corresponding ammonium hydrogen carbonate. Trace of carbonate

anion form could be characterized by infra-red spectrum, with a characteristic pic appearing at 835 cm^{-1}. The later would then react with the intermediate opened form of the epoxide, leading to the cyclic carbonate and the release of a water molecule. So, water does not to be introduced in stoichiometric amounts.

In our case, we have estimated that, in this absence of any drying treatments of benzonitrile and of CO_2 gas, a small molar fraction of water is present in the autoclave (c.a. 1 H_2O : 6 Salophen-M) which is much lower than the optimal concentration emphasized by Gao and co-workers in their paper.

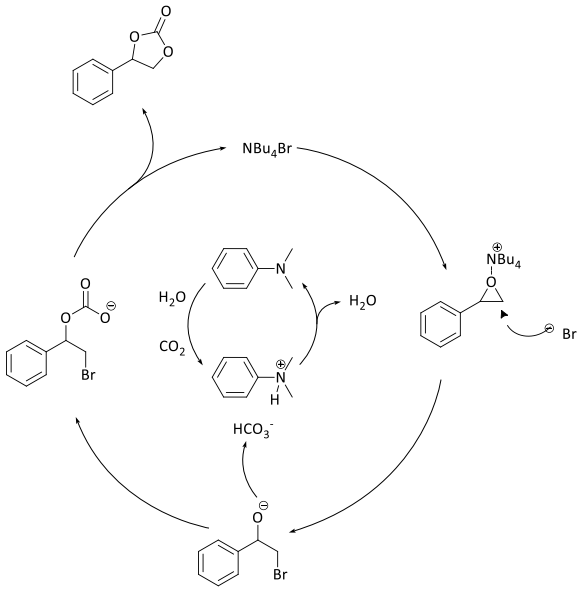

***Figure 70**: Proposed n-Bu_4NBr /tertiary amine catalysis mechanism for the cycloaddition of CO_2 onto styrene oxide.*

In order to investigate the in-situ formation of the bicarbonate form in our work, we thought that IR monitoring of the reaction medium under CO_2 pressure could be adapted.[22] However, the expected amount of HCO_3^- (1/6th of the co-catalyst) was too small to get a sensitive measurement. This is the reason why; it was decided with Dr T. Tassaing (from ISM in Bordeaux) to look at the direct interaction of CO_2 with KBr pellets of the co-catalyst in the presence of water. Such analyses were performed on **Salophen-tBu-Cr** and **Salophen-Me_2N-Cr** samples under 40 bar of CO_2 at temperatures of 40, 80 and 100 °C. The spectra (see **Appendix**) were acquired in the 400 - 4000 cm^{-1} spectral region. However, only the 700 - 1700 cm^{-1} range, which includes characteristic vibrational modes of the anion at 835 (carbonate anion form), 1300 (carbonate anion form) and 1650 cm^{-1} (amide form) will be presented in

Figure 71. The amide band of 1650 cm^{-1} could be seen at 1615 cm^{-1} and the expected band of 1300 cm^{-1} was not visible. A signal at 835 cm^{-1} was also observed but the later could not be directly linked to the presence of hydrogen carbonate form since it was also present on its corresponding blank spectrum. The temperature did not seem to play an important role since no significative differences could be observed by comparing the spectra performed at 40, 80 and 100 °C. Blank spectra were recorded before the measurement in the presence of CO_2. Again, no significative difference which could confirm the presence of the anion or the alteration of the structure of the Salophen catalyst could be emphasized. If present, IR is not sensitive enough to establish the in-situ formed formation of hydrogen carbonate.

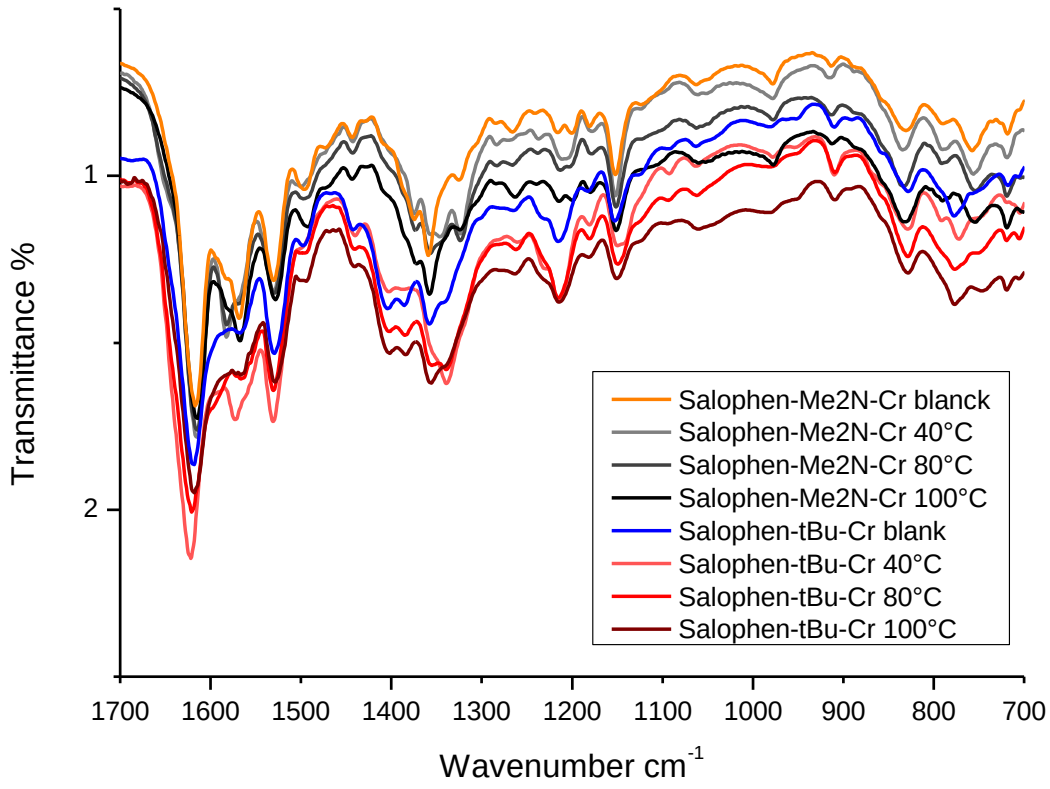

Figure 71: *IR spectra of two Salophen-Cr(III) complexes recorded in the presence of 40 bar of CO2 in a range of temperature of 40, 80 and 100°C. Blank of each compounds are also present (orange for Me2N complex and blue for tBu complex.*

IV.3.4 Conclusion

In this work, chromium(III) and manganese(III) Salophen complexes bearing tertiary dimethyl or diethyl amino groups in position 4 were successfully synthesized. These compounds were then tested as homogeneous co-catalysts for the cycloaddition of CO_2 on styrene epoxide under 11 bar of CO_2. Excellent yields of styrene carbonate were obtained after 23 h reaction at 60°C using Salophen-Et_2N-Cr and, even at 50°C, using Salophen-Me_2N-Cr. From the comparison of these results to those obtained with Salophen-tBu-Cr, a more classical Salophen ligand bearing -tBu substituents in 3,5 positions, it comes that the presence of tertiary amine groups on the aromatic cycles of Salophen clearly enhances the co-catalytic activity of the corresponding Cr(III) complexes. Best results were obtained by the association of *n*-Bu_4NBr with Salophen-Me_2N-Cr(III). The origin of this effect could be due to the reaction of the tertiary amino groups with residual water, leading to the in-situ formation of hydrogen carbonate species, even though such hypothesis could not be confirmed by IR spectra measurements.

References

[1] C. Baleizão, H. Garcia, Chiral salen complexes: An overview to recoverable and reusable homogeneous and heterogenous catalysts, *Chem. Rev.*, (**2006**), 106, 3987–4043.

[2] E.M. McGarrigle, D.G. Gilheany, Chromium-and manganese-salen promoted epoxidation of alkenes, *Chem. Rev.*, (**2005**), 105, 1563–1602.

[3] R.L. Paddock, Y. Hiyama, J.M. McKay, S.B.T. Nguyen, Co(III) porphyrin/DMAP: an efficient catalyst system for the synthesis of cyclic carbonates from CO_2 and epoxides, *Tetrahedron Lett.*, (**2004**), 45, 2023–2026.

[4] Y.M. Shen, W.L. Duan, M. Shi, Chemical fixation of carbon dioxide catalyzed by binaphthyldiamino Zn, Cu, and Co salen-type complexes, *J. Org. Chem.*, (**2003**), 68, 1559–1562.

[5] R.M. Haak, A. Decortes, E.C. Escudero-Adán, M.M. Belmonte, E. Martin, J. Benet-Buchholz, A.W. Kleij, Shape-Persistent Octanuclear Zinc Salen Clusters: Synthesis, Characterization, and Catalysis, *Inorg. Chem.*, (**2011**), 50, 7934–7936.

[6] F. Jutz, J.-D.D. Grunwaldt, A. Baiker, In situ XAS study of the Mn(III)(salen)Br catalyzed synthesis of cyclic organic carbonates from epoxides and CO_2, *J. Mol. Catal. A Chem.*, (**2009**), 297, 63–72.

[7] M. Alvaro, C. Baleizao, D. Das, E. Carbonell, H. García, CO_2 fixation using recoverable chromium salen catalysts: use of ionic liquids as cosolvent or high-surface-area silicates as supports, *J. Catal.*, (**2004**), 228, 254–258.

[8] D.J. Darensbourg, Making Plastics from Carbon Dioxide: Salen Metal Complexes as Catalysts for the Production of Polycarbonates from Epoxides and CO_2, *Chem. Rev.*, (**2007**), 107, 2388–2410.

[9] M. Ulusoy, Ö. Birel, O. Ahin, O. Büyükgüngör, B. Cetinkaya, Structural, spectral, electrochemical and catalytic reactivity studies of a series of N_2O_2 chelated palladium(II) complexes, *Polyhedron*., (**2012**), 38, 141–148.

[10] Z. Taşci, M. Ulusoy, Efficient pathway for CO_2 transformation to cyclic carbonates by heterogeneous Cu and Zn salen complexes, *J. Organomet. Chem.*, (**2012**), 713, 104–111.

[11] A.S. Abu-Surrah, H.M. Abdel-Halim, H.A.N. Abu-Shehab, E. Al-Ramahi, Iron and cobalt salicylaldimine complexes as catalysts for epoxide and carbon dioxide coupling: effects of substituents on catalytic activity, *Transit. Met. Chem.*, (**2017**), 42, 117–122.

[12] J.A. Castro-Osma, M. North, X. Wu, Synthesis of Cyclic Carbonates Catalysed by Chromium and Aluminium Salphen Complexes, *Chem. - A Eur. J.*, (**2016**), 22, 2100–2107.

[13] Y. Leng, D. Lu, C. Zhang, P. Jiang, W. Zhang, J. Wang, Ionic Polymer Microspheres Bearing a CoIII-Salen Moiety as a Bifunctional Heterogeneous Catalyst for the Efficient Cycloaddition of CO_2 and Epoxides, *Chem. - A Eur. J.*, (**2016**), 22, 8368–8375.

[14] W. Hou, G. Wang, X. Wu, S. Sun, C. Zhao, W.S. Liu, F. Pan, Lanthanide clusters as highly efficient catalysts regarding carbon dioxide activation, *New J. Chem.*, (**2020**), 44, 5019–5022.

[15] X. Wu, C. Chen, Z. Guo, M. North, A.C. Whitwood, Metal- and Halide-Free Catalyst for the Synthesis of Cyclic Carbonates from Epoxides and Carbon Dioxide, *ACS Catal.*, (**2019**), 9, 1895–1906.

[16] M. North, R. Pasquale, C. Young, Synthesis of cyclic carbonates from epoxides and CO_2, *Green Chem.*, (**2010**), 12, 1514–1539.

[17] P.A. Carvalho, J.W. Comerford, K.J. Lamb, M. North, P.S. Reiss, Influence of Mesoporous Silica Properties on Cyclic Carbonate Synthesis Catalysed by Supported Aluminium(Salen) Complexes, *Adv. Synth. Catal.*, (**2019**), 361, 345–354.

[18] F.F. Awwadi, H.A. Hodali, Anagostic interactions in chiral separation . Polymorphism in a [Co(II)(L)] complex : Crystallographic and theoretical studies, *J. Mol. Struct.*, (**2018**), 1154, 373–381.

[19] S. Republic, Synthesis and Study of Novel Coumarin Derivatives Potentially Utilizable as Memory Media, *Molecules*., (**2009**), 14, 4838–4848.

[20] F.F. Awwadi, H.A. Hodali, Anagostic interactions in chiral separation. Polymorphism in a [Co(II)(L)] complex: Crystallographic and theoretical studies, *J. Mol. Struct.*, (**2018**), 1154, 373–381.

[21] F. Castro-Gómez, G. Salassa, A.W. Kleij, C. Bo, A DFT study on the mechanism of the cycloaddition reaction of CO_2 to epoxides catalyzed by Zn(Salphen) complexes, *Chem. - A Eur. J.*, (**2013**), 19, 6289–6298.

[22] L. Ji, Z. Luo, Y. Zhang, R. Wang, Y. Ji, F. Xia, G. Gao, Imidazolium ionic liquids/organic bases: Efficient intermolecular synergistic catalysts for the cycloaddition of CO_2 and epoxides under atmospheric pressure, *Mol. Catal.*, (**2018**), 446, 124–130.

CHAPTER V

CUSTOM SYNTHESIS OF QUATERNARY AMMONIUM SALTS GRAFTED ON SILICA AND THEIR ECO-FRIENDLY CYCLOADDITION REACTION

(Work carried out in collaboration with Julie KONG (M2), Ludivine K/BIDI (M2) and Miguel ALONSO DE LA PENA (PhD student IRCELYON))

V.1 Introduction

Quaternary ammonium salts (QAS) are very often used as catalysts for the CO_2 cycloaddition onto epoxides to get cyclic carbonates. Most of the research conducted in this domain deal with the search of co-catalysts or the improvement of the nucleophilicity of their counter anion but such investigations are undertaken with soluble QAS. In the present part, we have focused our attention on supported QAS. Such approach would allow a better recovery at the end of the reaction avoiding the loss of these compounds during the work-up procedure as well as the contamination of the products. Commercially available anionic polymeric resins bearing quaternary ammoniums salts can be used but, like most of the polymers, they suffer from low textural parameters and their sensitivity to organic solvents (shrinkage or swelling effects). That is the reason why, functional materials based on inorganic supports, like mesoporous silica were rather investigated in our work. As usual, organic functions can be introduced either in the synthesis gel ("co-condensation pathway") of the silica support or using a post-synthesis strategy ("post-synthesis pathway"). Materials prepared following the co-condensation pathway are characterized by higher loadings but usually suffer from low textural parameters and elimination of the structure directing agent in these cases is difficult since calcination is no longer possible.[1,2]. On the other hand, the materials obtained using a post-synthesis pathway are characterized by better textural and structural properties when homogeneous distributions of the organic functions are reached with optimized experimental protocols affording a good diffusion of the reactants [1]. In all cases, quaternary ammonium salts bearing trialkoxysilane groups are necessary, but the scope of commercially available molecules is limited. Conventional synthesis modes used in organic chemistry to get QAS are based on the reaction of halogenoalkyl derivatives with tertiary amines. In the present context focusing on the grafted strategy, such syntheses can be performed either before grafting the above-mentioned molecules (*ex-situ* grafting strategy [3–6]) or by the reaction of an anchored group, i.e. amino-alkyl or halogeno-alkyl derivative with an alkylhalide or a tertiary amine (*in-situ* grafting strategy [7–9]). Such synthesis methods have already been described in the literature, whether with silica or other types of supports, but few of the materials hence obtained have been applied for CO_2 cycloaddition catalysis on epoxides.[9–11] A good overview of recent literature on the subject is given in **Table 22**.

***Table 22**: Most recent supported QAS catalytic systems used in the cycloaddition of CO_2 on epoxides.*

Entry	Reagent	Support	Concentration	Strategy	QAS	X	Ref.
1	$-NR_3$ (R = Me, Et, Bu)	Carbon nanotubes	1 $mmol.g^{-1}$	***ex-situ grafting***	$-N^+R_3$	Cl^-	[12]
2	BuBr	Silica $\{NH_2\}$-SiO_2-OH	0.96$mmol.g^{-1}$	***in-situ grafting***	$-N^+Bu_3$	Br^-	[13]
3	BuBr	Imidazole immobilized on {Cl}-MCM-41	1.5 $mmol.g^{-1}$	***in-situ* grafting**	$-[Im]N^+Bu$	Cl^-	[14]
4	BnCl	Fluorochem LC301 silica bearing alkyl groups with terminal Et_2N groups	0.43 to 1.21 $mmol.g^{-1}$	***In-situ* grafting**, then ion exchange of Cl^- with Br^-	$-N^+Et_2Bn$	Br^-	[15]
5	Alkyl halide BuX (X = I, Br, Cl); RBr (R = Et, Hex, Oct)	Porous polymer bearing N-vinylimidazole groups	0.84 to 1.02 $mmol.g^{-1}$	***in-situ grafting***	$-[Im]N^+(alkyl)$	Cl^-; Br^-; I^-	[16]
6	Quaternarized CPTMS	Silica SiO_2	4.4-4.7 $mmol.g^{-1}$	***ex-situ cP***	$-N^+Me_3$	Cl^-	[17]
7	Quaternarized CPTMS	Silica SiO_2	1.2-1.3 $mmol.g^{-1}$	***ex-situ cP***	$-N^+Me_3$	Cl^-	[18]
8	$BuMe_3NCl$	Fe_3O_4@SiO_2	1.5 $mmol.g^{-1}$	***in-situ cP***	$-N^+Et_3$	Cl^-	[19]
9	PEI	SiO_2	0.48%	***in-situ grafting***	$(CH_2\text{-}CH_2)N^+(CH_2\text{-}Ph)(CH_2\text{-}CH\text{-}OH\text{-}CH_3)$	Cl^-	[20]
10	acryloxyethyl-trimethylammonium chloride	SiO_2	0.235	***ex-situ cP***	$-N^+Me_3$	Cl^-	[21]

APTES: (3-Aminopropyl)trimethoxysilane, cP: co-condensation polymerization; PEI: polyethylenimine; Bn : Benzyl

Lots of selected examples (**Table 22, entries 2-5, 9**) are dealing with the *in-situ* grafting strategy which corresponds to nucleophilic substitution reactions between anchored amines with alkyl halides (**Table 22, entries 2, 4-5**) or anchored alkyl halides with amines (**Table 22, entry 3**). Other examples report polycondensation of materials with quaternary ammonium functions (**Table 22, entries 6-8, 10**). Only one example deals with the *ex-situ* grafting strategy (ex-situ strategy, see **Table 22 entry 1**). Generally, the concentration of grafted QAS tends to 1.0 $mmol.g^{-1}$. The nature of supported QAS varies as a huge diversity can be obtained, either by changing the alkyl chain length (Et, Bu, Hex or Oct) or the nature of the counter anion (usually halides, i.e. I^-, Br^-, Cl^-). Chloride and bromide are among the most representative examples.

In the scope of the cycloaddition reaction, as already seen in **Chapter II**, better catalytic properties are obtained with the use of bromides and QAS with a longer chain length such as butyl. Moreover, supported ammonium bromides have been little studied in the literature compared to other halogen such as chloride. Even better catalytic properties have been emphasized by some authors, including our group,[2] for soluble QAS bearing at least one hydroxyalkyl substituent which is able to interact through hydrogen bonding with the oxygen atom of the oxirane. Such observation led us, in a work conducted by C. Rocha, to synthesize supported -$Me_2(EtOH)N^+Cl^-$ onto SBA-15 silica using an *in-situ* grafting strategy based on the nucleophilic substitution of Cl of anchored chloropropyl groups by dimethylethanolamine (DMEA). Such material, despite a non-optimized synthesis and the use of Cl^- instead of Br^-, showed an interesting catalytic activity in the cycloaddition of CO_2 onto styrene oxide, with a yield of 73% of styrene carbonate after 23h at 120°C.

The aim of this chapter is the synthesis and characterization of QAS@SBA-15 materials showing good catalytic performances in the absence of co-catalyst. Our work will focus on the development of home-made QAS bearing either alkyl or hydroxyethyl substituents. As previously shown in our group, the later will be introduced onto pre-formed SBA-15 by using a grafting approach where i) either an organosilane bearing a halogen substituent will be grafted onto SBA-15 before the quaternization reaction (“in-situ approach”), ii) or an organosilane bearing a QAS (Si-QAS) will be synthesized before being grafting (“ex-situ approach”). Best QAS@SBA-15 materials will be tested in the CO_2 cycloaddition onto styrene

oxide in the absence of co-catalyst in order to evaluate the catalysts only and define the requirements for the co-catalysts if necessary.

In this part, QAS@SBA-15, will be prepared by the reaction of tertiary amines with chloropropyl or bromopropyl groups. Here, only QAS with bromide or chloride counter-ions will be synthesized despite the good reactivity of soluble QAS involving iodide as a counter-ion for CO_2 cycloaddition. Indeed, in the context of the whole study where CO_2 cycloaddition will be combined with an epoxidation step performed in the presence of hydrogen peroxide or dioxygen, iodide ions may be oxidized to iodine and may no longer be available for the oxirane nucleophilic attack.

V.2 Optimization of grafting protocols

Variations in reaction conditions were examined in detail for the grafting of 3-chloropropyl trimethoxysilane (CPTMS). Optimal anchoring conditions will be investigated and then be applied for the different halogenated organosilanes (*in-situ* route) or organosilanes bearing quaternary ammonium groups (ex-situ route). CPTMS has been selected over other alkyl halides due to its great accessibility.

V.2.1 A detailed study with 3-chloropropyltrimethoxysilane (CPTMS)

The experimental procedure described in the insert below was used. Optimization parameters were the volume of toluene (X, 5.5 to 25 $mL.g^{-1}$), the amount of CPTMS (Y, 2 or 4 $mmol.g^{-1}$) and the heating time under reflux (1 to 72 h).

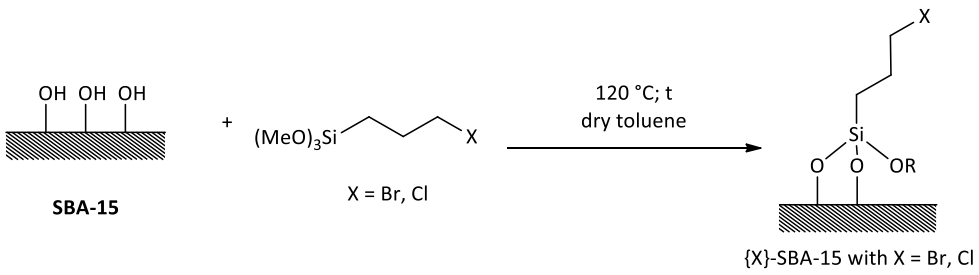

Figure 72: *Reaction scheme for the grafting of linkers or of organosilanes bearing QAS groups*

***Functionalization of SBA-15 by CPTMS**: SBA-15 was vacuum dried at 120°C for 3 h in a two-necked vessel connected to a condenser. After cooling at room temperature and under N_2 atmosphere, a volume of X mL of anhydrous toluene was added per gram of solid. Then, the suspension was immerged in an ultrasonic bath for 15 min. Under stirring, Y mmol of CPTMS was added dropwise per gram of SBA-15. The resulting suspension was stirred at room temperature for 2 h and heated at reflux for Z h. The white solid was recovered by filtration using a frit (porosity 4), washed with acetone and CH_2Cl_2 using a Soxhlet in order to get rid of physisorbed molecules. Finally, the solid was dried overnight at 50°C and vacuum-dried for a few hours.*

All the resulting {Cl}-SBA-15 materials were characterized by TGA in order to estimate the content of chloropropyl groups anchored onto SBA-15 **(Figure 73).**

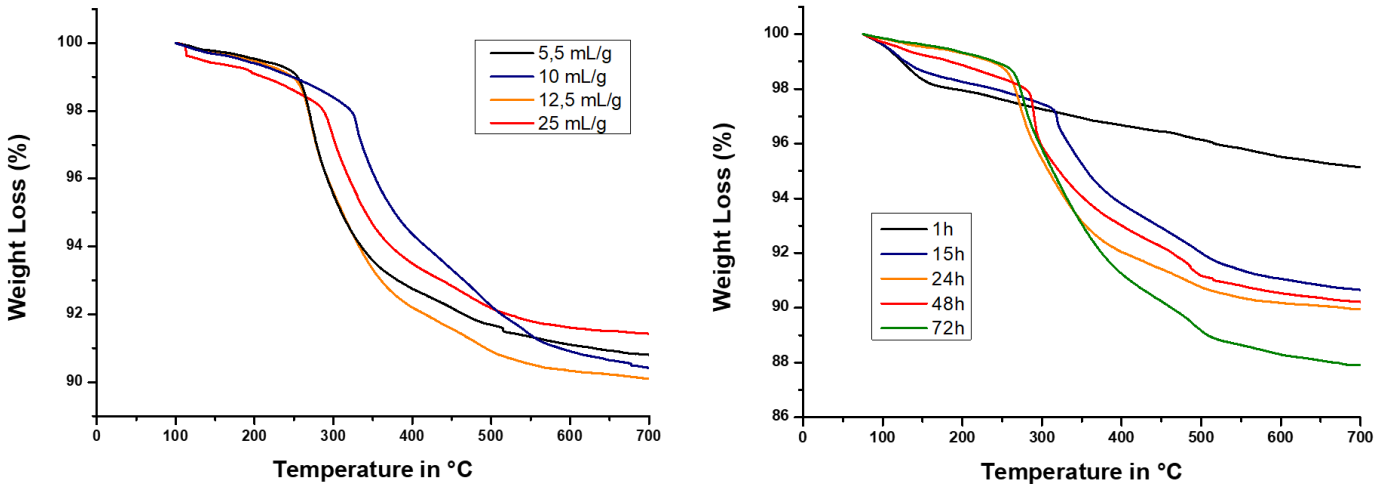

***Figure 73:** TGA of {Cl}-SBA-15 materials obtained with different toluene volumes (left) or heating times (right). All the curves were normalized at 100% for 100°C.*

Regarding the variation of the solvent volume using a nominal CPTMS loading of 4 mmol.g^{-1} and a heating time of 24 h (**Figure 73**, left), it can be stated that 25 mL g^{-1} was detrimental to the final uptake of chloropropyl groups (only 0.82 mmol.g^{-1}, **Table 23, entry 1**). The maximum experimental loading (1.08 mmol.g^{-1}) was reached with 12.5 mL of toluene .g^{-1} (**Table 23, entry 2**). Thus, it seemed to us that, the increase of the concentration of CPTMS in toluene promotes its grafting onto SBA-15. However, below 12 mL.g^{-1}, the grafting rate did not vary very much with an average experimental concentration of 0.9-1 mmol.g^{-1} (**Table 23, entries 3 and 4**).

Table 23 Impact of different parameters on the final loading of chloropropyl on the silica support

Entry	CPTMS quantity (mmol.g^{-1})	Dry toluene volume (mL.g^{-1})	Time (h)	[-PrCl] (mmol.g^{-1})
1	4	25	24	0.82
2	4	12.5	24	1.08
3	4	10	24	0.95
4	4	5.5	24	0.96
5	4	12	1	0.23
6	4	12	15	0.77
7	4	12	48	0.90
8	4	12	72	1.31
9	2	12	24	1.13

The grafting efficiency of CPTMS was then studied as a function of the reflux heating time keeping the toluene volume at 12 mL.g^{-1} and the organosilane nominal amount at 4 mmol.g^{-1}. As the reaction time increased, the concentration of chloropropyl functions increased from 0.23 mmol.g^{-1} for 1 h to 1.31 mmol.g^{-1} for 72 h. However, beyond 24 h, the experimental loading of organic functions varied only slightly, from 1.08 mmol.g^{-1} to 1.31 mmol.g^{-1} for 3 days of reaction (**Table 23**, **entries 2 and 8**). In the end, the same reaction was carried out reducing the nominal amount of CPTMS (from 4 to 2 mmol.g^{-1}) keeping the volume of toluene at 12 mL.g^{-1} and the heating time at 24 h (**Table 23, entry 9**). In this later case, the experimental loading of chloropropyl groups was not significantly different from the value obtained starting from 4 mmol.g^{-1}. So, it was possible to decrease the amount of CPTMS added without risking a decrease of the organosilane concentration on the support.

Thereafter, the grafting procedure of trialcoxy silanes on SBA-15 will be as follows:

***Functionalization of SBA-15 by organosilanes**: SBA-15 was vacuum dried at 120°C for 3 h in a two-necked vessel connected to a condenser. After cooling at room temperature and under N_2 atmosphere, a volume of 10 mL of anhydrous toluene was added per gram of solid. Then, the suspension was immerged in an ultrasonic bath for 15 min. Under stirring, 2 mmol of organosilane was added dropwise per gram of SBA-15. The resulting suspension was stirred at room temperature for 2 h and heated at reflux for 24 h. The white solid was recovered by filtration using a frit (porosity 4), washed with acetone and CH_2Cl_2 using a Soxhlet in order to get rid of physisorbed molecules. Finally, the solid was dried overnight at 50°C and vacuum-dried for a few hours.*

TGA alone does not allow to characterize the nature of the covalent bonding between silica and CPTMS. Further analysis, using ^{29}Si NMR CP MAS, was needed. Results obtained for the material prepared according to the conditions of **Table 23, entry 9** are reported in **Figure**

74, emphasizing T^1 signals (1 bond between the linker and SBA-15) at -48 ppm and T^2 signals (2 bonds between the linker and SBA-15) at -58 ppm. Such data are in good accordance with the literature.[22]

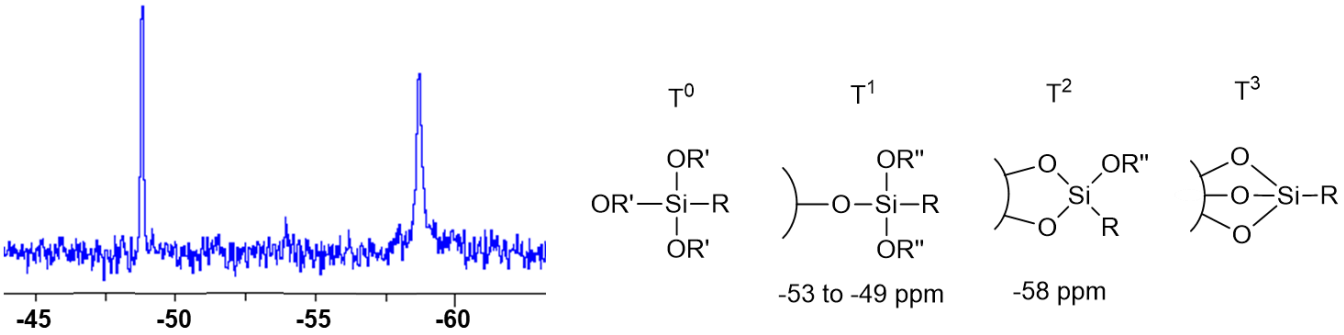

Figure 74: ^{29}Si NMR CP MAS spectrum of {Cl}-SBA-15 with reference values

V.2.2 Case of {Br}-SBA-15 – comparisons with {Cl}-SBA-15 and {NH_2}-SBA-15

{Br}-SBA-15 that will be used in the up-coming part for *in-situ* grafting of tertiary amines was synthesized from SBA-15 and BPTMS (bromopropyltrimethoxysilane) following the optimal procedure described before and characterized by TGA, XRD and N_2 sorption analyses. The results are displayed (in brown) in **Figure 75** as well as those for {Cl}-SBA-15 (green, see description before). In comparison, previously described {NH_2}-SBA-15 see in **Chapter IV.1**, that were prepared from APTES, was also displayed in the same figure. Bromopropyl loading in {Br}-SBA-15 evaluated by TGA was estimated to 1.29 mmol.g^{-1} which is in a range order similar to the loading of chloropropyl groups in {Cl}-SBA-15, but quite lower than 2.2 mmol.g^{-1} of aminopropyl groups in {NH_2}-SBA-15. One possible explanation to the difference of molar concentration would be the nature of alkoxy group present in the precursor structure. In this matter, trimethoxy silane groups were used in the case of {Br} and {Cl} functionalized silica, while triethoxy group was found in the case of {NH_2} function. Further studies should be investigated to validate or not this hypothesis.

Table 24: *Physicochemical properties of parent SBA-15 and of its corresponding grafted* forms

Sample	S_{BET} ($m^2.g^{-1}$)	Pore Vol. ($cm^3.g^{-1}$)	Average Pore diameter (nm)	Organic function loading ($mmol.g^{-1}$)
SBA-15	900	1.12	6.2	-
{Cl}-SBA-15	640	0.91	6.2	1.13
{Br}-SBA-15	570	0.74	5.9	1.29
{NH_2}-SBA-15	530	0.69	5.7	2.2

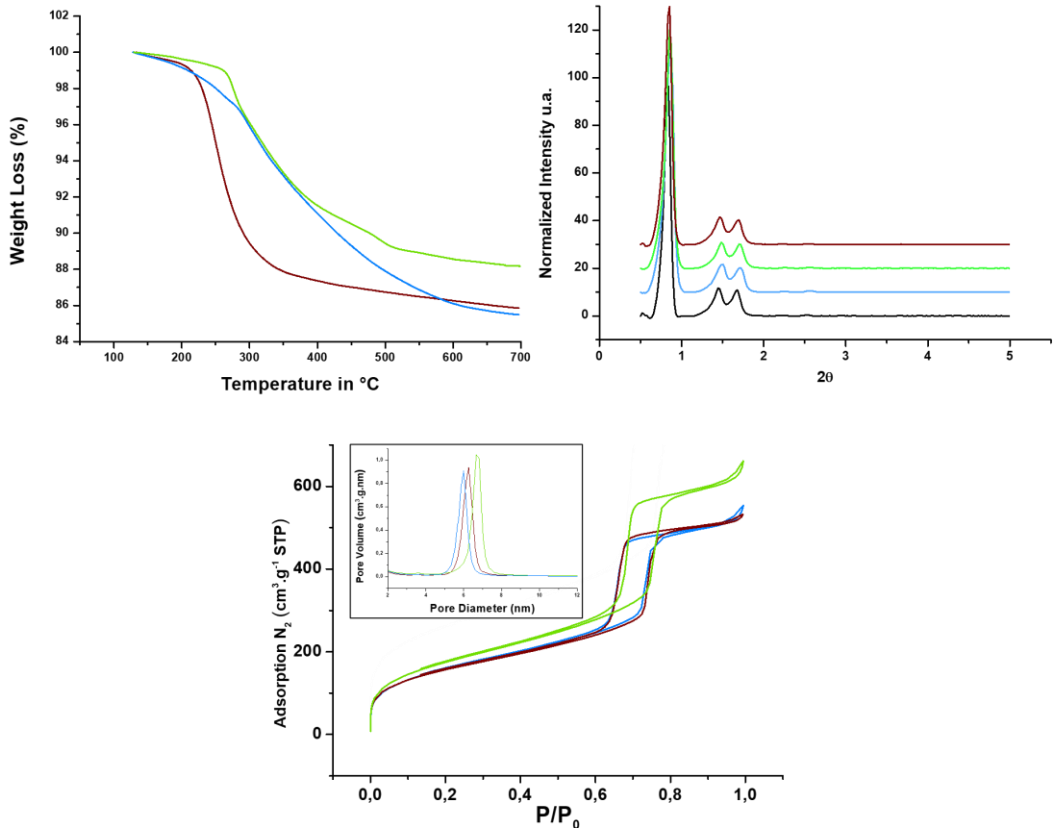

Figure 75: *(top left) TGA (All curves were normalized at 100°C) - (top right) X-ray Diffraction with SBA-15 reference (black) - (bottom) Nitrogen adsorption-desorption isotherms (77K) of {NH_2}-SBA-15 (blue), {Cl}-SBA-15 (green) and {Br}-SBA-15 (brown) with pore size distribution curves (inset)*

As shown by XRD, the SBA-15 silica support does not seem to be altered whatever the organosilane used. The signals related to the (100), (110) and (200) reticular planes characteristic of SBA-15 are still present in all the synthesized materials (**Figure 75**). In parallel, a decrease of all the textural parameters (specific surface area, pore volume and average pore diameter) was also observed in the resulting hybrid materials (see **Table 24**). These results are compatible with a homogeneous grafting of the bromopropyl and chloropropyl groups in the different pores of the SBA- 15 silica.

V.3 In-situ approach for the synthesis of supported QAS

Bromine being a better leaving group than chlorine in SN2 reactions, the in-situ synthesis of supported QAS was performed starting from {Br}-SBA-15 instead of {Cl}-SBA-15. Hence, {Br}-SBA-15 was reacted with 2 amine equivalents in acetonitrile (see experimental procedure in the insert below) to form supported QAS, as shown in **Figure 76.** The amines used were N,N,N triethylamine, N,N-dimethyl(2-hydroxyethyl)amine, N,N-di(2-hydroxyethyl)-N-methylamine and N,N,N-tri(2-hydroxyethyl)amine.

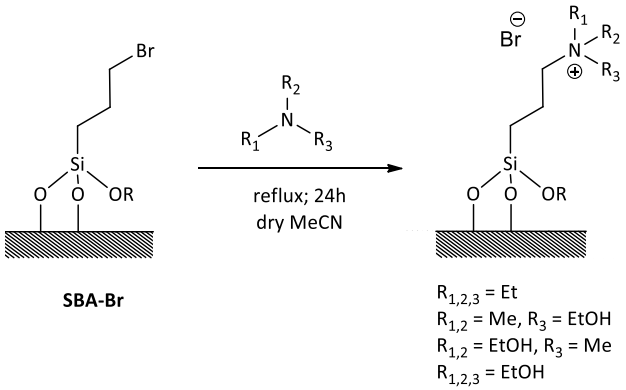

Figure 76: *In-situ synthesis of grafted ammonium salts*

> ***Preparation of {QAS}-SBA-15 (in-situ mode):*** *{Br}-SBA-15 was first dried under vacuum at 80°C for 3 h. After cooling down to room temperature, anhydrous acetonitrile (20 mL per gram of {Br}-SBA-15) was added under N_2 atmosphere. The resulting mixture was immerged in an ultrasonic bath for 15 min, then 2 amine equivalents per bromine atoms were added under magnetic stirring. The suspension was refluxed at 90°C for 24 h. The white solid obtained was recovered by filtration on a frit (porosity 4), washed with acetone, then CH_2Cl_2 using a Soxhlet. {QAS}-SBA-15 was then dried at 50°C overnight and dried under vacuum for a few hours.*

Thermogravimetric as well as Nitrogen adsorption-desorption analyses were conducted on the resulting materials (**Figure 77, left**), showing that no significant increase of mass loss was observed for materials {$Et_3N^+Br^-$}-SBA-15, {$(EtOH)_2MeN^+Br^-$}-SBA-15 and {$(EtOH)_3N^+Br^-$}-SBA-15 compared to the starting material {Br}-SBA-15. Thus, it can be concluded that the expected reaction did not occur efficiently with N,N,N triethylamine (predicted pKa = 10.62), N,N-di(2-hydroxyethyl)-N-methylamine (predicted pKa = 14.41) and N,N,N-tri(2-hydroxyethyl)amine (predicted pKa = 14.17) since it should have led to increasing amounts of organic loadings.

Table 25: Physicochemical properties of the materials recovered from the in-situ approach

Compound	S_{BET} ($m^2.g^{-1}$)	Pore Vol. ($cm^3.g^{-1}$)	Average Pore diameter (nm)	Organic function loading ($mmol.g^{-1}$)
{Br}-SBA-15	570	0.74	5.9	1.29
$\{Et_3N^+Br^-\}$-SBA-15	510	0.74	6.0	trace of QAS
$\{(EtOH)_2MeN^+Br^-\}$-SBA-15	434	0.73	6.2	trace of QAS
$\{(EtOH)_3N^+Br^-\}$-SBA-15	405	0.59	5.8	trace of QAS
$\{Me_2(EtOH)N^+Br^-\}$-SBA-15	290	0.49	5.9	0.50

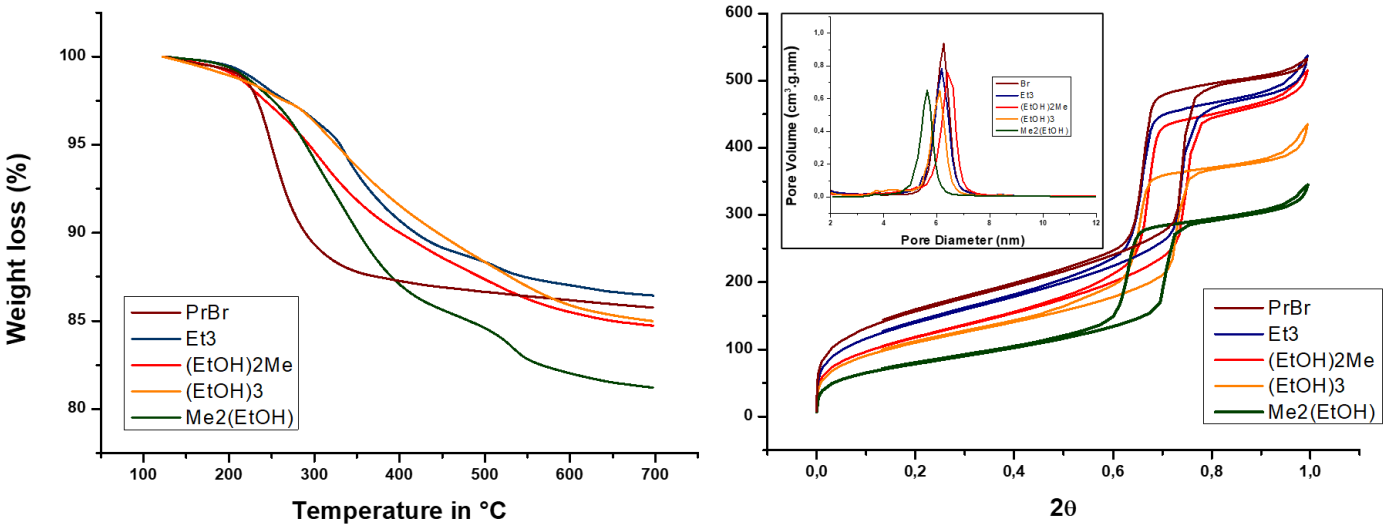

Figure 77: (left) TGA (All curves were normalized at 100°C) - (right) Nitrogen adsorption-desorption isotherms (77K) with pore size distribution curves (inset) for {Br}-SBA-15 (brown) and the materials ({QAS}SBA-15) recovered after its reaction with tertiary amine

TGA interpretations for $\{Et_3N^+Br^-\}$-SBA-15 and $\{(EtOH)_2MeN^+Br^-\}$-SBA-15 are further validated by the N_2 adsorption-desorption data (**Figure 77 (right)**). In both cases, the decrease of the specific surface area and of the pore volumes was not of significant importance in the resulting material in comparison with the starting solid, {Br}-SBA-15 (**Table 25**). Only, a slight decrease of the pore volume (0.59 $cm^3.g^{-1}$ instead of 0.74-73 $cm^3.g^{-1}$) could be noticed in the case of $\{(EtOH)_3N^+Br^-\}$-SBA-15 but, globally, the pore size distributions of materials were unchanged.

On the other hand, $\{(EtOH)Me_2N^+Br^-\}$-SBA-15 obtained from the reaction of N-(2-hydroxyethyl)-N,N-dimethylamine (predicted pKa = 14.88) with {Br}-SBA-15 presents significantly different TGA and N_2 sorption data (**Figure 77**). TGA of $\{Me_2(EtOH)N^+Br^-\}$-SBA-15 showed an increase in mass loss of 4.5 % compared to {Br}-SBA-15 allowing the estimation of the tertiary amine uptake to approximately 0.50 $mmol.g^{-1}$. However, TGA analyses alone

cannot confirm the efficiency of the expected nucleophilic substitution reaction. Indeed, it has been shown in the work of C. Rocha Carvalho [1] that tertiary amines can also interact with surface silanols through hydrogen bonds or even neutralize silanol groups through an acid-base reaction (see **Figure 78**).

As a first conclusion, it seems that *in-situ* synthesis of quaternary ammonium salts by the reaction of tertiary amines with bromopropyl substituted SBA-15, through a nucleophilic attack pathway, is not efficient. The superior reactivity of $Me_2(EtOH)N$ compared to those of

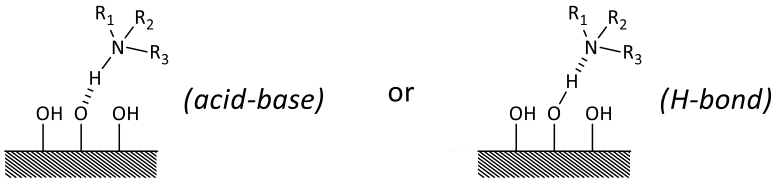

Figure 78: *Secondary reactions of tertiary amines with silanol groups of SBA-15*

$(EtOH)_2MeN$, Et_3N and $(EtOH)_3N$ cannot be explained by a favourable pKa value, but more probably by the lesser steric bulkiness of this amine. However, it cannot be totally excluded that the affinity of the amine with silica prevents a 100% nucleophilic substitution yield. As the result, an *ex-situ* synthesis of organosilanes bearing similar quaternary ammonium salts was also investigated and will be presented in the following part.

V.4 Ex-situ approach for the synthesis of supported QAS

V.4.1 Synthesis and characterization of organosilanes bearing quaternary ammonium salts (Si-QAS)

The synthesis of eight potentially interesting silylated quaternary ammonium was carried out using 1 equivalent of BPTMS or CPTMS and 1 equivalent of tertiary amine (**Figure 79**). Among the three solvents tested (MeCN, toluene, THF, **Table 6**) in reflux conditions, MeCN, dry MeCN (see experimental conditions in the inset below) led to the best results for compounds **of entries 1-4.**

***Si-QAS synthesis procedure**: In a Pyrex tube, under N_2 atmosphere, containing 1 mL of anhydrous acetonitrile, 4 mmol of halogenosilane were added. Then, 4 mmol of amine were introduced dropwise under magnetic stirring. The reaction mixture, once the tube has been sealed, was stirred under reflux (82 °C) during 17 h, then the yellow solution was analysed by ^{1}H NMR.*

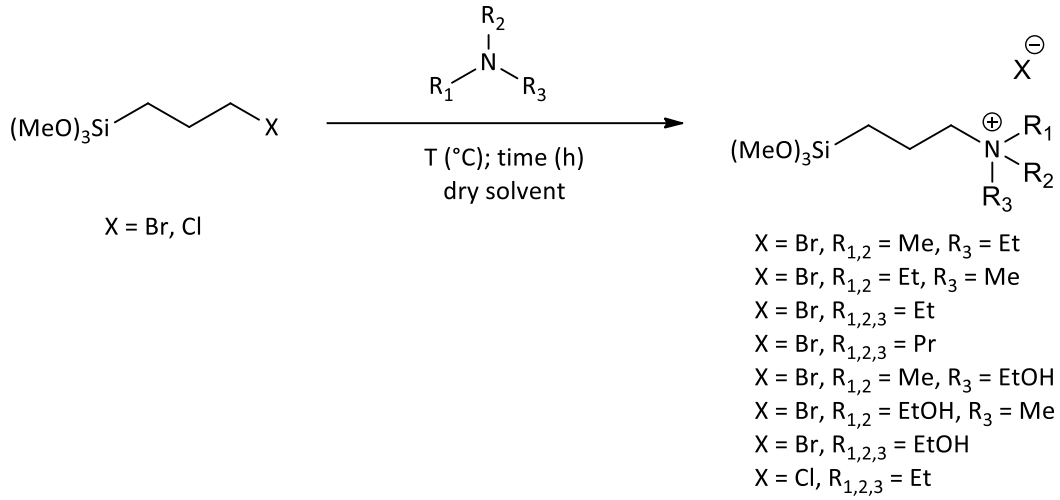

***Figure 79:** Ex-situ synthesis of organosilanes bearing quaternary ammonium salts*

***Table 26**: Experimental parameters and results of ex-situ quaternarisation of tertiary amines with silylated organo silane*

Entry	Silane	Amine	Halide	Dry solvent	Time (h)	T (°C)	NMR yield (%)
1	**2**	Me_2EtN	Br	MeCN	17	Reflux	98
2	**2**	$MeEt_2N$	Br	MeCN	17	Reflux	95
3	**2**	Et_3N	Br	MeCN	17	Reflux	92
4	**2**	Pr_3N	Br	MeCN	17	Reflux	42
5	**2**	$(Me)_2(EtOH)$ N	Br	MeCN	17	Reflux	trace
6	**2**	$(EtOH)_2MeN$	Br	MeCN	17	Reflux	trace
7	**2**	$(EtOH)_3N$	Br	MeCN	17	Reflux	trace
8	**3**	Et_3N	Cl	THF	24	Reflux	0
9	**3**	Et_3N	Cl	MeCN	24	Reflux	0
10	**3**	Et_3N	Cl	Toluene	64	Reflux	0
11	**3**	Et_3N	Cl	-	16	Reflux	0
12	**3** + 0.024 eq NaI	Et_3N	Cl	MeCN	24	Reflux	19

{$Me_2EtN^+Br^-$} (**entry 1**), {$Et_2MeN^+Br^-$} (**entry 2**) and {$Et_3N^+Br^-$} (**entry 3**) were obtained with almost complete yields of 98, 95 and 92% (on ^{1}H NMR basis) within 17 h (**Table 26**). In this matter, better results were obtained in this order: $Me_2EtN > Et_2MeN > Et_3N$. At first sight, it must be concluded that the less bulky the amine, the better the quaternization is. Indeed, compound **13** derived from Pr_3N (**Table 26, entry 4**) was obtained in a rather low yield (42%). Separation operations between non-reacted amine, the halogenosilane and the expected product are delicate if not complicated, and such mixture was not be used for further grafting on silica.

The tests carried out for the synthesis of Si-QAS bearing hydroxyethyl group(s) (**Table 26, entries 5-7**) were not conclusive. Indeed, a white solid that was insoluble in water, DMSO, ethanol and acetone was observed at the end of the reaction. This suggests that the solid is inorganic and, probably, the result of the undesired reaction between the hydroxyl groups of the amines and the methoxy groups of the halogenosilanes (see **Figure 80**).

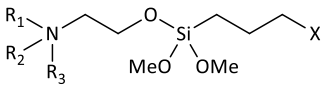

(condensation reaction)

Figure 80: *Secondary reaction of amines bearing hydroxyethyl groups with the halogenosilane*

These results also highlight the fact that the *in-situ* grafting based on the reaction between anchored bromopropyl groups and amines bearing hydroxyethyl substituents tested before had no chance to be conclusive. As the result, we suggest that the increase in mass loss obtained for {$Me_2(EtOH)N^+Br^-$}-SBA-15 compared to {Br}-SBA-15 (**Figure 77, left**) could be due to the above-mentioned secondary condensation reaction.

The reactivity of NEt_3 towards the chloropropyl group in CPTMS was also checked. As shown in **(Table 26 entries 8-12)**, CPTMS was not reactive enough to afford a good yield of the corresponding quaternary ammonium salt, even when varying the solvent and the reaction temperature. As bromine is a better leaving group than chlorine, a yield of 92% was achieved in the case of **entry 3**. In order to improve the yield a test was performed in the presence of NaI added in catalytic amount (1% mol.), leading to a 19% yield (**Table 26, entry 12**).

To conclude, three organosilanes bearing quaternary ammonium salts with ethyl and/or methyl substituents and bromide counter-anion (**10**, **11** and **12**) could be prepared in high yield (more than 92%) avoiding difficult separation procedures before use. Details on their grafting on SBA-15 and characterization of the obtained materials are described in the next section.

V.4.1.1 Grafting of Si-QASs and characterization of the resulting materials

Silylated quaternary ammonium salts seen in **section 4.1** were grafted on silica SBA-15, targeting QAS@SBA-15 materials (see **Figure 81**) following the optimal experimental procedure established in section **4** (see details in the inset below).

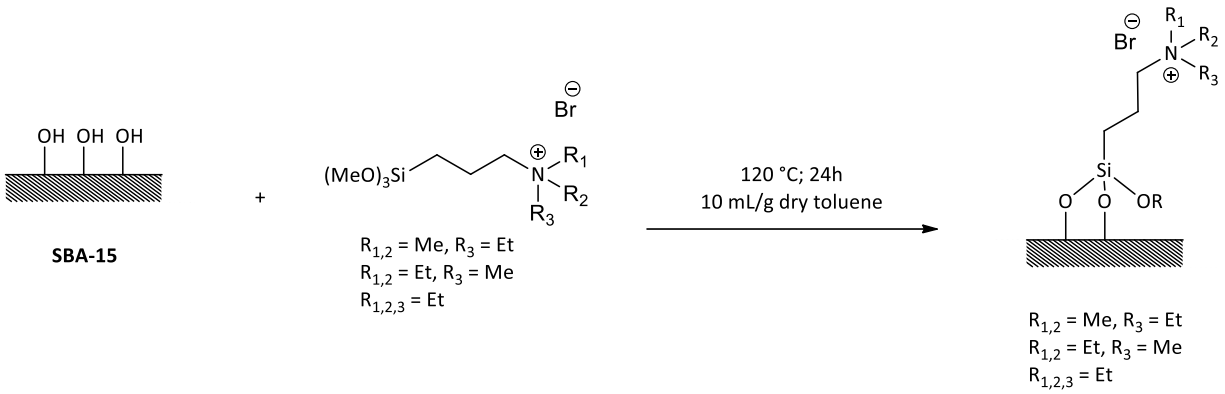

Figure 81: *Grafting of Si-QAS onto SBA-15 silica*

> ***Grafting of Si-QAS onto SBA-15****: SBA-15 was vacuum dried at 120°C for 3 h using a two-necked vessel connected to a condenser. After cooling to room temperature and under N_2 atmosphere, 10 mL of anhydrous toluene were added per gram of SBA-15. The resulting suspension was immerged in an ultrasonic bath for 15 min. Then, under stirring, 2 mmol of QAS (per gram of SBA-15) were added dropwise. The suspension was stirred at room temperature for 2 h and then, heated at reflux for 24 h. The white solid was recovered by filtration (frit with porosity 4), washed with acetone and CH_2Cl_2 using a Soxhlet. The obtained material was dried overnight at 50°C and vacuum dried for a few hours.*

TGA analyses (**Figure 82, left**) of the three materials synthesized following the *ex-situ* approach proved that the grafting was successful (see maximum loss rate at *c.a.* 243°C). The Si-QAS content of {$Me_2EtN^+Br^-$}-SBA-15 and {$Et_2MeN^+Br^-$}-SBA-15 materials could be estimated to 1 mmol.g^{-1} for 2 mmol.g^{-1}expected, corresponding to a grafting yield of 50% (**Table 7**). {$Et_3N^+Br^-$}-SBA-15 was obtained with 1.13 mmol.g^{-1} of functions for 2 mmol.g^{-1} (grafting yield of 57%, **Table 7**). It is noteworthy that additional X-ray fluorescence (XRF) measurements performed at IRCELYON gave similar results (see **Appendix**) regarding the bromide weight concentration (**Table 27**).

Table 27*: Physico-chemical properties of the functionalized materials and of the SBA-15 reference*

Sample	S_{BET} ($m^2.g^{-1}$)	Pore Vol. ($cm^3.g^{-1}$)	Average Pore diameter (nm)	Organic function loading			Yield (%)
				Molar conc. ($mmol.g^{-1}$)	%Br (TGA)	%Br (XRF)	
SBA-15	900	1.12	6.2		-		
{$Me_2EtN^+Br^-$}-SBA-15	433	0.56	5.3	1.26	10.1	9.8	50
{$Et_2MeN^+Br^-$}-SBA-15	320	0.50	5.6	1.17	9.4	9.7	49
{$Et_3N^+Br^-$}-SBA-15	415	0.54	5.3	1.22	9.7	6.8	57

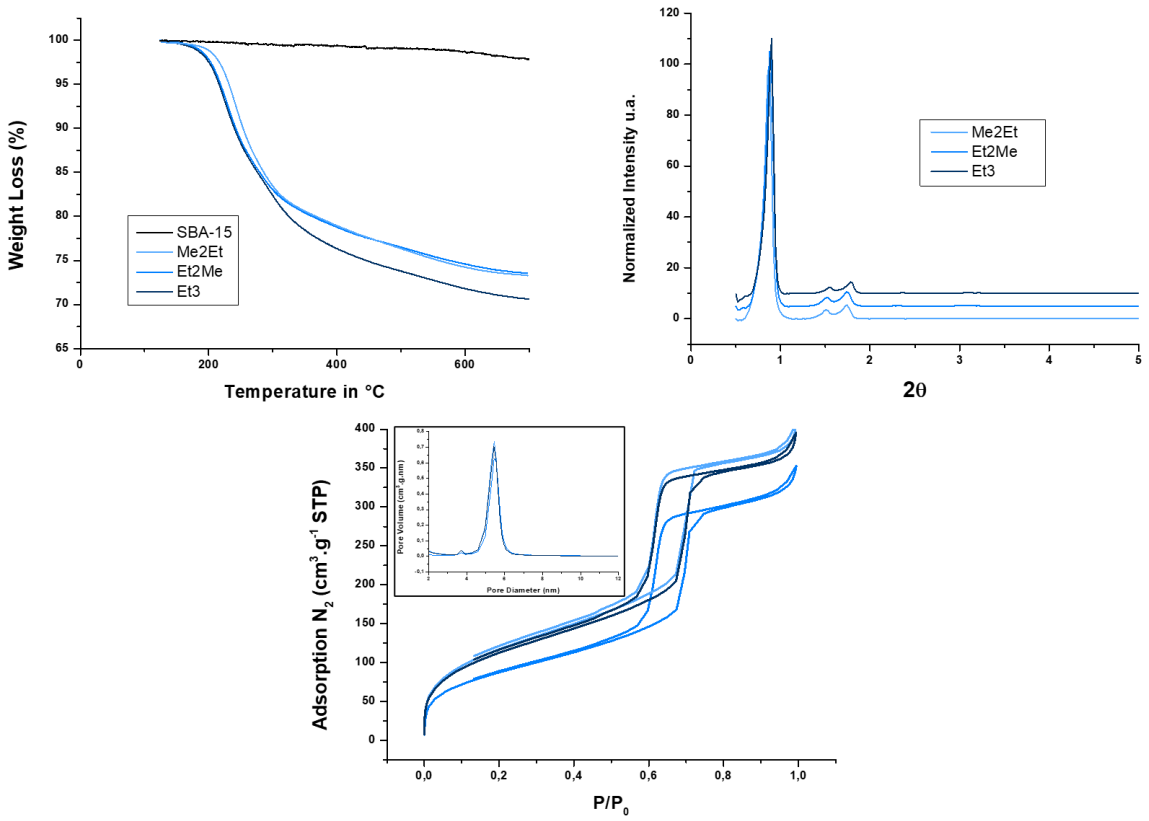

***Figure 82**: (top left) TGA (All curves were normalized at 100°C) - (top right) Low-angle XRD patterns of {Me2EtN+Br-}-SBA-15 (light blue), {Et2MeN+Br-}-SBA-15 (blue) and {Et3N+Br-}-SBA-15 (dark blue)*

Grafting of the Si-QASs onto SBA-15 did not affect the hexagonal pore structure of the support as indicated by the presence of the XRD peaks corresponding to the (100), (110) and (200) reticular planes characteristic of SBA-15 (see **Figure 82** (right)). An overall decrease of the specific surface area was observed, from 900 $m^2.g^{-1}$ to 415 $m^2.g^{-1}$ (**Table 7**), as well as for the pore volume (from 1.12 $cm^3.g^{-1}$ to 0.54 $cm^3.g^{-1}$) and the average pore diameter (from 6.2 nm to 5.3 nm) in the case of $\{Et_3N^+Br^-\}$-SBA-15. The same tendency was observed for the other materials, which is compatible with the incorporation of the silylated ammonium groups in the different pores of the SBA- 15 support.

X-ray photoelectron spectroscopy (XPS) analysis was also conducted on the three QAS@SBA-15 materials.

No matter the QAS@SBA-15 considered, the bromine XPS signal (**Figure 83**, top) could be deconvoluted in the Br $3d_{3/2}$ (69.2 eV) and Br $3d_{5/2}$ (68.1 eV) components ascribed to Br^-. [23] In the case of nitrogen, the main peak observed at 400.8 eV (N 1s) was that expected for a quaternary ammonium, but a much smaller one, at 398.0 eV, was also visible, meaning the presence of 2 types of nitrogen. Given that Si-QAS samples prepared were not purified before the grafting step, the additional N peak in the three XPS spectra was attributed to the presence of non-reacted tertiary amine. Logically, the XPS molar ratios between ammonium and bromide

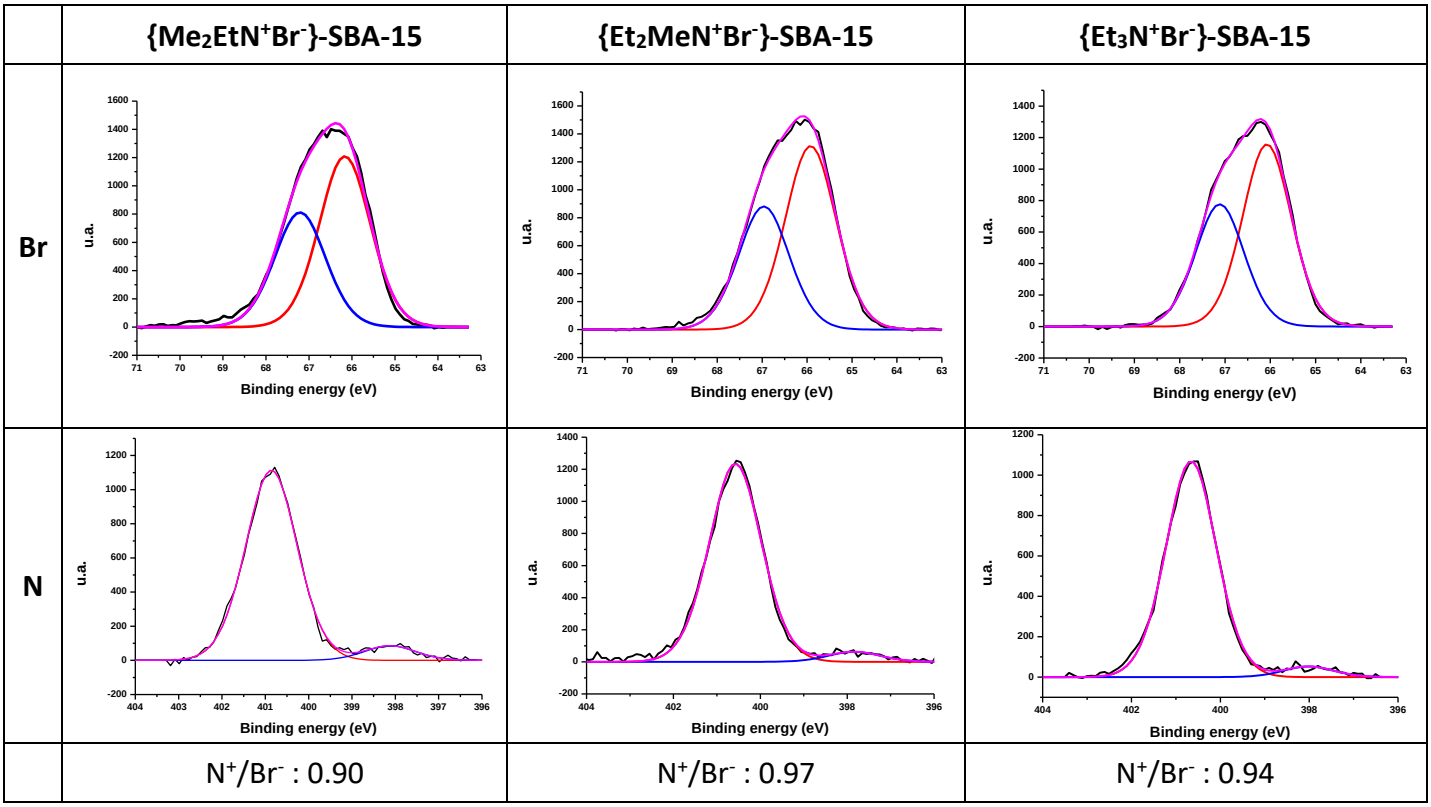

***Figure 83**: XPS analysis of bromine and nitrogen elements of the three QAS@SBA-15 materials. (Calibration was made from C1s C-C peak at 284.8 eV)*

V.4.1.2 Partial conclusions about the synthesis of QAs@SBA-15

Grafting experimental procedures of halogenopropyl groups or “ex-situ” prepared Si-QAS on SBA-15 were optimized with the highly available chloropropyltrimethoxysilane (CPTMS). A longer reaction time allowed to slightly improve the quantity of CPTMS grafted. Nevertheless, beyond a certain heating time, the gain of CPTMS anchored compared to the reaction time was no longer advantageous. Therefore, the reaction time was limited to 24 h for all other attempts. In these conditions, the maximum amount of chloropropyl groups that

could be grafted was around 1 mmol.g^{-1} while that of bromopropyl groups from BPTMS (bromopropyltrimethoxysilane) was slightly higher (1.3 mmol.g^{-1}) under the same conditions including two successive washings with a soxhlet. CP MAS ^{29}Si NMR confirmed the covalent attachment of the organic molecules on SBA-15 and, although those analyses were not performed systematically in this study, it can be assumed, that it was the same for the other materials prepared here. XRD analyses and N_2 physisorption measurements on SBA-15 grafted with chloropropyl groups showed that there is no degradation of the silica support but, in our opinion, the reduction of the specific surface area, of the average pore diameter and of the pore volume is a good indicator showing that the grafting took place homogeneously within the pores.

The attempt to anchor amines with ethyl or hydroxyethyl substituents by the *in-situ* ammonium approach did not work well with {Br}-SBA-15. Among the amines tested, only the less bulky one, *i.e.* $(Me)_2(EtOH)N$, turned out to be attached with 0.5 mmol.g^{-1} but, due to the possibilities of undesired side reactions, it could not be established that all the amine molecules were linked as expected in that case.

In the *ex-situ* approach, the quaternization worked well with bromotrimethoxysilane and tertiary amines with substituents like methyl or ethyl groups. Hence, a yield of 92% was obtained with trimethylamine instead of traces for the *in-situ* approach. Silylated quaternary ammonium salts were then grafted with a 50% yield onto SBA-15. In these cases, TGA analysis helped to establish a maximum loading of 1 mmol.g^{-1} of quaternary ammonium salts for substituents like Me_2Et, Et_2Me and Et_3. Moreover, XPS analyses showed that 100% of bromine atoms in QAS@SBA-15 were present in the Br^- form. In the case of nitrogen peaks, the presence of non-quaternized R_3N molecules was emphasized, thus confirming the incomplete quaternization of the precursors.

Amines bearing hydroxyalkyl substituents could not be quaternized following both approaches as the result of their bulkiness but also because these groups seemed to be incompatible with the methoxy groups of the halogenosilanes. To avoid side reactions, hydroxyl groups should be protected before, but this strategy further introduces additional steps. Last but not least, grafted chloropropyl groups (in-situ approach) or CPTMS (ex-situ approach) have to be abandoned as the result of the too low leaving group ability of Cl vs. Br.

V.4.2 Catalytic Tests

The catalytic activity of {$Me_2EtN^+Br^-$}-SBA-15, {$MeEt_2N^+Br^-$}-SBA-15 and {$Et_3N^+Br^-$}-SBA-15 was then investigated in the cycloaddition of CO_2 onto styrene oxide in the absence of co-catalyst and compared with that of soluble $Bu_4N^+Br^-$ and also that of {$Bu_3N^+Br^-$}-SBA-15 prepared by our colleagues at IRCELYON from the corresponding commercially available Si-QAS. The cycloaddition of CO_2 was carried out under 11 bar with temperatures from 80 to 120°C at reaction times of 3 h and 23 h following the procedure described below.

Cycloaddition of CO_2 on styrene oxide: *Styrene oxide (0.665 mL, 5.6 mmol), 20 mL of benzonitrile, {QAS}-SBA-15 (0.4 mmol) and 8.0 mmol of p-xylene (1 mL) used as internal standard were introduced in a Teflon vessel. The resulting suspension was stirred for 5 min at room temperature and then pressurized in a stainless-steel autoclave at 11 bar of CO_2. The mixture was then heated to 80 or 120°C for 3 to 23 h with a temperature increase of 2.5 °C/min. The autoclave was then cooled down at room temperature using ice and water and its content analysed by GC-FID (see results in table .*

As already mentioned in this work, silica SBA-15 alone did not show any catalytic activity (**Table 28 entry 1**).

Table 28*: Yields of styrene carbonate in the CO_2 cycloaddition onto styrene oxide in the presence of QAS@SBA-15*

Entry	cat	T (°C)	3h	23h
1	SBA-15	120	-	0
2	{ $Me_3N^+Cl^-$}-SBA-15	120	8	40
3	{$Me_2EtN^+Br^-$}-SBA-15	120	63	99
4	{$Me_2EtN^+Br^-$}-SBA-15	80	16	62
5	{$MeEt_2N^+Br^-$}-SBA-15	120	75	99
6	{$MeEt_2N^+Br^-$}-SBA-15	80	21	89
7	{$Et_3N^+Br^-$}-SBA-15	120	87	98
8	{$Et_3N^+Br^-$}-SBA-15	80	24	76
9	{$Bu_3N^+Br^-$}-SBA-15	120	97	99
10	{$Bu_3N^+Br^-$}-SBA-15	80	31	87
11	$Bu_4N^+Br^-$	120	62	84
12	$Bu_4N^+Br^-$	80	12	49

All the QAS@SBA-15 materials (bearing bromide counter-ions) afforded the complete conversion of styrene oxide into styrene carbonate within 23 h at 120°C (**Table 28, entries 3, 5, 7 and 9**). Such improvement of the catalytic activity is primarily related to the switch of Cl^- to Br^-. The formation of loose anion/cation pairs, as the result of the increase of the lipophilicity of the nitrogen substituents, may also be invoked when comparing the results obtained with {$Me_2EtN^+Br^-$}-SBA-15, {$MeEt_2N^+Br^-$}-SBA-15, {$Et_3N^+Br^-$}-SBA-15 and {$Bu_3N^+Br^-$}-

SBA-15. Indeed, the longer the alkyl chain, the better the yield of styrene carbonate (see the results at 120°C, 3 h with Br^-): Bu_3N > Et_3N > Et_2Me > Me_2Et. As such, styrene oxide conversion remained as high as 63% for {$Me_2EtN^+Br^-$}-SBA-15 at 120°C after 3h (**Table 28, entry 3**), 75% for {$MeEt_2N^+Br^-$}-SBA-15 (**Table 28, entry 5**), 87% for {$Et_3N^+Br^-$}-SBA-15 (**Table 28, entry 7**) and even 97% for {$Bu_3N^+Br^-$}-SBA-15 (**Table 28, entry 9**). However, none of those catalysts allowed the completion of the reaction at 80°C with yields < 31 % within 3 h or < 89% within 23 h (**Table 28, entries 4, 6, 8 and 10**).

From the comparison of the catalytic performances of {$Bu_3N^+Br^-$}-SBA-15 and $Bu_4N^+Br^-$ at 80°C (3 h or 23 h), it can be noted that grafting quaternary ammonium salts does not only lead to a greater recovery of the QAS but also to the improvement of its activity. With {$Bu_3N^+Br^-$}-SBA-15 (**Table 8, entry 10**), we thus got styrene carbonate in 87% yield after 23h reaction at 80°C while TBABr alone only afforded 49% yield (**Table 8, entry 11**). However, silica itself showed no activity at all even at 120°C (**Table 8, entry 1**). Once again in this manuscript, these results clearly emphasize the benefits of silica in terms reactivity of the resulting heterogeneous catalysts. As explained previously in **Chapter II**, hydroxyl groups would play a major role in styrene carbonate formation. They would apparently interact with oxiranes via hydrogen bonding and thus activate them towards the nucleophilic attack of Br^-.

V.5 Conclusion

In this chapter, we have investigated two grafting strategies for the incorporation of QAS onto SBA-15 silica. Preliminary work on commercially available organosilanes showed that c.a. 1 $mmol.g^{-1}$ of SBA-15 seems to be a threshold for the organotrimethoxysilanes (CPTMS and BPTMS) while 2 $mmol.g^{-1}$ could be reached with APTES, probably as the result of differences of reaction rates of silanols with trimethoxysilanes vs. triethoxysilanes. Optimized synthesis conditions for the grafting of CPTMS were adapted to BPTMS and the resulting material was tested as precursor for the *in-situ* grafting of QAS through the reaction of bromopropyl groups with four different tertiary amines (Et_3N, $(EtOH)_2MeN$, $(EtOH)_3N$ and $Me_2(EtOH)N$). However, only, the less bulky one ($Me_2(EtOH)N$) was grafted but only at 0.5 $mmol.g^{-1}$ in these conditions. We showed thereafter in *ex-situ* attempts to synthesize Si-QAS that the reaction of bromopropyl groups is already unfavourable with tertiary amines bearing

ethyl substituents instead of methyl ones and that hydroxyethyl substituents are responsible for secondary reactions. In the present work, best yields of Si-QAS were obtained for Me_2EtN, $MeEt_2N$ and Et_3N. Grafting of the resulting Si-QAS with trimethoxysilane functions in the conditions optimized for CPTMS allowed us to reach 1 mmol of QAS $.g^{-1}$ of silica support.

Then, the catalytic activity of the QAS@SBA-15 issued from the ex-situ approach has been investigated emphasizing greater results for the cycloaddition of CO_2 onto styrene oxide compared to soluble TBABr. Undoubtedly, QAS grafting on inert SBA-15 leads to significant improvements of their catalytic activity. However, in the context, of the present work dealing with the implementation of a catalytic system allowing the direct conversion of styrene into styrene carbonate in the presence of CO_2 and a green oxidant under mild conditions, it is clear, from the present study, that co-catalysts will be needed. Unfortunately, QAS@SBA-15 bearing longer alkyl chains or hydroxyethyl substituents could not be produced in this work. Indeed, the best material, $\{Bu_3N^+Br^-\}$-SBA-15, had to be synthesized starting from its expensive commercially available Si-QAS precursor. Further progresses are definitely needed to obtain better catalysts.

References

[1] C. Yang, B. Zibrowius, F. Schüth, A novel synthetic route for negatively charged ordered mesoporous silica SBA-15, *Chem. Commun.*, (**2003**), 1772–1773.

[2] C. Carvalho Rocha, PhD thesis: Towards a catalytic system allowing the “one-pot” conversion of alkenes into cyclic carbonates in the presence of dioxygen/carbon dioxide mixtures, Université de Paris, **2013**.

[3] T.-H. Kim, M. Jang, J.K. Park, Bifunctionalized mesoporous molecular sieve for perchlorate removal, *Microporous Mesoporous Mater.*, (**2008**), 108, 22–28.

[4] X. Wang, L. Shi, J. Zhang, J. Cheng, X. Wang, Self-assembly fabrication, microstructures and antibacterial performance of layer-structured montmorillonite nanocomposites with cationic silica nanoparticles, *RSC Adv.*, (**2017**), 7, 31502–31511.

[5] I. Rodriguez, S. Iborra, F. Rey, A. Corma, Heterogeneized Brönsted base catalysts for fine chemicals production: grafted quaternary organic ammonium hydroxides as catalyst for the production of chromenes and coumarins, *Appl. Catal. A Gen.*, (**2000**), 194–195, 241–252.

[6] S. Cerneaux, S.M. Zakeeruddin, J.M. Pringle, Y.-B. Cheng, M. Grätzel, L. Spiccia, Novel Nano-Structured Silica-Based Electrolytes Containing Quaternary Ammonium Iodide Moieties, *Adv. Funct. Mater.*, (**2007**), 17, 3200–3206.

[7] E.A. de Campos, A.A. da Silva Alfaya, R.T. Ferrari, C.M.M. Costa, Quaternary Ammonium Salts Immobilized on Silica Gel: Exchange Properties and Application as Potentiometric Sensor for Perchlorate Ions, *J. Colloid Interface Sci.*, (**2001**), 240, 97–104.

[8] A.R. Hajipour, N.S. Tadayoni, F. Mohammadsaleh, Nicotine functionalized-silica palladium (II) complex: a highly efficient, environmentally benign and recyclable nanocatalyst for C-C bond forming reactions under mild conditions, *Appl. Organomet. Chem.*, (**2016**), 30, 777–782.

[9] S. Udayakumar, S.-W. Park, D.-W. Park, B.-S. Choi, Immobilization of ionic liquid on hybrid MCM-41

system for the chemical fixation of carbon dioxide on cyclic carbonate, *Catal. Commun.*, (**2008**), 9, 1563–1570.
[10] M. Cokoja, M.E. Wilhelm, M.H. Anthofer, W.A. Herrmann, F.E. Kühn, Synthesis of Cyclic Carbonates from Epoxides and Carbon Dioxide by Using Organocatalysts, *ChemSusChem*., (**2015**), 8, 2436–2454.
[11] K. Motokura, S. Itagaki, Y. Iwasawa, A. Miyaji, T. Baba, Silica-supported aminopyridinium halides for catalytic transformations of epoxides to cyclic carbonates under atmospheric pressure of carbon dioxide, *Green Chem.*, (**2009**), 11, 1876–1880.
[12] S. Baj, T. Krawczyk, K. Jasiak, A. Siewniak, M. Pawlyta, Catalytic coupling of epoxides and CO_2 to cyclic carbonates by carbon nanotube-supported quaternary ammonium salts, *Appl. Catal. A Gen.*, (**2014**), 488, 96–102.
[13] Y. Zhang, Y. Zhang, L. Wang, H. Jiang, C. Xiong, Coconut Shell Activated Carbon Supported Quaternary Ammonium for Continuous Cycloaddition of CO_2 and Biogas Upgrading in a Packed Bed, *Ind. Eng. Chem. Res.*, (**2015**), 54, 5894–5900.
[14] D.-W. Kim, D.-O. Lim, D.-H. Cho, J.-C. Koh, D.-W. Park, Production of dimethyl carbonate from ethylene carbonate and methanol using immobilized ionic liquids on MCM-41, *Catal. Today*., (**2011**), 164, 556–560.
[15] M. North, P. Villuendas, Influence of Support and Linker Parameters on the Activity of Silica-Supported Catalysts for Cyclic Carbonate Synthesis, *ChemCatChem*., (**2012**), 4, 789–794.
[16] L. Han, H.-J. Choi, D.-K. Kim, S.-W. Park, B. Liu, D.-W. Park, Porous polymer bead-supported ionic liquids for the synthesis of cyclic carbonate from CO_2 and epoxide, *J. Mol. Catal. A Chem.*, (**2011**), 338, 58–64.
[17] L. Yu, M. Kanezashi, H. Nagasawa, N. Moriyama, T. Tsuru, K. Ito, Enhanced CO_2 separation performance for tertiary amine-silica membranes via thermally induced local liberation of CH_3Cl, *AIChE J.*, (**2018**), 64, 1528–1539.
[18] A. Dioum, S. Hamoudi, Mono- and quaternary-ammonium functionalized mesoporous silica materials for nitrate adsorptive removal from water and wastewaters, *J. Porous Mater.*, (**2014**), 21, 685–690.
[19] Z. He, D. Liu, R. Li, Z. Zhou, P. Wang, Magnetic solid-phase extraction of sulfonylurea herbicides in environmental water samples by Fe_3O_4@dioctadecyl dimethyl ammonium chloride@silica magnetic particles, *Anal. Chim. Acta*., (**2012**), 747, 29–35.
[20] J. Liu, S. Ma, L. Zang, Preparation and characterization of ammonium-functionalized silica nanoparticle as a new adsorbent to remove methyl orange from aqueous solution, *Appl. Surf. Sci.*, (**2013**), 265, 393–398.
[21] O. Valdés, A. Marican, Y. Mirabal-Gallardo, L.S. Santos, Selective and efficient arsenic recovery from water through quaternary amino-functionalized silica, *Polymers (Basel).*, (**2018**), 10,.
[22] T. Bein, R.F. Carver, R.D. Farlee, G.D. Stuckyl, Solid-state ^{29}Si NMR and Infrared Studies of the Reactions of Mono- and Polyfunctional Silanes with Zeolite Y Surfaces, *J. Am. Chem. Soc*., (**1988**), 110, 4546–4553. papers2://publication/uuid/9C85CFF7-9A7D-4B67-A68F-8B57A58A1D60.
[23] https://xpssimplified.com/elements/bromine.php, (n.d.),.

CHAPTER VI

EPOXIDATION OF STYRENE AND ITS DERIVATIVES USING O_2 OR H_2O_2

(Work carried out in collaboration with Asma MAYOUFI (ATER), Ludivine K/BIDI (M2)

VI.1 Introduction

As previously described, the purpose of this thesis is to develop a catalytic system able to perform both a green epoxidation step and the cycloaddition reaction using CO_2. More precisely, the goal is to combine oxidation and cycloaddition steps that are independently efficient and make them work together in similar conditions (solvent, time, temperature, and pressure). Prior results described in the experimental chapter dealing with cycloaddition (**Chapter II**) report good conversion of styrene oxide into styrene carbonate with temperatures as high as 80°C after 3 to 23h, depending on the catalyst used. It was even stated that the combination of *n*-Bu_4NBr and Salophen-Me_2N-Cr was the best catalytic system, affording complete conversion with temperature of 50°C after 23h reaction. It is now envisaged to look at the feasibility, in our hands, of the epoxidation of styrene using O_2 or H_2O_2 with conditions (benzonitrile, 80°C, 3 to 23h and 11 bar of CO_2) compatible with those of most of our tests on CO_2 cycloaddition.

In the case of O_2 (first part of this chapter), commercially available ((S,S)-(+)-N,N'-bis(3,5-di-tert-butylsalicylidene)-1,2-cyclohexanedialinomanganese (III) chloride), also noted Mn(salen)Cl or Jacobsen catalyst, was chosen as a reference catalyst. Indeed, preliminary work on the epoxidation of styrene by O_2 using such catalyst was done previously in our group by C. Rocha [1] but here, we want to investigate in more details the impact of the catalyst, the solvent, the reductant quantity and the oxidant delivery mode targeting the parameters allowing an optimum conversion and selectivity towards the desired epoxide. Then, other Salen type catalysts, synthesized in **Chapter IV.2 and IV.3** will be tested such as Salophen-tBu-Cr, -Et_2N-Cr and -Me_2N-Cr.

In the case of H_2O_2 (second part of this chapter), R. Villanneau and F. Launay already have a good experience in the epoxidation of cycloalkenes catalyzed by soluble or supported polyoxometalates, but what about styrene? A polyoxometalate catalyst such as $(n\text{-}Bu_4N)_3NaH[As^{III}W_9O_{33}\{P(O)(CH_2CH_2\,CO_2H)\}_2]$, also named TBA_3NaH-(POM-CO_2H), has been efficiently used in the epoxidation reaction of cyclohexene and cyclooctene in the presence of a stoichiometric amount of aqueous (30 wt.%) H_2O_2.[2] A 89 % yield of cyclooctene oxide was reached after 6h in acetonitrile at 20°C, with a cyclooctene/catalyst molar ratio of 250. Supported catalyst was also obtained with an amide covalent grafting at the surface of silica

support. Reasonable 50% yield of cyclooctene oxide was obtained after 24h reaction at 50°C.[3] The aim of this second study is to adapt the reaction conditions to styrene, as well as α or β methyl-styrene.

With styrene as a substrate, the problem is that the epoxidation reaction is coupled with side reactions, including the oxidative cleavage of the C=C bond, which results in the formation of benzaldehyde (Figure 1). Our aim is to investigate how it is possible to maximize the formation of epoxide at the expense of benzaldehyde, while maintaining a high conversion to styrene.

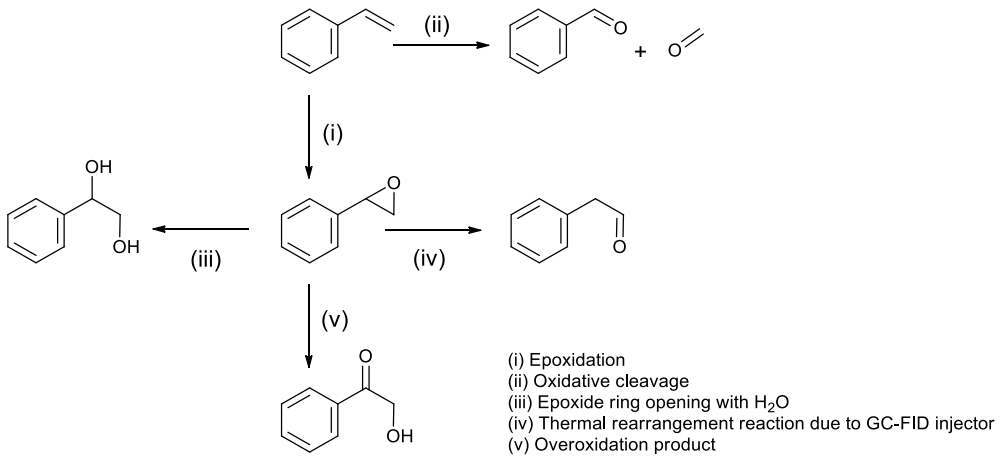

Figure 84: *Main epoxidation product and by-products obtained from styrene*

Other by-products may also appear such as styrene glycol and phenylacetaldehyde that are related to the hydrolysis or of the thermal degradation (GC analysis) of styrene oxide. Over-oxidation products are also possible as well as coupling products between the expected epoxide with the acid issued from the oxidation of the sacrificial reductant in the Mukaiyama route.

VI.2 Aerobic epoxidation

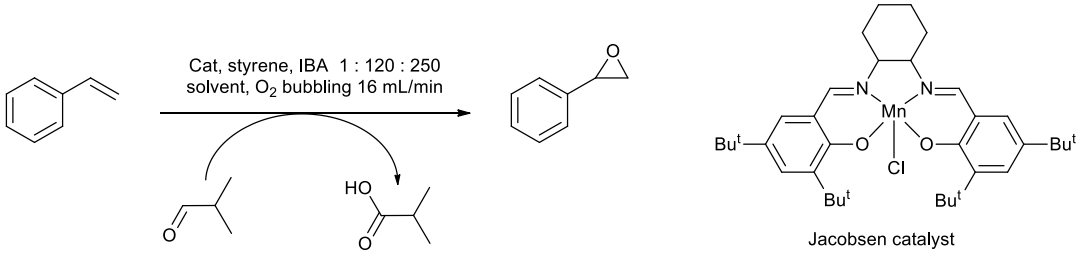

Figure 85: *Mukaiyama reaction experiment conditions and commercial Jacobsen catalyst*

Earlier C. Rocha showed in her thesis [1], that working, with Mn(salen)Cl, styrene and isobutyraldehyde with the following molar ratios 1 : 120 : 300 at a temperature of 80°C and an oxygen flow of 16 mL/min (**Figure 85**) afforded a good compromise between styrene conversion and styrene oxide yield. Under these conditions, the maximum selectivity in styrene oxide was about 55 % which is far from being sufficient for an overall process targeting the transformation of styrene into styrene carbonate. However, from our literature survey, it is noteworthy that some authors have reported in the literature styrene oxide yields up to 100% using the Mukaiyama approach for aerobic epoxidation, thus encouraging us to investigate a little bit more this system, looking for example at the influence of the catalyst and of the temperature. The typical procedure is as follows:

***Experimental conditions**: Styrene (St, 1 mL, 8.7 mmol), catalyst (Mn(salen)Cl, 46 mg, 72.4 µmol), isobutyraldehyde (IBA, 2 mL, 22 mmol), the GC internal standard (p-xylene, 1 mL, 8 mmol) and benzonitrile (solvent, 20 mL) were mixed in a round-bottom flask connected to a condenser at room temperature. Then, the mixture was heated at 80°C before introducing 16 mL/min of dioxygen through the solution. The reaction medium was stirred for 3h and the O_2 flow kept constant at all times of the experiment.*

VI.2.1 Impact of the catalyst and of the temperature

In order to elucidate the role of manganese and of the temperature in this reaction, a series of six experiments were carried out at 80, 60 and 50°C in the presence or in the absence of the catalyst, keeping all the other parameters constant.

At 80°C without any catalyst, surprisingly, the conversion of styrene was 84% and the yield of styrene oxide 65%. Benzaldehyde (15%) and styrene glycol (2%) were also found and the carbon balance was almost 100%. When Mn(salen)Cl was introduced, up to 99% of styrene was converted (**Figure 86_CAT_80°C**) but without affecting significantly the yields of styrene oxide and benzaldehyde compared to the blank test (**Figure 3_NO_CAT_80°C**). Only the yields of styrene glycol and other by-products increased to 10%.

The same pattern repeats itself for the experiments done at 60°C (**Figure 86_NO_CAT_60°C** and **Figure 86_CAT_60°C**). Again, styrene oxide and benzaldehyde were formed in the absence of Mn(salen)Cl and their yields were not improved after its addition. Only the overall styrene conversion increased in the presence of the catalyst leading to more styrene glycol and other by-products.

A significant influence of Mn(salen)Cl on the yield of styrene oxide (and of benzaldehyde) was observed only at 50°C. Without Mn(salen)Cl, the overall conversion of styrene was as low as 56% with a styrene oxide yield of 20% (**Figure 86_NO_CAT_50°C)** with a 20% loss of carbon balance. However, it is noteworthy that the introduction of Mn(salen)Cl at 50°C Figure **86_CAT_50°C)** afforded results very similar to those obtained at 60 and 80°.

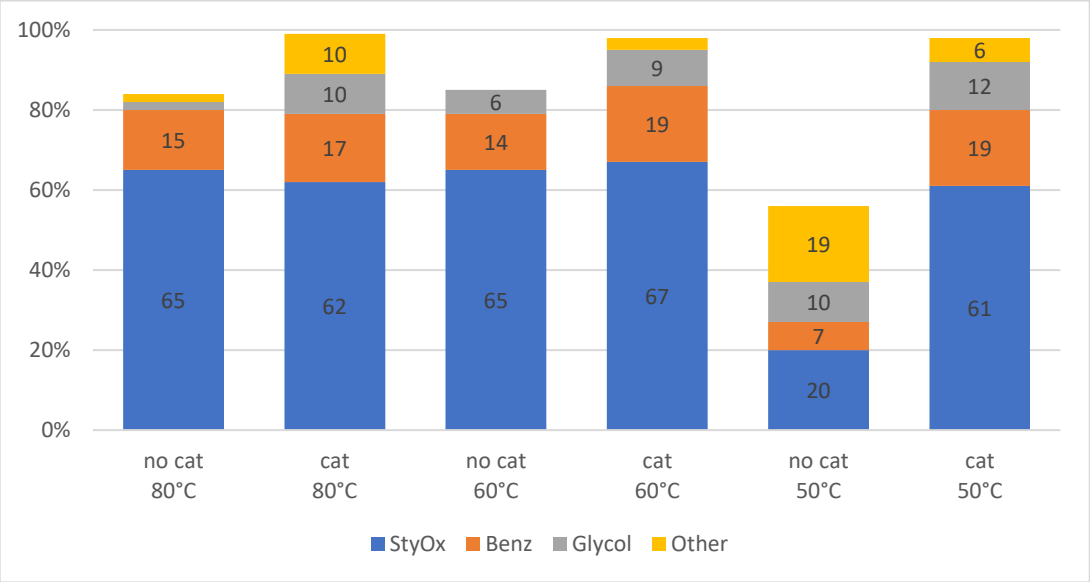

Figure 86: *Influence of the catalyst and of the temperature on the products yields and distribution obtained in the aerobic epoxidation of styrene. (Cat : styrene : IBA 1 : 120 : 300, O_2 bubbling 16 mL/min, 0.435M of styrene in PhCN, 3h)*

Such results mean that Mn(salen)Cl will be of greater help when considering the whole conversion of styrene into styrene carbonate at 50°C. Otherwise (60 or 80°C), it is possible that the "apparently" constant yield of epoxide and the increase of styrene glycol with the catalyst at a given temperature would be the consequence of a facilitated ring opening of the epoxide as the result of the Lewis acidity of Mn(salen)Cl.[4] We hope that such side-reaction involving water affording styrene glycol could be reduced in the presence of *n*-Bu_4NBr and CO_2 present in the whole transformation. Epoxidation tests described thereafter will be performed at 80°C since reasonably fast CO_2 cycloaddition reactions onto styrene oxide occurred at this temperature in the previous chapter.

VI.2.2 Impact of the solvent

In the very early work of Mukaiyama and co-workers, aerobic epoxidations were carried out in halogenated solvents. Later, acetonitrile was introduced due to its greener properties and its well-known resistance to oxidants. Unexpected above-mentioned results obtained in the absence of catalyst led us to question the role of benzonitrile itself. As a matter

of fact, a series of tests including Mn(salen)Cl was carried out here between 50 and 80°C with acetonitrile (ACN) and 1,2-dichloroethane (DCE) at 80°C in order to be compared with others carried out in the temperature range of 40-80°C(**Figure 87**). All experiments were performed during 3h.

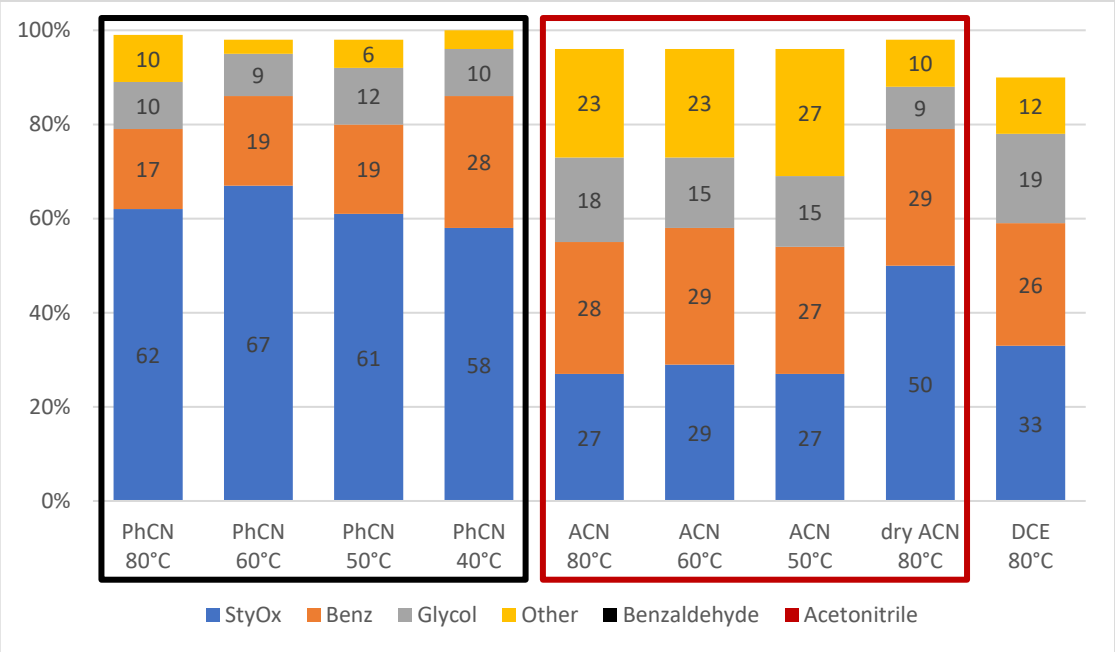

Figure 87: *Influence of the solvent and of the temperature on the products yields and distribution obtained in the aerobic epoxidation of styrene. (Cat : styrene : IBA 1 : 120 : 300, O_2 bubbling 16 mL/min, 0.435M of styrene in PhCN, 3h)*

Within the first series of tests performed using benzonitrile between 40 to 80°C (**Figure 87_PhCN** experiments), the maximum yield of styrene oxide was obtained at 80°C with 68% of selectivity while the lowest one was reached at 40°C (58% of selectivity). Benzaldehyde arising from the oxidative cleavage of the carbon-carbon double bond was favoured at lower temperature while higher temperatures led to the apparent conversion of benzaldehyde and styrene oxide into unknown compounds.

In the case of ACN, the distribution of the products was significantly different from that obtained with benzonitrile. A greater proportion of benzaldehyde (multiplied by *c.a.* 1.5 in ACN), styrene glycol (multiplied by *c.a.* 1.2 at 50°C to 1.8 at 80°C) and important amounts of other compounds (multiplied by *c.a.* 4.5 at 50°C to 2.3 at 80°C) could be emphasized (**Figure 87_ACN** *vs*. **Figure 87_PhCN**) while the styrene oxide yield was divided by c.a. 2.2-2.3 whatever the temperature considered. The higher hydrophilicity of ACN compared to benzonitrile led us to suspect that the higher yields of glycol obtained in acetonitrile would be related to the higher water content of this solvent. An experiment was thus conducted using

freshly distilled instead of non-treated ACN (**Figure 87_dryACN_80°C**). Indeed, as expected, the yield of styrene glycol could be divided by 2 but, more spectacularly the yield of styrene oxide was multiplied by 1.8 (from 27% with non-treated ACN (**Figure 87_ACN_80°C**) to 50% with dry CAN at 80°C (**Figure 87_dryACN_80°C**)). Excepted for styrene oxide and benzaldehyde, the yields of other products were very similar in benzonitrile and in dry acetonitrile at 80°C. Significant increase of the benzaldehyde yield in acetonitrile was confirmed (almost the same with non-treated and dry ACN), thus emphasizing the more important role of the nitrile itself (than water) in the selectivity of the aerobic oxidation reaction. The higher yield of styrene oxide in benzonitrile (62%) compared to dry acetonitrile (50%) at 80°C could be also another indication of the intrinsic role of the nitrile in the oxidation process.

A last test performed in the presence of non-distilled DCE (dichloroethane) at 80°C (**Figure 87_DCE_80°C)** led to a product distribution very similar to that obtained with non-distilled ACN (**Figure 87_ACN_80°C**).

In conclusion, our results show that the best compromise between high conversion of styrene and high selectivity of styrene oxide is reached in benzonitrile at 60 or 80°C, but the later temperature is more suitable for the whole process, from styrene to styrene carbonate. By then, future experiments will be conducted in benzonitrile only.

VI.2.3 Impact of the amount of reducing agent

A new series of eight experiments was conducted with different amounts of sacrificial reductant (0, 1, 2.5 or 5 molar equivalent(s) of isobutyraldehyde, IBA) at 80°C in the absence or presence of Mn(salen)Cl (see experimental details below).

***Experimental conditions**: Styrene (St, 1 mL, 8.7 mmol), Mn(salen)Cl (46 mg, 72.4 µmol), isobutyraldehyde (IBA, 0 to 4 mL, 0 to 44 mmol), the GC internal standard (p-xylene, 1 mL, 8 mmol) and benzonitrile (20 mL) were mixed at room temperature in a round-bottom flask connected to a condenser. Then, the mixture was heated under 80°C and 16 mL/min of dioxygen were bubbled through the solution. The reaction medium was stirred under these conditions for 3h and the O_2 flow was kept constant during all the experiment.*

In the absence of sacrificial aldehyde, no reaction occurred with (**Figure 88_CAT_0EQ**) or without (**Figure 88_NoCAT_0EQ**) Mn(salen)Cl meaning that the aldehyde is the essential component of the system.

In the presence or absence of catalyst, we showed earlier that, at 80°C, with a reducing agent/styrene molar ratio of 2, the yields of styrene oxide and benzaldehyde were very similar. The same occurred here for IBA/Styrene ratios of 1 and 2.5. Best results were observed for 2.5 equivalent of IBA added. Without Mn(salen)Cl, the yield of styrene oxide was 65% and with Mn(salen)Cl, 62%. It can be noted that the proportion of by-products is higher in the presence of catalyst. A decrease of styrene oxide yield and an increase of by-product proportion was observed at high IBA equivalent of 5 (see **Figure 88_CAT_5EQ**).

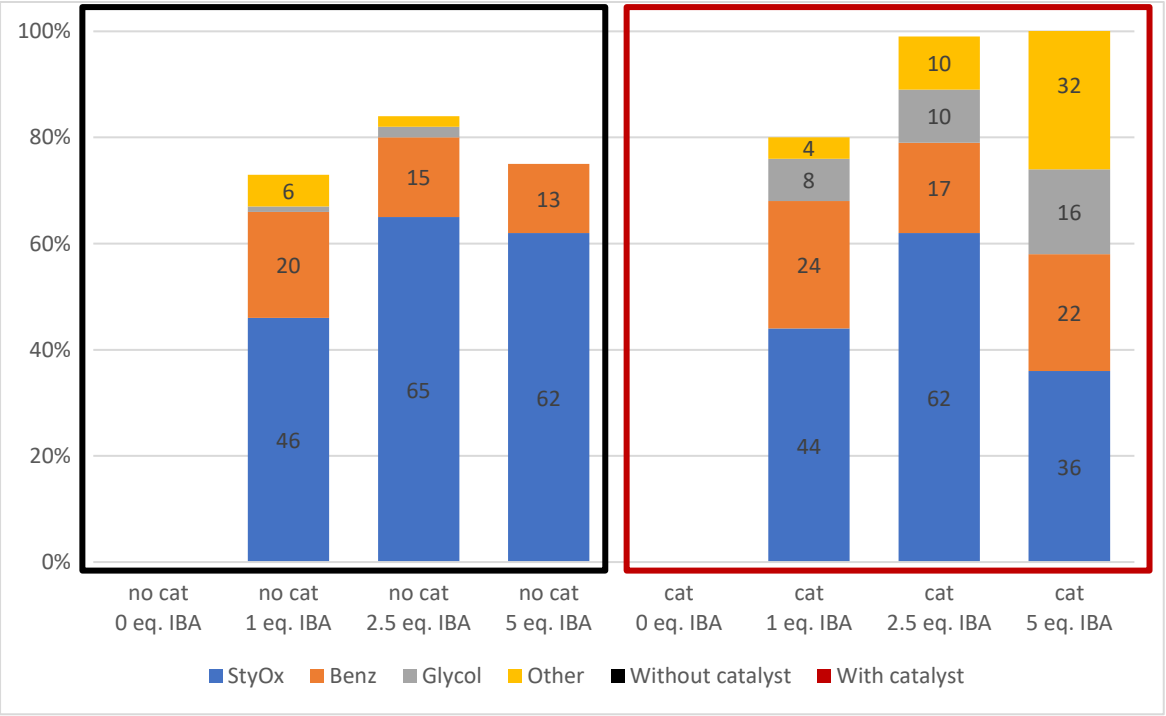

***Figure 88**: Influence of the amount of sacrificial reductant and of the catalyst on the products yields and distribution obtained in the aerobic epoxidation of styrene. (Cat : styrene : IBA 1 : 120 : 300, O_2 bubbling 16 mL/min, 0.435M of styrene in PhCN, 80°C, 3h)*

In conclusion, best results were found with 2.5 equivalents of sacrificial reductant IBA. It is expected that side-reactions related to the Lewis acidity of the catalyst and leading to the opening of the oxirane ring will be replaced by in-situ CO_2 cycloaddition in the whole transformation process. Future experiments will then be conducted in benzonitrile with optimal IBA molar quantity of 2.5.

VI.2.4 Impact of the oxygen supply

Positive results obtained in the absence of any catalysts led us to question the influence of oxygen introduction (method and amount). Above experiments were performed using bubbling with a metal needle (**c** case) with a flow of 16 mL/min. One hypothesis dealt with the possible involvement of soluble metal species issued from the corrosion of the needle. One way to avoid such corrosion was to replace the metal needle by a special glassware (**a** case). Another hypothesis concerned the flow rate and the O_2 concentration in the reaction solution leading us to test a gas flow over the solution (**b** case) instead of bubbling. Last but not least, with the goal of performing the whole process under static pressurized and not flowing O_2 and CO_2 gases, it was also important to test the aerobic epoxidation alone in an autoclave (**d** case).

To summarize, in this part, as shown in **Figure 89**, four modes of oxygen introduction were investigated using either a glass tube dipping inside (**a**) or located above the surface of the solution (**b**) or a metal needle dipping in the solution (**c**) or using an autoclave filled by 3.5 bar of O_2 at 80°C(**d**).

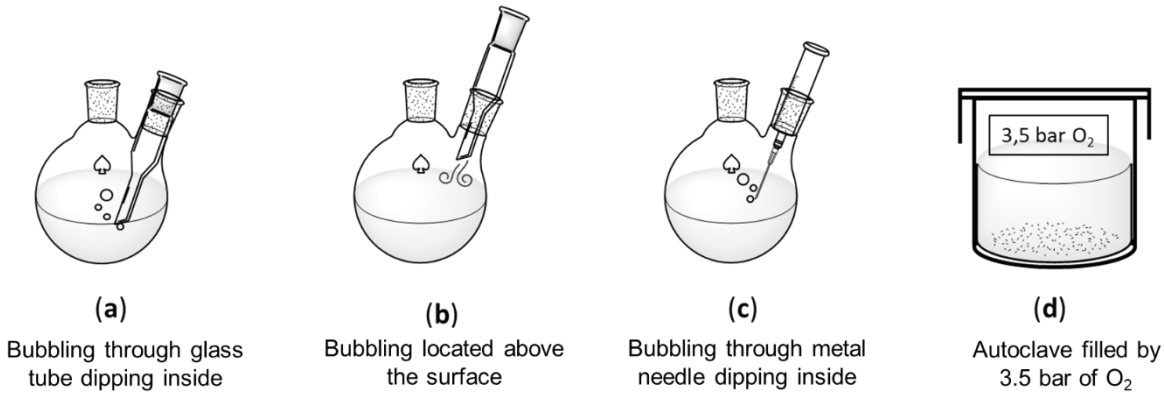

Figure 89: *Test of different forms of oxygen supply for the aerobic epoxidation of alkenes*

Modifications of the experimental procedures depending on the case studied are described below and the results reported in **Figure 90**.

***Experimental conditions**: Styrene (1 mL for experiments **a,b,c** : 8.7 mmol or 0.645 mL for experiment **d**: 5.6 mmol), Mn(salen)Cl (72.4 µmol for experiments **a,b,c** or 48.1 µmol for experiment **d**), isobutyraldehyde (IBA, 2 mL, 22 mmol for experiments **a,b,c** or 1.33 mL for experiment **d**), the GC internal standard (p-xylene, 1 mL, 8 mmol for experiments **a,b,c**; or 0.665 mL for experiment **d**) and benzonitrile (20 mL for experiments **a,b,c**; or 13 mL for experiment **d**) were mixed in a reactor (round-bottom flask connected to a condenser for experiments **a,b,c** or autoclave for experiment **d**) at room temperature. In the case of experiments, **a,b,c**, the mixture was heated under 80°C and dioxygen was then bubbled (16 mL/min). The reaction was stirred under these conditions of 3h (from the time of O_2 introduction) and the O_2 flow was kept constant during all the experiment. In the case of experiment **d**, the reactive medium was sealed inside 3.5 bar O_2 pressure (11.6 mmol) then heated at 80°C.*

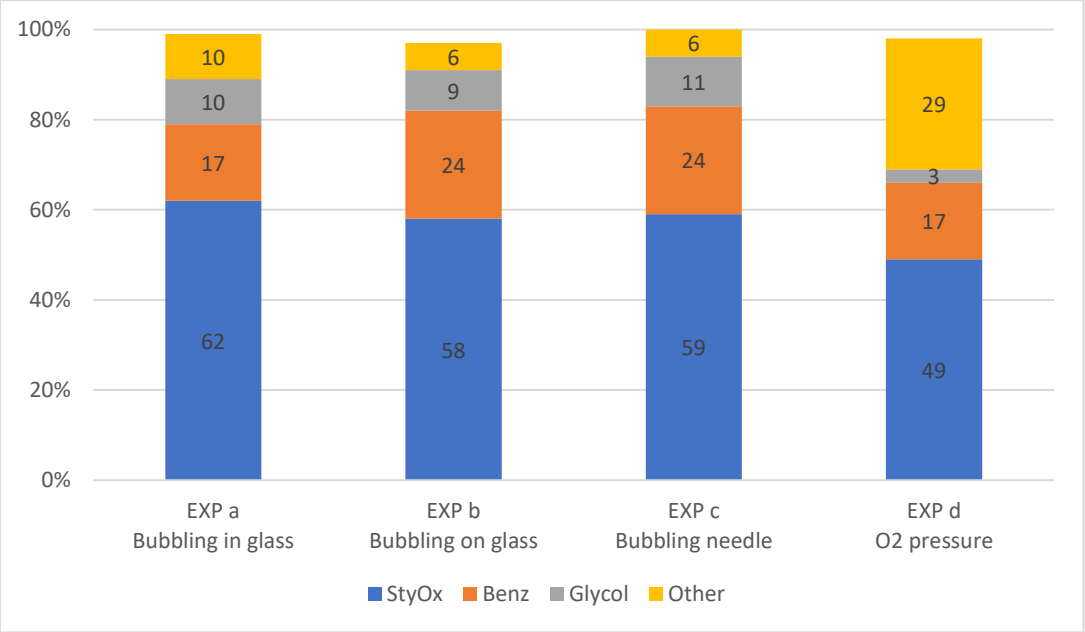

***Figure 90:** Influence of the oxidant supply on the products yields and distribution obtained in the aerobic epoxidation of styrene. (Cat : styrene : IBA 1 : 120 : 300, O_2 bubbling 16 mL/min or 3,5 bar, 0.435M of styrene in PhCN, 80°C, 3h)*

In the experiments **a** and **b** performed under O_2 flow at atmospheric pressure, the distribution of the different products was not modified compared to the experiment **c** (high conversion, *c.a.* 60% yield of styrene oxide, *c.a.* 20% yield of benzaldehyde and *c.a.* 10% yield of styrene glycol with *c.a.* 10% of by-products). Apparently, the method used for dioxygen introduction at atmospheric pressure does not seem to significantly alter the results obtained, thus helping us to discard hypotheses such as metal contamination of the reaction medium or the use of too high amounts of O_2 in the experiment **c**.

In the case of the experiment **d,** conducted under 3.5 bar of O_2 inside a sealed reactor, (**Figure 90_EXP_d**), significant differences compared to runs in **a**, **b** and **c** conditions were observed. Even if the conversion remains pretty high (98%), a decrease of styrene oxide yield (from 60 (average value for **a**, **b** and **c)** to 49%) as well as a decrease of the carbon balance could be emphasized.

Experiments (**a**, **b** and **c**) performed under O_2 flow at 16 $mL.min^{-1}$ were quite reproducible and did not depend on bubbling or on the material used for O_2 introduction. However, the results obtained under static conditions were different but it has to be noted that any attempt of optimization was performed.

VI.2.5 Impact of the catalyst

In this work, other Salen complexes, especially those with chromium (Salophen-tBu-Cr, Salophen-Et_2N-Cr and Salophen-Me_2N-Cr, see **Chapters IV.2 and IV.2**) have been designed in order to improve the cycloaddition reaction performances, but are these complexes, used in the same amounts, also efficient in the frame of the Mukaiyama epoxidation of styrene at 80°C during 3h in benzonitrile with 2.5 mol of IBA per mol of alkene and under 16 mL/min of O_2 bubbling? A series of experiments was carried out with the chromium complexes, as shown below and the results compared with those obtained with the Jacobsen catalyst in **Figure 91**.

***Experimental conditions**: Styrene (1 mL, 8.7 mmol), catalyst (72.4 µmol), isobutyraldehyde (IBA, 2 mL, 22 mmol, 2.5 eq. per styrene), GC internal standard (p-xylene, 1 mL, 8 mmol) and benzonitrile (20 mL) were mixed at room temperature in a round-bottom flask connected to a condenser. Then, the mixture was heated at 80°C and 16 mL/min of dioxygen were bubbled into the solution when the desired temperature was reached. The reaction mixture was stirred under these conditions for 3h (from the time of O_2 introduction) and the O_2 flow was kept constant at 16 mL/min during all the experiment.*

Salophen-tBu-Cr (**Figure 91_tBu_Cr**) led to a similar overall conversion of styrene with a decrease of styrene oxide yield (from 62 to 48%) and an increase of styrene glycol from 10 to 20%. Apparently, Cr(III) would further promote the cleavage of the oxirane ring through hydrolysis compared to Mn(III).

On the other hand, a decrease of the overall conversion and of the styrene oxide yield was always observed when using Salophen-Et_2N-MCl or Salophen-Me_2N-MCl, with M = Cr or Mn, (**Figure 91**). It has to be noted that, compared to t-Bu in 3,5 positions, the -Et_2N or -Me_2N

substituents in 4 position do not favour the epoxidation over the oxidative cleavage of the C=C bond. Indeed, the (epoxide+styrene glycol)/benzaldehyde molar ratio was close to 4 with the Jacobsen catalyst and Salophen-tBu-Cr while it was about 2.5-3 with the other complexes bearing Et_2N or Me_2N substituents.

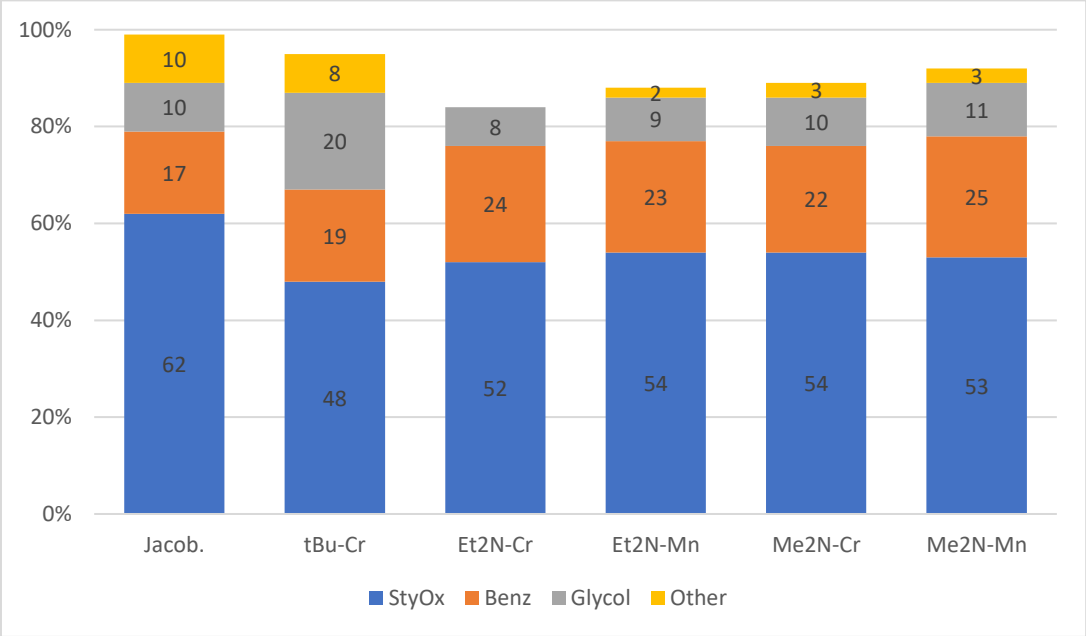

***Figure 91**: Influence of the catalyst nature on the products yields and distribution obtained in the aerobic epoxidation of styrene. (Cat : styrene : IBA 1 : 120 : 300, O_2 bubbling 16 mL/min, 0.435M of styrene in PhCN, 80°C, 3h)*

VI.2.6 Conclusion

Epoxidation of styrene was successfully conducted under Mukaiyama conditions using a 16 $mL.min^{-1}$ O_2 flow and IBA as an electron source at 80°C. With a 100% conversion of styrene, best styrene oxide yields were about 62-67% with the Jacobsen catalyst with the unavoidable formation of benzaldehyde (*c.a.* 20%) and styrene glycol (*c.a.* 10%) to a lesser extent. Optimum conditions involved the use of 2.5 eq of IBA per styrene molecule but, overall, of a convenient solvent such as benzonitrile whose intrinsic properties are determining to favour epoxidation over the C=C cleavage. Our study emphasized the very important influence of the aldehyde since in the absence of the later, no reaction occurred. On the other hand, the catalyst was shown to be useful at 50°C but its role appeared to be less crucial at 80°C, the temperature targeted for the whole conversion process of styrene to styrene carbonate in the presence of O_2 and CO_2. However, at 80°C, Salen complexes with tBu groups led to a more selective formation of styrene oxide (and glycol) than benzaldehyde

compared to others bearing amino substituents. At 80°C, the catalysts seemed to be responsible of an increase of the styrene conversion but the styrene oxide yield did not increase as the result of the in-situ hydrolysis of the epoxide encouraged by the Salophen complexes, especially those involving Cr(III).

VI.3 Epoxidation using H_2O_2

As reported in **Chapter I**, many times, polyoxometalates (POMs) [5,6] were shown to be efficient catalysts for H_2O_2-based oxidations. In the past, our group has synthesized lacunary hybrid polyoxometalates deriving formally from the Keggin structure that are efficient in the epoxidation of cycloalkenes by H_2O_2 under mild conditions and that can be grafted, thus affording supported homogeneous catalysts[2].

The aim of this part was to test these catalysts in the epoxidation of styrene by H_2O_2 instead of endocyclic alkenes like cyclooctene or cyclohexene which are more frequently used as models for the epoxidation reaction. One important question to answer concerned the epoxide/benzaldehyde/styrene glycol selectivity. Could it be different from that obtained using the Mukaiyama system? First, the synthesis of several POM catalysts will be described, and their catalytic activity will be further developed regarding the epoxidation reaction of alkenes. Styrene and its methyl substitutes α-methyl and β-methyl styrene will be tested in an attempt to reduce the proportion of secondary product benzaldehyde and glycol at the end. Process optimisation will also be studied by varying parameters such as the quantity of catalyst or oxidant as well as their delayed addition in the reactive medium.

VI.3.1 Synthesis and characterisation of $[As^{III}W_9O_{33}\{RP=O\}_2]^{5-}$ compounds

Two different species of general formula $[As^{III}W_9O_{33}\{RP=O\}_2]^{5-}$, *i.e.* POM-tBu and POM COOH (**Figure 92**) were synthesized starting from $Na_8[HAsW_9O_{33}].14H_2O$, tetra-n-butylammonium bromide (TBABr) and the corresponding phosphonic acids $(RP=O(OH)_2)$.

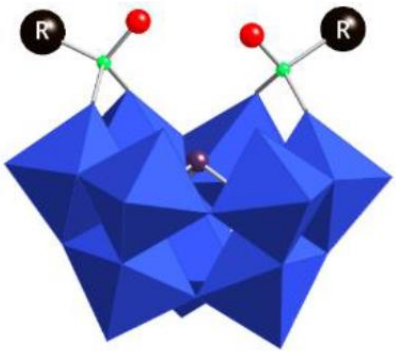

R = -^{t}Bu, -COOH

Figure 92: *Series of hybrid polyoxometalates ($[As_{III}W_9O_{33}\{P(O)tBu\}_2]^{5-}$ and $[As^{III}W_9O_{33}\{P(O)CH_2CH_2COOH\}_2]^{5-}$) synthesized from $Na_8[HAsW_9O_{33}].14H_2O$. WO_6 polyhedra are shown in blue and As, P, O and C atoms are shown, respectively, in prune, blue, red, and black*

The experimental procedure followed is reported below:

Synthesis of $[As^{III}W_9O_{33}\{RP=O\}_2]^{5-}$ compounds. $Na_8[HAsW_9O_{33}].14H_2O$ (1.39 mmol, 1 eq), Bu_4NBr (5.56 mmol, 4 eq) and $(OH)_2P(O)R$ (2.78 mmol, 2 eq) are dissolved in 30 mL of acetonitrile. Then, HCl (5.56 mmol, 4 eq) was added dropwise. The resulting reaction mixture was stirred overnight at reflux and then the suspension was hot-filtered (frit glass 4). Later, the filtrate was evaporated under vacuum to give a yellow oil. $[As^{III}W_9O_{33}\{RP=O\}_2]^{5-}$ with its ammonium counter-ions was precipitated by adding ethanol and diethyl ether, then the resulting white solid was washed with water, ethanol, and diethyl ether. After vacuum drying, the solid was weighed and characterized. **For all products**, the ^{1}H NMR (500 MHz, $CDCl_3$) signals of tetrabutylammonium are: 3.14 – 3.12 (m, 24H) ; 1.64 – 1.61 (m, 24H) ; 1.42 – 1.35 .(m, 24H) ; 0.99 – 0.96 (t, 36H). **POM-tBu** (**1**): ^{1}H NMR (500 MHz, $CDCl_3$): 1.28 (s, 9H) ; 1.24 (s, 9H). RMN ^{31}P (δ ppm): 33.05 (s). **POM-COOH** (**2**): ^{1}H NMR (500 MHz, $CDCl_3$): 2.90 – 2.70 (m, 2H); 2.30 – 2.18 (m, 2H). ^{31}P NMR (δ ppm): 26.01 (s).

Depending on the POM, yields varied between 46% (POM-*t*Bu) and 88% (POM-COOH) as seen in **Table 29**.

Table 29*: Yields and molecular weights of POMs synthesized*

POMs		M (g.mol^{-1})	Yield (%)
$(TBA)_3NaH[As^{III}W_9O_{33}\{P(O)tBu\}_2]^{5-}$	POM-tBu	3217.18	46
$(TBA)_3NaH[As^{III}W_9O_{33}\{P(O)CH_2CH_2COOH\}_2]^{5-}$	POM-COOH	3249.95	88

It should be noted that POM-COOH (**2**) was proposed by Villanneau and Launay for covalent anchoring (amide bond) on SBA-15 silica functionalized by aminopropyl groups.[7]

VI.3.2 Catalytic activity

Here, it was decided to investigate the epoxidation of styrene as well as α-methyl styrene and β-methyl styrene by H_2O_2 in the presence of the above-mentioned POMs. As shown earlier in **Chapter I**, several solvents can be used (EtOH, DCM) but acetonitrile leads to a better conversion and remains the most common solvent regardless of the catalysts described in the literature. Often reactions described are working at room temperature or at 50°C for short reaction times (4 h to 24 h). From our bibliographical survey, it appears that the order of reactivity is: β-methyl styrene > styrene > α-methyl styrene. In addition, differences in epoxidation kinetics have been highlighted in particular between *trans*- and *cis*-β-methyl styrene, the *cis* isomer reacting more rapidly and leading more selectively to the epoxide than the former.

The molecules expected during these reactions are the epoxides, but other products may also be formed arising from the oxidative cleavage of the alkenes, opening of the epoxides by water leading to the corresponding diol. Some epoxides can also undergo a Meinwald rearrangement [8–11]. In the present work, all aliquots of the reaction media were analysed by gas chromatography coupled with a flame ionization detector using a calibration curve with p-xylene as the internal standard. Volatile molecules resulting from the oxidative cleavage of alkenes, such as acetaldehyde and formaldehyde, could not be quantified. The catalysis tests were first carried out in acetonitrile and then in benzonitrile, which is currently the solvent used in our group for the cycloaddition reaction.

VI.3.3 Oxidation in acetonitrile

After various tests (variation of the amount of H_2O_2, the temperature and of the catalyst precursor), only few differences were found between the results obtained with POM-tBu and POM-COOH. In this matter, results obtained with POM-tBu only will be discussed in this section.

VI.3.3.1 Case of styrene

Styrene oxidation in the presence of POM-tBu was carried out at 50°C and in the presence of one equivalent of H_2O_2.

***Experimental conditions**: Styrene (0.69 mL, 6 mmol), catalyst (24 µmol), GC internal standard (p-xylene, 0.75 mL, 6 mmol) and dry ACN (20 mL) were mixed at room temperature in a round-bottom flask connected to a condenser. Then, the mixture was heated at 50°C and 6 or 12 mmol of H_2O_2 was added (0.6 or 1.2 mL) into the solution when the desired temperature was reached and when the catalyst was completely dissolved. The reaction mixture was stirred under these conditions for a certain amount of time (from the time of H_2O_2 introduction). For GC-FID analyses, 20 µL of reagent medium was taken and diluted in 10 mL of HPLC-grade dichloromethane.*

Conversion of styrene and the yields of the reaction products over time (up to 48 h) are displayed in the graph below (**Figure 93**). Styrene oxide, benzaldehyde, and styrene glycol were systematically obtained. In addition, 2-hydroxy-1-phenylethanone arising from over-oxidation of styrene glycol could be detected in small quantities by GC-FID and identified by GC-MS, as well as phenylacetaldehyde arising from the Meinwald rearrangement of styrene oxide. These two products correspond to the "other" category in Figure 10.

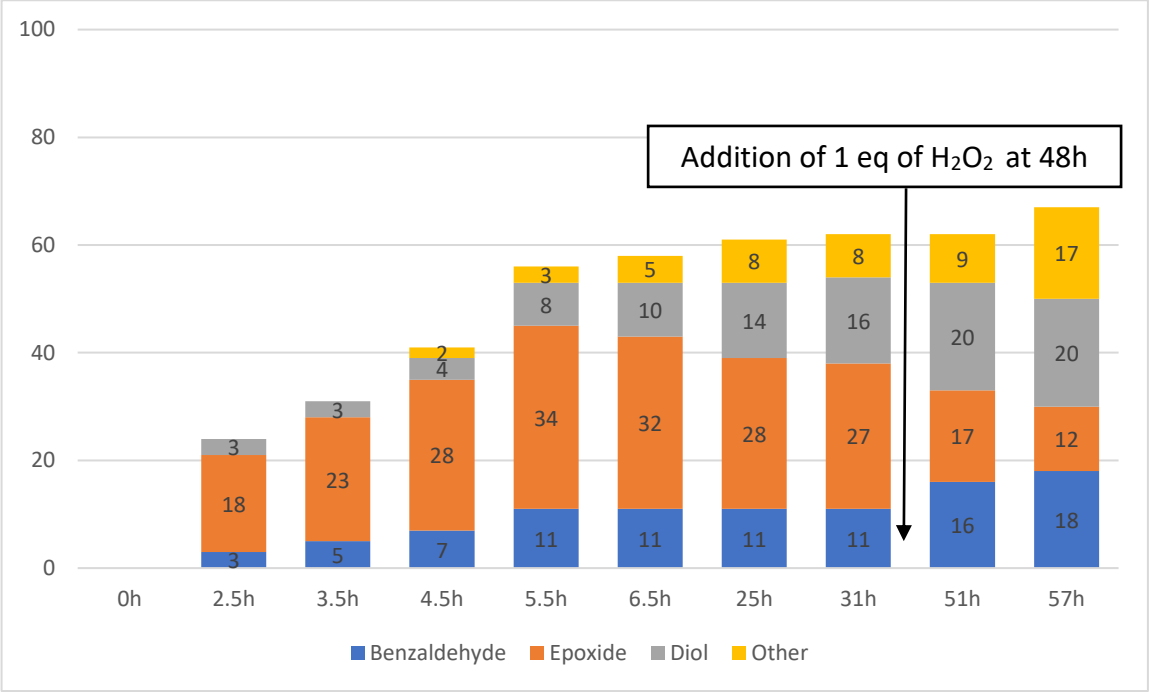

***Figure 93:** Kinetic profile of the products yields during styrene epoxidation by H_2O_2 in the presence of POM-tBu (catalyst/substrate/H_2O_2: 1/250/250 then 1/250/500 after addition of the second equivalent of H_2O_2, 50°C).*

Styrene oxide was clearly the major product with a maximum yield of 34% after 5.5 h before slowly decreasing from 5.5 h to 31 h. Meanwhile, the yield of benzaldehyde increased very slowly reaching a "plateau" of 11% after 25h. Clearly, the yield of styrene glycol increased gradually throughout the test and continued to increase as the amount of styrene oxide decreased. The maximum conversion of styrene (*c.a.* 60%) was reached after 6 h, probably as the result of a defect in hydrogen peroxide due to its dismutation. After, there was clearly a

re-distribution of styrene oxide into styrene glycol and other by-products. It has to be noted that the epoxide + styrene glycol / benzaldehyde ratio tends to 3.8.

A second equivalent of H_2O_2 was added at t = 48h in order to restart the reaction. In spite of what was expected, the styrene conversion changed very little afterwards for the next 9h reaction. Instead, the overall yield of styrene oxide decreased to 12%! At 57h, the epoxide + diol / benzaldehyde ratio was 1.8 as the result of the increase of benzaldehyde and the hydrolysis of styrene oxide and more probably its over-oxidation. The most likely hypothesis would be that the catalyst was modified in the first 48h. The appearance of an unidentified white solid after a few hours of reaction seems to confirm such evolution.

VI.3.3.2 Cases of α and or β methyl-styrene

α- and β-methyl styrene were also tested with the following catalyst/substrate/H_2O_2 ratio: 1/250/250 at 50°C (See experimental conditions for styrene).

In addition to the epoxide, the expected products that can be detected by GC in the case of α-methyl styrene (**Figure 94**) are acetophenone arising from the oxidative cleavage of the exocyclic double bond and α-methyl styrene glycol.

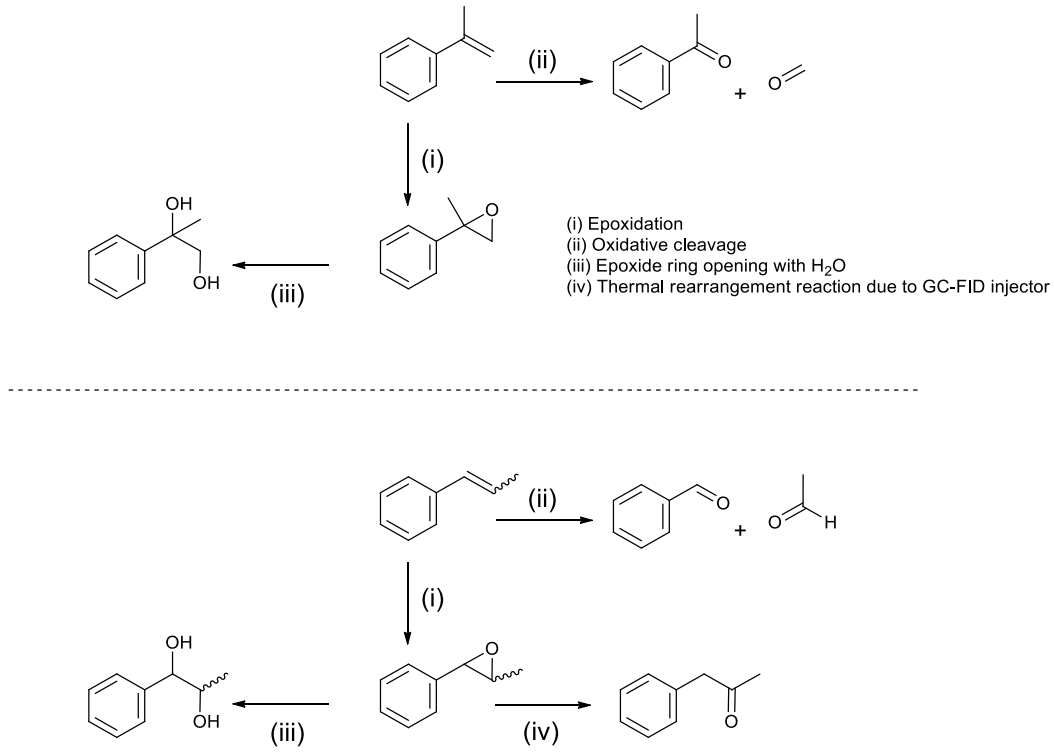

Figure 94: *Main oxidation products obtained from α and β methyl-styrene*

In the case of β-methyl styrene, it should be noted that a mixture of *trans*- and *cis*-β-methyl styrene has been used, and the epoxidation led to the two corresponding epoxides but also to the two diols as well. Similarly, to styrene oxide, β-methyl styrene oxides also partially isomerized (in the GC injector), thus affording phenylacetone. Oxidative cleavage of the exocyclic double bond led to the formation of benzaldehyde, as with styrene (**Figure 94**).

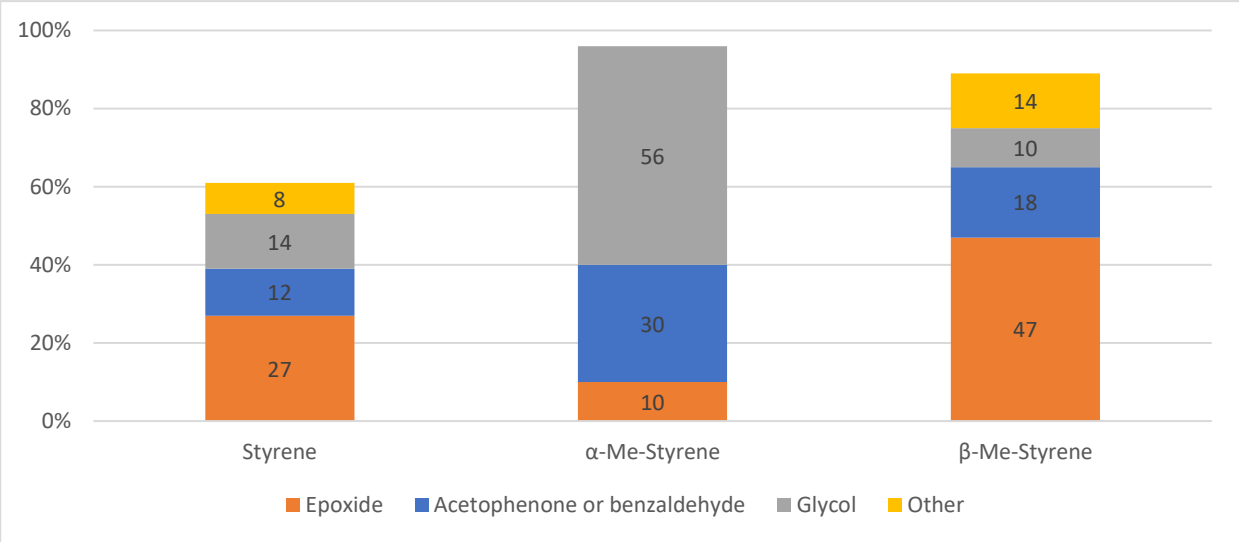

Figure 95: *24 h yields of the different products obtained in the oxidation of styrene, α-methystyrene and β-methylstyrene by H_2O_2 at 50°C (catalyst/substrate/H_2O_2 ratio: 1/250/250).*

Comparing the results obtained for α-, β-methyl styrene and styrene at 50°C (**Figure 95**), it can be stated that the alkene conversion measured after 24 h increased from 60% for styrene to 95% for α-methyl styrene and 90% for the mixture of the mixture of β-methyl styrene. The yields of the corresponding epoxides ranged from 47% for the mixture of trans- and cis-β-methyl styrene, 27% for styrene and only 10% for α-methyl styrene! It seems in this latter case that the epoxide was very sensitive to water since the amount of glycol was found to be very important compared to β-methyl styrene and styrene oxidations. Finally, 10% and 14% of trans- and cis-β-methyl styrene are converted into diol and unknown molecules.

VI.3.4 Oxidation in benzonitrile

Benzonitrile was also used as a solvent in the epoxidation of styrene and β-methyl styrene in the presence of POM-COOH (**Figure 96**).

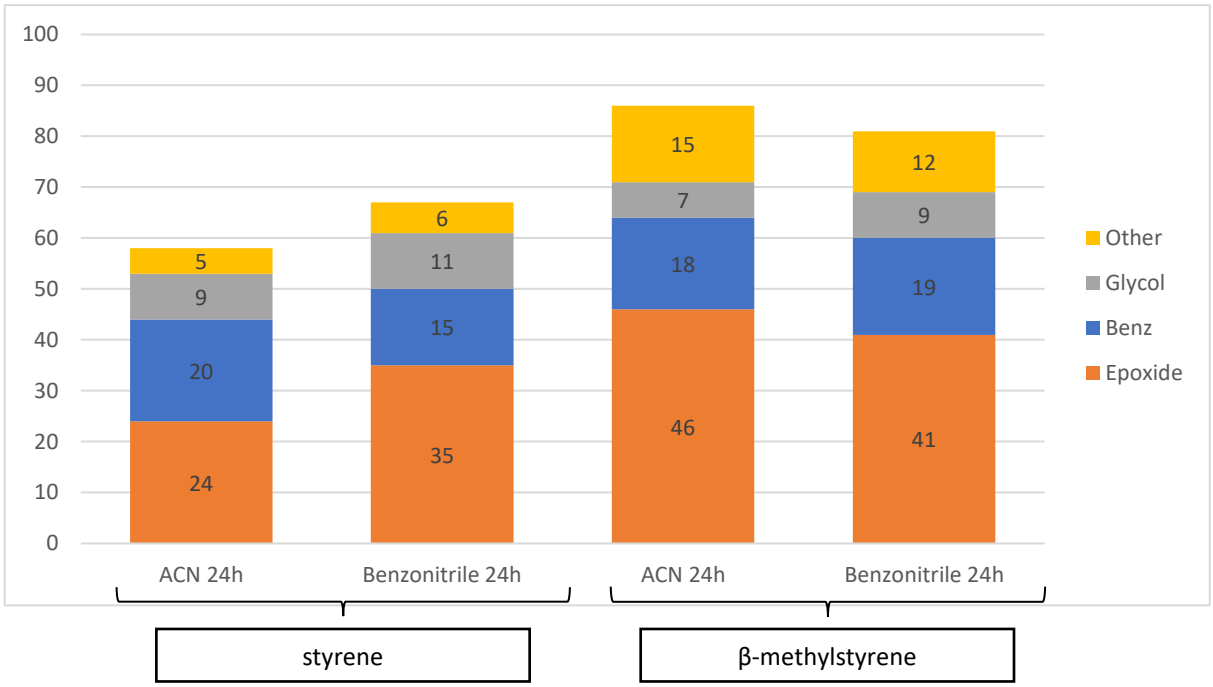

Figure 96: *Influence of the solvent (acetonitrile vs. benzonitrile) on the oxidation of styrene and β-methylstyrene after 24h at 50°C (ratio POM-COOH catalyst/substrate/H_2O_2 : 1/250/250).*

Clearly, the products were similar in acetonitrile and benzonitrile under identical operating conditions (50°C, POM-COOH catalyst/substrate/H_2O_2 ratio: 1/250/250, 24h). Regardless of the solvent used, the epoxides remained the major products for both substrates.

In the case of styrene, a small but significant improvement was noticed in conversion (65% in benzonitrile *vs.* 58% in acetonitrile). The yield of styrene oxide increased by 11% when changing solvents, whereas the yield of benzaldehyde decreased by 5%.

In the case of the β-methyl styrene, the change from acetonitrile to benzonitrile did not increase the substrate conversion (86% and 81%, respectively **in Figure 96**). The yields of benzaldehyde (18 and 19%) and styrene oxide (46 and 41%) also varied only slightly.

By comparing the oxidation results for these two substrates in each solvent, it can be concluded that solvent change has little effect on conversion rates and products distribution. More importantly, it appears that, with H_2O_2 and POMs, the distribution of the oxidation products is much less sensitive to the solvent than in the Mukaiyama catalytic system.

Unfortunately, conclusions regarding the change of solvent for α-methyl styrene could not be drawn due to co-elution problems between benzonitrile and α-methyl styrene in GC analyses.

VI.3.5 Partial conclusion

The epoxidation reactions of styrene and its derivatives in the presence of polyoxometallates (two examples were tested here without much difference) are not as selective as those of endocyclic alkenes. This is clearly related to the nature of the substrate as evidenced by the variations observed between styrene, α-meth styrene and β-methyl styrene. Styrene is clearly more difficult to oxidize than the other two: a maximum conversion of 60% has been achieved in both acetonitrile and benzonitrile. Further studies are required to improve this conversion, on the one hand, possibly by adjusting the rate of introduction of H_2O_2 or the substrate/POM ratio and, on the other hand, to limit the hydrolysis of the epoxide by introducing H_2O_2 in a non-aqueous form, which represents a constraint. With H_2O_2, the highest styrene oxide + styrene glycol / benzaldehyde ratio we were able to obtain was around 3.8.

VI.4 Conclusion

In this chapter, epoxidation of styrene in the presence of O_2 or H_2O_2 has been investigated using either Mn / Cr-based Salen complexes or W-based polyoxometalates. Several reaction parameters such as the temperature, the nature of the solvent, the oxidant supply or the nature of the catalyst were studied. Questions to be answered were : Are the catalytic systems efficient to promote epoxidation with good conversion and selectivity? Are the conditions implemented in good accordance with what is required for the cycloaddition reaction?

In the literature, aerobic Mukaiyama type epoxidation reactions often use Salen type catalysts. That is the reason why it was important for us to check if the Salophen complexes described in **Chapter IV** could also be efficient in the epoxidation process, hence avoiding to complicate the catalytic system for the whole process targeting the transformation of styrene into styrene carbonate with O_2 and CO_2. It was thus shown that the catalysts that led to the best performance in cycloaddition also displayed promising results in epoxidation. As such, an average yield of 51% of styrene epoxide at 80°C with 99% styrene conversion was obtained after 3h in benzonitrile in the presence of Salophen-Et_2N-Cr and Salophen-Me_2N-Cr. Optimal molar ratio observed for IBA : substrate : Salophen was 300 : 120 : 1 in the case of aerobic epoxidation reaction occurring at 80°C and below during 3h. For Mn(salen)Cl, the optimum

parameters have been established to be a 2.5 equivalent of isobutyraldehyde and benzonitrile as solvent. Under pure O_2, the Salophen complexes seem to be involved in the ring opening of styrene glycol by H_2O but we hope that, using both CO_2 and O_2 for the whole transformation, CO_2 will be able to compete with H_2O leading to styrene carbonate instead of too much styrene glycol. It has to be noted that most of the present work was performed using a O_2 flow. Only a few experiments were carried out under static conditions (O_2 pressure of 3.5 bar). In these conditions, the styrene oxide yield dropped by 10% (49% instead of 59%) in the presence of Mn(salen)Cl meaning that optimization is required.

With H_2O_2, using POM-tBu or POM-COOH as catalysts precursors and H_2O_2 : substrate POM ratio of 250:250:1, most of the alkene conversion occurred in less than 6 h at 50°C. Longer reaction times led to more hydrolysis of the epoxide by the water introduced with aqueous H_2O_2 which represents a severe drawback that could be more difficult to minimize in the whole transformation except if anhydrous H_2O_2 is used. β-methyl styrene oxide seems to be less sensitive to hydrolysis than styrene oxide and especially α-methyl styrene oxide which means that, without further optimization, the whole transformation with H_2O_2 and CO_2 in the presence of POMs and Salophen complexes should be at best performed on β-methyl styrene.

References

[1] C. Carvalho Rocha, PhD thesis: Towards a catalytic system allowing the “one-pot” conversion of alkenes into cyclic carbonates in the presence of dioxygen/carbon dioxide mixtures, Université Pierre et Marie Curie, **2013**.

[2] F. Bentaleb, O. Makrygenni, D. Brouri, C. Coelho Diogo, A. Mehdi, A. Proust, F. Launay, R. Villanneau, Efficiency of Polyoxometalate-Based Mesoporous Hybrids as Covalently Anchored Catalysts, *Inorg. Chem.*, (**2015**), 54, 7607–7616.

[3] O. Makrygenni, D. Brouri, A. Proust, F. Launay, R. Villanneau, Immobilization of polyoxometalate hybrid catalysts onto mesoporous silica supports using phenylene diisothiocyanate as a cross-linking agent, *Microporous Mesoporous Mater.*, (**2019**), 278, 314–321.

[4] A. Lidskog, Y. Li, K. Wärnmark, Asymmetric Ring-Opening of Epoxides Catalyzed by Metal–Salen Complexes, *Catalysts*., (**2020**), 10, 705.

[5] S.T. Oyama, Mechanisms in Homogeneous and Heterogeneous Epoxidation Catalysis, **2008**.

[6] S.S. Wang, G.Y. Yang, Recent Advances in Polyoxometalate-Catalyzed Reactions, *Chem. Rev.*, (**2015**), 115, 4893–4962.

[7] R. Villanneau, A. Marzouk, Y. Wang, A. Ben Djamaa, G. Laugel, A. Proust, F. Launay, Covalent grafting of organic-inorganic polyoxometalates hybrids onto mesoporous SBA-15: A key step for new anchored homogeneous catalysts, *Inorg. Chem.*, (**2013**), 52, 2958–2965.

[8] J.M. Fraile, J.A. Mayoral, L. Salvatella, Theoretical study on the BF_3-catalyzed meinwald rearrangement reaction, *J. Org. Chem.*, (**2014**), 79, 5993–5999.

[9] N. Humbert, D.J. Vyas, C. Besnard, C. Mazet, An air-stable cationic iridium hydride as a highly active and general catalyst for the isomerization of terminal epoxides, *Chem. Commun.*, (**2014**), 50, 10592–10595.

[10] A. Rezaeifard, R. Haddad, M. Jafarpour, M. Hakimi, $\{Mo_{132}\}$ nanoball as an efficient and cost-effective catalyst for sustainable oxidation of sulfides and olefins with hydrogen peroxide, *ACS Sustain. Chem. Eng.*, (**2014**), 2, 942–950.

[11] J.R. Lamb, M. Mulzer, A.M. Lapointe, G.W. Coates, Regioselective Isomerization of 2,3-Disubstituted Epoxides to Ketones: An Alternative to the Wacker Oxidation of Internal Alkenes, *J. Am. Chem. Soc.*, (**2015**), 137, 15049–15054.

CHAPTER VII

Global reaction using O_2 and CO_2

VII.1 Introduction

As previously described in **Chapter III**, only a few catalytic systems allowing the conversion of styrene into styrene carbonate in the presence of O_2 (or H_2O_2) and CO_2 have been reported.

Among them, Bai *et al* obtained a rather high yield of styrene carbonate (76%) with 100% selectivity using a dual homogeneous catalytic system based on Bu_4NI as main cycloaddition catalyst and a ruthenium metalloporphyrin for the epoxidation step. Such reaction worked well under 5 bar of O_2 and 11 bar of CO_2 at 30°C during 48h but the amount of catalysts was relatively high ([Ru] : Bu_4NI : styrene 1 : 2 : 25). Another system developed later by Jain *et al*. in 2015 and made of $Ph_3P^+Br^-$ and $Mo(acac)_2$ grafted on a magnetic chitosan support afforded styrene carbonate with a 67% yield after 10 h at 100°C in the presence of IBA as sacrificial reductant.

This chapter is devoted to the investigation of the catalysis potential of the combination of a Salen complex and a quaternary ammonium salt (QAS) for the targeted global reaction transformation of styrene into styrene carbonate with O_2 and CO_2.

Another option of dual catalysis based on the use of supported quaternary ammonium bromides (as synthesized **Chapter V**) partially exchanged by POMs was initially envisaged but had to be abandoned. Indeed, the simple addition of a soluble bromide, such as *n*-Bu_4NBr, into the homogeneous epoxidation catalysis test of *trans*- and *cis*-β-methyl styrene running with POM and H_2O_2 under conditions similar to those of **Chapter VI** (50°C, 24h, ratio catalyst/substrate/H_2O_2 : 1/250/250) showed that only little or no conversion of alkene to epoxide was noticed after 24h of reaction.

The implementation of a global reaction involving oxidation and cycloaddition steps should at best:

- use a unique solvent with similar reagents concentrations. In our case, benzonitrile was shown to be adequate **(Chapter IV, V and VI)** and the concentrations of the reagents adjusted to c.a. 112 : 2 : 1 (Salophen : *n*-Bu_4NBr : substrate) for both reactions .

- work, if possible, under unique pressure and temperature conditions. In our case, it has been demonstrated in **Chapter IV** and **Chapter VI** that both oxidation and cycloaddition could be carried out efficiently at 80°C and below.
- work ideally with both catalysts (Salophen/n-Bu_4NBr) and both reactants introduced at the beginning of the operation.

However, we may not exclude that, due to possible interferences, oxidation and cycloaddition reactions would have to be performed one after the other.

Preliminary experiments dealing with the use of O_2 and CO_2 are presented here in order to conclude on the feasibility of the global reaction.

VII.2 Towards a unique set of conditions

In order to investigate the feasibility of the whole reaction in a unique set of conditions (solvent, temperature, concentrations, all catalysts and reagents at the beginning), our initial idea was to look at the impact of the reagents of one reaction on the other one. To do so, the strategy used consisted in adapting a classical epoxidation reaction carried out under 3.5 bar of O_2 (**Chapter VI)** and to test the effect of CO_2 and/or of the cycloaddition catalyst. Typical experimental conditions are described below and the tested parameters presented in **Table 30** with the corresponding styrene conversion rate and the yields of the main products in **Figure 97**.

***Protocol for experiments 1.1 to 1.6 (see Table 1)**: Styrene (0.70 mL, 5.6 mmol), isobutyraldehyde (1.33 mL, 15 mmol), n-Bu_4NBr (31.1 mg, 96.2 µmol) and commercially available Jacobsen complex or Salophen-tBu-Cr (48.3 µmol), GC internal standard (p-xylene, 0.66 mL, 5.3 mmol) and 13.3 mL of benzonitrile were mixed in a Teflon pot that was further introduced in a stainless-steel autoclave equipped with a magnetic stirrer and an electric heater. The autoclave was then purged with O_2, the system was pressurized with 3.5 bar of O_2 then 11 bar of CO_2 and heated at 80°C. The reaction mixture was stirred for x (3 or 23) h (see **Table 30**). After each catalytic test, the resulting solutions were analysed by gas chromatography after dilution (samples of 25 µL diluted in 10 mL of CH_2Cl_2).*

Table 30: *Sets of experimental conditions used to test the influence of the reactants and catalysts of each single reaction on the other one in the frame of the whole conversion of styrene into styrene carbonate.*

Experiment	**1.1**	**1.2**	**1.3**	**1.4**	**1.5**	**1.6**
t (h)	3	3	3	3	3	**23**
Ox. catalyst	-	**Jacobsen**	Jacobsen	**tBu-CrCl**	tBu-CrCl	tBu-CrCl
Cyclo. catalyst	-	-	-	-	***n*-Bu$_4$NBr**	*n*-Bu$_4$NBr
P O_2 (bar)	3.5	3.5	3.5	3.5	3.5	3.5
P CO_2 (bar)	-	-	**11**	11	11	11

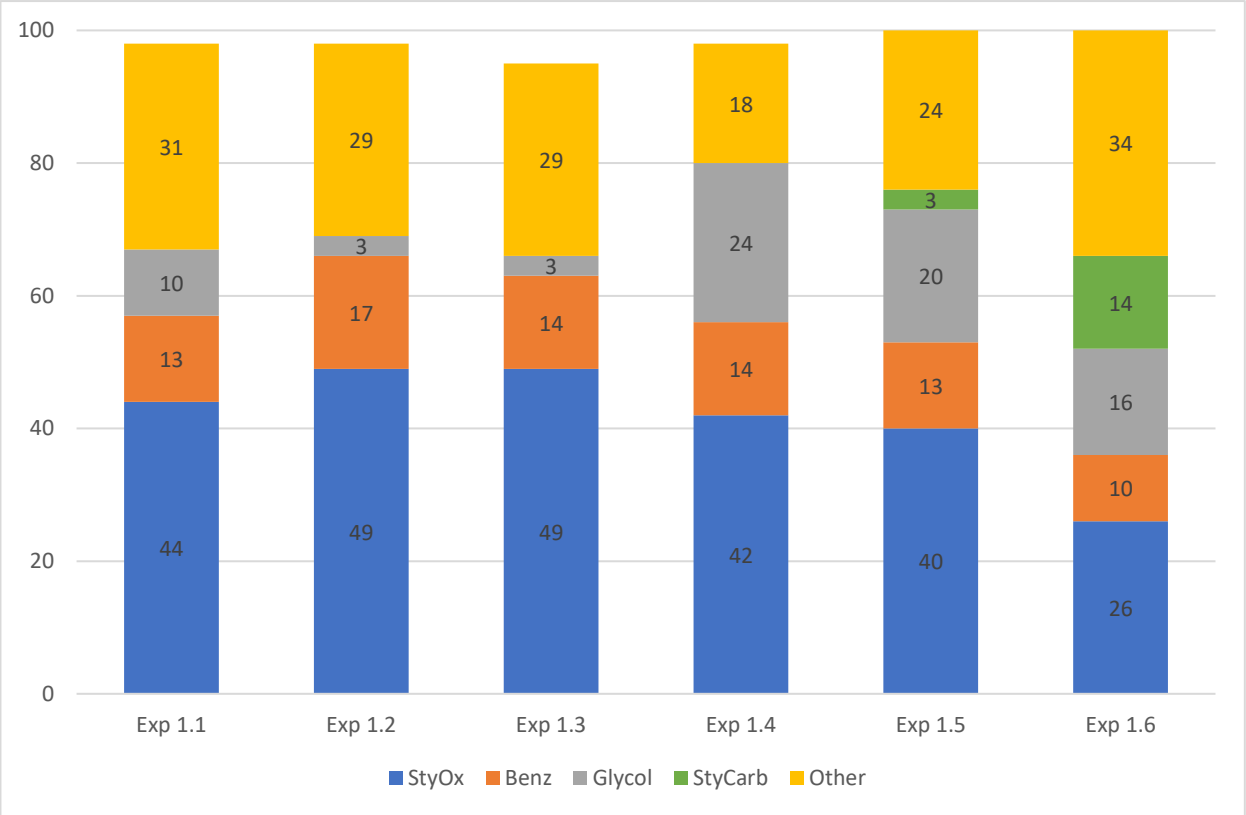

Figure 97: Conversion of styrene and yields of the different products depending on the experimental conditions (see ***Table* 30** *). Styrene (5.6 mmol), isobutyraldehyde (15 mmol), commercially available Jacobsen complex or Salophen-tBu-Cr (0.05 mmol), n-Bu$_4$NBr (0.1 mmol), in 13.3 mL of benzonitrile at 80°C under 3.5 bar of O_2 and 11 bar of CO_2.*

A typical styrene epoxidation was performed without (**Figure 97_Exp1.1**) or with Mn-Salen-Cl (**Figure 97_Exp1.2**) under 3.5 bar of O_2 only during 3 h. Both reactions led to a nearly complete conversion of styrene with 49% yield of styrene oxide, 17% yield of benzaldehyde and 29% of unknown species. A small amount of styrene glycol was also obtained.

What about the influence of CO_2? The same reaction was repeated under 3.5 bar of O_2 and 11 bar of CO_2 (**Figure 97_Exp1.3**) showing that the addition of CO_2 did not impact

significantly the yields of styrene oxide (49%), benzaldehyde (14 instead of 17%), styrene glycol (3%) and of the by-products after 3 h. A similar reaction (**Figure 97_Exp1.4)** was carried out with Salophen-tBu-Cr which showed better catalysis performances (**Chapter IV.2**) in styrene aerobic epoxidation than Mn-Salen-Cl despite a very similar structure. On one hand, after 3 h, the yield of benzaldehyde was unchanged (14%) and a relatively good yield of styrene oxide was obtained in comparison with Mn-Salen-Cl ((**Figure 97_Exp1.3)** 42% vs. 49%) but, on the other hand, a strong increase of the amount of styrene glycol could be emphasized (24% instead of 3%). Such variation could be the result of the activation of styrene oxide towards the attack of water molecules as the result of the more important Lewis acidity of Cr(III). It can be noticed that in Exp1.4, the (styrene oxide + styrene glycol) / benzaldehyde molar ratio was 4.7. At first glance, it would seem that the styrene conversion and the styrene oxide yield are very little influenced by the presence of CO_2 (at least up to 11 bar) and the nature of the catalyst (Cr vs. Mn).

As a further step, the experiment was now conducted in the presence of the main cycloaddition catalyst, *i.e.* *n*-Bu_4NBr (**Figure 97_Exp1.5**) allowing the synthesis of styrene carbonate, but in a low yield (3%). Clearly, styrene carbonate was formed at the expense of styrene glycol (slight decrease from 24 (**Exp1.4**) to 20% (**Exp1.5)**) and styrene oxide (slight decrease from 42 (**Exp1.4**) to 40% (**Exp1.5)**). Hopefully, a higher yield of styrene carbonate (14%) was observed after 23h at 80°C (see **Figure 97_Exp1.6**) with a consequent loss of styrene oxide yield from 40 to 26%, but also of styrene glycol (from 20 to 16%). Our hypothesis here is that styrene carbonate formed comes from the styrene oxide and that the hydrolysis of styrene oxide may be slowed down by the competitive reaction of epoxide with CO_2 instead of H_2O. It seems that benzaldehyde was formed early and that the cycloaddition step had little impact on it but a high proportion of unknown by-products could be detected (balance default of 34%). One of the possible sources of secondary products could be the reaction of styrene oxide with the isobutyric acid formed as a side-product of the oxidation of the sacrificial aldehyde. Indeed, epoxides are known to react with carboxylic acids to form 1,2-diol mono-esters in the presence of imidazolium ionic liquids.[1]

To conclude, we confirmed the ability of the *n*-Bu_4NBr / Salophen-tBu-Cr catalytic system to induce the production of styrene carbonate from styrene in the presence of O_2 and CO_2. However, after 23 h, the yield of styrene carbonate was low (14%). The apparent rather

low activity of the *n*-Bu_4NBr/Salophen-tBu-Cr catalytic system towards CO_2 cycloaddition onto styrene oxide was surprising. Indeed, we showed earlier, that under similar conditions (80°C, 11 bar CO_2 and 23h), 99% styrene carbonate yield could be obtained with 100% selectivity (see **Chapter IV.2**).

Seemingly, the reagents (IBA, O_2) or the by-products (isobutyric acid) of the epoxidation step would have a negative influence on the cycloaddition catalyst. Thus, further work was carried out using styrene oxide as a substrate focusing our attention of the perturbation of this reaction by the oxidation step by O_2 and IBA, especially. The experimental procedure of the different tests, performed here with Salophen-tBu-Cr, is summarized below and in **Table 31.**

***Protocol for experiments 2.1 to 2.4 (see Table 2)**: Styrene oxide (0.66 mL, 5.6 mmol), isobutyraldehyde (1.33 mL, 15 mmol), n-Bu_4NBr (31.1 mg, 96.2 µmol), Salophen-tBu-Cr (32.4 mg, 48.3 µmol), GC internal standard (p-xylene, 1 mL, 8 mmol) and 13.3 mL of benzonitrile were mixed in a Teflon pot that was further introduced in a stainless-steel autoclave equipped with a magnetic stirrer and an electric heater. The autoclave was then purged with O_2, and pressurized with 3.5 bar of O_2, then 11 bar of CO_2 and heated at 80°C. The reaction mixture was stirred for 3h or 23h (see **Table 31**). After each catalytic test, the resulting solutions were analysed by gas chromatography after dilution (samples of 25 µL diluted in 10 mL of CH_2Cl_2).*

Table 31: Sets of experimental conditions used to test the influence of the reactants and catalysts of each single reaction on the other one in the frame of the cycloaddition reaction of CO_2 onto styrene oxide in O_2/CO_2 atmosphere

Experiment	**2.1**	**2.2**	**2.3**	**2.4**
t (h)	3	3	3	23
IBA	-	yes	yes	yes
P O_2 (bar)	3.5	-	3.5	3.5
CO_2 (bar)	11	11	11	11
Medium color	**red**	**red**	**yellow**	**yellow**

Corresponding styrene oxide conversions and styrene carbonate yields (100% selectivity) are displayed in **Figure 98**. First, the influences of O_2 and of IBA were investigated separately in experiments **2.1** and **2.2** at 80°C within 3 h (**Figure 98_Exp2.1** and **Figure 98_Exp2.2**) showing results very similar to those of **Chapter IV.2**. Neither O_2, nor IBA alone had a negative effect on the cycloaddition step. However, when both components were added together, things got worse (**Figure 98_Exp2.3**) with a clear decrease of the catalytic activity, but the catalysts still worked! Indeed, after 3 h, the styrene oxide conversion was 17% and the carbonate yield was only 12%. It has to be noted that this yield subsequently increased to 76%

after 23h (**Figure 98_Exp2.4**). In each case the selectivity of styrene carbonate remained high and only the conversion of styrene oxide was lowered.

As a reminder, at 80°C, the yield of styrene carbonate in the presence of *n*-Bu_4NBr alone was 12% after 3 h reaction (**Chapter IV.2**) and 99% after 23 h meaning, probably, in our case, that O_2 and IBA could be responsible for a deactivation of the Salen complex. It is also noteworthy that the final color of the reaction mixture was purple red in **Exp. 2.1 and 2.2**, but yellow in **Exp. 2.3 and 2.4**. Such change could result from the evolution of the Salen complex as a result either from the degradation of the ligand or from the variation of the Cr oxidation state, or both.

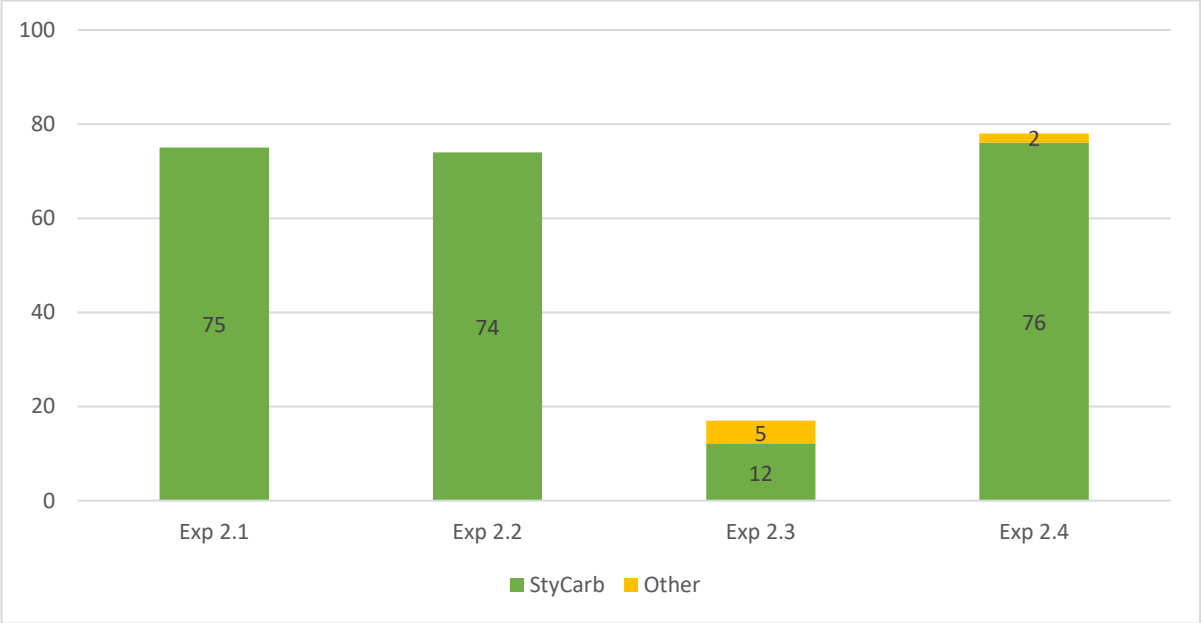

*Figure 98: Influence of O_2, IBA or both on the conversion of styrene oxide and on the yields of products (see experimental details in **Table 31**). Styrene oxide (5.6 mmol), isobutyraldehyde (1.33 mL, 15 mmol), Salophen-tBu-Cr (0.05 mmol), n-Bu_4NBr (0.1 mmol) in 13.3 mL of benzonitrile at 80°C under 3.5 bar of O_2 and 11 bar of CO_2 for 3 or 23 h.*

The hypothesis of the variation of the oxidation state of Cr(III) to Cr(V) or Cr(VI) was quickly verified using ^{1}H NMR. Indeed, Cr(III) in the starting complex is paramagnetic and its ^{1}H NMR spectrum shows wide and undefined signals. Here, a first analysis of the crude reaction mixture of **Exp2.4** by ^{1}H NMR gave rise to a spectrum with well-defined peaks, more typical of a diamagnetic form of Cr, probably Cr(VI) hence allowing us to discard the hypothesis of the formation of a paramagnetic Cr(V) here. A complementary UV-Vis analysis of the reaction media resulting from **Exp2.1** and **Exp2.4** was also carried out (see experimental details in **Appendix A)** after the dilution of the Cr species to 10^{-4} M showing that the spectra (**Figure 99**) were very different.

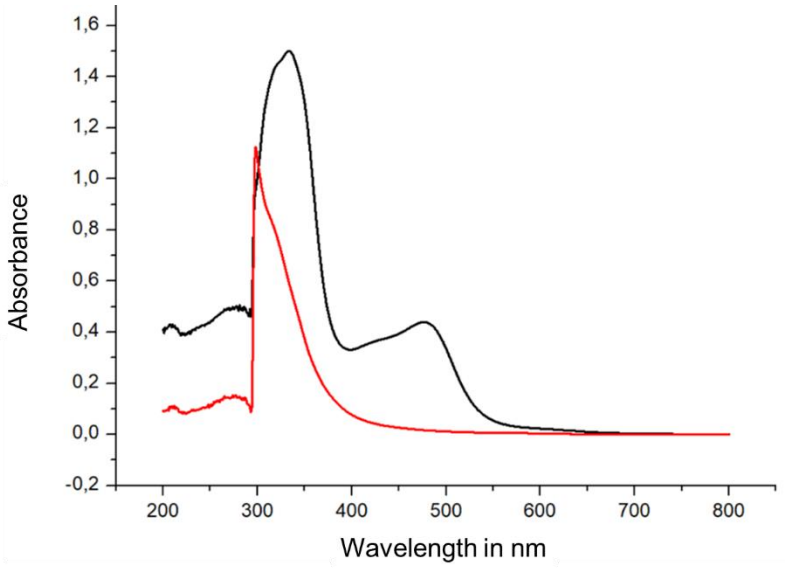

*Figure 99: UV-Vis. spectra of the diluted crude reaction mixtures of **Exp2.1** (O_2 only, black) and **Exp2.4** (O_2 and IBA, red) after the catalysis test.*

Clearly, the shape of the spectrum of the solution corresponding to **Exp2.1** is in agreement with the presence of Cr(III). In this case, the absorbance peak at 482 nm led to a calculated value of ε of 4 800 $l.mol^{-1}.cm^{-1}$ that would correspond to a **d – π*** ligand to metal charge transfer [2]. In the case of the solution corresponding to **Exp2.4**, no peak was detected near 400-500 nm, which could be explained by the oxidation of Cr(III) to Cr(VI) characterized by the absence of d electrons.

To conclude, it appears that for the whole conversion of styrene into styrene carbonate in the presence of IBA, O_2, CO_2, Salophen-tBu-Cr and *n*-Bu_4NBr, the *in-situ* change in the oxidation state of Cr would be responsible for the slower conversion of styrene oxide into styrene carbonate. Since we showed earlier in **Chapter VI**, that the Salen complex is not really needed during the oxidation step at 80°C (see also **Figure 97_Exp1.1**), Salen complexes involving cations such as Al^{3+} or Zn^{2+} should be preferred but they were not synthesized in this work. So, in a last attempt, we propose to carry out, first, the epoxidation reaction under O_2 atmosphere only, then to add in the same pot, before the second step, the *n*-Bu_4NBr/Salophen catalytic system. This "one-pot" strategy is detailed in the following section.

VII.3 Global reaction with a delayed introduction of CO_2 and of the catalysts

A series of experiments involving the delayed introduction of Salophen-R-Cr (with R = -tBu or Me_2N) catalysts were performed. In each case, the epoxidation of styrene was conducted first during 3h at 80°C with IBA under 3.5 bar of O_2. After cooling, molecular oxygen was evacuated, then *n*-Bu_4NBr and Salophen were introduced. The pressure was then set at 11 bar of CO_2 and the reaction carried out again at 80°C. Salophen-Me_2N-Cr was also tested here as it proved earlier to be the best homogeneous co-catalyst for the CO_2 cycloaddition (see **Chapter IV.3**). Experimental settings for the different tests are presented below with the conditions details in **Table 32** and the results are displayed in **Figure 100.**

***Typical experimental conditions**: Styrene (0.70 mL, 5.6 mmol), isobutyraldehyde (1.33 mL, 15 mmol), GC internal standard (p-xylene, 0.66 mL, 5.3 mmol) and 13.3 mL of benzonitrile were mixed in a Teflon pot that was further introduced in a stainless-steel autoclave equipped with a magnetic stirrer and an electric heater. The autoclave was then purged and pressurized with 3.5 bar of O_2 and heated at 80°C. After 3 h, the autoclave was cooled down to room temperature, the oxygen evacuated, and the mixture stirred during 5 min. Later, n-Bu_4NBr (31.1 mg, 96.2 µmol) and Salophen-R-Cr (48.3 µmol) were added. The autoclave was then purged and pressurized with 11 bar of CO_2 and heated at 80°C. Later, the autoclave was cooled down to room temperature. After each catalytic test, the resulting solutions or suspensions were analysed by gas chromatography after dilution (samples of 25 µL diluted in 10 mL of CH_2Cl_2).*

***Table 32:** Sets of experimental conditions used to test the influence of the two steps global oxidative cycloaddition reaction, starting with O_2 atmosphere, and followed by a cycloaddition in 11 bar of CO_2. Respective times and catalysts inside are presented.*

Exp	**3.1**	**3.2**	**3.3**
t (h) Ox. / Cyclo.	3 / 3	3 / 20	3 / 20
Salophen	tBu-CrCl	tBu-CrCl	Me_2N-CrCl
Cyclo. catalyst	*n*-Bu_4NBr	*n*-Bu_4NBr	*n*-Bu_4NBr
P O_2 (bar)	3.5	3.5	3.5
P CO_2 (bar)	11	11	11

After 3h epoxidation under 3.5 bar of O_2 without any catalyst followed by 3h of cycloaddition under 11 bar of CO_2 in the presence of Salophen-tBu-Cr and *n*-Bu_4NBr at 80°C, 100% conversion of styrene was reached with a 7% yield of styrene carbonate only (**Exp3.1**). It has to be noted that the yield of cyclic carbonate increased up to 16% after 20h cycloaddition (**Exp3.2**). However, the proportion of unknown by-products increased from 11% to 35% after 3h to 20h cycloaddition while the yields of benzaldehyde and styrene glycol did not evolve.

Actually, the products distribution resulting from this modified procedure (**Exp3.2**) did not change very much from those of **Exp1.6**.

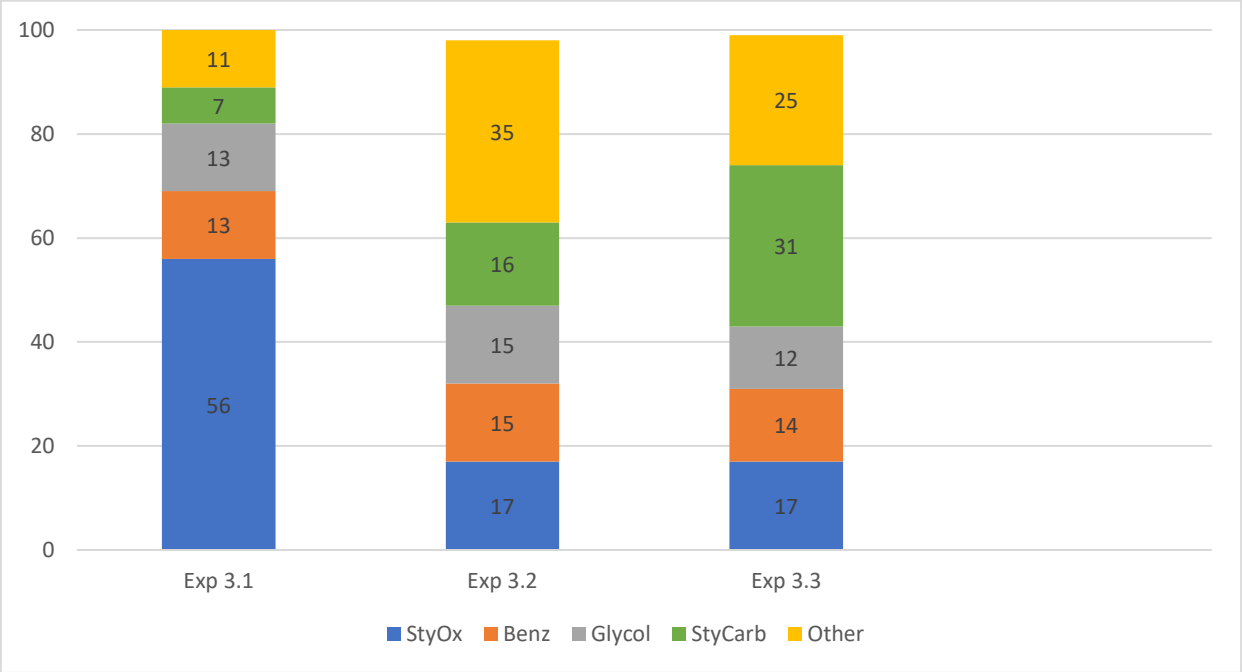

Figure 100: Influence of the Salophen complex and of time on the conversion of styrene and of the yields of products. Styrene (5.6 mmol), isobutyraldehyde (1.33 mL, 15 mmol), commercial Jacobsen or Salophen-tBu-Cr (0.05 mmol), n-Bu_4NBr (0.1 mmol), in 13.3 mL of benzonitrile at 80°C under 3.5 bar of O_2 and 11 bar of CO_2. (see experimental details in Table 32*).*

Another cycloaddition co-catalyst, Salophen-Me_2N-Cr, was also tested due to its high catalytic activity observed for CO_2 cycloaddition in **Chapter IV.3** After a 3h period for styrene epoxidation, followed by 20 h for CO_2 addition on styrene oxide, once again, a complete styrene conversion was observed with the highest value, in this work, for styrene carbonate yield (31%) (**Figure 100_Exp3.3**). Clearly, Salophen-Me_2N-Cr led to less unknown by products and the overall yield of known products not issued from C=C cleavage reached 60% (*i.e.* 17% for styrene oxide + 12% for styrene glycol + 31% for styrene carbonate)!

VII.4 Conclusion

The conversion of styrene into styrene carbonate was conducted at 80°C under O_2 and CO_2 either under a unique set of reactants and catalysts or by adding later the Salophen complex, the quaternary ammonium salt and CO_2.

In the "one-step" transformation carried out with IBA, Salophen-tBu-Cr and *n*-Bu_4NBr under a O_2/CO_2 atmosphere, the maximum yield of styrene carbonate reached after 23h at

80°C was 14% while the yields of benzaldehyde, unknown by-products and products not issued from a C=C cleavage (styrene oxide, styrene glycol and styrene carbonate) were 10%, 34% and 56%, respectively. Apparently, the *in-situ* oxidation of Cr(III) to Cr(VI) was suspected to lower the kinetics of cycloaddition and favour the formation of by-products.

A "two-steps" transformation based on the prior epoxidation of styrene in the presence of IBA and O_2 (3.5 bar) only, followed by the CO_2 cycloaddition in the presence of *n*-Bu_4NBr and Salophen-R-Cr catalysts under 11 bar of CO_2, after purging O_2 was also investigated. In this case, the maximum yield of styrene carbonate, obtained after 3h epoxidation and 20h cycloaddition (with Salophen-Me_2N-Cr), was 31% at 80°C while the yields of benzaldehyde, unknown by-products and products not issued from a C=C cleavage (styrene oxide, styrene glycol and styrene carbonate) were 14%, 25% and 60%, respectively. This highest yield was apparently related to the use of Salophen-Me_2N-Cr that allowed to minimize the amount of unknown by-products.

To conclude, interesting directions to follow, in order to perform the one-step transformation of styrene into styrene carbonate in the presence of O_2 and CO_2, would be the use of Salophen-Me_2N-Cr or Salophen complexes that have no redox properties such as those based on Zn(II) or Al(III).

References

[1] M.N.S. Rad, S. Behrouz, The base-free chemoselective ring opening of epoxides with carboxylic acids using [bmim]Br: A rapid entry into 1,2-diol mono-esters synthesis, *Mol. Divers.*, (**2013**), 17, 9–18.

[2] M. Alvaro, C. Baleizao, D. Das, E. Carbonell, H. García, CO_2 fixation using recoverable chromium salen catalysts: use of ionic liquids as cosolvent or high-surface-area silicates as supports, *J. Catal.*, (**2004**), 228, 254–258.

[3] T. Buchecker, P. Schmid, S. Renaudineau, O. Diat, A. Proust, A. Pfitzner, P. Bauduin, Polyoxometalates in the Hofmeister series, *Chem. Commun.*, (**2018**), 54, 1833–1836.

[4] Selectivity (SBA resins), http://dardel.info/IX/other_info/selectivity_a.html, (**2020**),.

[5] Rohm and Haas, Ion exchange resins, *Https://Www.Lenntech.Com/Products/Resins/Rohm-Haas/Rohm-Haas-Ion-Exchange-Resins.Html* (**2020**),.

CHAPTER VIII

PRELIMINARY WORKS TOWARDS CATALYTIC SYSTEMS BASED ON BOTH QAS AND METAL SALOPHEN COMPLEX (Exploratory study)

VIII.1 Introduction

In the previous section, we concluded that both a quaternary ammonium salt (catalyst) and a co-catalyst are needed to facilitate the CO_2 cycloaddition onto epoxides in reaction conditions favourable with the prior epoxidation step which is the target of the whole project. Various strategies are available in order to integrate both Lewis basic (main catalyst) and acidic functions (co-catalyst) inside only one structure. In the recent literature, the strategies reported are based either on completely soluble species bearing the two functions (homogeneous catalysis) or on heterogeneous catalytic systems, the latter being obtained by successive graftings of the two functions on the solid support or by using a heterogeneous catalyst involving both functions in its core structure. Some typical systems with their advantages and drawbacks are presented below.

A relevant example of the approach based on soluble species is given by the bimetallic aluminium salen catalyst developed in 2011 by North and co-workers.[1] The firstly synthesized aluminium salen bearing tertiary amine substituents could be easily quaternized via a nucleophilic substitution reaction, affording a structure bearing both aluminium metal centres and QAS functions. A heterogenized version of such a structure has also been successfully obtained by the reaction of the previous aluminium salen bearing tertiary amines with MCM-41 silica functionalized by bromoalkyl linkers using an *in-situ* grafting strategy for the formation of QAS. Homogeneous and supported catalytic systems showed good performances in CO_2 cycloaddition reaction on styrene oxide, with 89% yield of styrene carbonate after 6h at 26°C under 1 bar of CO_2 and using 2.5% mol catalyst without needing the addition of external TBABr. Fewer yield was obtained in the case of a supported catalyst within the same reaction conditions.

Other metal complexes have also been developed. Hence, Jing and co-workers worked on a zinc metalloporphyrin functionalized by 2 equivalents of $Bu_3N^+X^-$ (with X = Br, I, F and Cl).[2] Best yields of propylene carbonate (99%) were obtained with bromides within 6h at 120°C under 20 bar of CO_2 and using rather high molar ratios of cat : oxide = 1 : 5000. Such entity was able to run efficiently without the need of additional soluble QAS. Although interesting results could be reached with several epoxides, yields of propylene carbonate dropped with the temperature, with only 40% at 80°C and 17% at 60°C.

Since the precursor work of North and co-workers [1], other heterogeneous catalytic systems have been reported in the literature. Indeed, Leng and co-workers successfully grafted a Salen-Et_2N-Co catalyst on functionalized polymer microspheres bearing bromoalkyl groups by using an *in-situ* formation approach of QAS through nucleophilic substitution. [3] This allowed the grafting of Salen-Co with a quaternary ammonium covalent bond, thus leading to a supported catalyst with 5 wt.% of cobalt. According to the authors, the two amine functions borne by each Salen were quaternized, leading to 2 equivalents of QAS per equivalent of cobalt atom. Using only 0.2% molar ratio of cobalt (0.4% of QAS), styrene carbonate was successfully synthesized with 96% yield at 80°C after 6h under 10 bar of CO_2. It is noteworthy that this heterogeneous catalytic system could be recycled showing a constant activity over 5 runs.[3]

As a conclusion of this partial review on catalytic systems bearing both functions, it can be noted that most of them worked without needing the addition of an external source of quaternary ammonium salt. Despite these interesting properties, only a few of these catalytic systems were heterogenized (see example of North.[1]). More importantly, the description of bifunctional heterogenized catalysts remain scarce and progress needs to be made in order to lower the catalysis tests conditions (lower temperature and CO_2 pressure). Further development should also be assessed in order to simplify the catalysts developed.

In another approach, we will look at the co-grafting of Si-QAS obtained by an ex-situ synthesis (see **Chapter V)** and of the aminopropyl linker that can be used for the grafting of Salophen complexes as shown in **Chapter IV** of this manuscript.

VIII.2 Towards an independent anchoring of quaternary ammoniums salts and of salophen complexes

Earlier, we have shown that: i) Salophen complexes bearing a carboxylic group can be grafted up to 0.15 mmol.g^{-1} through amide bonds on SBA-15 silica bearing up to 2.2 mmol.g^{-1} of aminopropyl groups (**Chapter IV.2**),and ii) quaternary ammonium salts, such as -NEt_3^+,Br^-, bearing trimethoxysilylane groups prepared in an *ex-situ* mode could be grafted up to 1.13 mmol.g^{-1} directly onto SBA-15 (**Chapter V**).

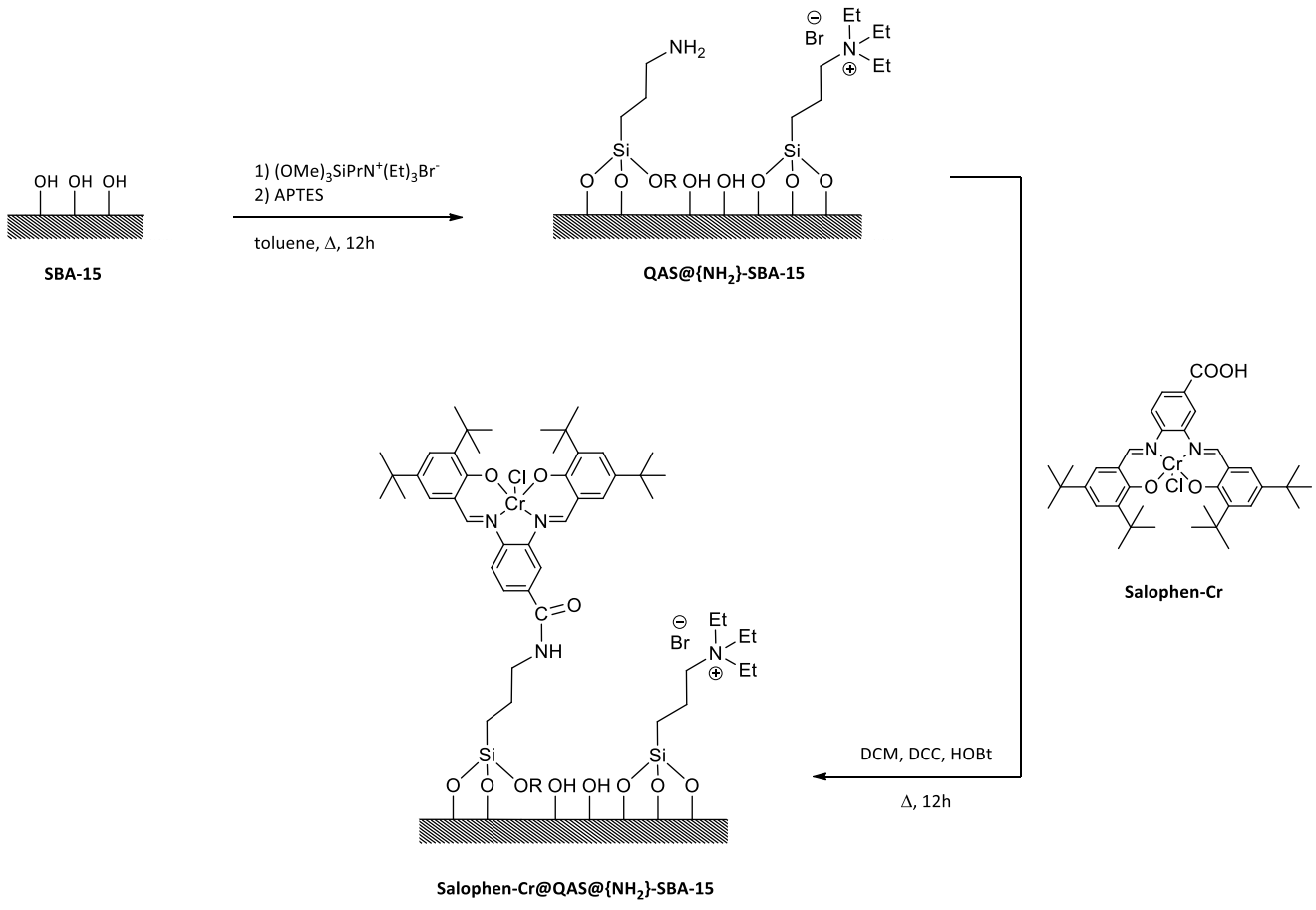

Figure 101: *General strategy for an independent anchoring of quaternary ammoniums salts and of salophen complexes*

So, in order to minimize the number of synthetic steps, we propose here to perform the grafting of Si-QAS and APTES together on SBA-15, affording QAS@{NH_2}-SBA-15, followed by the coupling step of the salophen complex bearing a carboxylic group (**Figure IV**).

VIII.2.1 Co-grafting of APTES and Si-QAS

Considering our previous experience, and especially the grafting efficiency of triethylammonium bromide (aminopropyl)triethoxysilane on one hand, and of 3-(aminopropyl)triethoxysilane, on the other hand, we have proposed the following co-grafting procedure in order to reach the 2 : 1 ratio of QAS : Salophen already employed in homogenous conditions.

Co-grafting of triethylammonium bromide (aminopropyl)triethoxysilane and of 3-(aminopropyl)triethoxysilane on SBA-15: *SBA-15 silica (500 mg) previously dried at 80°C under vacuum for 12 h was dispersed in 17 mL of anhydrous toluene using an ultrasound bath for 5 min and magnetic stirring. Then, triethylammonium bromide (aminopropyl)triethoxysilane (1 mL dissolved in dry acetonitrile, 1.2 mmol) and 3-(aminopropyl)triethoxysilane (APTES) (140 µL, 0.6 mmol) were added and, after 1 h, the resulting mixture heated up to 130°C. Reflux was maintained for 20 h, after which the suspension was filtered. The recovered white solid was washed with toluene, acetonitrile, and ethanol (15 mL of each), then air dried. The resulting solid was extracted with ethanol using a soxhlet for 24 h, then dried at air (m = 585 mg).*

Resulting white solid, QAS@{NH_2}-SBA-15, was characterized by TGA, thus emphasizing the attachment of organic functions (**Figure 102**). In case of total grafting of both groups, the total weight loss could be estimated to c.a. 25 wt.% vs. 22 here, which appears as a very satisfying result.

The weight loss derivative curve of QAS@{NH_2}-SBA-15 was compared to those of {NH_2}-SBA-15 and {$Et_3N^+Br^-$}-SBA-15 (Figure 5) in order to try to quantify both functions. Hence, it seems that {$Et_3N^+Br^-$}-SBA-15 is mostly thermally degraded between 180°C and 400°C (with a maximum at 200°C) while {NH_2}-SBA-15 is decomposed mostly at higher temperature maximum at 300°C. Unfortunately, there is some overlapping since the degradation of the amino groups occurs between 180 and 500°C. Using an arbitrary partition before 270°C for {$Et_3N^+Br^-$}-SBA-15 and after 270°C for {NH_2}-SBA-15, -$NEt_3^+Br^-$ and -NH_2 loadings were

estimated to 0.36 mmol.g^{-1} and 1.43 mmol.g^{-1}, but this later is superior to the expected value (1.2 mmol.g^{-1}).

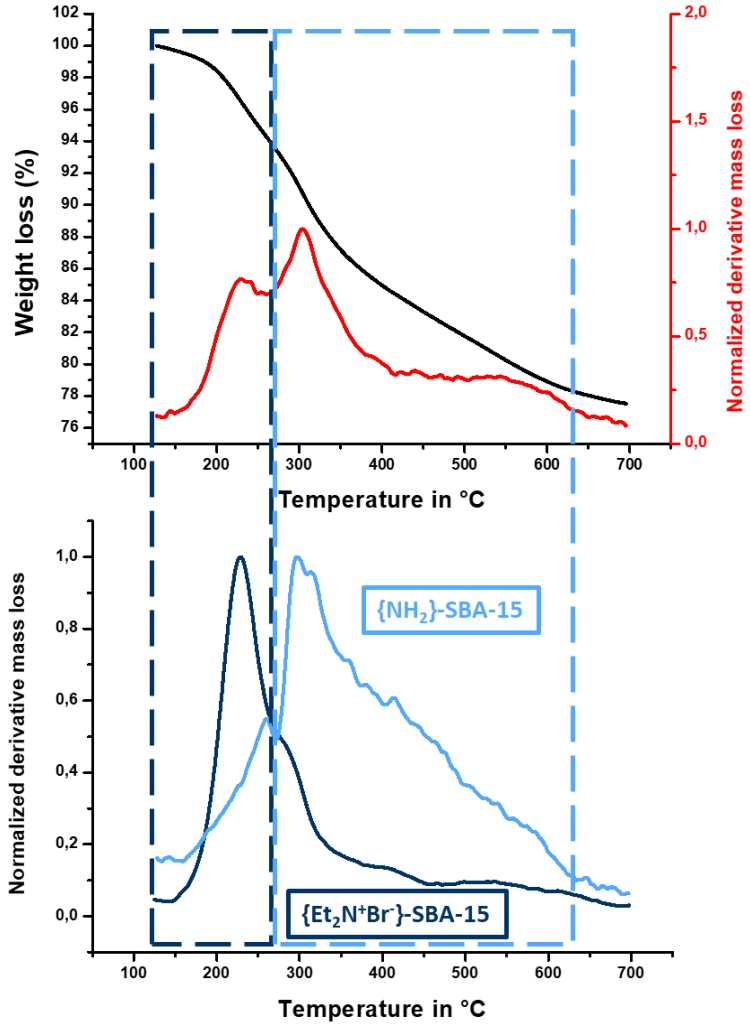

Figure 102: *Thermogravimetric analysis of the solid bearing both {-NH2} and {Et2N+Br}- functions (the weight loss derivative curves of the solid and of {NH2}-SBA-15 and of {Et2N+Br-}-SBA-15 are also represented for a better interpretation).*

QAS@{NH_2}-SBA-15 was also analysed by XPS **(Figure 103)**. The nitrogen XPS signal could be deconvoluted in 2 components, corresponding to the ammonium of -$NEt_3^+Br^-$ at 402.4 eV and the amine of -NH_2 at 399.3 eV.[4] In the case of Br, expected Br^- was identified by the two deconvolution peaks at 68.7 eV (Br $3d_{3/2}$) and 67.6 eV (Br $3d_{5/2}$).[5] Elements atomic concentrations were also determined, with 1.5 atomic% for Br^-, 1.2% for N in -NH_2 and 1.8 found for N in -$NEt_3^+Br^-$. As the result, the Br^-/N(-NEt_3^+) atomic ratio equals 0.83 which is relatively acceptable for an expected quaternary ammonium salt.

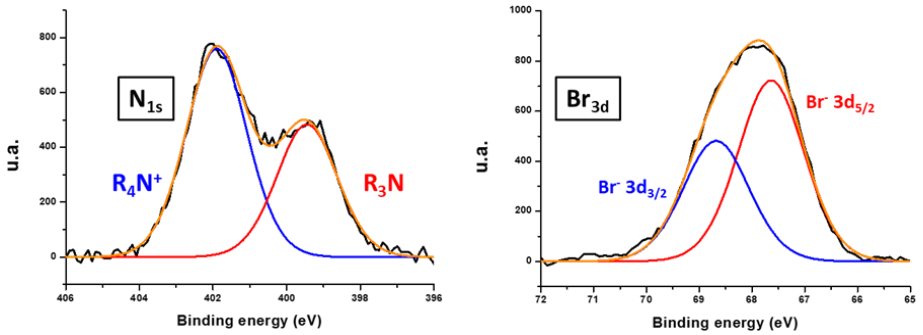

Elements	Atomic ratio
Br^-	1,5
N	1,2
N^+	1,8

Figure 103: *XPS analysis of bromide and nitrogen in QAS@{NH_2}-SBA-15. (Calibration was made from C1s peak at 284.8 eV).*

Considering that the atomic ratio of N(-NH_2)/Br^- is 0.8 and taken into account the total weight loss measured by TGA (**Figure 102**), we have been able to obtain a more plausible quantification of the loading of each function (see details below).

M ($Et_3N^+Br^-$)-$(CH_2)_3$ = 223.17 g.mol^{-1}
M (NH_2)-$(CH_2)_3$ = 58.10 g.mol^{-1}

Atomic ratio N/Br^- = 0.80

Total mass lost in TGA : 218.83 mg / 1g SBA

*($Et_3N^+Br^-$)-$(CH_2)_3$ → **0.81 mmol.g^{-1}** → 181.1 mg loss/ 1g SBA*
*(NH_2)-$(CH_2)_3$ → **0.65 mmol.g^{-1}** → 37.7 mg loss/ 1g SBA*

Total mass lost obtained from molar concentration: 181.1 + 37.7 = 218.8 mg
*Molar ratio N/Br^- = **0.65 / 0.81** = 0.80*

Hence, the c.a. 22 wt.% loss and the N(-NH_2)/Br^- of 0.8 measured by TGA and XPS, respectively turned out to be compatible with a loading of 0.81 mmol.g^{-1} of QAS (68% yield) and of 0.65 mmol.g^{-1} of aminopropyl groups (54% yield).

In conclusion, a SBA-15 type material bearing similar amounts of quaternary ammonium salt and of primary amine was successfully synthesized in one step. Further functionalisation by coupling Salophen-tBu-Cr through covalent amide bonds was investigated in the following part.

VIII.2.2 Coupling of Salophen-tBu-Cr with QAS@{NH_2}-SBA-15

As shown in **Chapter IV.2**, the covalent coupling of the Salophen-tBu-Cr complex with the aminopropyl groups of QAS@{NH_2}-SBA-15 was undertaken in the presence of DCC and HOBT as described in the inset below.

Covalent grafting of Salophen-tBu-Cr onto QAS@{NH_2}-SBA-15. *QAS@{NH_2}-SBA-15 (300 mg, [-RNH_2] = 0.65 mmol g^{-1}, corresponding to 0.20 mmol of {-NH_2} functions) and Salophen-tBu-Cr (33 mg, 0.050 mmol) were dried under vacuum overnight in two distinct schlenk tubes. Then, Salophen-tBu-Cr was dissolved in dichloromethane (DCM, 5 mL). In parallel, 1-hydroxy-1H-benzotriazole (HOBT, 0.002 g, 0.014 mmol) and N,N'-dicyclohexylcarbodiimide (DCC, 0.015 g, 0.064 mmol) were dissolved in 2 mL of DCM and the resulting solution was added to the solution of Salophen and the mixture was stirred for 40 min at room temperature. Meanwhile, 10 mL of DCM were added to QAS@{NH_2}-SBA-15 and the resulting suspension immerged in an ultra-sound bath for 15 min. The solution of Salophen was then transferred into the suspension of silica and the resulting mixture refluxed overnight under N_2. After cooling, the red solid was recovered by filtration, washed successively with methanol and acetone using a Soxhlet, respectively for 3 days and 24 h affording 330 mg of Salophen-tBu-Cr@QAS@{NH_2}-SBA-15.*

Thermogravimetric analysis of Salophen-tBu-Cr@QAS@{NH_2}-SBA-15 material **(Figure 104)** was performed, showing an increase of the weight loss starting around 385 °C (with a maximum of the derivative curve at c.a. 400°C) that would correspond to the Salophen complex. The loss was of 4% instead of *c.a.* 10%, leading to an estimated concentration of 0.06 mmol.g^{-1}. Compared to the 0.6 mmol per gram of SBA, the resulting reaction yield was only of 36%.

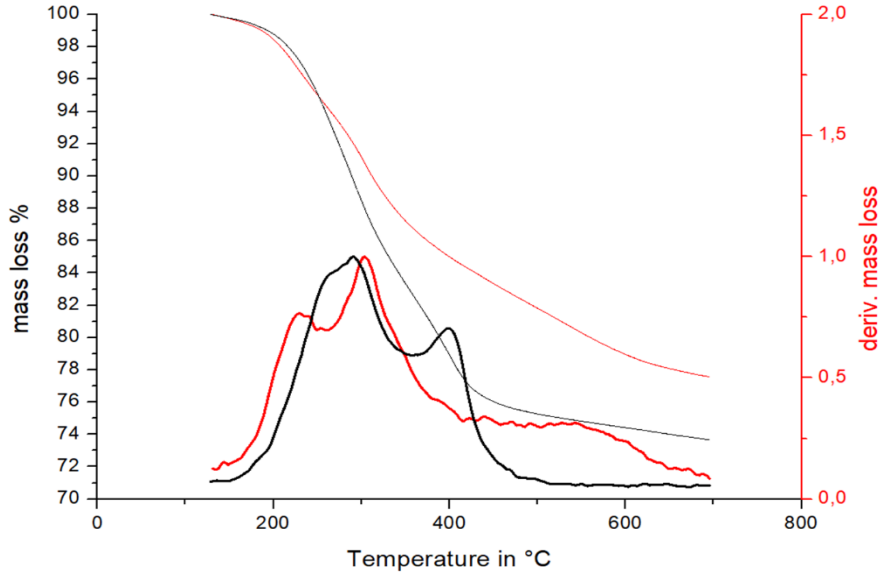

Figure 104: *TGA of Salophen-tBu-Cr@QAS@{NH2}-SBA-15 (black) and QAS@{NH2}-SBA-15 (red) mass loss (top) and mass loss (bot) derivative are represented*

A complementary analysis of Salophen-tBu-Cr@QAS@{NH_2}-SBA-15 was carried out using XPS looking more particularly at the signals of Br, Cr and N. As shown before, the bromine XPS signal (**Figure 105**) could be deconvoluted in two components Br and Br^- as reported before.[5] In the case of nitrogen, two distinct species could be observed with signals at 402.2 eV (for R_4N^+) and 399.3 eV (for free amines and amides)[6] which is not very different from QAS@{NH_2}-SBA-15, excepted for the area distribution of both peaks. The Br^-/R_4N^+ atomic ratio was estimated to 0.65 compared to 0.83 in the starting material which could indicate that part of Br^- would have been exchanged during this last step. But more importantly, the chromium peak was very weak which is, as first sight, in contradiction with TGA data. The only explanation that can be formulated would be that some demetallation occurred during the coupling step.

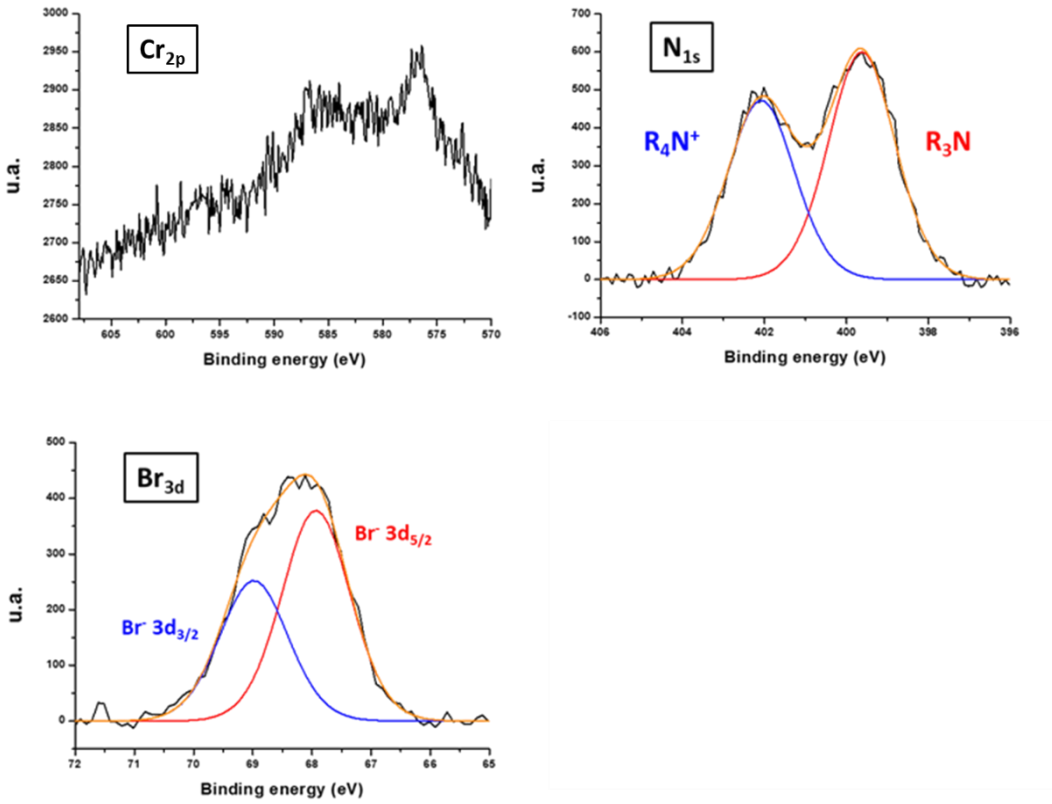

Figure 105: *XPS spectra of chromium, bromine and nitrogen in Salophen-tBu-Cr@QAS@{NH2}-SBA-15 and atomic ratios (Calibration was made from C1s peak at 284.8 eV).*

VIII.3 Conclusion

Here, the incorporation of a quaternary ammonium salt and of a Salophen complex onto a SBA-15 type silica was based on the grafting of the Si-QAS and of the Salophen complex. Both used independent linkers with a two-step protocol from SBA-15 to the end material. In that way, we have been able to anchor simultaneously 0.81 mmol.g^{-1} of {$Et_3N^+Br^-$} function and 0.65 mmol.g^{-1} of {NH_2} in one step, as revealed by a cross-interpretation of TGA and XPS data. However, it seems that Cr was lost (by a demetallation process?) during the coupling step between its Salophen complex bearing carboxylic functions and the supported aminopropyl groups.

References

[1] J. Melendez, M. North, P. Villuendas, C. Young, One-component bimetallic aluminium(salen)-based catalysts for cyclic carbonate synthesis and their immobilization, *Dalt. Trans.*, (**2011**), 40, 3885–3902.

[2] X. Jiang, F. Gou, X. Fu, H. Jing, Ionic liquids-functionalized porphyrins as bifunctional catalysts for cycloaddition of carbon dioxide to epoxides, *J. CO_2 Util.*, (**2016**), 16, 264–271.

[3] Y. Leng, D. Lu, C. Zhang, P. Jiang, W. Zhang, J. Wang, Ionic Polymer Microspheres Bearing a CoIII-Salen Moiety as a Bifunctional Heterogeneous Catalyst for the Efficient Cycloaddition of CO_2 and Epoxides, *Chem. - A Eur. J.*, (**2016**), 22, 8368–8375.

[4] XPS spectrum of Nitrogen, https://xpssimplified.com/elements/nitrogen.php, (n.d.),.

[5] https://xpssimplified.com/elements/bromine.php, (n.d.),.

[6] J. Ederer, P. Janoš, P. Ecorchard, J. Tolasz, V. Štengl, H. Beneš, M. Perchacz, O. Pop-Georgievski, Determination of amino groups on functionalized graphene oxide for polyurethane nanomaterials: XPS quantitation vs. functional speciation, *RSC Adv.*, (**2017**), 7, 12464–12473.

GENERAL CONCLUSION

The main objective of this work was to study the feasibility of a **catalytic process for the one-pot formation of cyclic carbonates from alkenes using green oxidants (O_2/H_2O_2) and CO_2**. As stated in the introduction, the development of an efficient catalytic system operating under unique conditions for both reactions (epoxidation, CO_2 cycloaddition) was the bottleneck that needed to be tackled. A secondary objective was the immobilisation of these catalysts on mesoporous silica through a covalent grafting approach.

Below, we have summarised the main achievements of our research for the CO_2 cycloaddition onto styrene oxide, the epoxidation of styrene using O_2 or H_2O_2 and for the one-pot conversion of styrene into styrene carbonate.

- **Cycloaddition**

Two metal salophen complexes (Salophen-tBu-Mn(III) and -tBu-Ni(II)) with pending -CO_2H groups have been synthesised. Both complexes were shown to improve the cycloaddition of CO_2 onto styrene oxide in the presence of *n*-Bu_4NBr (**Chapter IV.1**). Indeed, a 100% yield of styrene carbonate was obtained within **3h in benzonitrile at 120°C** in the presence of Salophen-tBu-Mn instead of 62% without. These salophen complexes were then anchored, with up to **1 wt.% of metal,** by a covalent amide bond onto {NH_2}-SBA-15. The resulting supported complexes showed an enhanced co-catalytic activity compared to their soluble counterpart that could be due to the activation of the epoxide and/or CO_2 by the remaining aminopropyl groups. In the case of Salophen-tBu-Ni, a 100% conversion of styrene oxide was reached after 7h at 120°C instead of 85% in solution (styrene oxide : n-Bu_4NBr : Salophen was **112 : 56 : 1)**. Ni solid co-catalyst could be recycled without a significant loss of activity after 4 runs.

Cr(III) was also tested in order to lower the reaction temperature. Hence, Salophen-tBu-Cr(III) has been synthesized and was successfully grafted onto {NH_2}-SBA-15 (**Chapter IV.2**) and high yields of styrene carbonate could be obtained with a **complete conversion** of styrene oxide after **7h at 80°C** or **23h at 60°C** in the presence of Salophen-tBu-Cr(III) and *n*-Bu_4NBr but, surprisingly, the yields were significantly lower (decrease of styrene

carbonate yield of 15%) with the heterogenized form. However, this chromium co-catalyst made the cycloaddition reaction feasible at temperatures in the range of 50 to 80°C, *i.e.* adapted to the epoxidation step .

Further optimization was possible by varying the nature of the substituent in the 4,4' positions of the Salophen ligand. Et_2N-MCl and Me_2N-MCl (M = Mn, Cr) complexes were successfully synthesized and tested in the presence of *n*-Bu_4NBr in the CO_2 cycloaddition onto styrene oxide (**Chapter IV.3**) showing that the tertiary **amino groups enhanced the co-catalytic activity** compared to the -tBu groups in the 3,3',5,5' positions. The best result was obtained with the association of *n*-Bu_4NBr and **Salophen-Me_2N-Cr(III),** with a complete conversion of styrene oxide into styrene carbonate after 23h at 50°C under 11 bar of CO_2 (67% in the case of Salophen-tBu-Cr).

Meanwhile, the anchoring of customized quaternary ammonium salts (playing the role of the main catalyst in CO_2 cycloaddition) was investigated either by an *in-situ* or an *ex-situ* grafting protocol (**Chapter V**). The *ex-situ* approach was the most successful in our hands. Hence, quaternization of several tertiary amines could be performed in solution, by substitution reactions with organotrimethoxysilanes bearing either chloropropyl or bromopropyl groups (CPTMS or BPTMS), with good yields in the case of Me_2EtN, Et_2MeN and Et_3N and BPTMS. Such strategy led to an average **1 mmol.g^{-1}** of QAS loading onto SBA-15 while 2 mmol.g^{-1} could be reached with APTES, probably as the result of differences of reaction rates of silanols with trimethoxysilanes vs. triethoxysilanes. However, the reaction of bromopropyl group was only effective with tertiary amine bearing ethyl substituents instead of propyl. Moreover, reactions of BPTMS with tertiary amines bearing hydroxyethyl substituents were not successful due to secondary reactions.

Clearly, higher yields of styrene carbonate could be obtained with {QAS}-SBA-15 materials issued from the *ex-situ* approach (with the following reactivity order : **Et_3N > Et_2MeN > Me_2EtN**) compared to *n*-Bu_4NBr in solution. Indeed, a 76% yield of styrene carbonate could be reached after **23h at 80°C under 11 bar of CO_2** without any metal complex. Even though supported quaternary ammonium salt catalysts may be enough, addition of Salophen complexes is still required to obtain high yields of cyclocarbonate in shorter time and at lower temperature. Unfortunately, QAS@SBA-15 bearing longer alkyl chains or

hydroxyethyl substituents, known to be more efficient in homogenous conditions, could not be produced in this work.

In this part, cycloaddition reaction conditions were made acceptable to be coupled with epoxidation. Indeed, use of Chromium(III) and addition of tertiary amine substituents led to high yields of styrene carbonate at **temperature as low as 50°C.** Furthermore, catalytic activity could be further improved by **grafting the catalyst function** over SBA-15 silica, by amide covalent bond for Salophen co-catalysts or *ex-situ* anchoring in the case of QAS.

- **Mukaiyama epoxidation**

Epoxidation of styrene involving O_2 or H_2O_2 was investigated with the idea to improve the styrene oxide yield at the expense of benzaldehyde.

Styrene aerobic epoxidation, following Mukaiyama protocol (**Chapter VI**), was conducted in the presence of the Jacobsen catalyst and IBA used as electron donor. An optimized yield of 62% of styrene oxide could be obtained with a 100% conversion in benzonitrile after 3h under a 16 mL/min O_2 flow (**IBA : substrate : Salophen molar ratios of 300 : 120 : 1**)**.** Even though styrene oxide could be obtained without any catalyst at 80°C (65% yield), the presence of the latter was required at **50°C**. More importantly, good yields of styrene oxide were obtained (51%) after **3h at 80°C** in the presence of Salophen-Et_2N-Cr and **Salophen-Me_2N-Cr**, which showed earlier excellent co-catalytic properties in the cycloaddition step. Under non-optimized static conditions, with 3.5 bar of O_2, the yield of styrene oxide was 49%, but with an average 30% of unknown by-products.

In the case of H_2O_2, two hybrids of lacunary polyoxometalates, POM-tBu and POM-COOH, were tested at 50°C in benzonitrile (molar ratio of H_2O_2 : substrate POM **250:250:1**) leading to a 67% conversion of styrene with only 35% yield of styrene oxide with POM-COOH. Longer reaction times led to more **hydrolysis of the epoxide** by the water formed or present in aqueous H_2O_2, which represents a severe drawback. Two other styrene

derivatives were also investigated, i.e. α-methyl and β-methyl styrene, whose corresponding epoxide tend to be **less sensitive to hydrolysis than styrene oxide**.

At this stage of our work, it was thus shown that the cycloaddition and epoxidation steps were able to operate under common operating conditions (temperature of **80°C**, **benzonitrile** as solvent, and similar **catalyst and substrate concentrations**). However, for the sake of efficiency, the transformation of styrene into styrene carbonate (global reaction) will be carried out only in the presence of CO_2 and O_2.

- **Global reaction**

First attempts of the global reaction were carried out at 80°C in benzonitrile in the presence of n-Bu_4NBr, metal Salophen, IBA under O_2 and CO_2 atmosphere (**Chapter VII**). A 14% yield of styrene carbonate was obtained in the presence of Salophen-tBu-Cr after 23h, apparently as the result of Cr(III) to Cr(VI) oxidation, which would induce a lower co-catalytic activity in the cycloaddition step. We checked independently that n-Bu_4NBr and CO_2 did not interfere with the aerobic epoxidation of styrene. A "one-pot/two-steps" protocol was then conducted to avoid the deactivation of the cycloaddition co-catalyst. Hence, an epoxidation step was conducted during 3 h at 80°C in the presence of IBA under 3.5 bar of O_2, then the cycloaddition catalysts were added, as well as 11 bar of CO_2, thus affording a **styrene carbonate yield of 31%** with Salophen-Me_2N-Cr (20 h, 80°C).

In the end, an exploratory study was conducted towards the synthesis of functionalized SBA-15 bearing both the QAS catalyst and the Salophen-tBu-Cr co-catalyst (**Chapter VIII**). Interesting results were obtained by applying the ex-situ grafting strategy optimized in **Chapter V** in order to introduce simultaneously aminopropyl groups (0.65 $mmol.g^{-1}$) and the $Et_3N^+Br^-$ quaternary ammonium salt (0.81 $mmol.g^{-1}$) onto silica as proved by TGA and XPS. Covalent grafting of Salophen-tBu-Cr(III) complex bearing -COOH was then operated following the protocol described in **Chapter IV.1**. Unfortunately, effectiveness of the grafting could not be confirmed by TGA and XPS analysis. It would seem that Cr metal was lost due to a demetallation process.

APPENDIX : EXPERIMENTAL TECHNIQUES

Characterization techniques

Atomic absorption

Atomic absorption measurements for Ni/Mn analyses were performed with a Perkin Elmer Analyst 100 spectrophotometer. Samples of Salophen-Ni@{NH_2}-SBA-15 or Salophen-MnCl@{NH_2}-SBA-15 (25 mg, ca. 1% wt Ni or Mn) were dissolved in 10 mL of a sulfonitric acid solution (3: 2 v: v of concentrated sulfuric acid: nitric acid) for 24 h. A violet acidic solution and a white silica powder were thus obtained. The acidic suspension was filtered on a sintered glass and the liquid phase was collected and then diluted 25 times in a 2% nitric acid solution (Ni metal concentration *c.a.* 1 mg L^{-1}). The diluted solution was then analysed by atomic absorption using a Ni (232 nm) or a Mn (279.5 nm) atomic absorption cathode lamp.

Gas chromatography analysis

The gas chromatography analyses were performed on an AF Shimadzu NEXIS-GC-2030 instrument, equipped with a split/splitless injector, a flame ionization detector and a GC SH-Rxi-5MS capillary column (ID: 0.25 mm; film thickness: 0.25 µm; length: 30 m). Helium was the carrier gas (1.5 mL/min) and the oven temperature was programmed as follows: ramp from 70 to 250°C at 10°C/min, then isotherm at 250°C for 10 min. Calibrations were performed by dilution in dichloromethane using commercial reagents (p-xylene (internal standard, 3 mmol) and reagents to quantify (3 mmol for the sum) in 10 mL ACN, then dilution 20 µL in 10 mL DCM).

High pressure transmission infrared spectroscopy (ISM Bordeaux)

Fourier transform infrared spectra were recorded using a Nicolet 6700 spectrometer (Thermo Scientific) in the range of 4000 – 400 cm^{-1} with a nominal resolution of 4 cm^{-1}. In order to measure the spectrum of CO_2 in interaction with selected materials investigated in this study, the catalyst was dispersed in a KBr pellet (10 wt.% of the catalyst, typically 0.012 g in 0.11 g of KBr). Then, the pellet was “stuck up” between the two Ge windows of the high-pressure transmission homemade cell (see ref below for details). A spectrum of the catalysts loaded KBr pellet under atmospheric pressure was taken using the FTIR spectrometer described above (32 scans, 4 cm^{-1} resolution, in transmission mode) after which CO_2 was introduced into the cell at a pressure of 4 MPa.

Bergeot, V.; Tassaing, T.; Besnard, M.; Cansell, F.; Mingotaud, A.-F., *J. Supercrit. Fluids*, **2004**, *28*, 249-261

High Resolution Mass Spectroscopy

Analysis were performed on an ESI/ LTQ Orbitrap XL with resolution scale from 200 to 4000 m/z. 1 mL of sample was prepared from a dilution at 10 µg/mL in LC quality MeOH inside 11x32 flask.

Infrared spectroscopy

Solids were characterised by attenuated total reflexion infrared spectroscopy, using a Bruker Tensor 27 FTIR spectrometer equipped with a ZnSe crystal with resolution better than 1 cm^{-1} with a number of scans of 128.

Nitrogen adsorption-desorption

A micromeritics ASAP 2020 – Physisorption Analyzer was used to carry out the adsorption of N_2 at -196 °C. Before analysis, samples were thermally treated at 110°C for 0.5 h and 200°C for 6 h with an evacuation rate of 0.0067 bar/s.

The specific surface area was determined by the Brunauer, Emmett and Teller (BET) method with P/P^0 values in the range of about 0.05 – 0.25. The pore size distribution was estimated from the desorption branch of the isotherms using the Barrett-Joyner-Halenda (BJH) method. Finally, total pore volumes were obtained from the total amount of nitrogen adsorbed at $P/P^0 = 0.97$.

Nuclear magnetic resonance (NMR)

All NMR experiments were performed at 27 °C using a Bruker Avance III 400 MHz NMR spectrometer operating at a ^1H Larmor frequency of 400 MHz with a 5 mm broadband probe head (^1H / ^{31}P - ^{15}N). The ^1H-NMR spectra were recorded using a pulse sequence of proton with a spectral width of 7212 Hz, an acquisition time of 4.5 s and a relaxation delay of 5s. The spectra were analysed with TOPSPIN 3.6 (Bruker). ^{13}C CP MAS NMR spectra were recorded at 176.09 MHz on a Bruker AVANCE III 700 (16.4 T) spectrometer with a 4 mm Bruker probe and at a spinning frequency of 10 kHz (Recycle delay = 5 s, contact time = 10 ms).

Raman

Raman spectra were recorded on solid samples on a Kaiser Optical Systems RXN1 spectrometer equipped with a diode laser (785 nm).

Thermogravimetric analysis

Thermogravimetric analysis (TGA) were performed on a SDT Q600 system (TA Instruments, Inc.) under air flow (100 mL/min) at a heating rate of 5 °C/min, in the temperature range 25-700 °C.

X-ray diffraction

The X-ray diffraction (XRD) patterns were recorded on a Bruker AXS D8 diffractometer operated at 30 kV and 30 mA using a Cu Kα radiation (α = 1.54184 Å) as X-ray source. For the low angles diffraction experiments, the data were collected in the 2θ range from 0.5 to 5° with a step of 0.02° and a counting time of 6 s/step.

XRF (IRCELYON)

Elemental composition of samples was determined by ED-XRF Epsilon 4 from PANALYTICAL. Analyses were conducted using a X-Ray tube with Ag anode (15W – 3Ma). Resolution was 135 eV (Mn Kα)

X-ray photoelectron spectroscopy

XPS analyses were performed using an Omicron Argus X-ray photoelectron spectrometer, equipped with a monochromated AlKα radiation source (hv = 1486.6 eV) and a 280 W electron beam power. The emission of photoelectrons from the sample was analysed at a takeoff angle of 45° under ultra-high vacuum conditions (≤10^{-9} mBar). Spectra were carried out with a 100-eV pass energy for the survey scan and 20 eV pass energy for the C_{1s}, O_{1s}, N_{1s}, Br_{3d}, Mn_{2p} and Cr_{2p} regions. Binding energies were calibrated against the Si 2p peak at 103.3 eV, and element peak intensities were corrected by Scofield factors. The peak areas were determined after subtraction of a Shirley background. The spectra were fitted using Casa XPS v.2.3.15 software (Casa Software Ltd, U.K.).

Catalytic tests

Analysis method

Reactions samples were collected at precise reaction times for analysis by GC-FID.

Carbon balances were estimated for every catalytic test and are defined as the ratio of the molar quantities of the present species (reactants and products) that are quantified vs the initial molar quantity of reactants.

$$\text{Carbon balance} = \frac{n_{reactants} + n_{quantified\ products}}{n_{initial\ reactants}}$$

Calculation methods for the results of the cyclocarbonatation of epoxides

Styrene oxide and styrene carbonate amounts were obtained from the integration of their GC peaks and their comparison with that of the internal standard. The consumption of styrene and formation of styrene carbonate was monitored over time and quantified using the following formulas:

$$\text{Styrene oxide (SO) conversion: \%C} = \frac{n_{SO,t=0} - n_{SO,t}}{n_{SO,t=0}} \text{ x 100}$$

$$\text{Styrene carbonate (SC) selectivity: \%S} = \frac{n_{SC,t}}{n_{SO,t=0} - n_{SO,t}} \text{ x 100}$$

$$\text{Styrene carbonate (SC) yield: \%Y} = \frac{n_{SC,t}}{n_{SO,t=0}} \text{ x 100}$$

Incertitude values for the results were calculated on the basis of four injections per sample and are of 2% (absolute uncertainty). Similar calculation methods could be drawn for the determination of styrene conversion and styrene oxide yield regarding the epoxidation reaction.

Table of Reagents regarding the epoxidation or cycloaddition tests

List of reagents used	Purity/Brand
Epoxidation and cycloaddition tests	
Styrene	99% Acros Organics
Styrene oxide	97% Aldrich chemistry
α-methyl styrene	99% Sigma Aldrich
Trans-β-methyl styrene	99% Sigma Aldrich
p-Xylene	99% Acros organics
H_2O_2	30% aqueous, Sigma Aldrich
Urea H_2O_2	97% Aldrich chemistry
Solvents	
Benzonitrile	99% Acros Organics
Acetonitrile	HPLC, Sigma Aldrich
Dichloromethane	For analysis, Carlo Ebra